STUDIES ON A CATALYTIC CADOGAN CYCLIZATION BY $P^{III}/P^{V}=O$ REDOX CYCLING

By

Tyler S. Harrison

B.S., Chemistry, 2015
University of Massachusetts, Lowell

Submitted to the Department of Chemistry
in Partial Fulfillment of the Requirements for the Degree of

MASTER OF SCIENCE
IN CHEMISTRY

at the
Massachusetts Institute of Technology
February 2018

Signature redacted

Signature of Author: _____
Department of Chemistry
February 9, 2018

Signature redacted

Certified by: _____
Alexander T. Radosevich
Associate Professor of Chemistry
Thesis Supervisor

Signature redacted

Accepted by: _____
Robert W. Field
Chairman, Departmental Committee on Graduate Students

Studies on a Catalytic Cadogan Cyclization by P^{III}/P^{V}=O Redox Cycling

by

Tyler S. Harrison

Submitted to the Department of Chemistry
on February 9, 2018 in Partial Fulfillment of the
Requirements for the Degree of Master of Science in
Chemistry

ABSTRACT

Organophosphorus reagents offer potential for developing catalytic protocols by inclusion of a reductant such as hydrosilanes to (re)generate the chemically active phosphine in situ. In our research, we have successfully adapted this concept to the Cadogan reductive cyclization by using a strained 4-membered phosphetane precatalyst, which proved to be more competent than acyclic and 5-membered analogs for P(III)/P(V)=O redox cycling. A variety of substrates were found to successfully undergo catalytic Cadogan indazole cyclization. The mechanism of the cyclization has been expanded. The resting state of phosphorus was determined to be the P^{III} phosphetane, and this phosphetane proved to be 8 times faster than the acyclic *n*-Bu_3P at driving the reductive cyclization of N-phenyl o-nitrobenzaldimine to 2-phenylindazole. A nitrosoarene, presumed an intermediate in the overall cyclization, was found to undergo cyclization under reaction conditions. In addition, a new unique oxazaphosphetane was observed as an intermediate during the course of cyclization, which may lead to a more complete understanding of other-phosphorus mediated deoxygenations, including nitro reduction. Initial studies in nitro reduction have been undertaken, though further work is necessary to fully develop a phosphorus-mediated catalytic protocol.

Thesis Supervisor: Alexander T. Radosevich
Title: Associate Professor of Chemistry

TABLE OF CONTENTS

LIST OF FIGURES

LIST OF TABLES

ACKNOWLEDGEMENTS

Firstly, I would like to greatly thank Professor Alexander T. Radosevich for all of his guidance and advice over the course of my graduate career. Thank you for your faith in my ability to succeed at MIT. I would also like thank Professor Stephen L. Buchwald and Professor Jeremiah A. Johnson for the time they sacrificed to serve on my committee. I would like to also thank the late Professor Daniel J. Sandman of the University of Massachusetts Lowell, without whom I would not have considered pursuing research in organic chemistry.

I would like to thank the members of the Radosevich group, both former and current, for their guidance, discussion, and support, without which I may have not lasted so long in the program.

Finally, I would like to acknowledge my brother, Brett, and my parents, Steven and Terri Harrison, for all of their support and all they have given me throughout my life. None of this would be possible without them, and I am grateful for all the opportunities and experiences you have been able to afford me.

Chapter 1

The Advancement of P^{III}/P^{V}=O Redox Cycling in Catalysis

Organic phosphorus compounds undergoing the conversion $P^{III} \rightarrow P^{V}$=O have seen great utility in a variety of chemical transformations. The use of stoichiometric amounts of such phosphorus reagents limits their utility due to the phosphine oxide waste generated, which would be rectified by the development of protocols that reduce the phosphine oxide in situ and therefore close a catalytic P^{III}/P^{V}=O redox cycle. This chapter will detail considerations necessary for designing a P^{III}/P^{V}=O redox cycle and prior successes in the field as a prelude to the studies that are the subject of this thesis.

1.1 – Phosphine Oxides in Organic Synthesis

Organophosphorus compounds have seen extensive utility in the realm of synthetic transformations. Due to the ability for phosphorus to accommodate both +3 and +5 oxidation states while spanning coordination numbers of 1 to 6, organophosphorus compounds can be considered suitable for redox chemistry. Redox chemistry broadly involves the net transfer of electrons from one chemical species to another, resulting in a change of oxidation state. In organophosphorus chemistry, the most common redox reaction a P^{III} species can undergo is oxide formation, which involves the generation a P^{V}=O bond. This bond is strong, with a bond dissociation energy of about 128-139 kcal/mol,[1] owing in part to the ability for oxygen lone pairs to donate into σ* orbitals on the phosphorus moiety (Figure 1.1).[2]

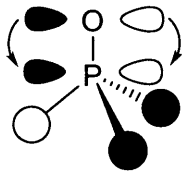

Figure 1.1. Descriptor of relevant orbitals involved in P=O π bonding ($n_O \rightarrow \sigma^*_{PR3}$).

As a result of this bond strength, the formation of P=O bonds provides the thermodynamic driving force behind a variety of chemical transformations, including the Wittig reaction,[3] the Appel reaction,[4] and the Mitsunobu reaction.[5] In each of these reactions, a phosphine undergoes net oxygenation, concomitant with the formation of olefins, halides, and functionalized alcohols respectively. The phosphine oxide is frequently discarded as chemical waste, being produced as a stoichiometric byproduct to the reaction of interest. This point demonstrates the limited atom economy[6] provided by typical organophosphorus-based reactions. Catalytic turnover of the phosphine oxide could, in principle, address these challenges.

1.2 – Reduction of Phosphine Oxides

In order to render an organophosphorus-based reaction catalytic, the generated phosphine oxide must be reduced in situ to reform the chemically active phosphine. A variety of methods to reduce phosphine oxides have been explored in the literature,[7] including aluminum hydrides, boranes, and silanes.

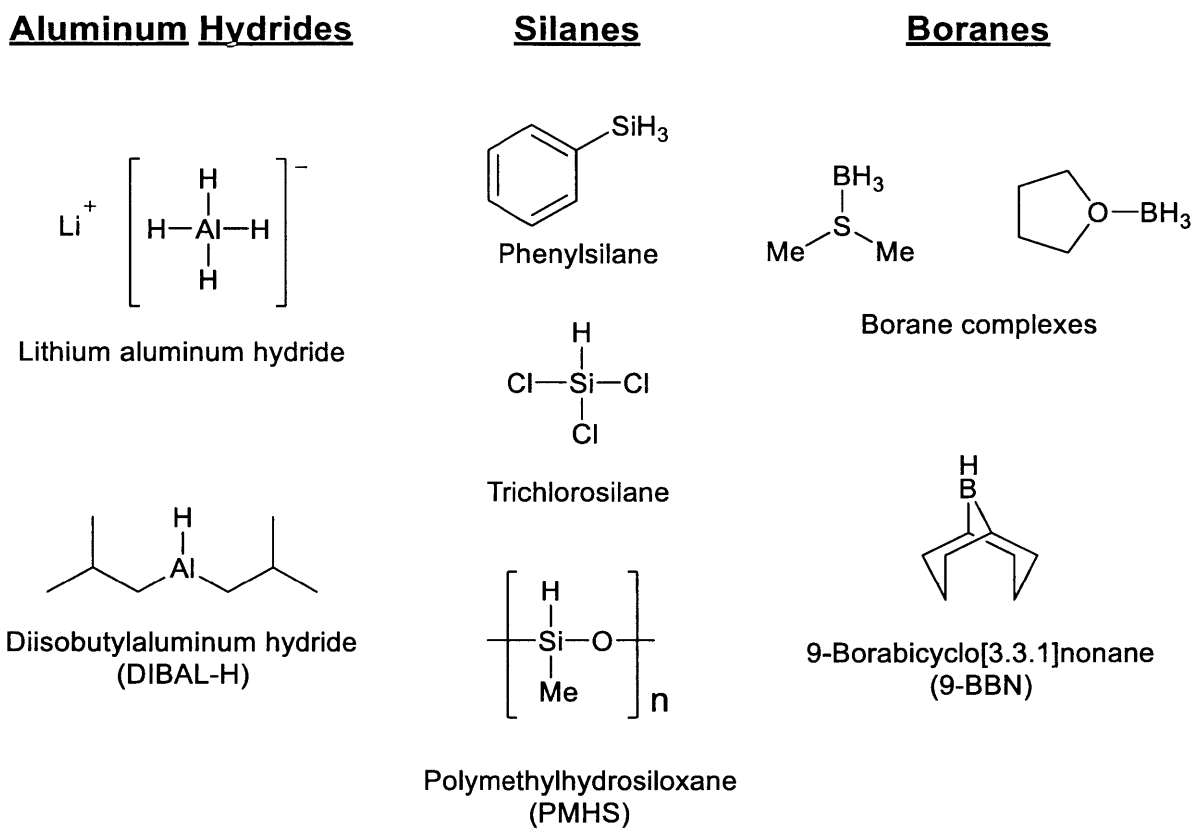

Figure 1.2. Examples of reducing agent classes for the conversion $R_3P{=}O \rightarrow R_3P$.

Aluminum hydride reagents are strong reducing agents, and as such suffer from poor chemoselectivity—in addition to necessitating a Lewis acid for efficient reduction of arylphosphines under mild conditions,[8] they undergo unfavorable side reactions with other reducible functionalities (ketones, aldehydes, disulfides)[9] and facile cleavage of P–O,[10] P–N,[11] and $P–C_{aryl}$[12] bonds.

Borane reagents can be used as a means to produce stable, easy-to-handle borane-protected phosphines from phosphine oxides.[13] However, reformation of the phosphine from this borane-phosphine complex typically requires treatment with excess amines, such as diethylamine[14] or N,N,N,N-tetramethyldiaminoethane,[15] which could be problematic with acidic functionalities.

Silanes can be used as efficient, chemoselective reductants of arylphosphine oxides, although the reduction of trialkylphosphine oxides require a Lewis basic additive such as trimethylamine.[16] Silanes also range in terms of reducing strength and commercial availability, and an excess is generally required for efficient phosphine oxide reduction, although additives such as $Ti(OiPr)_4$ have been used to reduce the silane loading.[17]

Despite their issues, silanes would appear to offer the most favorable means of reducing phosphine oxides in situ for catalytic turnover. In particular, their chemoselectivity towards phosphine oxide reduction and the generation of the chemically-active phosphine without further work-up are both attractive features for their broad applicability in P^{III}/P^{V}=O redox cycling.

While silanes are suitable phosphine oxide reductants, these reductions are typically kinetically slow. According to the currently accepted mechanism (Figure 1.3),[18] the reduction process first involves the conversion of the pseudotetrahedral phosphine oxide into a trigonal bipyramidal phosphorane by addition of Si–H across the P=O moiety. Collapse of this phosphorane results in the reformation of the phosphine oxide, as well as a silanol. Based on computational data by Krenske,[19] the barrier to this process arises in part from the need for geometric reorganization at phosphorus upon initial addition of Si–H.

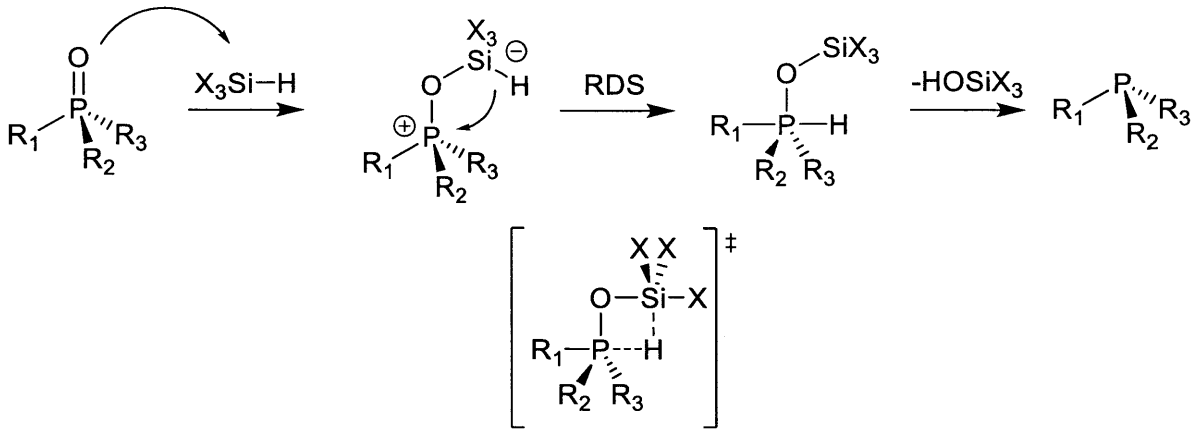

Figure 1.3. Mechanistic course of hydrosilane-mediated reduction of phosphine oxides.

Given that a geometric reorganization at phosphorus is involved in the rate-limiting step, constraining the geometry around phosphorus minimizes the energetic barrier, and thereby speeds the rate of phosphine oxide reduction.[20,21,22] As has been noted by Hudson[23] and Westheimer,[24] constraining phosphorus valence angles within a ring increases the electrophilic character at phosphorus, which should assist in phosphine oxide reduction.

1.3 – Approaches to Catalysis in Phosphine-Mediated Transformations

The notion of using geometric constraint at phosphorus to improve reduction has been utilized by a number of researchers in their attempts to achieve phosphorus-based catalysis.

The earliest success in this area was performed by O'Brien and colleagues[21] in their adaptation of a catalytic protocol to the Wittig reaction by using one of two constrained, 5-membered phosphacyclic catalysts—3-methyl-1-phenylphospholane and 1-phenylphospholane—generated from their oxides by diphenylsilane as an in situ reductant. With only 4-10 mol% of the phosphine oxide precatalyst, they were able to demonstrate the synthesis of olefins in good to excellent yields (66-96%). Further work by O'Brien, in their development of a room temperature variant, has indicated that acyclic phosphine oxides can be utilized, but only with the addition of a protic acid to enhance the rate of reduction.[25]

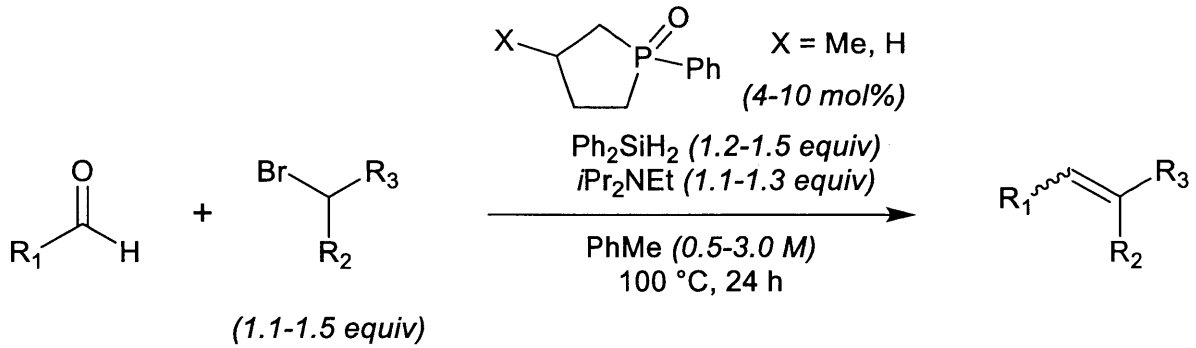

Figure 1.4. Catalytic Wittig reaction developed by O'Brien.

Similarly, van Delft and colleagues[26] have achieved success in developing a catalytic Appel reaction using a constrained, 5-membered phosphacyclic catalyst—5-phenyldibenzophosphole—with diphenylsilane as the reductant. The phospholane utilized by O'Brien proved unsuitable, as it reacted with the bromide source utilized (diethyl 2-bromomalonate). Using this protocol, primary alkyl bromides could be synthesized in moderate to good yields (45-72%) with only 10 mol% of the phosphine catalyst, while secondary alkyl bromides generally exhibited poor reactivity.

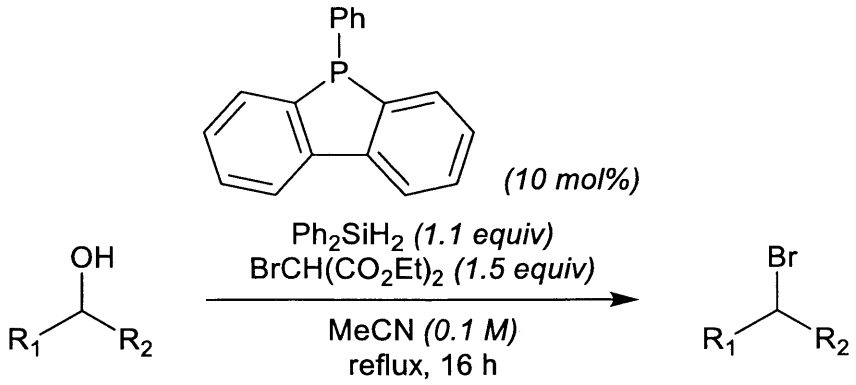

Figure 1.5. Catalytic Appel reaction developed by van Delft

Radosevich and colleagues[27] have successfully adapted a catalytic protocol for the deoxygenative condensation of α-keto esters with carboxylic acids via a Kukhtin-Ramirez reaction using phenylsilane as a reductant and a constrained, 4-membered phosphacyclic precatalyst—*P*-pyrrolidino-2,2,3,4,4-pentamethylphosphetane oxide. These condensation products were synthesized in moderate to excellent yields (65-94%) with a range of electronics, sterics, and functionalities. Despite the general chemoselectivity of silanes towards phosphine oxide reduction, the authors did note that overreduction of their phosphetane catalyst (i.e. formation of P–H from the P–N bond) occurred with high equivalencies of hydrosilane reductant.

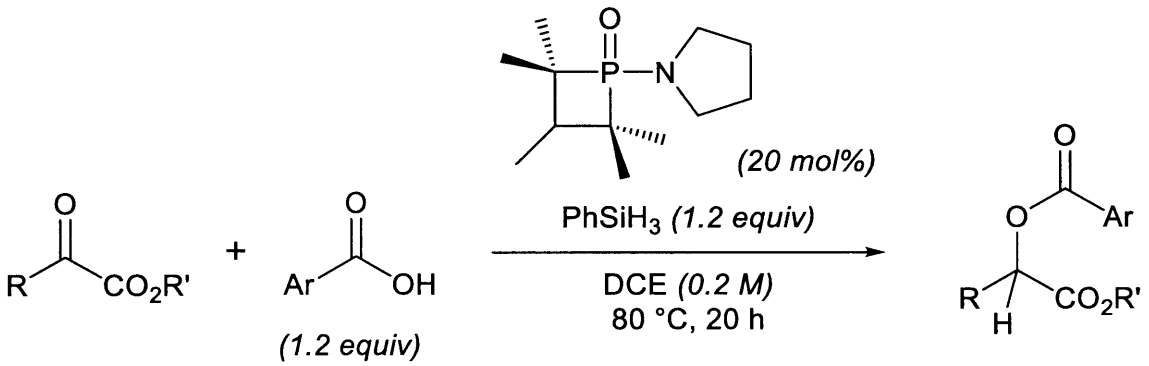

Figure 1.6. Catalytic deoxygenative condensation of α-keto esters and carboxylic acids developed by Radosevich.

In each of these cases, it was found that, without additional additives, unconstrained phosphine oxides, such as triphenylphosphine and larger (6^+-membered) phosphacycles, proved unsuitable as catalysts. This lends credence to the notion that constraining the geometry at phosphorus is necessary for reducing phosphine oxides effectively and swiftly in order to utilize P^{III}/P^{V} redox cycling.

1.4 – Summary and Looking Ahead

In view of the vast literature on their stoichiometric reactivity, organophosphorus reagents offer clear potential for developing catalytic protocols. This development would require in situ reduction of a phosphine oxide to regenerate the chemically reactive phosphine, and hydrosilanes are promising chemoselective reductants for this transformation. Several researchers have demonstrated this kind of reactivity with the use of constrained phosphines, which have been noted as potential platforms for facile reduction. Given this precedent, 4-membered phosphacycles appear to be a most promising avenue for further work in developing catalytic phosphine-based protocols of stoichiometric reactions. This thesis will examine our advances in developing P^{III}/P^{V}=O redox catalysis in the deoxygenation reactions of nitroarenes, as well as mechanistic insights into said reaction using 4-membered phosphacycles as the platform of choice.

1.5 – References

[1] Hudson, R. F. *Structure and Mechanism in Organo-Phosphorus Chemistry*; Blomquist, A. T., Ed.; Academic Press: New York, NY, 1965; pp 68-70.

[2] Gilheany, D. G. "No d Orbitals but Walsh Diagrams and Maybe Banana Bonds: Chemical Bonding in Phosphines, Phosphine Oxides, and Phosphonium Ylides." *Chem. Rev.* **1994**, *94*, 1339–1374.

[3] (a) Wittig, G.; Geissler, G. "Course of reactions of pentaphenylphosphorus and certain derivatives." *Justus Liebigs Ann. Chem.* **1953**, *580*, 44-57. (b) Wittig, G.; Schollkopf, U. "Triphenylphosphinemethylene as an olefin-forming reagent. I." *Chem. Ber.* **1954**, *97*, 1318-1330. (c) Wittig, G.; Haag, W. "Triphenylphosphinemethylene as an olefin-forming reagent. II." *Chem. Ber* **1955**, *88*, 1654-1666.

[4] Appel, R. "Tertiary Phosphane/Tetrachloromethane, a Versatile Reagent for Chlorination, Dehydration, and P–N Linkage." *Angew. Chem. Int. Ed. Engl.* **1975**, *14*, 801–811.

[5] (a) Mitsunobu, O.; Yamada, M.; Mukaiyama, T. "Preparation of esters of phosphoric acid by the reaction of trivalent phosphorus compounds with diethyl azodicarboxylate in the presence of alcohols." *Bull. Chem. Soc. Jpn.* **1967**, *40*, 935-939. (b) Mitsunobu, O.; Yamada, M. "Preparation of esters of carboxylic and phosphoric acid via quaternary phosphonium salts." *Bull. Chem. Soc. Jpn.* **1967**, *40*, 2380-2382.

[6] Trost, B. M. "The Atom Economy--a Search for Synthetic Efficiency." *Science* **1991**, *254*, 1471–1477.

[7] Hérault, D.; Nguyen, D. H.; Nuel, D.; Buono, G. "Reduction of secondary and tertiary phosphine oxides to phosphines." *Chem. Soc. Rev.* **2015**, *44*, 2508–2528.

[8] Imamoto, T.; Takeyama, T.; Kusumoto, T. "Facile Reduction of Organic Halides and Phosphine Oxides with $LiAlH_4$–$CeCl_3$." *Chem. Lett.* **1985**, *14*, 1491–1492.

[9] Bootle-Wilbraham, A.; Head, S.; Longstaff, J.; Wyatt, P. "Alane–A Chemoselective Way to Reduce Phosphine Oxides." *Tetrahedron Lett.* **1999**, *40*, 5267–5270.

[10] Zhu, J.-L.; Bau, J.-S.; Shih, Y.-C. "$LiAlH_4$-Induced Reductive Dephosphonylation of α,α-Dialkyl Triethyl β-Phosphonyl Esters: Mechanistic Study and Synthetic Application." *Synlett* **2012**, *23*, 863–866.

[11] Henson, P. D.; Ockrymiek, S. B.; Markham, R. E. "Reductive Cleavage of Phosphinanilides with Lithium Aluminum Hydride." *J. Org. Chem.* **1974**, *39*, 2296–2298.

[12] Higham, L. J.; Clarke, E. F.; Müller-Bunz, H.; Gilheany, D. G. "P-Chirogenic Phosphines. MOP/diPAMP Hybrids, Their Oxide Crystal Structures, Reduction Studies and Alternative Syntheses." *J. Organomet. Chem.* **2005**, *690*, 211–219.

[13] Köster, R.; Morita, Y. "Triphenylphosphin Aus Triphenylphosphinoxyd Durch Reduktion Mit Boranen." *Angew. Chem.* **1965**, *77*, 589–590.

[14] Imamoto, T.; Oshiki, T.; Onozawa, T.; Kusumoto, T.; Sato, K. "Synthesis and Reactions of Phosphine-Boranes. Synthesis of New Bidentate Ligands with Homochiral Phosphine Centers via Optically Pure Phosphine-Boranes." *J. Am. Chem. Soc.* **1990**, *112*, 5244–5252.

[15] Ohff, M.; Holz, J.; Quirmbach, M.; Börner, A. "Borane Complexes of Trivalent Organophosphorus Compounds. Versatile Precursors for the Synthesis of Chiral Phosphine Ligands for Asymmetric Catalysis." *Synthesis* **1998**, 1391–1415.

[16] Fritzsche, H.; Hasserodt, U.; Korte, F. "Reduktion Organischer Verbindungen Des Fünfwertigen Phosphors Zu Phosphinen, II. Reduktion Tertiärer Phosphinoxyde Zu Tertiären Phosphinen Mit Trichlorsilan." *Chem. Ber.* **1965**, *98*, 171–174.

[17] Berthod, M.; Favre-Réguillon, A.; Mohamad, J.; Mignani, G.; Docherty, G.; Lemaire, M. "A Catalytic Method for the Reduction of Secondary and Tertiary Phosphine Oxides." *Synlett* **2007**, 1545–1548.

[18] Zhang, K.; Cai, L.; Yang, Z.; Houk, K. N.; Kwon, O. "Bridged [2.2.1] Bicyclic Phosphine Oxide Facilitates Catalytic γ-Umpolung addition–Wittig Olefination." *Chem. Sci.* **2018**, Advance Article.

[19] (a) Krenske, E. H. "Reductions of Phosphine Oxides and Sulfides by Perchlorosilanes: Evidence for the Involvement of Donor-Stabilized Dichlorosilylene." *J. Org. Chem.* **2012**, *77*, 1–4. (b)

Krenske, E. H. "Theoretical Investigation of the Mechanisms and Stereoselectivities of Reductions of Acyclic Phosphine Oxides and Sulfides by Chlorosilanes." *J. Org. Chem.* **2012**, *77*, 3969–3977.

[20] Rowley, A. G. "Deoxygenations using Phosphorus(III) Reagents 1: General Functional Group Conversions." In *Organophosphorus Reagents in Organic Synthesis*. Cadogan, J. I. G., Ed. Academic Press: London, 1979; pp. 295-350.

[21] O'Brien, C. J.; Tellez, J. L.; Nixon, Z. S.; Kang, L. J.; Carter, A. L.; Kunkel, S. R.; Przeworski, K. C.; Chass, G. A. "Recycling the Waste: The Development of a Catalytic Wittig Reaction." *Angew. Chem. Int. Ed.* **2009**, *48*, 6836–6839.

[22] Keglevich, G.; Fekete, M.; Chuluunbaatar, T.; Dobó, A.; Harmat, V.; Tőke, L. "One-pot transformation of cyclic phosphine oxides to phosphine-boranes by dimethylsulfide-borane." *J. Chem. Soc., Perkin Trans. 1* **2000**, 4451-4455.

[23] Hudson, R. F.; Brown, C. "Reactivity of heterocyclic phosphorous compounds." *Acc. Chem Res.* **1972**, *5*, 204-211.

[24] Westheimer, F. H. "Pseudo-rotation in the hydrolysis of phosphate esters." *Acc. Chem Res.* **1968**, *1*, 70-78.

[25] O'Brien, C. J.; Lavigne, F.; Coyle, E. E.; Holohan, A. J.; Doonan, B. J. "Breaking the Ring through a Room Temperature Catalytic Wittig Reaction." *Chem. Eur. J.* **2013**, *19*, 5854–5858.

[26] van Kalkeren, H. A.; Leenders, S. H. A. M.; Hommersom, C. R. A.; Rutjes, F. P. J. T.; van Delft, F. L. "In Situ Phosphine Oxide Reduction: A Catalytic Appel Reaction." *Chem. Eur. J.* **2011**, *17*, 11290–11295.

[27] Zhao, W.; Yan, P. K.; Radosevich, A. T. "A Phosphetane Catalyzes Deoxygenative Condensation of α-Keto Esters and Carboxylic Acids via P^{III}/P^{V}=O Redox Cycling." *J. Am. Chem. Soc.* **2015**, *137*, 616–619.

Chapter 2

Development of a Catalytic Cadogan Reductive Cyclization

This chapter details the reductive cyclization of *o*-nitrobenzaldimines by trivalent phosphorus reagents, and our success in developing a catalytic protocol.

2.1 - Background

Given the previous success of developing a catalytic protocol for the deoxygenative condensation of α-keto esters and carboxylic acids,[1] we sought to investigate the possibility of rendering catalytic other phosphorus-mediated deoxygenations, leading us to the Cadogan reductive cyclization.[2] Broadly, this transformation involves double deoxygenation of a nitroarene by a R_3P^{III} reagent, resulting in a nitrene or nitrenoid intermediate which undergoes cyclization with a pendant functionality (Figure 2.1a). The presence of a nitrene intermediate has been postulated by comparison of byproducts also observed when an explicit nitrene is generated by thermolysis of an aryl azide.[3] The Cadogan transformation has been used to synthesize a wide variety of heterocycles, such as carbazoles, indazoles, phenazines, phenothiazines, and others (Figure 2.1b).

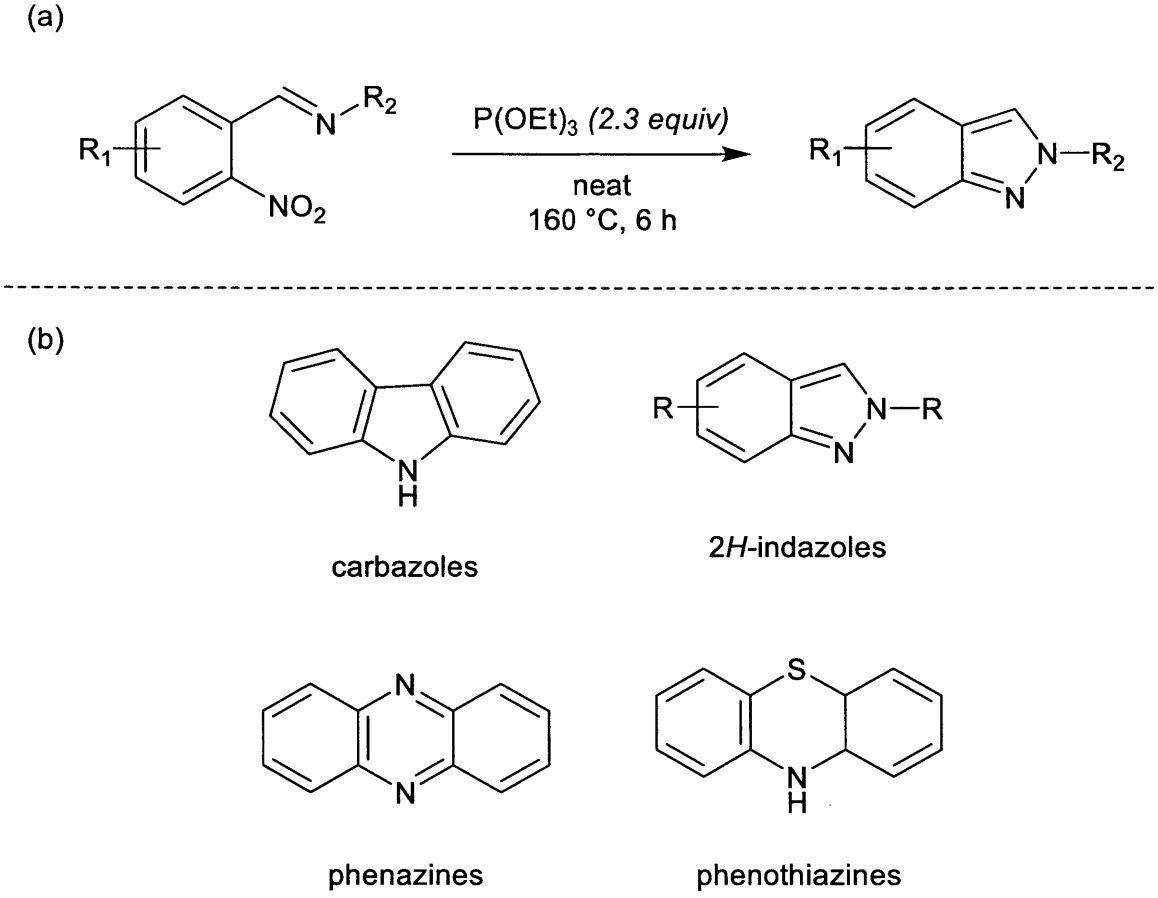

Figure 2.1. (a) General classical Cadogan indazole heterocyclization. (b) Examples of heterocycles synthesized by Cadogan reductive cyclization.

Most commonly, this transformation uses superstoichiometric amounts of the phosphorus reagents at an elevated temperature (traditionally neat refluxing triethylphosphite).[2] However, in 2014, Genung reported a mild, one-pot condensation–Cadogan cyclization method towards the synthesis of 2*H*-indazoles.[4] After first forming the imine substrate from condensation of *o*-nitroaldehydes with aromatic and aliphatic amines in isopropanol at 80 °C, treatment of the reaction mixture with three equivalents of tri-*n*-butylphosphine at 80 °C resulted in the synthesis of 2*H*-indazoles in moderate yields (37-87%). While this modified Cadogan method has advantages over the traditional protocol (i.e. lower reaction temperature, non-phosphite solvent,

one-pot condensation and reductive transformation), the possibility of catalysis was not considered.

2.2 – Developing a Catalytic Protocol to Cadogan Indazolation

In accord with Figure 2.1a, a potential catalytic Cadogan indazolation would require two phosphorus-based redox reactions operating in tandem: 1) reductive *O*-atom transfer from nitro substrate to phosphorus reagent, and 2) hydrosilane-mediated turnover of the in situ formed phosphine oxide. To validate each of these half reactions independently, we first carried out stoichiometric studies. Specifically, substrate **2.17** was reacted with 3 equiv of 2,2,3,4,4-pentamethyl-1-phenylphosphetane **2.7** (prepared by one-pot McBride[5] synthesis from 2,4,4-trimethylpent-2-ene and $PhPCl_2$) in toluene at 75 °C, resulting in formation of indazole **2.18** in 49% isolated yield. Complementarily, treatment of 2,2,3,4,4-pentamethyl-1-phenylphosphetane oxide **2.7**•[O] with phenylsilane cleanly converted to **2.7** within 3 h at 80 °C. Having demonstrated the requisite stoichiometric reactivity, a proof-of-principle catalytic variant was attempted. Reacting substrate **2.17** in the presence of 25 mol% of **2.7**•[O] with 2.5 equiv of phenylsilane in toluene at 100 °C resulted in an isolated indazole **2.18** yield of 83% in 20 h following column chromatographic purification.

Assuming that ready reduction of the phosphine oxide by hydrosilane is a necessary prerequisite for efficient $P^{III}/P^{V}=O$ catalysis, a suite of phosphorus precatalysts (Figure 2.2) including acyclic, 5-membered, and 4-membered phosphine oxides were reacted with a variety of silanes ($PhSiH_3$, Ph_2SiH_2, $(EtO)_3SiH$, Me_6Si_2, PMHS) in order to judge their ability to undergo rapid deoxygenation. In each experiment, the phosphine oxide was dissolved in toluene-d_8 (1.0 M) in an NMR tube. The hydrosilane (10 equiv) was added at room temperature, and the NMR tube was placed into a bath set at 100 °C. After 20 h, the reaction mixture was analyzed by ^{31}P NMR

spectroscopy to determine whether the phosphine oxide had been reduced; the phosphine oxide was considered successfully reduced if the signals corresponding to the phosphine oxide, determined by independent analysis, were no longer present. To note, these studies were performed with the assistance of Trevor Nykaza.

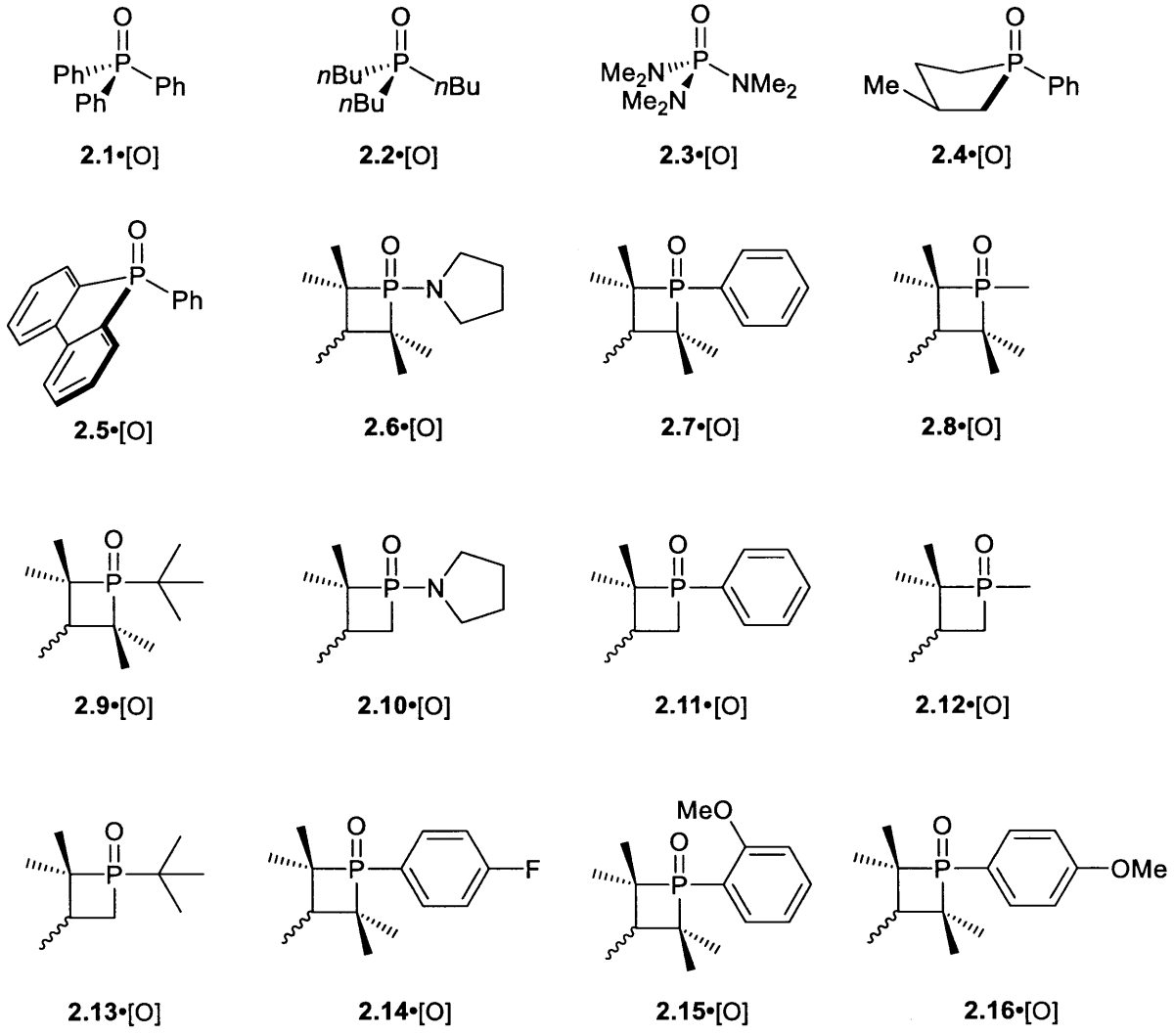

Figure 2.2. Potential phosphine oxide precatalysts for catalytic Cadogan cyclization.

From this initial triage, several catalyst/reductant combinations underwent full deoxygenation (see Table 2.1 for successful combinations). In general, $PhSiH_3$, Ph_2SiH_2, and

PMHS were efficient in reducing the majority of the phosphine oxides, with the exception of partial conversion of triphenylphosphine oxide **2.1**•[O] and hexamethylphosphoramide **2.3**•[O]. Notably, however, while PMHS was found to be suitable for reduction, operational issues prevented us from further study—the reaction mixture became a gel, likely due to crosslinking of the siloxane, hindering the efficiency of mixing. Hexamethyldisilane was insufficient in all cases, and $(EtO)_3SiH$ was capable of reducing the majority of the phosphacycles. However, $(EtO)_3SiH$ was not further considered, owing to concerns regarding toxicity and potential production of flammable silane (SiH_4).

Each of the suitable catalyst/reductant combinations were then subjected to a standard Cadogan cyclization—the synthesis of 2-phenyl-2*H*-indazole **2.18** (Table 2.1). It was found that both phenylsilane and diphenylsilane proved to be competent reductants and could be interchanged without significant effects on GC yield. In addition, the 4-membered phosphacycles proved to have the highest yield. After consideration of the relative phosphine structures, the four highest yielding candidates were advanced for further study (Table 2.1, entries 5, 7, 9, and 13).

Table 2.1. Successful catalyst/reductant combinations subjected to a standard Cadogan cyclization

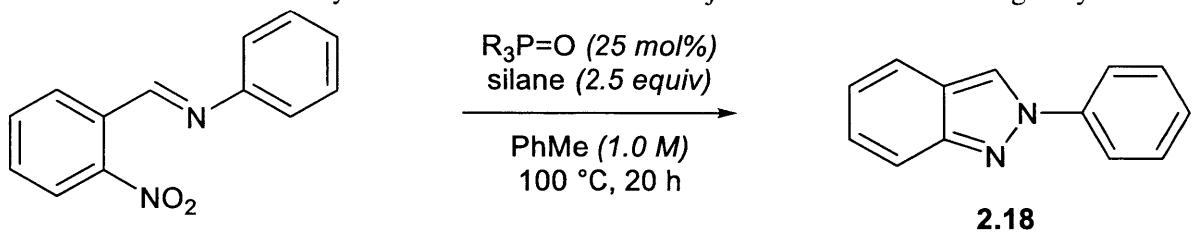

2.17 **2.18**

Entry	R_3P=O	Silane	Yield [a]
1	**2.2**•[O]	$PhSiH_3$	57%
2	**2.4**•[O]	Ph_2SiH_2	21%
3	**2.4**•[O]	$PhSiH_3$	45%
4	**2.7**•[O]	Ph_2SiH_2	78%
5	**2.7**•[O]	$PhSiH_3$	83%
6	**2.8**•[O]	$PhSiH_3$	78%
7	**2.8**•[O]	Ph_2SiH_2	84%
8	**2.11**•[O]	$PhSiH_3$	79%
9	**2.11**•[O]	Ph_2SiH_2	85%
10	**2.13**•[O]	$PhSiH_3$	74%
11	**2.14**•[O]	$PhSiH_3$	77%
12	**2.16**•[O]	Ph_2SiH_2	77%
13	**2.16**•[O]	$PhSiH_3$	89%

[a] Yields determined by GC with respect to dodecane internal standard.

Given that the deoxygenations were presumed to proceed through transient, zwitterionic intermediates, a polar high-boiling solvent (i.e. *N,N*-dimethylformamide) was tested as a potential substitute. This alteration resulted in higher GC yields for **2.7**•[O] and **2.8**•[O] (89% and 95% respectively), while **2.11**•[O] and **2.16**•[O] had decreased yields (84% and 85% respectively). Of these two successes, it was observed that **2.8**•[O] proceeded much faster than **2.7**•[O], with the reaction reaching completion in as little as 2 h with a 85% yield by GC; conversely, **2.7**•[O] had undergone 66% conversion with 53% yield by GC in the same time frame. As such, 1,2,2,3,4,4-hexamethylphosphetane oxide **2.8**•[O] was selected as the precatalyst of choice.

Upon further study, the use of diphenylsilane resulted in an isolable side product that co-elutes with desired product **2.18**. Single crystals of this byproduct were obtained by slow

evaporation from hexanes, and a crystal structure suitable to establish connectivity showed cyclic 2,2,4,4,6,6-hexaphenylcyclotrisiloxane **2.19** (Figure 2.3). Evidently, the silanediol formed following phosphine oxide reduction undergoes cyclocondensation to form the observed cyclotrisiloxane.[6] Attempts to remove cyclotrisiloxane **2.19** by chromatography with 10% KF on silica stationary phase[7] proved unsuccessful. Consequently, we opted to employ phenylsilane, which has similar performance in the catalytic reaction but is more readily removed during purification.

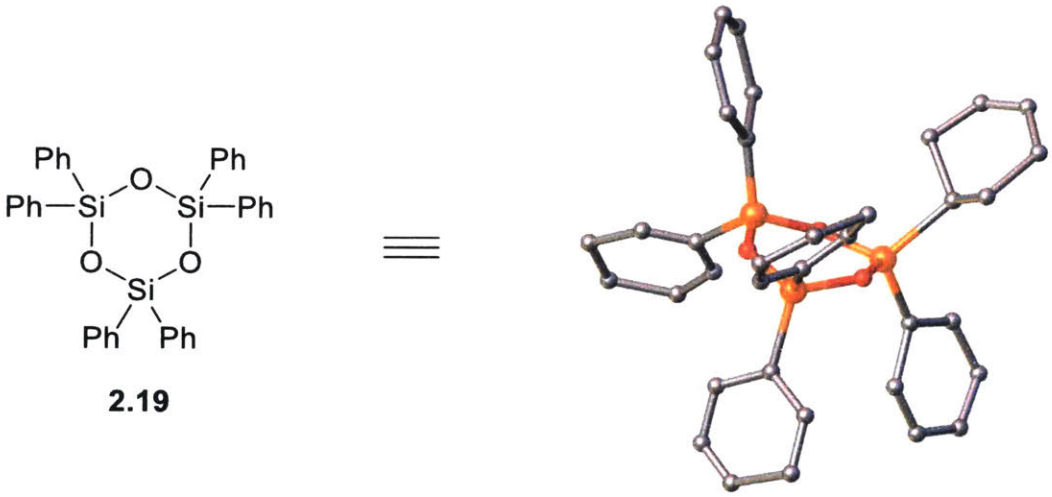

Figure 2.3. Crystal structure of the byproduct 2,2,4,4,6,6-hexaphenylcyclotrisiloxane.

Ultimately, a screen of catalyst loading, silane loading, and temperature led to the use of 15 mol% of **2.8**•[O]and 2 equiv of phenylsilane at 100 °C in toluene (Table 2.2, top).

2.3 – Substrate Scope

The scope of the indazolization method was probed (Table 2.2).[8] Aromatic substrates of varied substitution proved to be suitable, including electron-rich (**2.20**) and sterically demanding *N*-aryl substituted substrates (**2.25**). Free hydroxyl moieties (**2.23**, **2.26**) did not inhibit deoxygenative cyclization, although such substrates may undergo in situ silylation; a desilylative workup with tetrabutylammonium fluoride ensured recovery of the target compound. A range of reducible functionalities were preserved, including amides (**2.27**) and esters (**2.21**, **2.22**), but ketones (**2.24**) were at least partially reduced in situ. Substituents adjacent to the nitro moiety (**2.22**) hindered reactivity, promoting the reduction of the imine rather than cyclization.

Cyclization was not observed in several cases, although the specific reasons are not presently clear. The thiazole derivative (**2.28**) may have been unsuccessful due to the naphthalene branches adjacent to the nitro moiety, but experiments to determine the exact nature of incompatibility were not performed. Substrates deriving from (thio)hydrazones (**2.29**, **2.31**) and carboxylic acids (**2.32**), and substrates where the pendant functionality is an amide (**2.30**) also appear to not tolerate the cyclization.

Table 2.2. Examples of catalytic Cadogan cyclization [a]

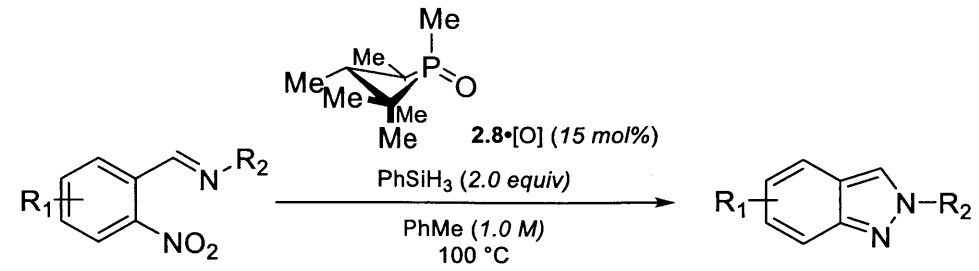

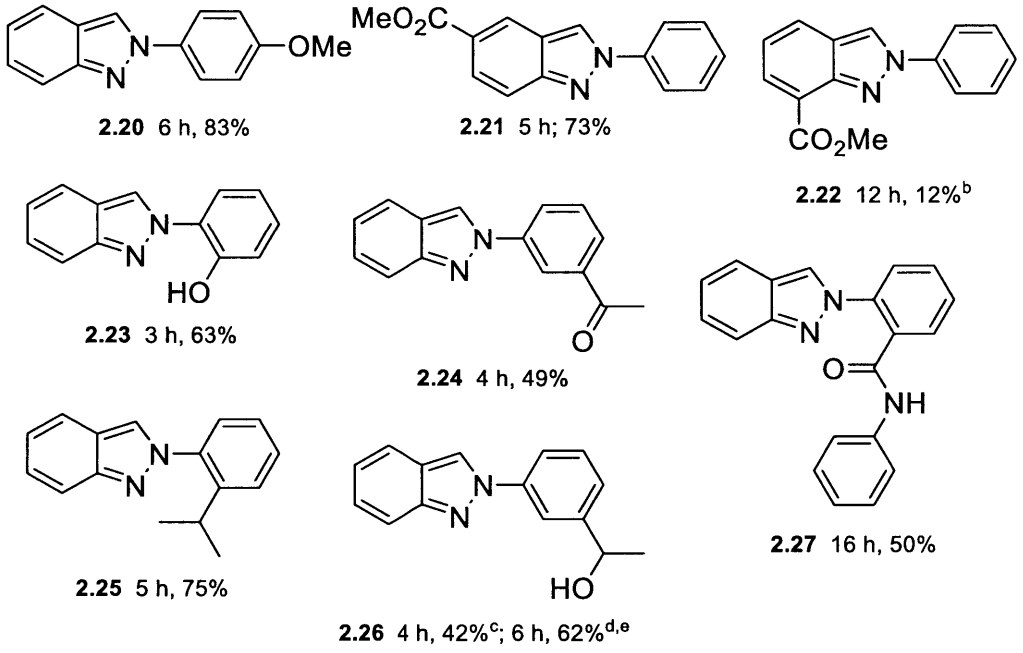

2.20 6 h, 83%

2.21 5 h; 73%

2.22 12 h, 12%[b]

2.23 3 h, 63%

2.24 4 h, 49%

2.27 16 h, 50%

2.25 5 h, 75%

2.26 4 h, 42%[c]; 6 h, 62%[d,e]

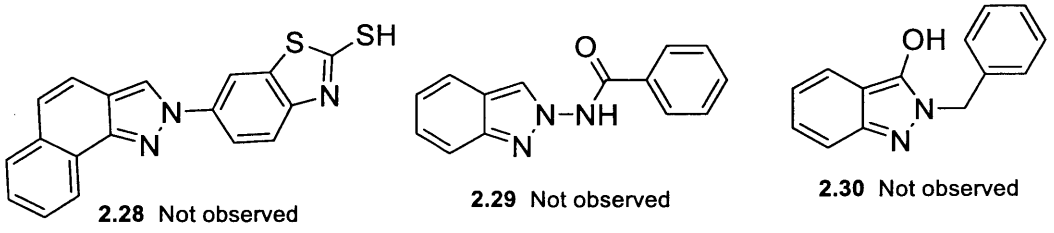

2.28 Not observed

2.29 Not observed

2.30 Not observed

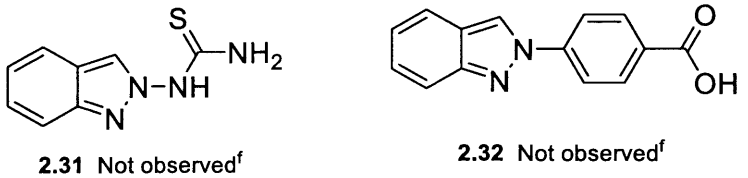

2.31 Not observed[f]

2.32 Not observed[f]

[a] Yields reported for isolated products. [b] 37% of secondary amine observed. [c] Yield obtained along with intact ketone **2.24**. [d] Yield obtained from authentic secondary alcohol substrate. [e] Treatment with TBAF prior to silica gel chromatography. [f] DMF used as the solvent.

2.4 – Summary

We have successfully developed a catalytic protocol to the Cadogan reductive cyclization by using a strained, 4-membered phosphacyclic precatalyst in the presence of an in situ hydrosilane reductant. These 4-membered phosphetanes proved to be more competent in the reductive cyclization than acyclic phosphines and 5-membered phospholanes. Diphenylsilane was found to undergo cyclization following the phosphine oxide reduction, limiting its utility as a reductant, but phenylsilane proved comparable. A range of substrate sterics, electronics, and functional groups were compatible with the cyclization, though it is unclear why some substrates were not. Insight into the mechanism of the transformation is studied in the next chapter.

2.5 – References

[1] Zhao, W.; Yan, P. K.; Radosevich, A. T. "A Phosphetane Catalyzes Deoxygenative Condensation of α-Keto Esters and Carboxylic Acids via P^{III}/P^{V}=O Redox Cycling." *J. Am. Chem. Soc.* **2015**, *137*, 616–619.

[2] Cadogan, J. I. G.; Cameron-Wood, M. Mackie, R. K.; Searle, R. J. G. "The Reactivity of Organophosphorus Compounds. Part XIX. Reduction of Nitro-Compounds by Triethyl Phosphite: A Convenient New Route to Carbazoles, Indoles, Indazoles, Triazoles, and Related Compounds." *J. Chem. Soc.* **1965**, 4831-4837.

[3] Cadogan, J. I. G.; Todd, M. J. "Reduction of Nitro- and Nitroso-Compounds by Tervalent Phosphorus Reagents. Part IV. Mechanistic Aspects of the Reduction of 2,4,6-Trimethyl-2′-Nitrobiphenyl, 2-Nitrobiphenyl, and Nitrobenzene." *J. Chem. Soc. C* **1969**, *20*, 2808-2813.

[4] Genung, N. E.; Wei, L.; Aspnes, G. E. "Regioselective Synthesis of 2*H*-Indazoles Using a Mild, One-Pot Condensation-Cadogan Reductive Cyclization." *Org. Lett.* **2014**, *16*, 3114–3117.

[5] McBride, J. J.; Jungermann, E.; Killheffer, J. V.; Clutter, R. J. "A New Phosphorylation Reaction of Olefins. II. A Novel Synthesis of a Four-Membered Phosphorus-Containing Ring Compound." *J. Org. Chem.* **1962**, *27*, 1833–1836.

[6] Greenwood, N. N.; Earnshaw, A. "Organosilicon compounds and silicones." In *Chemistry of the Elements*; Elsevier: Boston, MA, 1997; pp. 361-366.

[7] Harrowven, D. C.; Guy, I. L. "KF-Silica as a stationary phase for the chromatographic removal of tin residues from organic compounds." *Chem. Commun.* **2004**, 1968-1969.

[8] Nykaza, T. V.; Harrison, T. S.; Ghosh, A.; Putnik, R. A.; Radosevich, A. T. "A Biphilic Phosphetane Catalyzes N-N Bond-Forming Cadogan Heterocyclization via P^{III}/P^{V}=O Redox Cycling." *J. Am. Chem. Soc.* **2017**, *139*, 6839-6842.

Chapter 3

Mechanistic Investigations into Cadogan Cyclization

This chapter details the studies performed in order to assess the mechanism of Cadogan-type cyclizations, in particular with regard to indazolation and carbazolation. These investigations lead to a direct observance of an unprecedented nitrenoid intermediate, previously proposed but not characterized.

3.1 – Background

While the Cadogan reductive cyclization has been known for over 50 years, there are few explicit details regarding each step of the mechanism. As stated before, the Cadogan cyclization involves a double deoxygenation of a nitroarene by a R_3P^{III} reagent, which generates a nitrene or nitrenoid intermediate that undergoes cyclization. The identity of this intermediate, however, has not been explicitly observed, but rather postulated by comparison of similar byproducts when an explicit nitrene is generated from an aryl azide.[1] In addition, the intermediate formed from the first deoxygenation step, a nitrosoarene, while generally not detected, is considered an obligate intermediate for the transformation.[2] In fact, Cadogan has demonstrated that 2-nitrosobiphenyl can be converted to carbazole with triethylphosphite stoichiometrically at room temperature.[3] Our catalytic variant of the Cadogan cyclization also leads to an additional step to consider—the in situ reduction of phosphine oxide. Given these holes in the understanding of the reaction, we saw opportunity to investigate the mechanism more thoroughly.

3.2 – Catalytic Resting State of Phosphorus

To provide information related to both the mechanistic course as well as the speciation of the active phosphorus compounds during catalysis, in situ spectral monitoring of the catalytic reactions was performed for both the synthesis of indazoles[4] and carbazoles.[5]

In the synthesis of indazoles,[4] ^{1}H NMR spectra of a standard catalytic transformation showed the appearance of **3.3** over the course of approximately 1.5 h, with complete consumption of **3.2**. No long-lived intermediates were observed. Simultaneously, ^{31}P NMR spectra show the rapid (ca. 15 min) conversion of phosphetane P^{V}=O (δ 53.2 ppm) **3.1**•[O] to an epimeric mixture of the corresponding P^{III} phosphetane diastereomers (δ 32.4 (major, *anti*); δ 18.9 ppm (minor, *syn*)) in a 3:1 ratio, which persist in solution over the remainder of the reaction. Independent synthesis confirms the identity of these diastereomers.

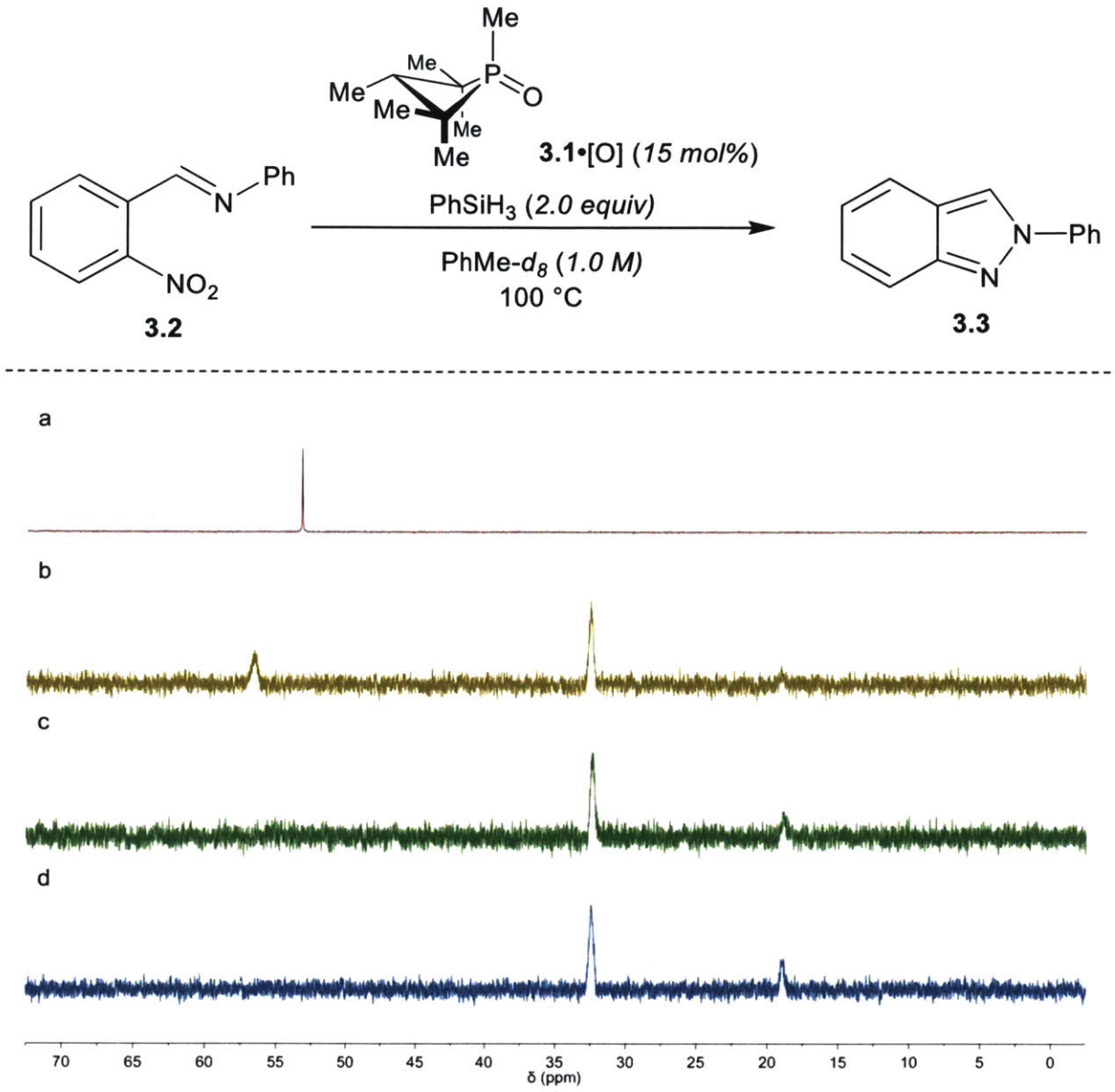

Figure 3.1. Time-stacked in situ ^{31}P NMR spectra of cyclization of imine **3.2** during catalysis. (a) t = 0 min; (b) t = 15 min; (c) t = 30 min; (d) t = 60 min. Chemical shifts (δ): *anti*-**3**•[O], 53.2 ppm; *anti*-**3**, 32.4 ppm; *syn*-**3**, 18.9 ppm.

Complementarily, a similar procedure was adapted for the synthesis of carbazoles.[5] ^{1}H NMR spectra of the standard catalytic transformation showed the consumption of 2-nitrobiphenyl **3.4** over approximately 4 h with concomitant appearance of carbazole **3.5** as the major product. No long-lived intermediates were observed. Simultaneously, ^{31}P NMR spectra show the rapid conversion ($t_{1/2}$ = 5 min) of phosphetane P^{V}=O (δ 53.5 ppm) **3.1**•[O] to an epimeric mixture of the corresponding P^{III} phosphetane diastereomers (δ 32.4 (major, *anti*); δ 18.9 ppm (minor, *syn*)) in a 5:1 ratio, which persist in solution over the remainder of the reaction.

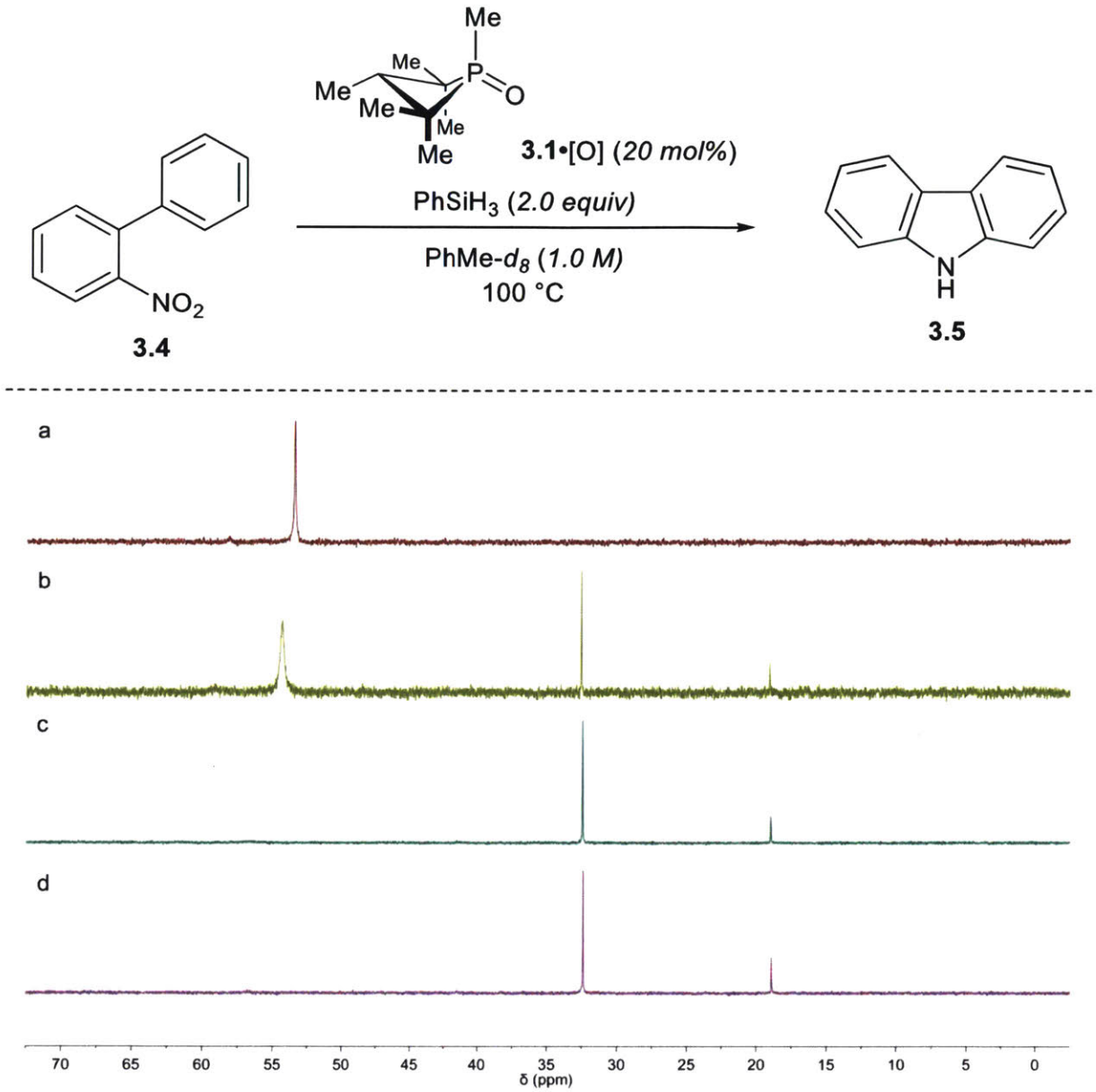

Figure 3.2. Time-stacked in situ ^{31}P NMR spectra of cyclization of nitroarene **3.4** during catalysis. (a) t = 0 min; (b) t = 5 min; (c) t = 30 min; (d) t = 60 min. Chemical shifts (δ): *anti*-**3.1**•[O], 53.5 ppm; *anti*-**3.1**, 32.5 ppm; *syn*-**3.1**, 19.0 ppm.

In accord with literature precedent,[6] the lack of stereospecificity in the phosphetane P^V=O reduction in both cases is thought to be indicative of a pentacoordinate phosphorane intermediate with a sufficient lifetime during hydrosilane-mediated phosphine oxide reduction to permit

pseudorotation, leading to stereochemical scrambling. At this time, however, this intermediate was not directly observed.

From this data, we inferred that the P^{III} phosphetane represents the catalytic resting state of both cyclizations, and as such might be representative of other catalytic Cadogan cyclizations. In addition, the data suggests that the turnover-limiting step involves the initial deoxygenation of the nitro substrate by P^{III} phosphetane, and that phosphetane oxide reduction is more rapid than *O*-atom transfer.

3.3 –Rate Improvement of Phosphetanes

It was previously discussed that 4-membered phosphetanes proved more competent than acyclic phosphines in the Cadogan reductive cyclization. To further quantitate this enhancement, a standard cyclization was performed under stoichiometric pseudo-first order conditions with excess phosphine, comparing constrained phosphetane **3** with acyclic *n*-Bu_3P. The phosphetane **3.1** was markedly faster than that of *n*-Bu_3P ($k_{rel} \approx 8$; Figure 3.3) for the cyclization of imine **3.2**.

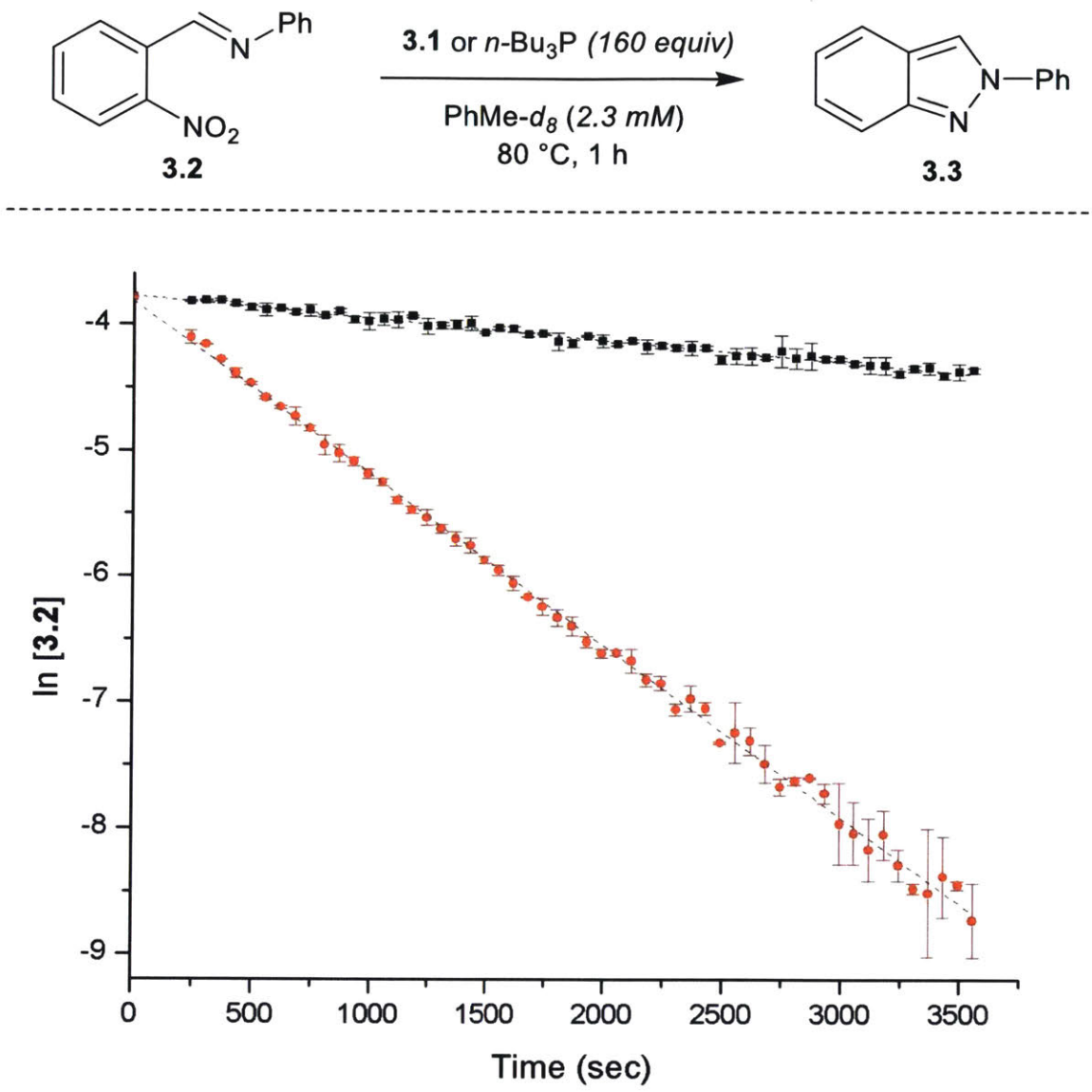

Figure 3.3. Plot of ln [**3.2**] vs time for reaction with excess phosphetane **3.1** (●; equation: $y = -1.37 \cdot 10^{-3} x - 3.82$; $R^2 = 0.9978$) and *n*-Bu_3P (■; equation: $y = -1.74 \cdot 10^{-4} x - 3.77$; $R^2 = 0.9811$), respectively, under pseudo-first order conditions.

The differential reactivity of phosphetane **3.1** and *n*-Bu_3P can be rationalized by DFT calculations.[4] The lowest energy pathway involves a rate-controlling (3+1) cheletropic addition of phosphetane and nitro substrate to give a pentacoordinate azadioxaphosphetane, followed by subsequent retro-(2+2) fragmentation. Further modeling of the transition structure indicates that

the LUMO of the phosphetane resides at a lower energy than the LUMO of the acyclic phosphine, while their HOMOs are of nearly identical energy. Thus, constraining the geometry around phosphorus serves to lower the LUMO energy, which permits a more favorable interaction between the nitro and the phosphorus.

3.4 – Role of Nitroso Intermediate in Cadogan Cyclization

Despite the apparent absence of detectable intermediates during various in situ spectroscopic monitoring, the intermediacy of a nitrosoarene was considered. Due to the difficulty in synthesizing *o*-nitrosobenzaldimines, 2-nitrosobiphenyl **3.6** was considered. Subjection of **3.6** to the catalytic conditions found that carbazole **3.3** was produced in 67% yield. In addition, 2-aminobiphenyl **3.7** was also produced in 11% yield.

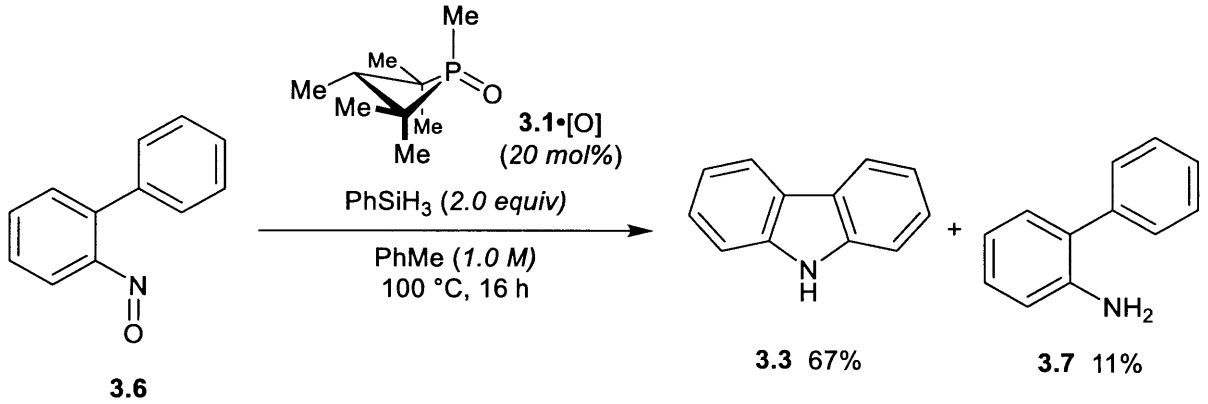

Figure 3.4. Subjection of nitroso **3.6** to catalytic conditions leads to carbazole **3.3** and 2-aminobiphenyl **3.7**.

This data suggests that 2-nitrosobiphenyl is indeed a viable intermediate en route to carbazole under catalytic conditions. The presence of 2-aminobiphenyl **3.7** suggests that there must be competition between alternative pathways at the relatively high concentration of nitroso **3.6** in this experiment. It remains postulated that the nitroso is a viable intermediate towards other Cadogan-type cyclizations, although this has not yet been formally tested.

To further investigate the role of a nitroso intermediate, low temperature VT-NMR studies were performed. A toluene-d_8 solution of phosphetane **3.1** (0.13 M) was frozen in liquid nitrogen, and a cold (−78 °C) solution of 2-nitrosobiphenyl **3.6** (1.3 equiv, 0.11 M) was layered on top via syringe injection. This heterogeneous mixture was inserted into a −60 °C thermostatted NMR probe where it thawed and underwent diffusional mixing over the course of approximately 80 min.

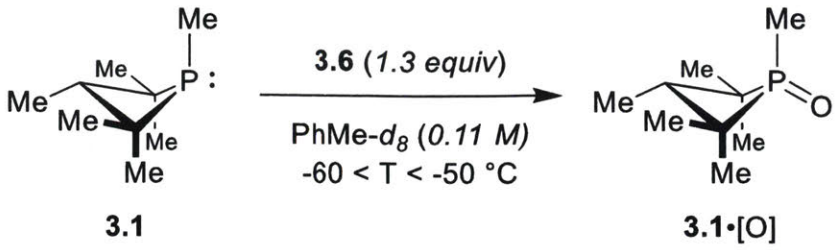

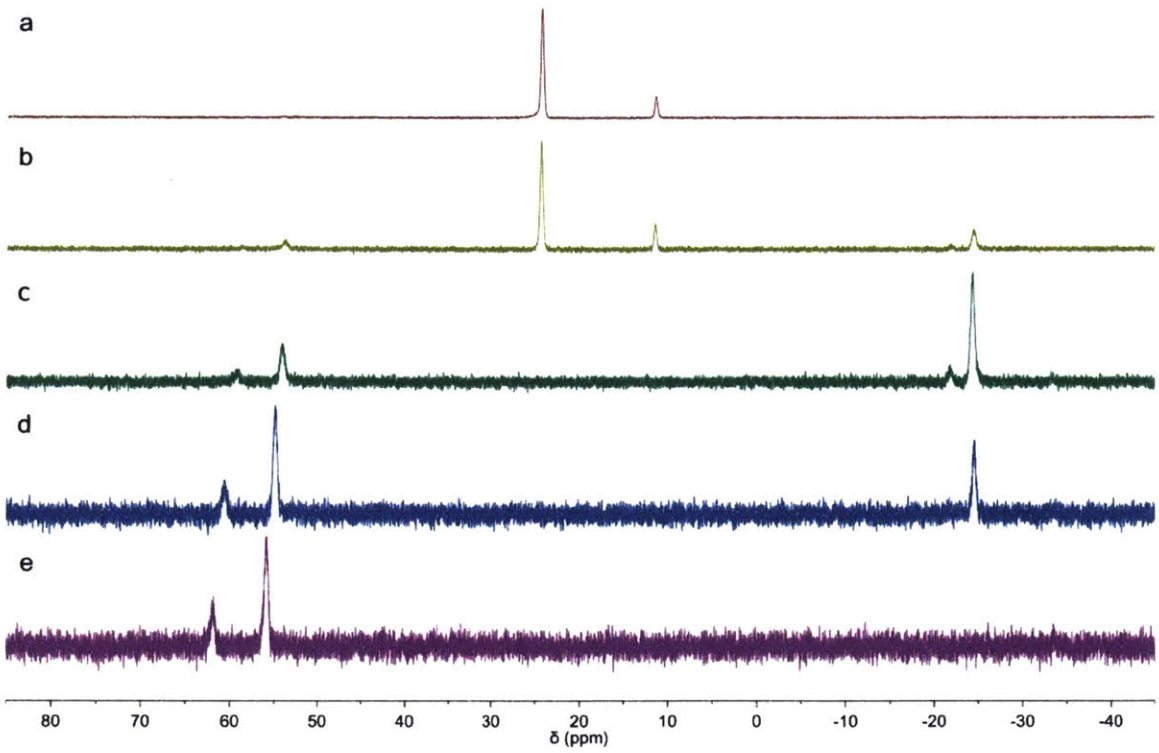

Figure 3.5. Time-stacked in situ ^{31}P NMR spectra of cyclization of nitrosoarene **3.6** by phosphetane **3.1**. (a) t = 0 min; (b) t = 120 min; (c) t = 200 min; (d) t = 300 min; (e) t = 390 min. Chemical shifts (δ): *anti*-**3.1**•[O], 54.1 ppm; *syn*-**3.1**•[O], 61.8 ppm; *anti*-**3.1**, 24.2 ppm; *syn*-**3.1**, 11.3 ppm; *syn*-**3.8**, −21.8 ppm; *anti*-**3.8**, −24.4 ppm.

^{31}P NMR spectra, recorded subsequently at 10 min intervals, showed the initial consumption of phosphetane **3.1** (δ 24.2 *major*, 11.3 *minor* ppm) and conversion to two new resonances with an upfield chemical shift (δ −24.4 *major*, −21.8 *minor* ppm). Over time, these resonances diminished concomitant with the growth of signals corresponding to the phosphetane oxide **3.1**•[O] (δ 24.2

major, 11.3 *minor* ppm). Upon termination of the experiment, an aliquot subjected to GC/MS analysis showed the presence of carbazole **3.3** and phosphetane oxide **3.1**•[O] as the only observable products. The observed ^{31}P NMR resonances at δ −24.4 and −21.8 ppm are postulated to correspond to a metastable intermediate **3.8** towards the production of carbazole from reaction between the diastereomeric phosphetanes **3.1** and 2-nitrosobiphenyl **3.6**.

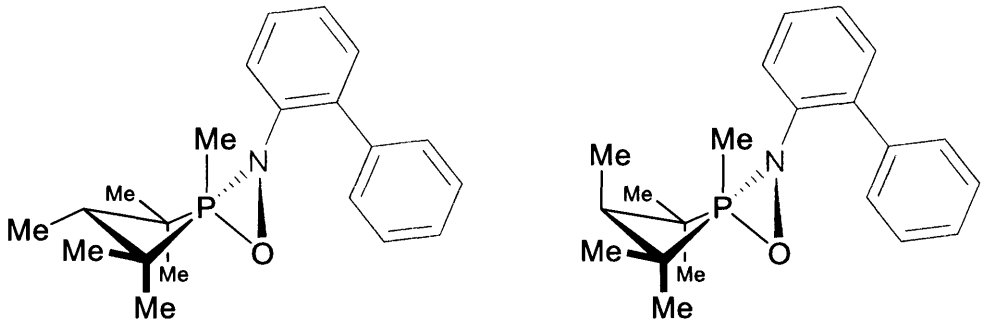

3.8 (8:1 *dr*)

δ -24.4 ppm *major* δ -21.8 ppm *minor*

Figure 3.6. Postulated intermediate diastereomers in reaction of nitroso **3.6** and phosphetane **3.1**.

A similar procedure was followed for the reaction between phosphetane **3.1** and isotopically labeled 2(^{15}N)--nitrosobiphenyl **3.6**. The new resonances at δ −24.4 ppm and δ −21.8 ppm exhibited ^{31}P–^{15}N scalar couplings with J = 40.8 Hz and J = 39.5 Hz respectively. In the ^{15}N NMR spectrum, complementary doublets centered at δ 239 ppm (*major*, J = 40.6 Hz) and δ 241 ppm (*minor*, J = 39.6 Hz) were simultaneously observed.

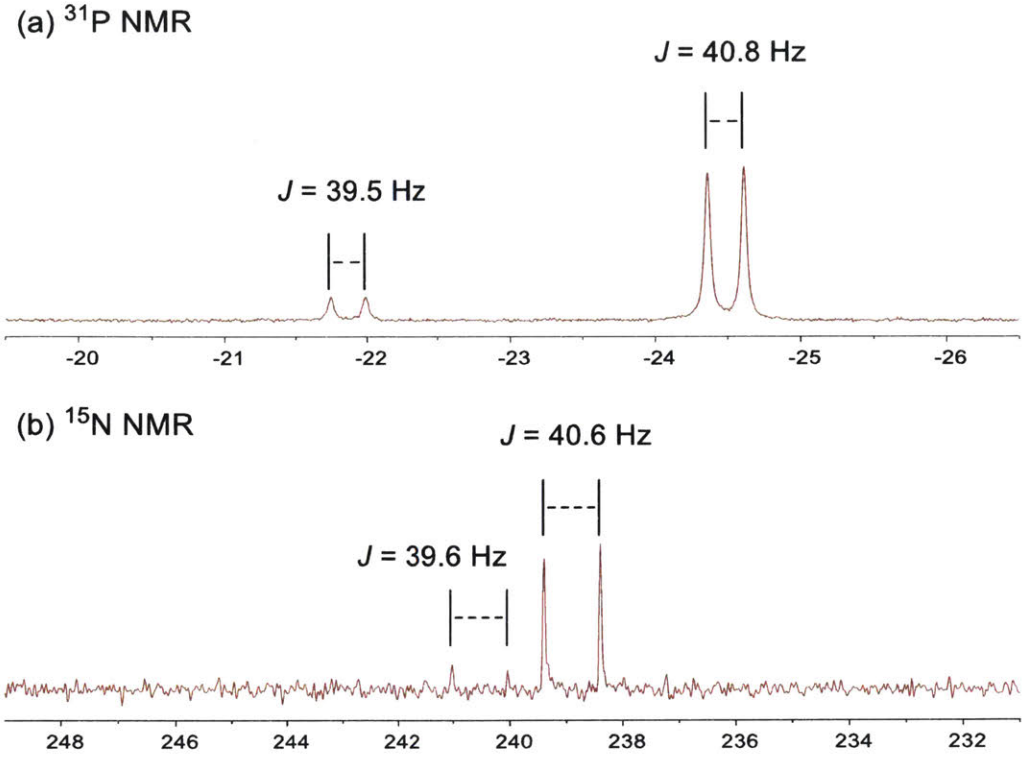

Figure 3.7. Heteronuclear NMR spectra of reaction of phosphetane 3.1 and 2-(^{15}N)nitrosobiphenyl **3.6** (–60 °C < T < –50 °C, toluene-d_8). Units are ppm relative to 85% H_3PO_4 (^{31}P, δ = 0.0 ppm) and liquid NH_3 (^{15}N, δ = 0.0 ppm). (a) Annotated ^{31}P NMR spectrum. (b) Annotated ^{15}N NMR spectrum.

The magnitude of this coupling constant falls within the expected range for direct one-bond $^1J_{P-N}$ coupling,[7,8] and the upfield ^{31}P chemical shift is most consistent with a pentacoordinate phosphorane.[9,10] Thus, we postulated that the P^V oxazaphosphirane structures **3.8** give rise to the observed ^{31}P NMR resonances. This type of structure, the oxazaphosphirane, has not been previously directly observed to our knowledge, although it has been postulated as a potential nitrenoid intermediate by both Cadogan[1] and Sundberg.[11]

3.5 – Summary

The mechanism of the catalytic Cadogan reductive cyclization has been expanded. The resting state of phosphorus was determined to be the P^{III} phosphetane by analysis by ^{31}P NMR spectroscopy. The strained phosphetane **3.1** appears to react approximately 8 times faster than the acyclic *n*-Bu_3P, and this enhancement arises from the lowering of the LUMO of the phosphetane. A nitrosoarene, presumed to be an intermediate in the overall Cadogan cyclization, was found to successfully undergo reaction to the corresponding carbazole. Low temperature, heteronuclear NMR spectroscopy has also enabled us to observe a unique oxazaphosphirane intermediate over the course of cyclization. The chemistry of this intermediate may assist in our understanding of other phosphorus-mediated deoxygenations.

3.6 – References

[1] Cadogan, J. I. G.; Todd, M. J. "Reduction of Nitro- and Nitroso-Compounds by Tervalent Phosphorus Reagents. Part IV. Mechanistic Aspects of the Reduction of 2,4,6-Trimethyl-2′-Nitrobiphenyl, 2-Nitrobiphenyl, and Nitrobenzene." *J. Chem. Soc. C* **1969**, 2808–2813.

[2] For theoretical studies and discussion of related downstream events, see: Davies, I. W.; Guner, V. A.; Houk, K. N. "Theoretical Evidence for Oxygenated Intermediates in the Reductive Cyclization of Nitrobenzenes." *Org. Lett.* **2004**, *6*, 743–746.

[3] Bunyan, P. J.; Cadogan, J. I. G. "Reactivity of organophosphorus compounds. XIV. Deoxygenation of aromatic C-nitroso compounds by triethyl phosphite and triphenylphosphine: a new cyclization reaction." *J. Chem. Soc.* **1963**, 42-49.

[4] Nykaza, T. V.; Harrison, T. S.; Ghosh, A.; Putnik, R. A.; Radosevich, A. T. "A Biphilic Phosphetane Catalyzes N-N Bond-Forming Cadogan Heterocyclization via P^{III}/P^{V}=O Redox Cycling." *J. Am. Chem. Soc.* **2017**, *139*, 6839-6842.

[5] Nykaza, T. V.; Ramirez, A.; Harrison, T. S.; Luzung, M. R.; Radosevich, A. T. "Biphilic Organophosphorus-Catalyzed Intramolecular C_{sp2}-H Amination: Evidence for a Nitrenoid in Catalytic Cadogan Cyclizations." *J. Am. Chem. Soc.* **2018,** DOI: 10.1021/jacs.7b13803.

[6] (a) Mislow, K. "Role of pseudorotation in the stereochemistry of nucleophilic displacement reactions." *Acc. Chem. Res.* **1970**, *3*, 321-331. (b) Marinetti, A.; Carmichael, D. "Synthesis and Properties of Phosphetanes." *Chem. Rev.* **2002**, *102*, 201-230.

[7] Gombler, W.; Kinas, R. W.; Stec, W. J. "$^{31}P-^{15}N$ Coupling Constants and $^{15}N/^{14}N$ Isotope Effects on ^{31}P NMR Chemical Shifts of 2-Phenylamino-2-oxo(-thioxo, -selenoxo)- 4-methyl-1,3,2-dioxaphosphorinanes and Related Compounds." *Z. Naturforsch., B: Anorg. Chem., Org. Chem.* **1983**, *38*, 815–818.

[8] Viljanen, T.; Klika, K. D.; Fülöp, F.; Pihlaja, K. "Coupling constants ^1J (^{15}N,^{31}P) as a probe for the conformational equilibria of 2-amino-substituted 1,3,2λ^5-oxazaphosphinan-2-ones." *J. Chem. Soc., Perkin Trans. 2* **1998**, 1479–1482.

[9] Kojima, S.; Sugino, M.; Matsukawa, S.; Nakamoto, M.; Akiba, K. "First Isolation and Characterization of an Anti-Apicophilic Spirophosphorane Bearing an Oxaphosphetane Ring: A Model for the Possible Reactive Intermediate in the Wittig Reaction." *J. Am. Chem. Soc.* **2002**, *124*, 7674–7675.

[10] Reichl, K. D.; Dunn, N. L.; Fastuca, N. J.; Radosevich, A. T. "Biphilic Organophosphorus Catalysis: Regioselective Reductive Transposition of Allylic Bromides via P^{III}/P^{V} Redox Cycling." *J. Am. Chem. Soc.* **2015**, *137*, 5292–5295.

[11] Sundberg, R. J.; Lang, C.-C. "Structure-Reactivity Studies of Deoxygenation Reactions." *J. Org. Chem.* **1971**, *36*, 300–304.

Chapter 4

Toward Catalytic Nitro Reduction via P^{III}/P^{V}=O Redox Cycling

This chapter describes the approaches and initial results toward developing this phosphorus-mediated deoxygenation towards other nitro-based transformations, specifically reduction to the aniline.

4.1 – Background

In our investigations of 2-nitrosobiphenyl as a potential intermediate, as noted in Chapter 3, 2-aminobiphenyl was observed as a byproduct. We sought to investigate the origin of this reduced product.

The reduction of nitro compounds to their respective amines has been a continuing source of scientific study since the first report by Béchamp over 150 years ago.[1] Due to the numerous utilities that amines possess in the production of pharmaceuticals, materials, and dyes, a suite of synthetic options to obtain amines is of great interest. In synthetic chemistry, nitro compounds can act as Michael donors[2] and acceptors,[3] electron-deficient arene directors, and carbanion nucleophiles;[4] as such, they can be used to access different amine derivatives that may be otherwise difficult to prepare, such as chiral amines.

Due to their great interest, numerous methods of reducing nitro groups have previously been developed,[5] such as hydrogenation, transfer hydrogenation, hydride-transfer, dissolving metal, and metal-free reductions (Figure 4.1). In hydrogenation,[6] H_2 gas is used in conjunction with a metal such as palladium or nickel to facilitate reduction of the nitro group. However, this method can be unselective towards nitro groups and may result in reductions occurring at olefins, imines, haloarenes, and other reducible functionalities; incomplete hydrogenation of the nitro is also possible, resulting in hydroxylamines.[7] Transfer hydrogenation shares similarities, but do not

explicitly utilize H_2 gas; instead, compounds like HCO_2NH_4,[8] *i*-PrOH,[9] and H_2NNH_2[10] are used as hydrogen sources. In hydride-transfer reactions, reagents such as aluminum hydrides,[11] borohydrides,[12] and organosilanes(-oxanes)[13] are used in conjunction with a metal catalyst to effect reduction. Some of their limitations have been described in Chapter 1, albeit focusing on their utility as phosphine oxide reductants; nevertheless issues with regards to chemoselectivity and reactivity are applicable. Dissolving metal reduction typically involves using a low oxidation state metal (e.g. Al,[14] Fe,[15] Zn,[16] etc.) with a proton source (e.g. water, AcOH, NH_4Cl, etc.) to facilitate reduction. Metal-free reductions have also been studied, leading to the use of sodium dithionite[17] and trichlorosilane in the presence of tertiary amines,[18] among other reagents.

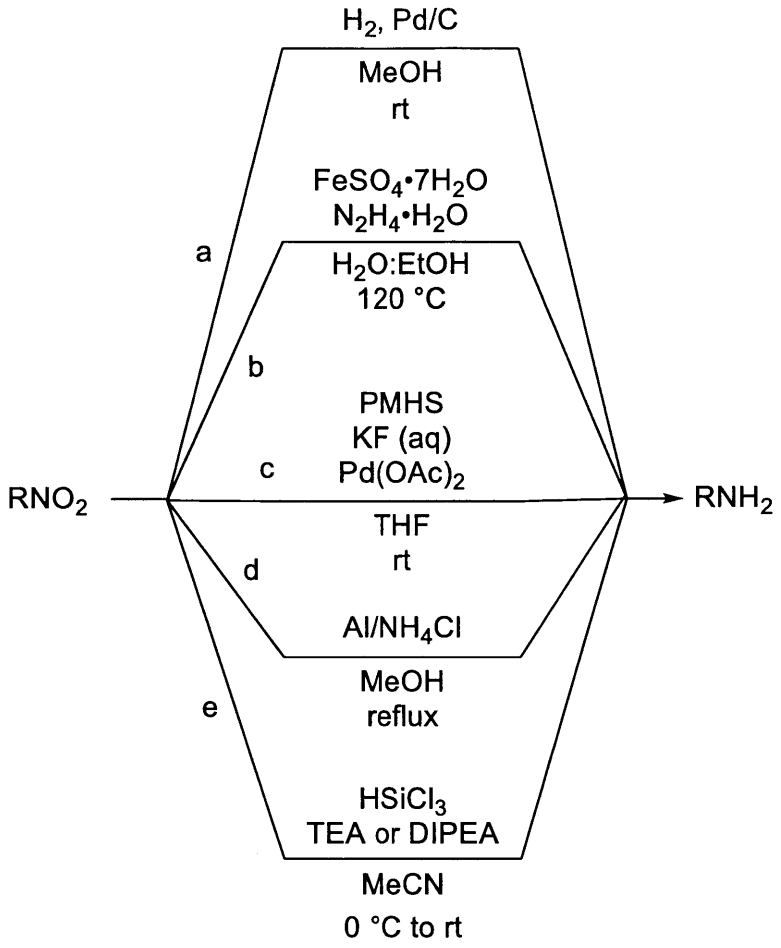

Figure 4.1. Examples of nitro reduction. (a) Hydrogenation. (b) Transfer hydrogenation. (c) Hydride-transfer. (d) Dissolving metal reduction. (e) Metal-free reduction.

Considering these precedents, nitro reduction via $P^{III}/P^{V}=O$ redox cycling presents an attractive avenue for study, potentially providing a metal-free, chemoselective, scalable means to synthesize amines. In addition, given the likelihood of the oxazaphosphirane intermediate described in Chapter 3 also playing a role nitro reduction by $P^{III}/P^{V}=O$ redox cycling, this also represents a useful means to determine conditions that may yield either the cyclized or the reduced product, enabling more synthetic utility, as well as the beginnings of further study into the reactivity of this previously unobserved structure.

4.2 – Initial Optimization

Previous optimization investigations of carbazole synthesis suggested that nitro substrates may be reduced by using methyl phosphetane *P*-oxide **4.1**•[O], phenylsilane, and 2,2,2-trifluoroethanol. Considering the previous successes of this phosphetane/silane combination, we sought to determine the generality of this observation as a method for nitro reduction. Experimental investigations began with a test of solvent dependence on the reduction of *p*-nitrotoluene (**4.2**, Table 4.1). After reaction of **4.2** with 15 mol % of **4.1**•[O] and phenylsilane for 22 h, ^{1}H NMR spectroscopy indicated minor reduction to the amine in *n*-butanol and toluene (entries 2 and 4), but none in other acidic and alcoholic media (entries 3, 5, and 6). In fact, the phosphetane **4.1**•[O] was not observed at all in acetic acid (entry 3) or in TFE at 70 °C (entry 1).

Table 4.1. Solvent screen for reduction of *p*-nitrotoluene.[a]

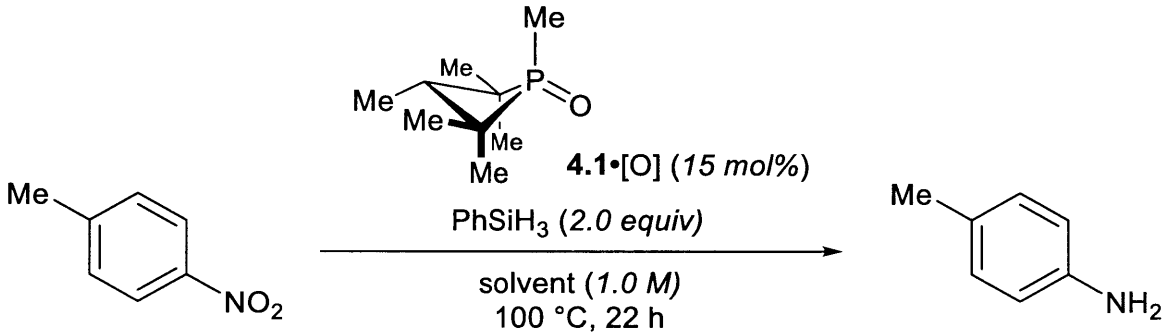

4.2 **4.3**

Entry	Solvent	Conversion (%)
1[b]	TFE	0[c]
2	*n*-BuOH	3
3	AcOH	0[c]
4	PhMe	4
5	Ethylene glycol	0
6	Glycerol	0

[a] Conversion determined by relative ^{1}H NMR integration (integration of amine / integration of amine and nitro). [b] Reaction performed at 70 °C. [c] Reduction of phosphetane *P*-oxide **4.1**•[O] not observed in absence of substrate.

More electronically deficient substrates were then studied. Reduction of *p*-chloronitrobenzene **4.4** was attempted in TFE and *n*-BuOH but only trace amounts of the anticipated aniline **4.5** was formed (Table 4.2). By contrast, *p*-dinitrobenzene **4.6** was observed to undergo a greater degree of conversion when subjected to reaction with phosphetane **4.1**•[O] and phenylsilane (Table 4.3), and alteration to the catalyst and silane identity increased further the amount of observed aniline (Table 4.4).

Table 4.2. Experiments involving electronically deficient *p*-chloronitrobenzene..[a]

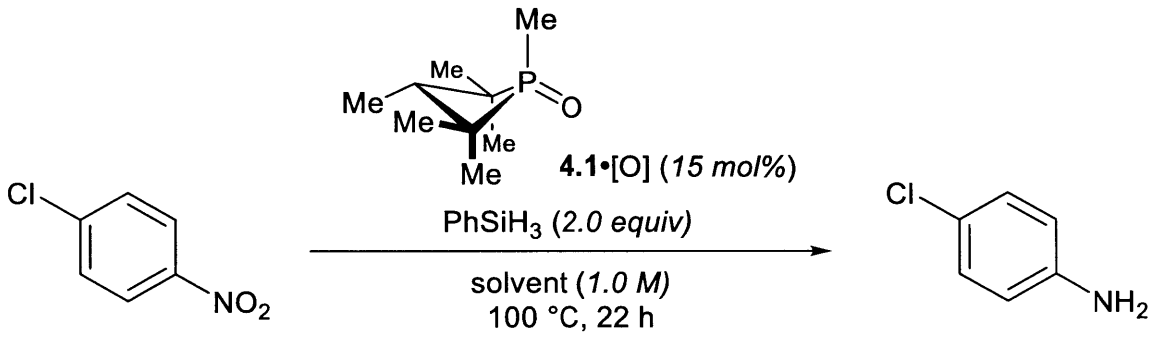

4.4 **4.5**

Entry	Solvent	Conversion (%)
1	TFE	1
2	*n*-BuOH	Trace[b]

[a] Conversion determined by relative ^{1}H NMR integration (integration of amine / integration of amine and nitro). [b] Trace aniline observed, but other signals prevent integration.

Table 4.3. Optimization experiments involving *p*-dinitrobenzene without internal standard.[a]

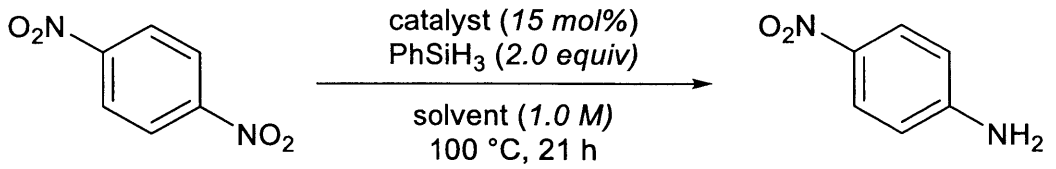

4.6 **4.7**

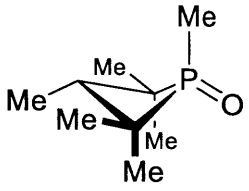

4.1•[O]

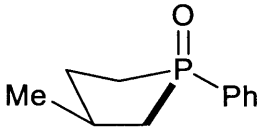

4.8•[O]

Entry	Catalyst	Solvent	Conversion (%)
1	**4.1**•[O]	TFE	2
2	**4.1**•[O]	n-BuOH	10
3	**4.8**•[O]	TFE	42
4	**4.8**•[O]	n-BuOH	19

[a] Conversion determined by relative ^{1}H NMR integration (integration of amine / integration of amine and nitro).

Table 4.4. Optimization experiments involving *p*-dinitrobenzene with internal standard.[a]

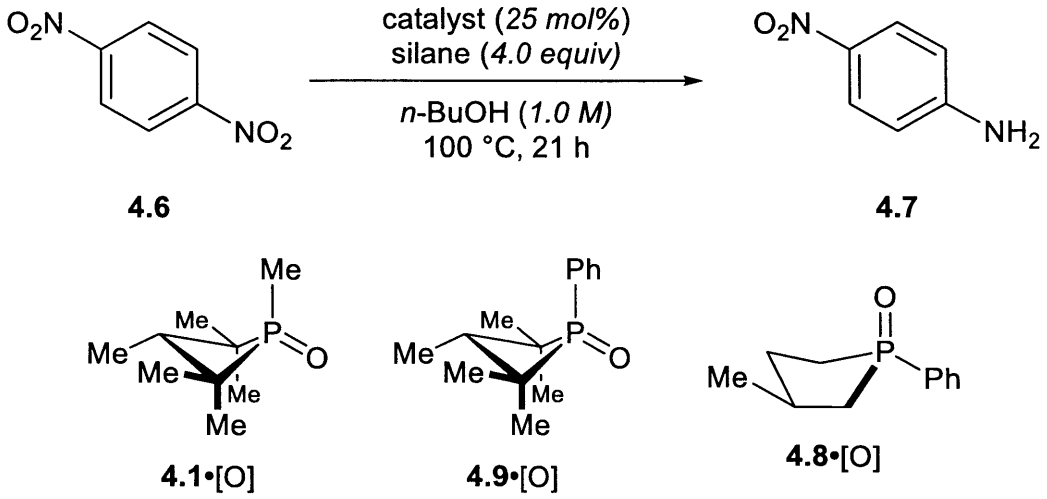

Entry	Catalyst	Silane	Conversion (%)	Yield (%)
1	**4.1**•[O]	$PhSiH_3$	97	36
2	**4.1**•[O]	$(MeO)_2MeSiH$	56	7
3	**4.1**•[O]	$(EtO)_2MeSiH$	64	9
4	**4.9**•[O]	$PhSiH_3$	59	28
5[b]	**4.8**•[O]	$PhSiH_3$	78	51

[a] Conversion and yield determined by ^1H NMR with respect to 1,3,5-trimethoxybenzene internal standard. [b] TFE used as solvent.

However, in most cases, observed conversion substantially exceeded the product yield. This discrepancy with respect to mass balance appears to be a general phenomenon, although its origin remains unknown and its magnitude varies with substrate. For instance, attempted reduction of *p*-nitrobenzonitrile leads to conversions that are in excess of the observed yield of aniline (Table 4.5), but to a lesser extent. In this latter case, an additional species was observed by GCMS with $m/z = 251$ (**4.13**) whose identity remains under investigation.

Table 4.5. Optimization experiments involving *p*-nitrobenzonitrile.

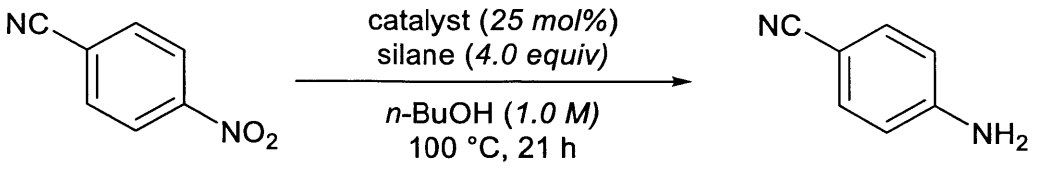

4.10 **4.11**

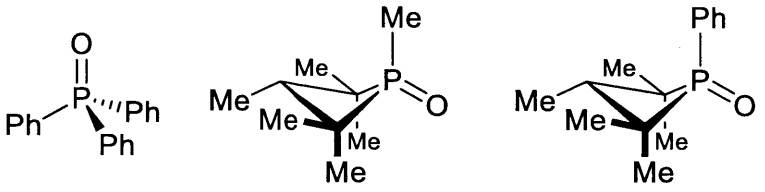

4.12•[O] **4.1•[O]** **4.9•[O]**

Entry	Catalyst	NMR Conversion (%) [a]	NMR Yield (%) [a]	GCMS Conversion (%) [b]	GCMS Yield (%) [b]	Unknown Yield (%) [b,c]
1	**4.12•[O]**	13	Trace	79[c]	Trace[c]	79
2	**4.1•[O]**	97	19	87	10	83
3	**4.9•[O]**	63	31	70	34	64

[a] Conversion and yield determined with respect to 1,3,5-trimethoxybenzene internal standard. [b] Conversion and yield determined with respect to dodecane internal standard. [c] Yield determined by relative GC integration (area of interest / sum of unknown, nitro, aniline areas).

Control experiments to elucidate the origin of this unknown product were performed (Table 4.6). Having noticed in previous GCMS traces a species that may contain a long alkyl chain, in the absence of the dodecane internal standard a substantial amount of the unknown product was observed. Subjection of the desired reduced product **4.11** to the reaction conditions did result in production of this unknown. Switching the silane to diphenylsilane retained the conversion (99%), and in fact did not lead to the unknown product, but resulted in low yields of the desired aniline derivative (24%). Switching the solvent from *n*-BuOH to toluene, however, resulted in 99% conversion of substrate and 86% yield of the aniline product, with no presence of the unknown product.

Table 4.6. Control experiments to determine source and identity of unknown product. [a]

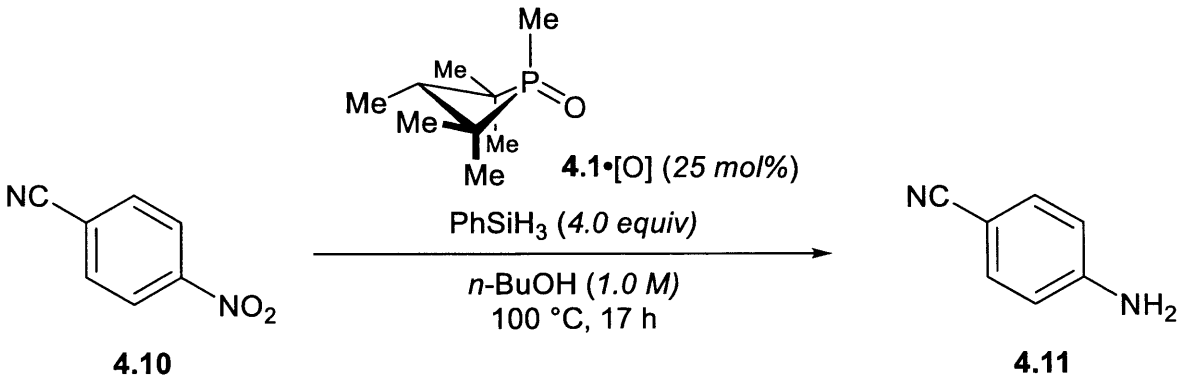

4.10 **4.11**

Entry	Variation	Conversion (%)	Yield of **4.11** (%)	Yield of unknown **4.13** (%)[b]
1	No internal standard	87[b]	6[b]	81
2	**4.11** as substrate	n/a	43[b]	57
3	Use of Ph_2SiH_2 as reductant	99	24	0
4	Use of PhMe as solvent	99	86	0
5	Use of PhMe as solvent, 2h	96	74	0

[a] Conversion and yields determined by GC with respect to dodecane internal standard.
[b] Determined by relative GC integration (area of interest / sum of unknown, nitro, aniline areas).

The reduction of *p*-nitrobenzonitrile was then examined in toluene with other catalysts to determine both the dependence of the unknown on *n*-BuOH and the effectiveness of the catalysts (Table 4.7). As expected, using triphenylphosphine oxide resulted in only trace conversion. *P*-phenyl phosphetane **4.9**•[O] enabled moderate conversion, but only a fraction of the desired aniline **4.11** was observed. Interestingly, phospholane **4.8**•[O] did completely consume the nitro **4.10**, but only 11% of the aniline was observed.

Table 4.7. Optimization in toluene. [a]

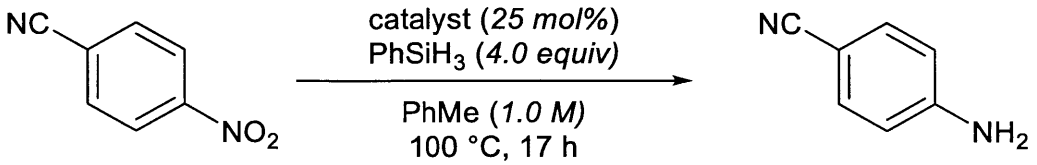

4.10 **4.11**

Entry	Catalyst	Conversion (%)	Yield (%)
1	**4.12**•[O]	1[b]	1[b]
2	**4.9**•[O]	68	19
3	**4.8**•[O]	100	11

[a] Conversion and yields determined by GC with respect to dodecane internal standard.
[b] Determined by relative GC integration (area of interest / sum of unknown, nitro, aniline areas).

4.3 –Future Work

The optimization experiments above provide an initial framework within which to study more thoroughly the phosphorus-catalyzed reduction of nitroarenes. Two immediate avenues appear prudent. The first would be to minimize the loading of both the catalyst and silane, and the second would be to determine how to reduce nitroarenes more electronically-rich than *p*-cyanonitrobenzene. Of the two aims, broadening the scope of nitroarenes is the more challenging but offers the greatest opportunity to better understand catalyst design principles.

Given our previous phosphine oxide reduction studies, the successful catalyst/silane combinations could each be tested against a standard reduction, such as reducing *p*-nitrotoluene. However, this would not necessarily lead us to a system where nitro reduction is most efficient, especially considering that the use of phosphetane **4.1**•[O] and $PhSiH_3$ already appears to give the highest yield, but not the highest conversion. It is presently unknown, when using phospholane **4.8**•[O], where the rest of the material is ending up, but investigating this discrepancy will help better understand how nitro reduction differs mechanistically from Cadogan cyclization. This may

also help determine why the 5-membered phosphacycle **4.8**•[O] converts the nitroarene so thoroughly. Previous stoichiometric studies should be consulted to consider other reaction pathways, such as the formation of azepines, which could account for this discrepancy.

In addition, our previous experimentation with nitrosoarene-phosphine reactions at low temperature indicates the presence of an oxazaphosphirane intermediate. Presumably, from the principle of microscopic reversibility, this intermediate is also generated in the reduction of nitroarenes and therefore represents a point at which either nitro reduction or Cadogan cyclization can occur. Since the oxazaphosphirane moiety is not previously reported in the literature, it is not clear under what conditions that reduction or cyclization predominates, but previous experiments seem to indicate that the hydrosilane is responsible for producing the hydrogen involved in nitro reduction. Reaction with deuterated hydrosilane could determine whether this is the case. The lack of experimental precedent of oxazaphosphiranes also presents a wealth of opportunity for new discoveries, despite their apparent thermal instability.

4.4 – Summary and Outlook

We have successfully adapted a catalytic protocol to the Cadogan reductive cyclization that utilizes a strained phosphacycle in the presence of an in situ reductant. Our work has led to a richer understanding of the mechanism of this reaction, in particular the oxazaphosphirane intermediate which has not previously been observed. This intermediate represents a potential branching point between different reactions possible for nitroarenes. Further study of both this intermediate and other nitro deoxygenations will lead to more accurate phosphorus catalyst design principles for applying P^{III}/P^{V}=O redox cycling to a wider variety of chemical systems.

4.5 – References

[1] Béchamp, A. "De l'action des protosels de fer sur la nitronaphtaline et la nitrobenzine. nouvelle méthode de formation des bases organiques artificielles de Zinin." *Ann. Chim. Phys.* **1854**, *42*, 186-196.

[2] Ballini, R.; Bosica, G.; Fiorini, D.; Palmieri, A.; Petrini, M. "Conjugate Additions of Nitroalkanes to Electron-Poor Alkenes: Recent Results." *Chem. Rev.* **2005**, *105*, 933–972.

[3] Li, X.; Peng, F.; Zhou, M.; Mo, M.; Zhao, R.; Shao, Z. "Catalytic Asymmetric Synthesis of 1,3-Enyne Scaffolds: Design and Synthesis of Conjugated Nitro Dienynes as Novel Michael Acceptors and Development of a New Synthetic Methodology." *Chem. Commun.* **2014**, *50*, 1745–1747.

[4] Dauzonne, D.; Royer, R. "A Convenient Route to Substituted Phenylalanines." *Synthesis* **1987**, *1987*, 399–401.

[5] Orlandi, M.; Brenna, D.; Harms, R.; Jost, S.; Benaglia, M. "Recent Developments in the Reduction of Aromatic and Aliphatic Nitro Compounds to Amines." *Org. Process Res. Dev.* **2016**. DOI: 10.1021/acs.oprd.6b00205.

[6] Blaser, H. U.; Siegrist, U.; Steiner, H.; Studer, M. "Aromatic Nitro Compounds." In *Fine Chemicals through Heterogeneous Catalysis*; Sheldon, R. A., van Bekkum, H., Eds.; Wiley-VCH: New York, NY, 2001; pp 389–406.

[7] Gallagher, W. P.; Marlatt, M.; Livingston, R.; Kiau, S.; Muslehiddinoglu, J. "The Development of a Scalable, Chemoselective Nitro Reduction." *Org. Process Res. Dev.* **2012**, *16*, 1665–1668.

[8] Lou, X.-B.; He, L.; Qian, Y.; Liu, Y.-M.; Cao, Y.; Fan, K.-N. "Highly Chemo- and Regioselective Transfer Reduction of Aromatic Nitro Compounds Using Ammonium Formate Catalyzed by Supported Gold Nanoparticles." *Adv. Synth. Catal.* **2011**, *353*, 281–286.

[9] Gawande, M. B.; Guo, H.; Rathi, A. K.; Branco, P. S.; Chen, Y.; Varma, R. S.; Peng, D.-L. "First Application of Core-Shell Ag@Ni Magnetic Nanocatalyst for Transfer Hydrogenation Reactions of Aromatic Nitro and Carbonyl Compounds." *RSC Adv.* **2012**, *3*, 1050–1054.

[10] Sharma, U.; Verma, P. K.; Kumar, N.; Kumar, V.; Bala, M.; Singh, B. "Phosphane-Free Green Protocol for Selective Nitro Reduction with an Iron-Based Catalyst." *Chem. Eur. J.* **2011**, *17*, 5903–5907.

[11] Nystrom, R. F.; Brown, W. G. "Reduction of Organic Compounds by Lithium Aluminum Hydride. III. Halides, Quinones, Miscellaneous Nitrogen Compounds." *J. Am. Chem. Soc.* **1948**, *70*, 3738–3740.

[12] Periasamy, M.; Thirumalaikumar, M. "Methods of Enhancement of Reactivity and Selectivity of Sodium Borohydride for Applications in Organic Synthesis." *J. Organomet. Chem.* **2000**, *609*, 137–151.

[13] Rahaim, R. J.; Maleczka, R. E. "Pd-Catalyzed Silicon Hydride Reductions of Aromatic and Aliphatic Nitro Groups." *Org. Lett.* **2005**, *7*, 5087–5090.

[14] Nagaraja, D.; Pasha, M. A. "Reduction of Aryl Nitro Compounds with Aluminium/NH_4Cl: Effect of Ultrasound on the Rate of the Reaction." *Tetrahedron Lett.* **1999**, *40*, 7855–7856.

[15] Chandrappa, S.; Vinaya, K.; Ramakrishnappa, T.; Rangappa, K. S. "An Efficient Method for Aryl Nitro Reduction and Cleavage of Azo Compounds Using Iron Powder/Calcium Chloride." *Synlett* **2010**, 3019–3022.

[16] Desai, D. G.; Swami, S. S.; Hapase, S. B. "Rapid and Inexpensive Method for Reduction of Nitroarenes to Anilines." *Synth. Commun.* **1999**, *29*, 1033–1036.

[17] Park, K. K.; Oh, C. H.; Joung, W. K. "Sodium Dithionite Reduction of Nitroarenes Using Viologen as an Electron Phase-Transfer Catalyst." *Tetrahedron Lett* **1993**, *34*, 7445–7446.

[18] Orlandi, M.; Tosi, F.; Bonsignore, M.; Benaglia, M. "Metal-Free Reduction of Aromatic and Aliphatic Nitro Compounds to Amines: A $HSiCl_3$-Mediated Reaction of Wide General Applicability." *Org. Lett.* **2015**, *17*, 3941–3943.

Chapter 5

Experimental Section

I. General Notes

All reactions were carried out using dry glassware and standard Schlenk techniques (when applicable) unless otherwise noted. All reagents were purchased from commercial vendors (Sigma-Aldrich, Alfa Aesar, Acros, TCI, or Oakwood Chemical) and used as received unless otherwise noted. All solvents were purified and collected under argon using a Glass Contour Solvent Purification System. Column chromatography was performed using 230-400 mesh silica gel (Silicycle) as the stationary phase unless otherwise noted. ^{1}H, ^{13}C, ^{19}F and ^{31}P NMR spectra were recorded with Varian Mercury 300, Bruker AV-360, DRX-400, or AVANCE-400 spectrometers and processed using MestReNova software. ^{1}H NMR chemical shifts are given in ppm with respect to the residual $CDCl_3$ peak (δ 7.26 ppm), residual DMSO-d_6 (δ 2.50 ppm), residual acetonitrile-d_3 (δ 1.94 ppm), or an internal TMS standard (δ 0.00 ppm), $^{13}C\{^{1}H\}$ NMR shifts are given in ppm with respect to $CDCl_3$ (δ 77.16 ppm), DMSO-d_6 (δ 39.52 ppm), acetonitrile-d_3 (δ 1.32, 118.26 ppm). ^{31}P shifts are given in ppm with respect to 85% H_3PO_4 (δ 0.0 ppm), and ^{15}N shifts are given in ppm with respect to liquid NH_3 (δ 0.00 ppm). Coupling constants are reported as *J*-values in Hz. High resolution DART mass spectra were obtained from the Department of Chemistry Instrumentation Facility (DCIF) at MIT using a Bruker Daltonics APEXIV 4.7 Tesla Fourier Transform Ion Cyclotron Resonance Mass Spectrometer. High resolution EI and ESI mass spectra were obtained from the Mass Spectrometry Laboratory at the School of Chemical Sciences, University of Illinois at Urbana-Champaign. Gas chromatography analyses were performed on either an Agilent 7890A gas chromatograph fitted with a J&W DB-1 column (10 m, 0.1 I.D.) or a Shimadzu GC-2010 gas chromatograph fitted with a SHRXI-5MS

column (30 m, 0.25 I.D.). Quantitative GC measurements were calibrated with samples of authentic analytes. HPLC analysis was conducted on an Agilent 1200 series chromatograph with Chiralcel AD-H columns at ambient temperature. Additional high-resolution mass spectra were collected at Bristol-Myers Squibb on an Agilent 6200 series TOF/6500 series Q-TOF B.06.01 (B6172 SP1). All yields reported are isolated yields unless stated otherwise.

II. Preparation of Phosphorus Compounds

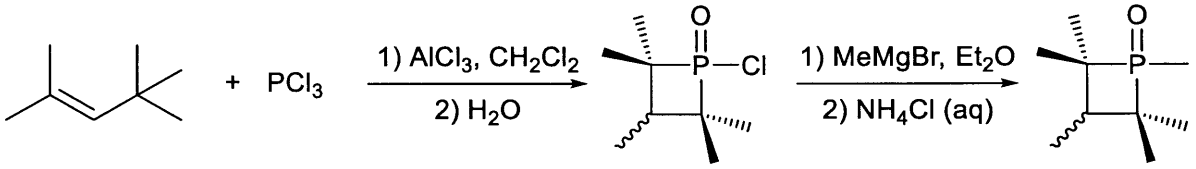

5.1

Figure 5.1. Two-step synthesis of 1,2,2,3,4,4-hexamethylphosphetane 1-oxide (**2.8**•[O]).

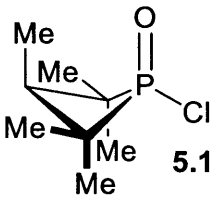

5.1

major isomer

1-Chloro-2,2,3,4,4-pentamethylphosphetane 1-oxide (**5.1**): A round-bottom flask equipped with a stir bar and septum was charged with 6.7 g (50 mmol) of $AlCl_3$, then evacuated and back-filled with nitrogen. Methylene chloride (30 mL) was added via syringe and the mixture was cooled to 0 °C with stirring. Phosphorus trichloride (4.4 mL, 50 mmol) was added via syringe and stirred for 5 min. 2,4,4-Trimethyl-2-pentene (7.79 mL, 50 mmol) was then added via syringe over a period of 10 min and stirring was continued at 0 °C for 2 h. The reaction was quenched by the slow addition of distilled water (30 mL) over 30 min. The organic phase was separated and the aqueous layer was extracted with methylene chloride (2 x 50 mL). After setting the aqueous layer aside, the organic layer was washed with an additional portion of water (30 mL) and then the combined aqueous phases were extracted with methylene chloride (50 mL). The combined organic phases were dried over anhydrous sodium sulfate, filtered, and concentrated by rotary evaporation. The product was

further dried in vacuo giving product S1 as a white solid (8.957 g, 92% yield, dr > 15:1), which could be used in the next step without additional purification. ^{1}H NMR (400 MHz, $CDCl_3$) δ 1.78 (qd, J = 7.1, 3.9 Hz, 1H), 1.39 – 1.27 (m, 12H), 0.92 (d, J = 7.1 Hz, 3H). ^{13}C NMR[1] (101 MHz, $CDCl_3$) δ 56.92 (d, J_{PC} = 56.8 Hz), 42.39 (d, J_{PC} = 1.5 Hz), 25.99 (d, J_{PC} = 6.8 Hz), 18.24 (d, J_{PC} = 3.4 Hz), 7.32 (d, J_{PC} = 30.5 Hz). ^{31}P NMR (162 MHz, $CDCl_3$) δ 81.49 (major), 80.63 (minor). This compound will slowly hydrolyze in the presence of moisture; it may be stored in a sealed container in a −20 °C freezer for an extended period.

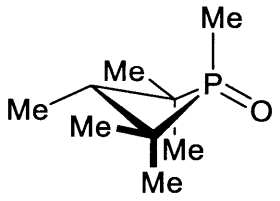

major isomer

1,2,2,3,4,4-hexamethylphosphetane 1-oxide (**2.8**•[O]): Chlorophosphetane oxide **5.1** (8.957 g, 46.02 mmol) was added to a two-neck round-bottom flask containing a stir bar and fitted with a reflux condenser. The top of the reflux condenser and the second neck were both fitted with a rubber septum. Following evacuation and back-filling with nitrogen, diethyl ether (32 mL) was added via syringe and the mixture was cooled to 0 °C (ice bath) with stirring. A solution of MeMgBr (3 M in diethyl ether, 16.11 mL, 48.33 mmol, 1.05 equiv.) was added over a period of 10 min. After the addition, the mixture was heated at 35 °C for 4 h then cooled to 0 °C (ice bath). The reaction was quenched by addition of saturated aqueous ammonium chloride (8 mL) at which time solids precipitated. The organic and aqueous layers were decanted into a separatory funnel and an additional 25 mL of water was added; the layers were then partitioned and the aqueous phase was extracted with methylene chloride (2 x 20 mL). The precipitated solids in the reaction vessel were triturated with methylene chloride (2 x 100 mL), then filtered. The resulting methylene chloride phases was then transferred to a separatory funnel and washed with water (2x30 mL). The combined organic phases were dried over anhydrous sodium sulfate, filtered, and concentrated by rotary evaporation. The isolated off-white solid was slurried with diethyl ether (40

mL) and collected by vacuum filtration with rinsing by an additional 50 mL of diethyl ether. Phosphetane oxide **2.8**•[O] was obtained as a white solid (3.474 g, 43%, dr 25:1). ^{1}H NMR (400 MHz, $CDCl_3$) δ 1.54 – 1.44 (m, 4H), 1.28 – 1.05 (m, 12H), 0.85 (d, J = 8.8 Hz, 3H). ^{13}C NMR (101 MHz, $CDCl_3$) δ 45.55 (d, J_{PC} = 59.6 Hz), 42.75 (d, J_{PC} = 5.9 Hz), 24.83 (d, J_{PC} = 3.5 Hz), 17.53 (d, J_{PC} = 4.3 Hz), 9.98 (d, J_{PC} = 41.0 Hz), 7.07 (d, J_{PC} = 23.5 Hz). ^{31}P NMR (162 MHz, CDCl3) δ 62.98 (minor), 59.38 (major).

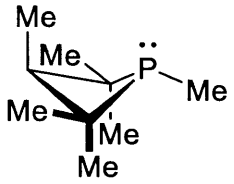

major isomer

1,2,2,3,4,4-Hexamethylphosphetane: Phosphine oxide **2.8**•[O] (1.10 g, 6.31 mmol) was added to a flame-dried round-bottom flask with a stir bar and fitted with a septum. Following evacuation and back-filling with nitrogen, benzene (13 mL, 0.5 M) was added via syringe and stirring was commenced. At room temperature, triethylamine (0.92 mL, 1.05 equiv.) was added, followed by trichlorosilane (0.67 mL, 1.05 equiv.) of over 5 min. The reaction mixture was heated at 75 °C for 20 h, then quenched with aqueous NaOH (8 mL, 10% w/v) and cooled to room temperature. The benzene layer was transferred via cannula to a nitrogen-purged vessel containing anhydrous sodium sulfate. The aqueous phase was extracted additional times with benzene and transferred similarly. The combined organic phases were dried by stirring with sodium sulfate for 20 min, then the benzene supernatant was removed via syringed into a clean, dried Schlenk flask under nitrogen. Solvent was removed in vacuo to give the desired product as an air-sensitive light yellow oil (397 mg, dr 35:1, 40%). The vessel was brought into an inert atmosphere glovebox for storage. ^{1}H NMR (400 MHz, $CDCl_3$) δ 2.61 (q, J = 7.2 Hz, 1H), 1.23 (s, 6H), 1.19 (s, 3H), 0.95 (d, J = 7.3 Hz, 6H), 0.74 (d, J = 7.2 Hz, 3H). ^{13}C NMR (101 MHz, $CDCl_3$) δ 51.41 (d, J_{PC} = 4.2 Hz), 26.91 (d, J_{PC} = 9.9 Hz), 25.22, 24.93, 9.41, 6.88 (d, J_{PC} = 29.7 Hz). ^{31}P NMR (162 MHz, $CDCl_3$) δ 28.77 (major), 16.11 (minor).

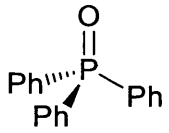

2.1•[O]

Triphenylphosphine oxide (**2.1**•[O]): Purchased from Aldrich (98%, CAS: 791-28-6, LOT BCBC3475) and used without further purification.

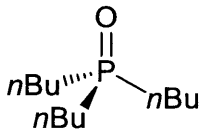

2.2•[O]

Tri-n-butylphosphine oxide (**2.2**•[O]): Purchased from Alfa Aesar (97%, CAS: 814-29-9, LOT W11A007) and stored/handled in an inert atmosphere glovebox due to hygroscopicity. Used without further purification.

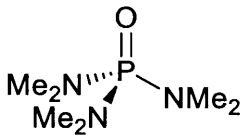

2.3•[O]

Hexamethylphosphoramide (**2.3**•[O]): Purchased from Sigma-Aldrich (99%, CAS: 680-31-9, LOT MKBF1080V) and stored/handled in an inert atmosphere glovebox due to hygroscopicity. Used without further purification.

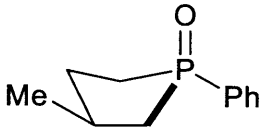

3-Methyl-1-phenylphospholane 1-oxide: Prepared according to the literature procedure[2] via hydrogenation (Pd/C) of commercially available 3-methyl-1-phenyl-2-phospholene 1-oxide. Spectral data are in agreement with the literature reported values.

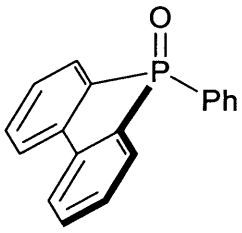

2.5•[O]

5-Phenylbenzo[b]phosphindole 5-oxide (**2.5**•[O]): According to the literature procedure,[2,3] triphenylphosphine oxide was treated with phenyllithium, and the corresponding phosphine (5-phenyl-5*H*-benzo[b]phosphindole) was oxidized using H_2O_2. The phosphine can be columned prior to oxidation (silica, 20% ethyl acetate – 80% hexanes) and recrystallized in ethyl acetate if necessary. Spectral data are in agreement with the literature reported values.

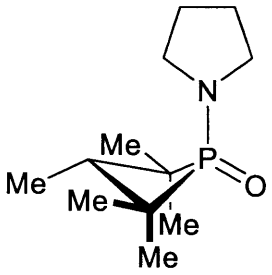

2.6•[O]

2,2,3,4,4-Pentamethyl-1-(purrolidin-1-yl)phosphetane 1-oxide (**2.6•**[O]): Prepared according to the literature procedure[4] by phosphoramidation of 1-chloro-2,2,3,4,4-pentamethylphosphetane 1-oxide (**5.1**) with 1.1 equiv. of pyrrolidine and 1.2 equiv. of trimethylamine in dry toluene (1.0 M) at 60 °C overnight. Spectral data are in agreement with the literature reported values.

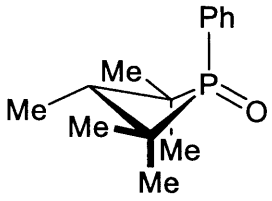

2,2,3,4,4-Pentamethyl-1-phenylphosphetane 1-oxide: Prepared according to a modification of the literature procedure.[5] In a round-bottom flask equipped with a stir bar and septum, $AlCl_3$ (2.7 g, 20 mmol) was charged under inert nitrogen atmosphere. Methylene chloride (20 mL) was added via syringe and stirring was commenced. After cooling to 0 °C, dichlorophenylphosphine (2.7 mL, 20 mmol) was added via syringe. The mixture was stirred for 5 min, then 2,4,4-trimethyl-2-pentene (3.2 mL, 20 mmol) was added via syringe over a period of 10 min. Stirring was continued at 0 °C for 2 h. Distilled water (20 mL) was then added slowly over 30 min. The organic phase was separated and the aqueous layer was extracted with CH_2Cl_2 (2 x 20 mL). After setting the aqueous layer aside, the organic layer was washed with an additional 20 mL of water and the combined aqueous phases were back-extracted with CH_2Cl_2 (20 mL). The combined organic phase was dried over anhydrous sodium sulfate, filtered, then concentrated by rotary evaporation to give an oil. Cyclohexane (25 mL) was added to the residue and the volatiles removed by rotary evaporation to give product **xx•**[O] as an off-white solid (3.741 g, 79%, 6:1 dr, δ 52.8 ppm (major)) which can be recrystallized in cyclohexane if necessary. Multiple fractional recrystallizations give a single isomer if desired. Spectral data are in agreement with the literature reported values.

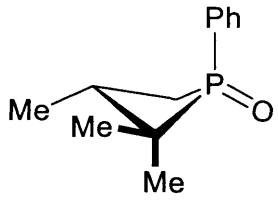

2.11•[O]

1-Phenyl-2,2,3-trimethylphosphetane 1-oxide (**2.11•**[O]): Prepared according to the literature procedure.[6] Spectral data are in agreement with the literature reported values.

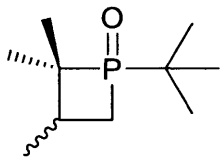

2.13•[O]

1-tert-Butyl-2,2,3-trimethylphosphetane 1-oxide (**2.11•**[O]): Prepared according to a modification of the literature procedure.[7] Spectral data are in agreement with the literature reported values.

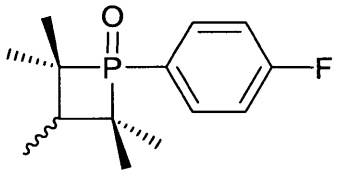

2.14•[O]

1-(4-Fluorophenyl)-2,2,3,4,4-pentamethylphosphetane 1-oxide (**2.14•**[O]): Prepared according to the literature procedure.[6] Spectral data are in agreement with the literature reported values.

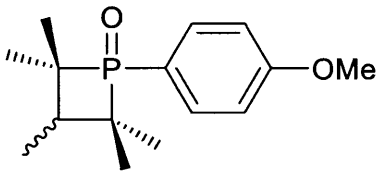

2.16•[O]

1-(4-Methoxyphenyl)-2,2,3,4,4-pentamethylphosphetane 1-oxide (**2.16•**[O]): Prepared according to the literature procedure.[8] Spectral data are in agreement with the literature reported values.

III. Optimization of Catalytic Cadogan Reaction Conditions

A. General Procedures

Reduction of Organophosphorus Catalysts:

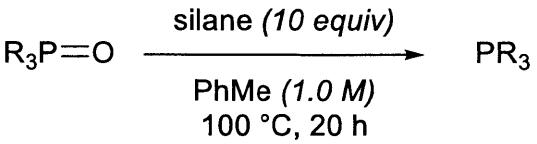

Selected phosphine oxide (0.5 mmol, 1 equiv.) was added to an oven-dried NMR tube equipped with a septum. After exchange of atmosphere for nitrogen, toluene (0.5 mL, 1.0 M) was added via syringe, and the NMR tube was briefly heated to dissolve the phosphine oxide. Selected silane (5.0 mmol, 10 equiv.) was then added via syringe. The NMR tube was then placed into a 100 °C sand bath. After 20 h, the NMR tube was removed from the bath, and the reaction mixture was analyzed by ^{31}P NMR.

Cyclization of (2-nitrobenzylidene)aniline 2.17:

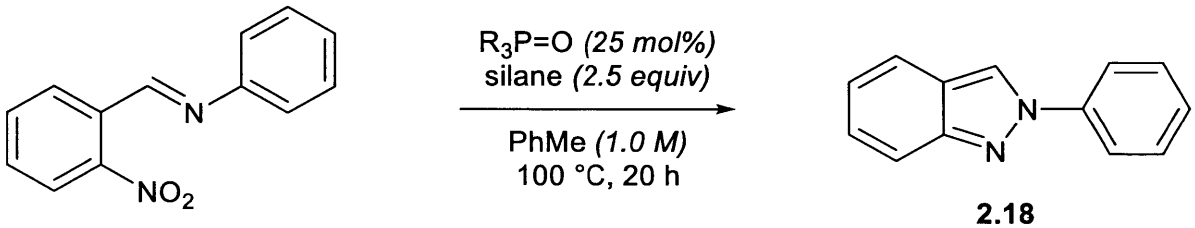

2.17 **2.18**

Imine **2.17** (113 mg, 0.5 mmol), selected phosphine oxide (0.125 mmol, 25 mol%), and dodecane (~85 mg, 0.5 mmol) were added to an oven-dried 4 mL screw cap vial equipped with a septum and a stir bar. After exchange of atmosphere for nitrogen, solvent (0.5 mL, 1.0 M) was added via syringe, followed by silane (1.25 mmol, 2.5 equiv.) The sample was heated for 3-20 h, then cooled to 0 °C and diluted with CH_2Cl_2 (1.0 mL). After stirring, 20 μL of the diluted reaction mixture was added to 1.5 mL of dichloromethane inside of a GC vial, and the sample was analyzed (0.7 μL

injection) using a Shimadzu GC-2010 gas chromatograph fitted with a SHRXI-5MS column (30 m, 0.25 I.D.). Retention times: 9.53 min (dodecane), 17.50 min (2*H*-indazole **2.18**), 18.10 min (imine **2.17**). Calibration curves were made using authentic analytes prior to the start of this study.

B. Catalyst/Silane Screen and Data

Table 2.1 (from text). Successful catalyst/reductant combinations subjected to a standard Cadogan cyclization

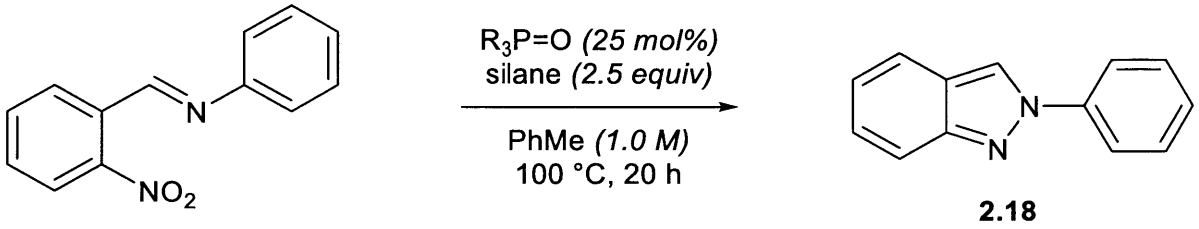

2.17 **2.18**

Entry	R_3P=O	Silane	Yield [a]
1	**2.2**•[O]	$PhSiH_3$	57%
2	**2.4**•[O]	Ph_2SiH_2	21%
3	**2.4**•[O]	$PhSiH_3$	45%
4	**2.7**•[O]	Ph_2SiH_2	78%
5	**2.7**•[O]	$PhSiH_3$	83%
6	**2.8**•[O]	$PhSiH_3$	78%
7	**2.8**•[O]	Ph_2SiH_2	84%
8	**2.11**•[O]	$PhSiH_3$	79%
9	**2.11**•[O]	Ph_2SiH_2	85%
10	**2.13**•[O]	$PhSiH_3$	74%
11	**2.14**•[O]	$PhSiH_3$	77%
12	**2.16**•[O]	Ph_2SiH_2	77%
13	**2.16**•[O]	$PhSiH_3$	89%

[a] Yields determined by GC with respect to dodecane internal standard.

Chromatographs for data tabulated in Table 2.1.

Table 2.1, Entry 1

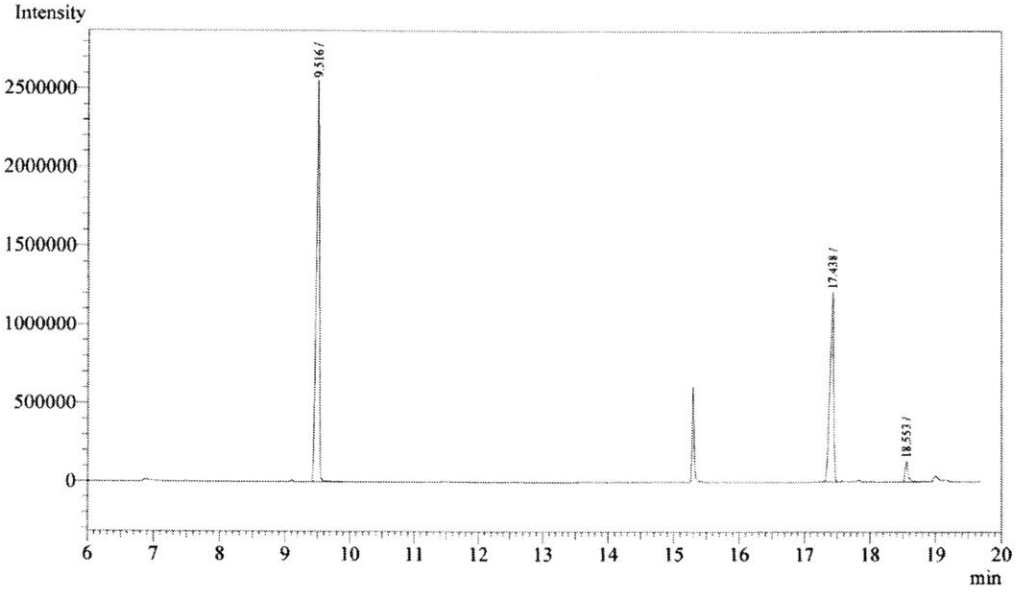

Peak#	Ret.Time	Area	Height	Conc.	Unit	Mark	ID#	Cmpd Name
1	9.516	7922927	2502735	60.112				
2	17.438	4849049	1201987	36.790				
3	18.553	408292	133638	3.098				
Total		13180268	3838360					

Table 2.1, Entry 2

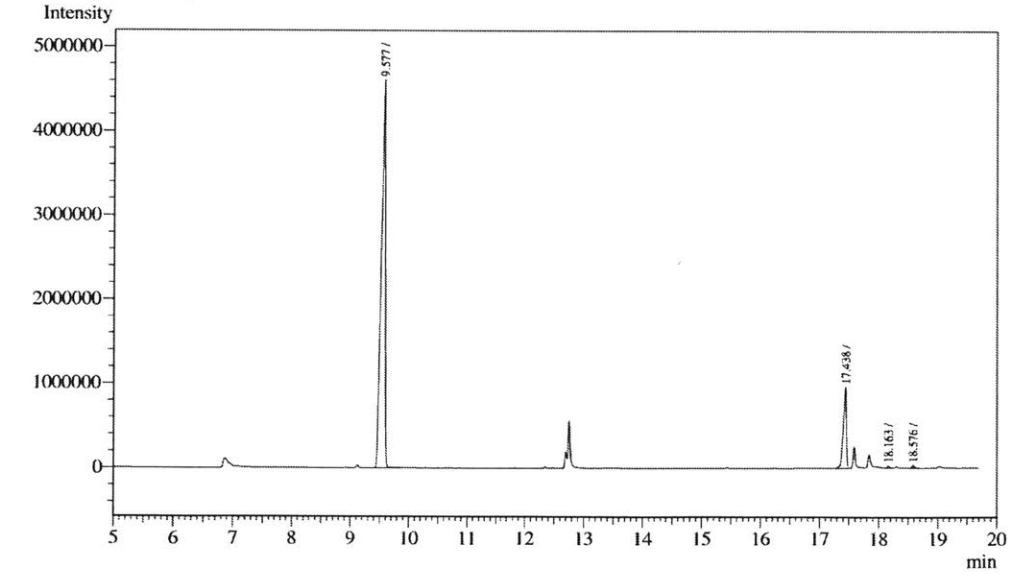

Peak#	Ret.Time	Area	Height	Conc.	Unit	Mark	ID#	Cmpd Name
1	9.577	21628697	4584427	85.608				
2	17.438	3475001	962689	13.754				
3	18.163	61970	27193	0.245				
4	18.576	99261	34035	0.393				
Total		25264929	5608344					

Table 2.1, Entry 3

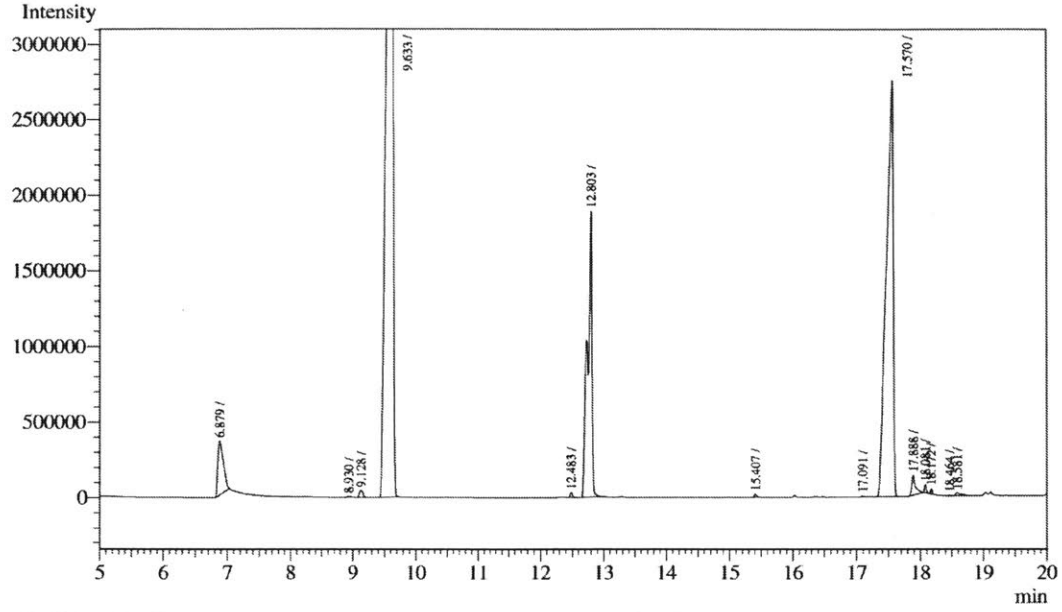

Peak#	Ret.Time	Area	Height	Conc.	Unit	Mark	ID#	Cmpd Name
1	6.879	2128577	355387	2.786				
2	8.930	25502	7231	0.033				
3	9.128	177730	46243	0.233				
4	9.633	43098803	6905457	56.414				
5	12.483	91560	32719	0.120				
6	12.803	9189695	1883357	12.029				
7	15.407	62713	23022	0.082				
8	17.091	20844	9468	0.027				
9	17.570	20779903	2733541	27.200				
10	17.888	523634	129341	0.685				
11	18.081	101119	53207	0.132				
12	18.172	66004	35185	0.086				
13	18.464	7364	3790	0.010				
14	18.581	124561	19478	0.163				
Total		76398009	12237426					

Table 2.1, Entry 4

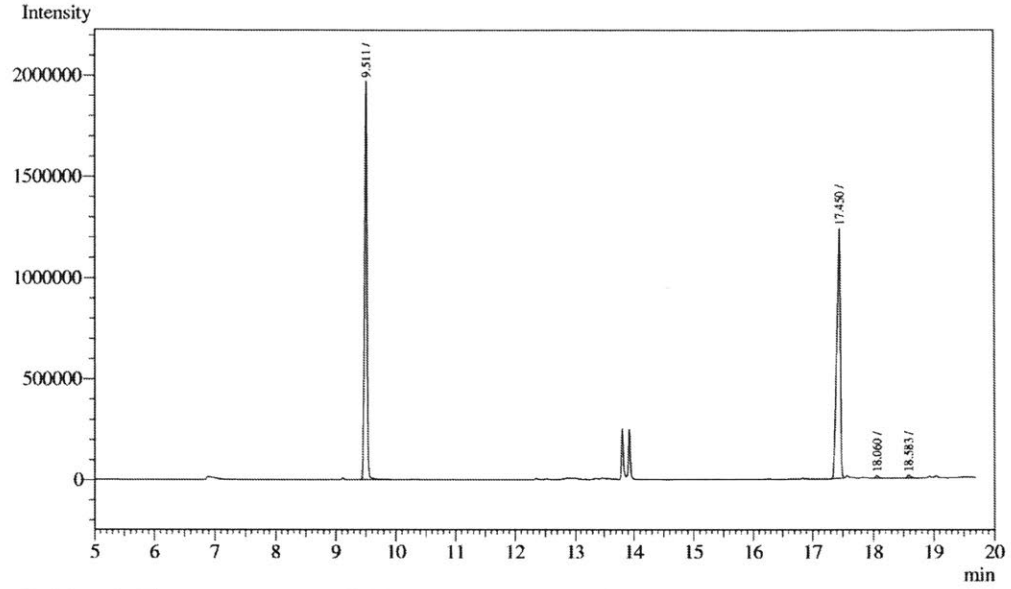

Peak#	Ret.Time	Area	Height	Conc.	Unit	Mark	ID#	Cmpd Name
1	9.511	5541838	1936005	51.875				
2	17.450	5040245	1222504	47.180				
3	18.060	45885	14222	0.430				
4	18.583	55058	15403	0.515				
Total		10683026	3188134					

Table 2.1, Entry 5

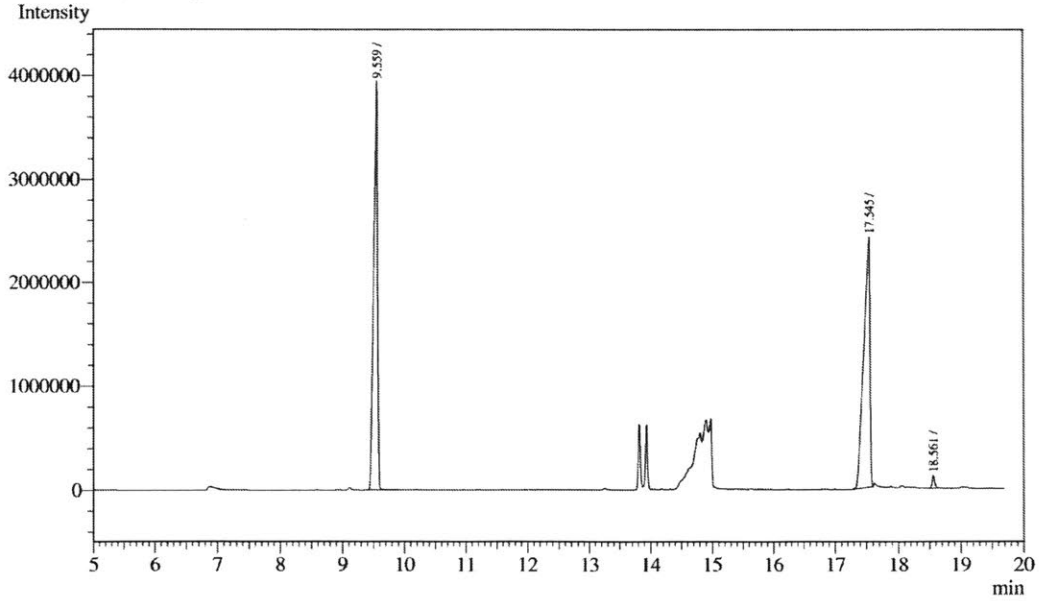

Peak#	Ret.Time	Area	Height	Conc.	Unit	Mark	ID#	Cmpd Name
1	9.559	16566546	3905818	49.378				
2	17.545	16650195	2407432	49.627				
3	18.561	333654	119016	0.994				
Total		33550395	6432266					

Table 2.1, Entry 6

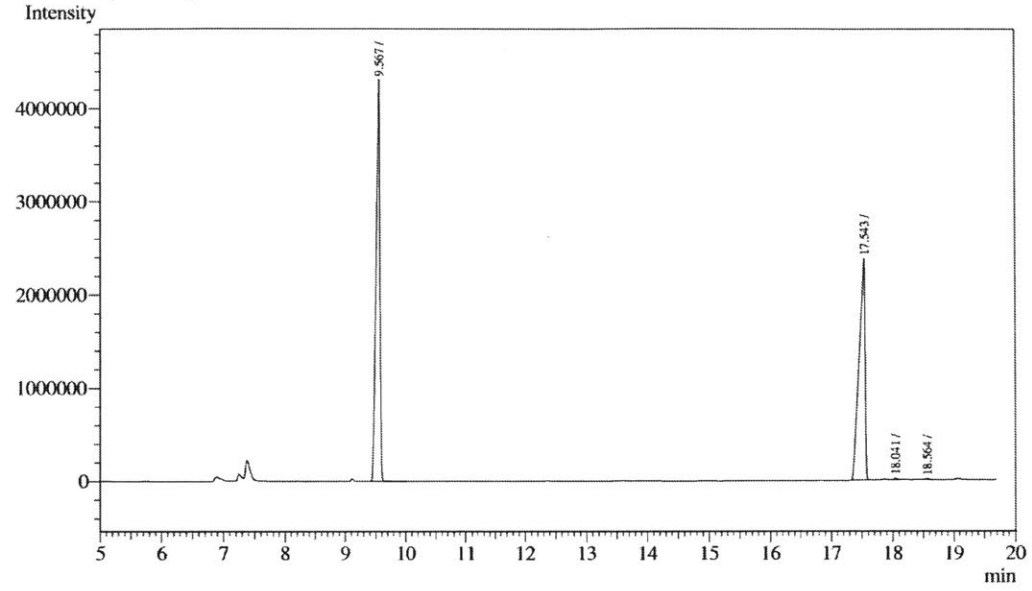

Peak#	Ret.Time	Area	Height	Conc.	Unit	Mark	ID#	Cmpd Name
1	9.567	19053685	4253658	54.850				
2	17.543	15600773	2355704	44.910				
3	18.041	45897	18895	0.132				
4	18.564	37402	9853	0.108				
Total		34737757	6638110					

Table 2.1, Entry 7

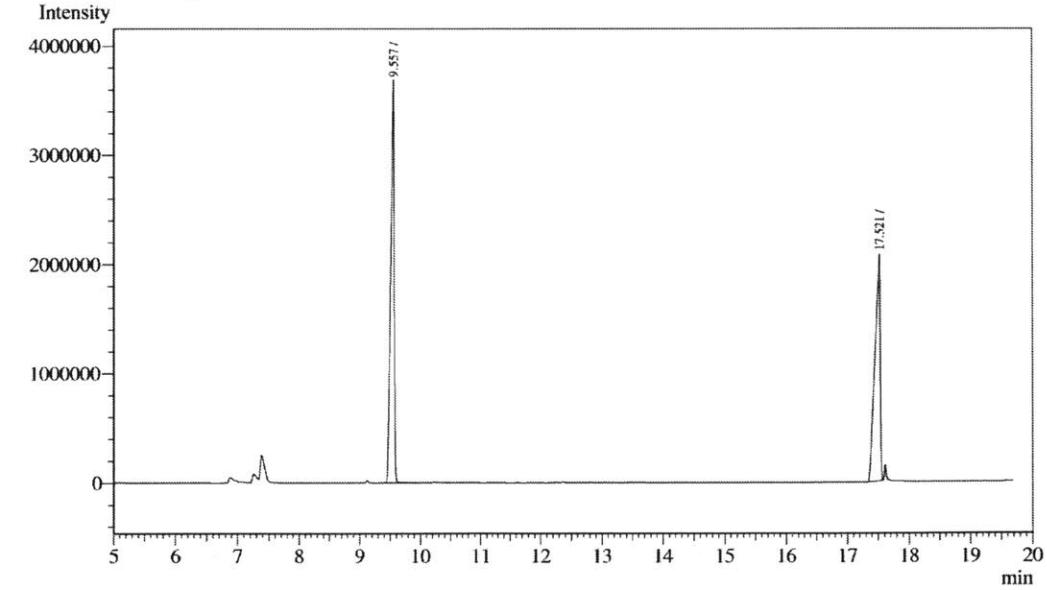

Peak#	Ret.Time	Area	Height	Conc.	Unit	Mark	ID#	Cmpd Name
1	9.557	14471590	3639413	54.033				
2	17.521	12311454	2075623	45.967				
Total		26783044	5715036					

Table 2.1, Entry 8

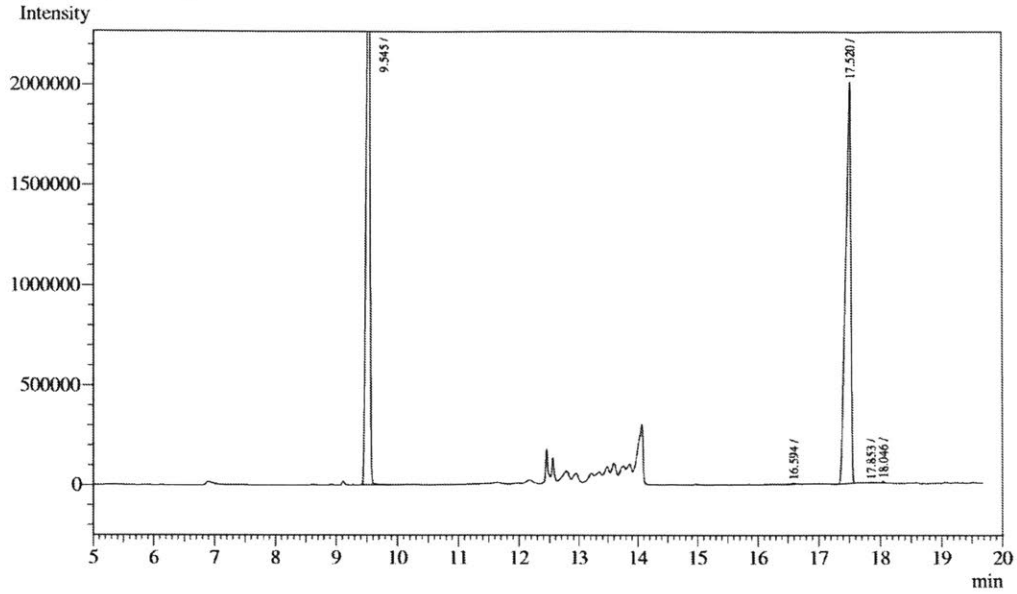

Peak#	Ret.Time	Area	Height	Conc.	Unit	Mark	ID#	Cmpd Name
1	9.545	12940102	3415677	52.441				
2	16.594	14654	4919	0.059				
3	17.520	11692924	1999524	47.387				
4	17.853	9240	2284	0.037				
5	18.046	18575	6880	0.075				
Total		24675495	5429284					

Table 2.1, Entry 9

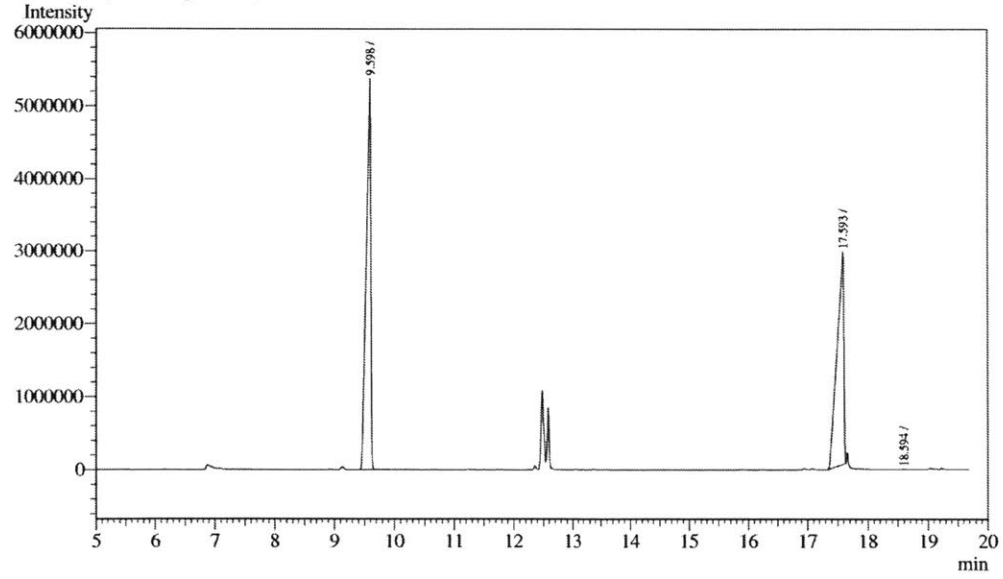

Peak#	Ret.Time	Area	Height	Conc.	Unit	Mark	ID#	Cmpd Name
1	9.598	27784717	5348931	55.007				
2	17.593	22711546	2905799	44.964				
3	18.594	14643	5162	0.029				
Total		50510906	8259892					

Table 2.1, Entry 10

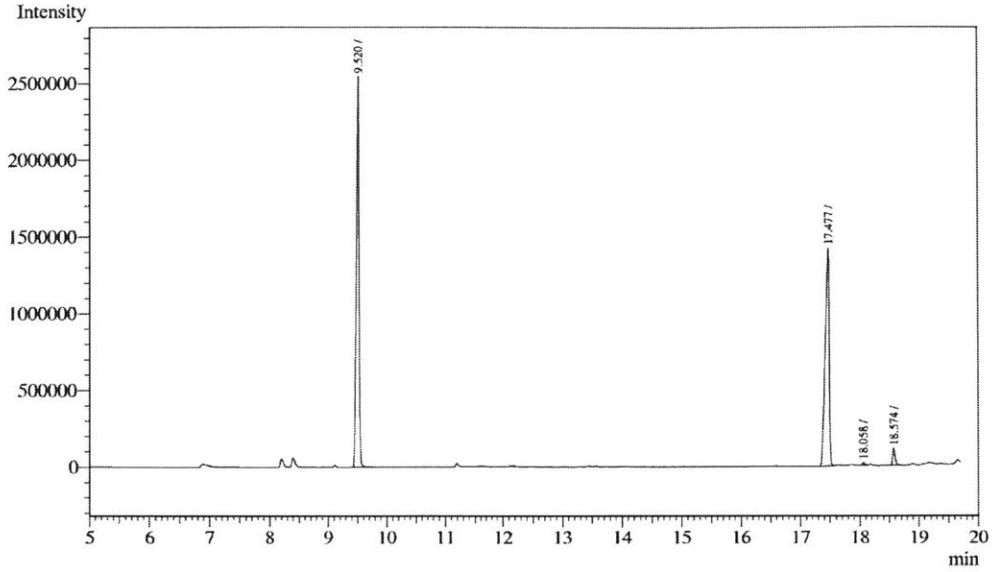

Peak#	Ret.Time	Area	Height	Conc.	Unit	Mark	ID#	Cmpd Name
1	9.520	8163362	2513356	53.416				
2	17.477	6749714	1411791	44.166				
3	18.058	51801	18964	0.339				
4	18.574	317666	108239	2.079				
Total		15282543	4052350					

Table 2.1, Entry 11

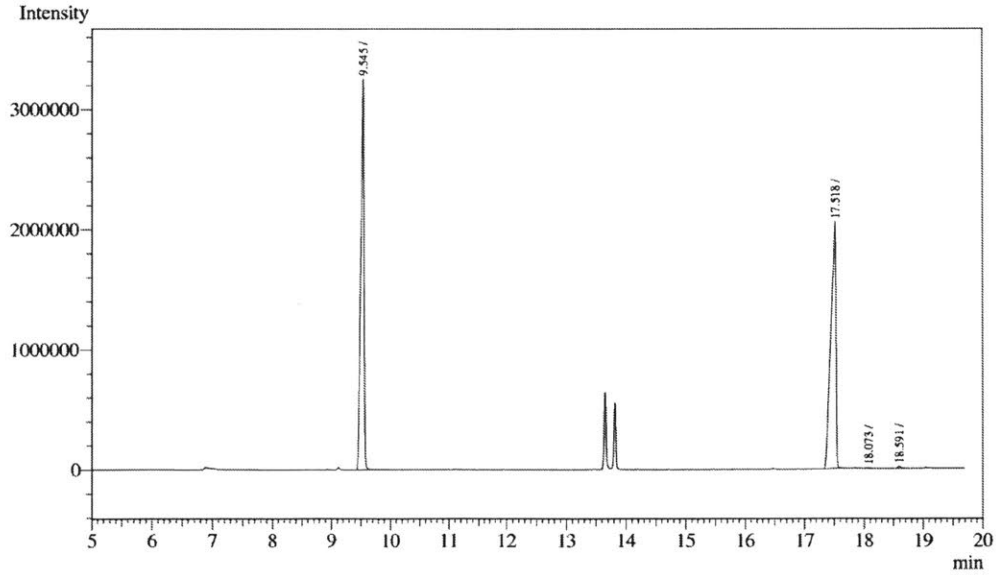

Peak#	Ret.Time	Area	Height	Conc.	Unit	Mark	ID#	Cmpd Name
1	9.545	12037718	3233581	49.898				
2	17.518	12022215	2041437	49.833				
3	18.073	11764	4119	0.049				
4	18.591	53084	17012	0.220				
Total		24124781	5296149					

Table 2.1, Entry 12

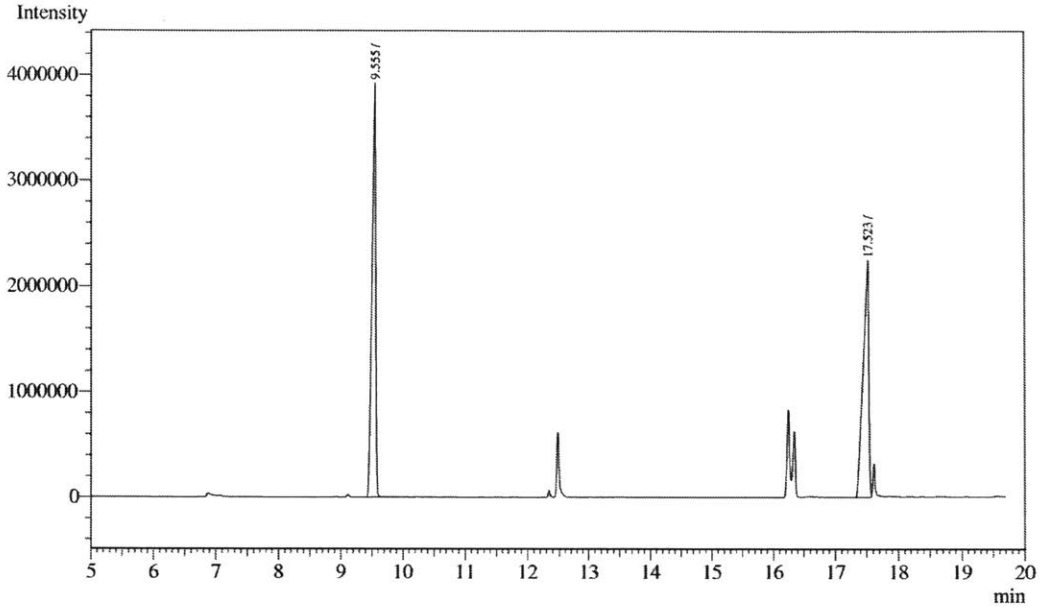

Peak#	Ret.Time	Area	Height	Conc.	Unit	Mark	ID#	Cmpd Name
1	9.555	16541530	3913237	54.214				
2	17.523	13969936	2230796	45.786				
Total		30511466	6144033					

Table 2.1, Entry 13

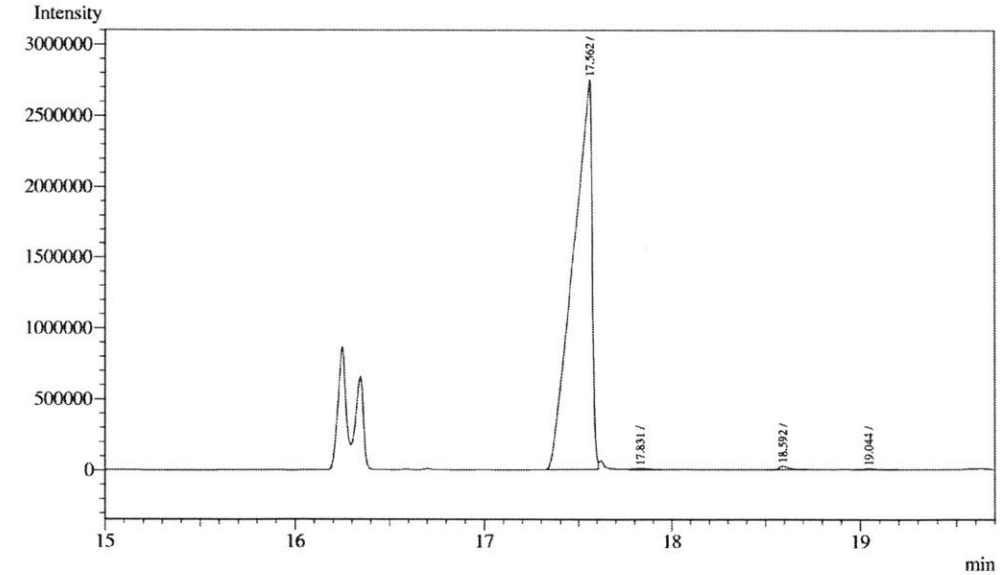

Peak#	Ret.Time	Area	Height	Conc.	Unit	Mark	ID#	Cmpd Name
1	9.573	21273375	4602300	51.244				
2	17.562	20053277	2743419	48.305				
3	17.831	76682	10399	0.185				
4	18.592	86900	25377	0.209				
5	19.044	23681	5637	0.057				
Total		41513915	7387132					

C. Polar Solvent Screen and Data

Table 5.1. Test of polar solvents in catalytic Cadogan cyclization.

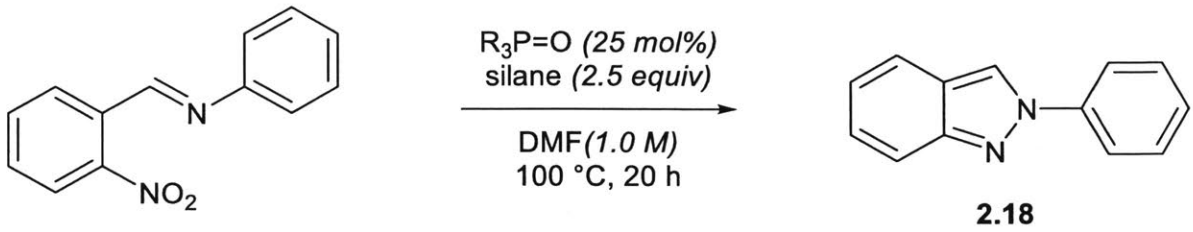

2.17 **2.18**

Entry	R_3P=O	Silane	Yield [a]
1	**2.7**•[O]	$PhSiH_3$	89%
2	**2.8**•[O]	Ph_2SiH_2	95%
3	**2.11**•[O]	Ph_2SiH_2	84%
4	**2.16**•[O]	$PhSiH_3$	85%

[a] Yields determined by GC with respect to dodecane internal standard.

Chromatographs for data tabulated in Table 5.1.

Table 5.1, Entry 1

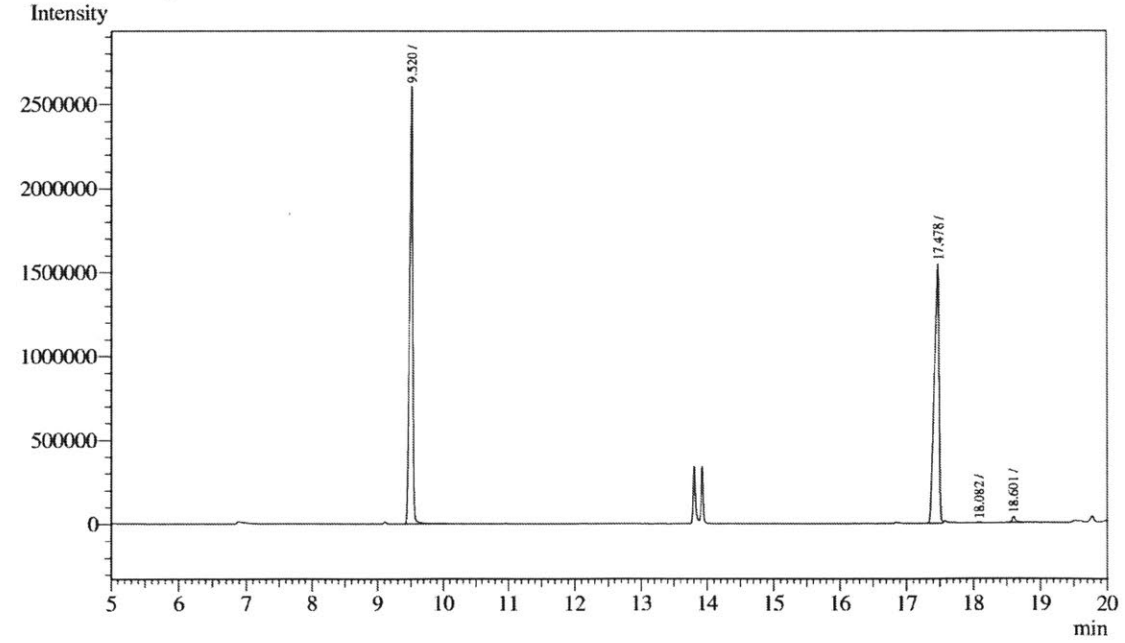

Peak#	Ret.Time	Area	Height	Conc.	Unit	Mark	ID#	Cmpd Name
1	9.520	8418694	2565554	52.367				
2	17.478	7511491	1538104	46.724				
3	18.082	9847	2739	0.061				
4	18.601	136278	35155	0.848				
Total		16076310	4141552					

Table 5.1, Entry 2

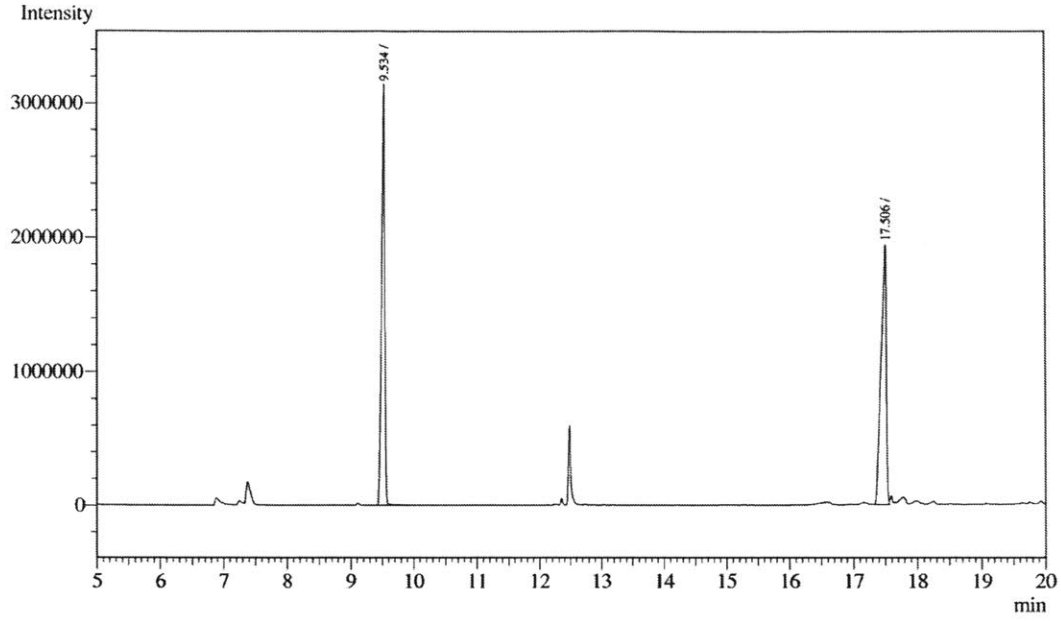

Peak#	Ret.Time	Area	Height	Conc.	Unit	Mark	ID#	Cmpd Name
1	9.534	11029105	3094560	50.414				
2	17.506	10847883	1941772	49.586				
Total		21876988	5036332					

Table 5.1, Entry 3

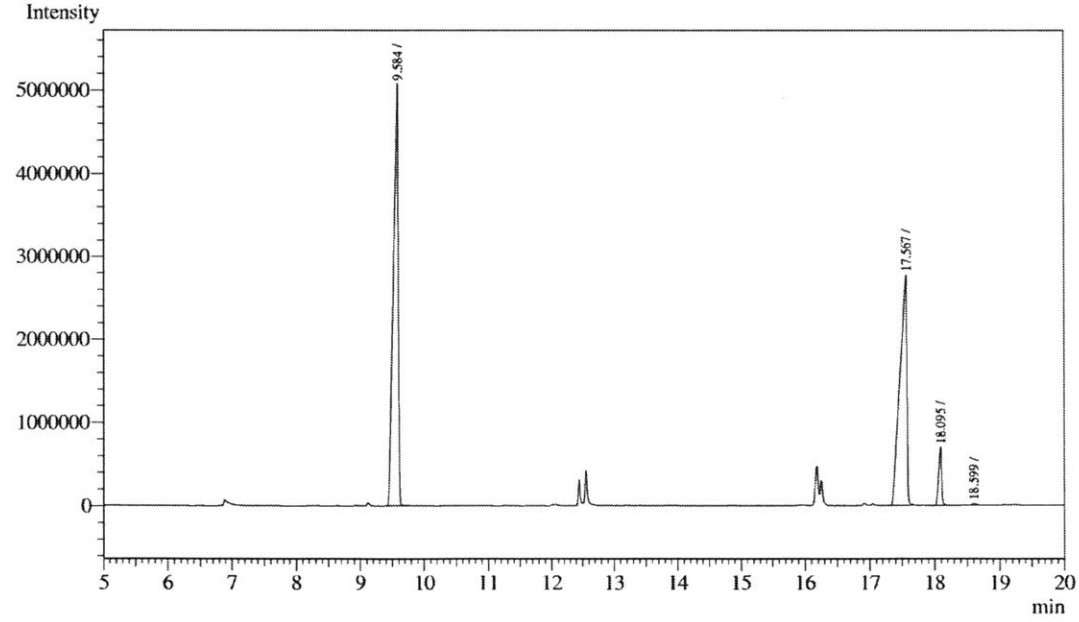

Peak#	Ret.Time	Area	Height	Conc.	Unit	Mark	ID#	Cmpd Name
1	9.584	25365427	5034219	52.278				
2	17.567	20828091	2766454	42.926				
3	18.095	2233321	694985	4.603				
4	18.599	93603	23133	0.193				
Total		48520442	8518791					

Table 5.1, Entry 4

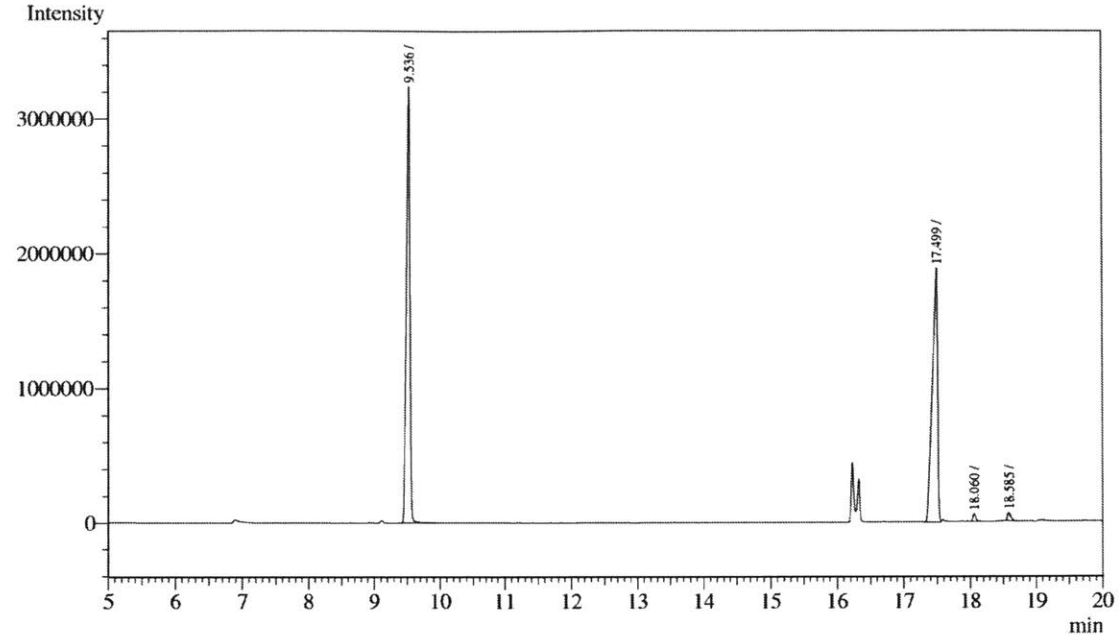

Peak#	Ret.Time	Area	Height	Conc.	Unit	Mark	ID#	Cmpd Name
1	9.536	11851025	3221398	52.787				
2	17.499	10212884	1882800	45.491				
3	18.060	179573	57437	0.800				
4	18.585	207071	59247	0.922				
Total		22450553	5220882					

D. Reaction Time Screen and Data

Table 5.2. Screen of reaction time in catalytic Cadogan cyclization.

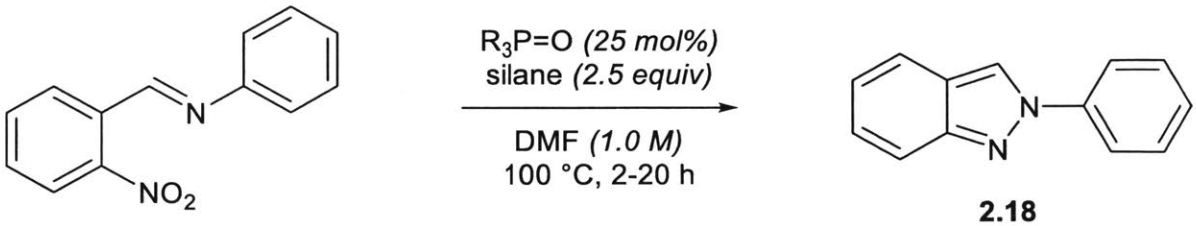

2.17 **2.18**

Entry	R_3P=O	Silane	Time (h)	Yield [a]
1	**2.7**•[O]	$PhSiH_3$	20	89%
2	**2.7**•[O]	$PhSiH_3$	2	34%
3	**2.8**•[O]	Ph_2SiH_2	20	95%
4	**2.8**•[O]	Ph_2SiH_2	2	85%

[a] Yields determined by GC with respect to dodecane internal standard.

Chromatographs for data tabulated in Table 5.2.

Table 5.2, Entry 1

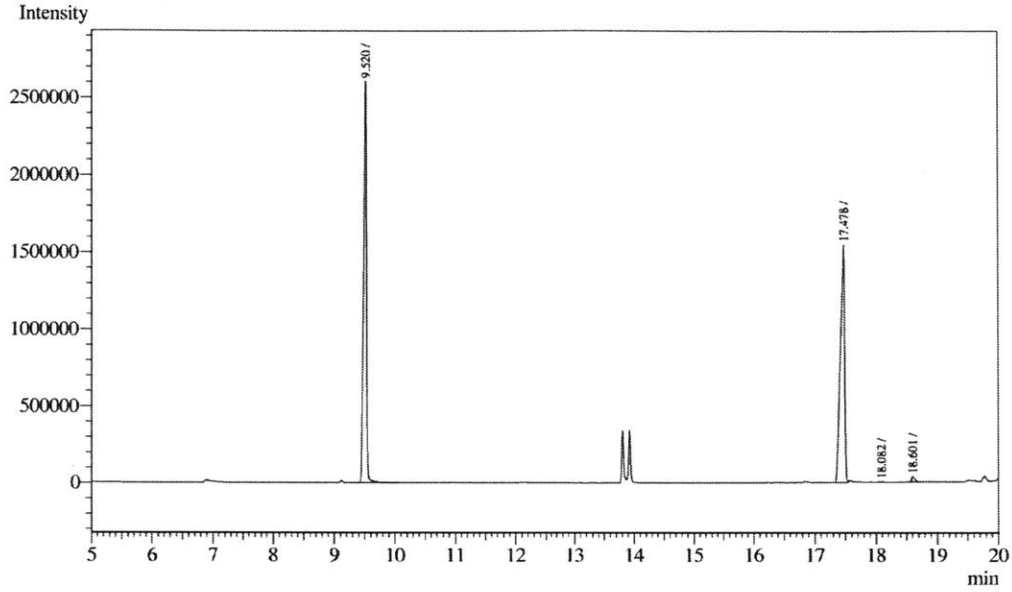

Peak#	Ret.Time	Area	Height	Conc.	Unit	Mark	ID#	Cmpd Name
1	9.520	8418694	2565554	52.367				
2	17.478	7511491	1538104	46.724				
3	18.082	9847	2739	0.061				
4	18.601	136278	35155	0.848				
Total		16076310	4141552					

Table 5.2, Entry 2

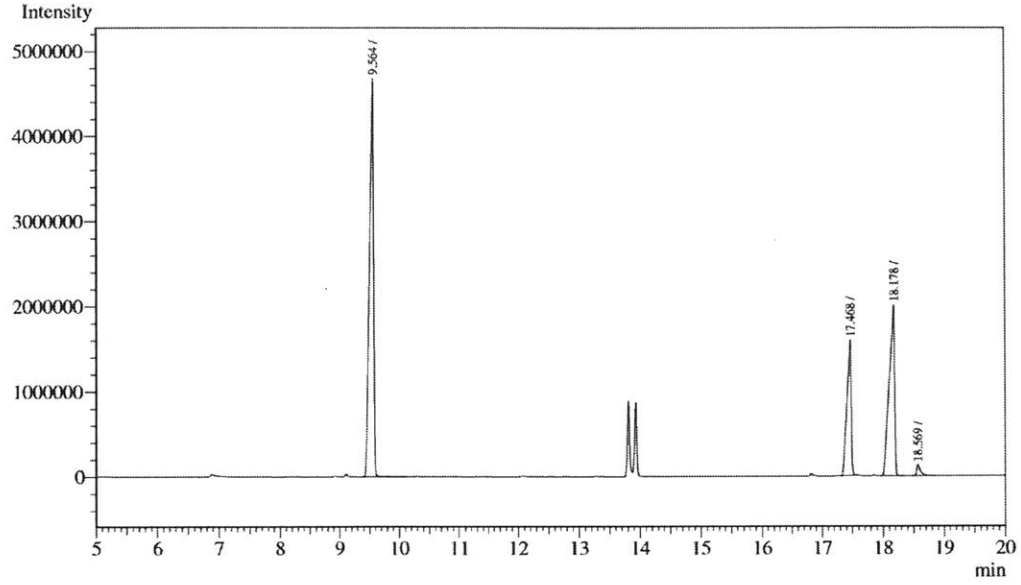

Peak#	Ret.Time	Area	Height	Conc.	Unit	Mark	ID#	Cmpd Name
1	9.564	21990767	4668251	51.768				
2	17.468	7805821	1579511	18.376				
3	18.178	12149108	2004683	28.600				
4	18.569	533530	128300	1.256				
Total		42479226	8380745					

Table 5.2, Entry 3

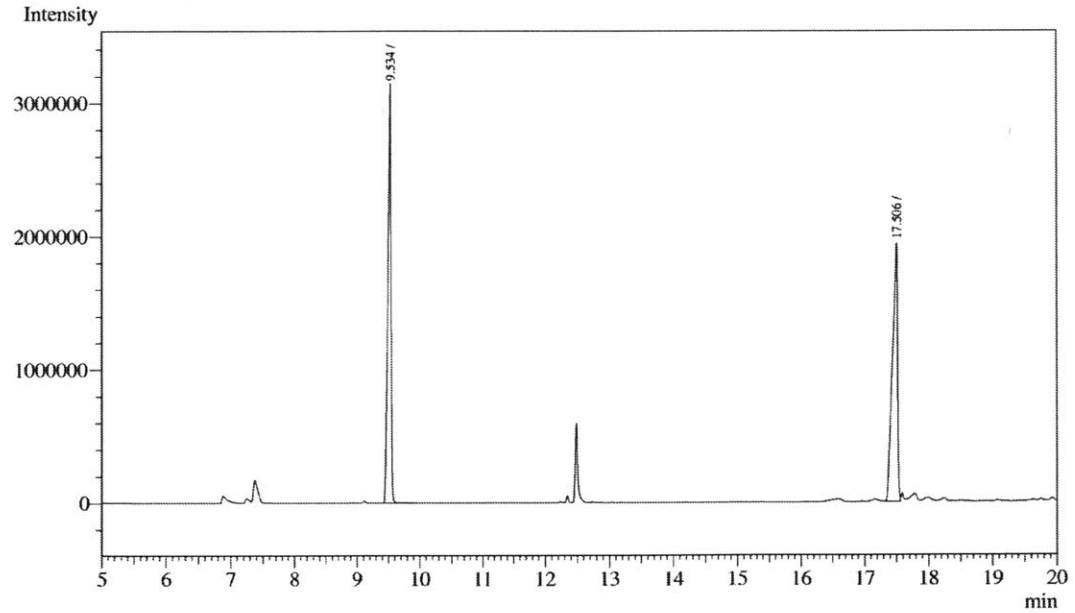

Peak#	Ret.Time	Area	Height	Conc.	Unit	Mark	ID#	Cmpd Name
1	9.534	11029105	3094560	50.414				
2	17.506	10847883	1941772	49.586				
Total		21876988	5036332					

Table 5.2, Entry 4

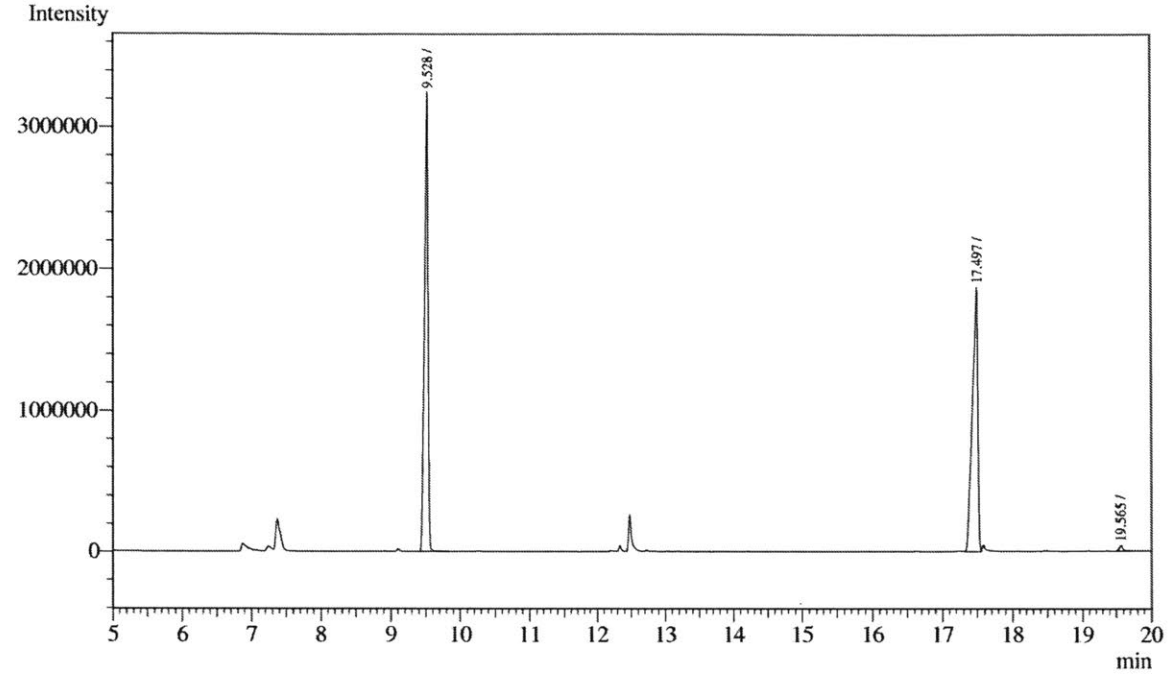

Peak#	Ret.Time	Area	Height	Conc.	Unit	Mark	ID#	Cmpd Name
1	9.528	11771386	3229422	53.290				
2	17.497	10180140	1871271	46.086				
3	19.565	137763	40188	0.624				
Total		22089289	5140881					

E. Isolation of Cyclotrisiloxane 2.19

To an oven-dried 4 mL screw cap vial equipped with a magnetic stir bar was added imine **2.17** (0.5 mmol, 1.0 equiv.) and phosphetane oxide **2.8**•[O] (9 mg, 0.05 mmol, 10 mol%). The vial was then sealed with a Teflon-wrapped septum cap, and the atmosphere was replaced with nitrogen. Toluene (0.5 mL, 1.0 M), then diphenylsilane (0.19 mL, 1 mmol, 2.0 equiv.) were added sequentially. The vial was heated to 100 °C for 3 h. The siloxane was isolated by column chromatography (100% hexanes on silica gel) and subsequently recrystallized in hexanes twice. Crystals were brought to the Penn State X-Ray Crystallography Facility for analysis.

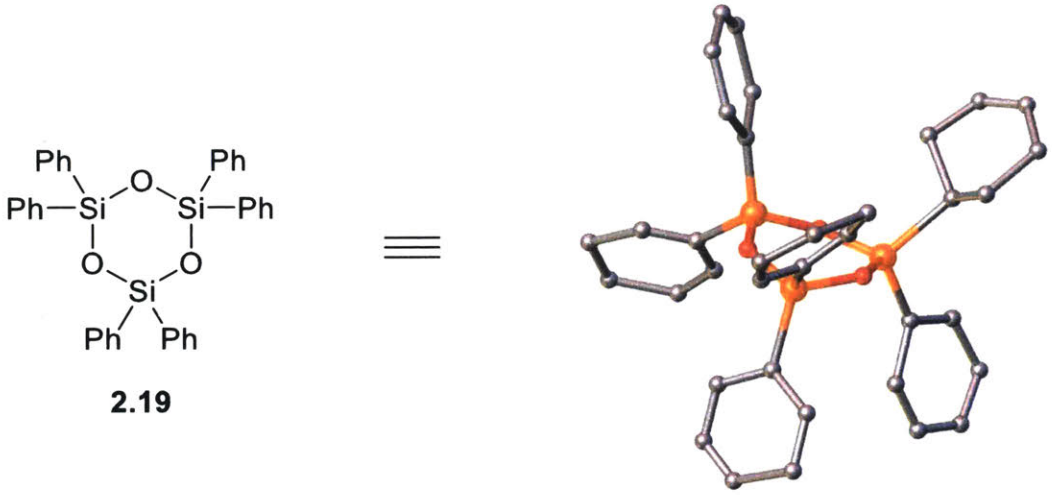

2.19

Figure 2.3 (from text)

IV. Catalytic Reductive Cyclization Reactions

A. Preparation of Substrates and Characterization Data

Imine preparation – general procedure: Nitrobenzaldehyde (1.0 equiv.), absolute ethanol (1.0-2.0 M), and the aniline or hydrazine (1.05 equiv.) were added sequentially to a 20 mL vial equipped with a stir bar. The vial was then sealed and heated to 70-80 °C with monitoring by TLC on alumina until completion. Following slow cooling, crystals commonly formed that could be collected by filtration. If further purification was needed, recrystallization in ethanol or column chromatography using neutral or basic alumina (often 25% ethyl acetate in hexanes) provided quality imine substrates.

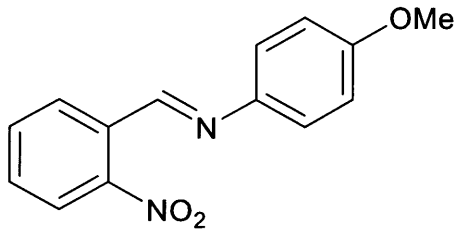

N-(4-methoxyphenyl)-1-(2-nitrophenyl)methanimine (**2.20s**): ^{1}H NMR (360 MHz, $CDCl_3$) δ 8.96 (s, 1H), 8.32 (d, J = 7.7 Hz, 1H), 8.06 (d, J = 8.1 Hz, 1H), 7.72 (t, J = 7.6 Hz, 1H), 7.59 (t, J = 7.5 Hz, 1H), 7.32 (d, J = 8.9 Hz, 2H), 6.96 (d, J = 8.8 Hz, 2H), 3.85 (s, 3H).

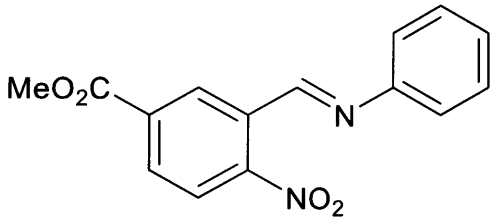

Methyl 4-nitro-3-((phenylimino)methyl)benzoate[9] (**2.21s**): ^{1}H NMR (400 MHz, $CDCl_3$) δ 8.97 (s, 1H), 8.70 (s, 1H), 8.42 (d, J = 8.2 Hz, 1H), 8.36 (d, J = 9.6 Hz, 1H), 7.48 – 7.40 (m, 2H), 7.35 – 7.28 (m, 3H), 4.01 (s, 3H). ^{13}C NMR (75 MHz, $CDCl_3$) δ 164.53, 154.69, 150.57, 149.15, 134.40, 133.87, 132.78, 130.09, 129.36, 127.45, 125.76, 121.32, 52.95. HRMS (DART) calculated for $C_{15}H_{12}N_2O_4$ $[M+H]^+$ 285.0870, found 285.0864.

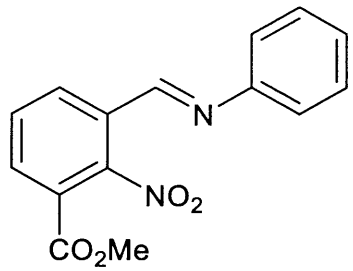

Methyl 2-nitro-3-((phenylimino)methyl)benzoate[9] (**2.22s**): ^{1}H NMR (360 MHz, Chloroform-*d*) δ 8.54 (dd, *J* = 7.9, 1.5 Hz, 1H), 8.38 (s, 1H), 8.13 (dd, *J* = 7.7, 1.5 Hz, 1H), 7.69 (t, *J* = 7.8 Hz, 1H), 7.42 (t, *J* = 7.6 Hz, 2H), 7.35 – 7.15 (m, 5H), 3.95 (s, 3H).

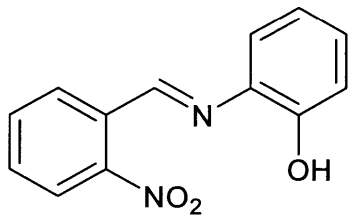

2-((2-nitrobenzylidene)amino)phenol (**2.23s**): ^{1}H NMR (360 MHz, $CDCl_3$) δ 9.17 (s, 1H), 8.26 (d, *J* = 7.7 Hz, 1H), 8.07 (d, *J* = 8.1 Hz, 1H), 7.75 (t, *J* = 7.5 Hz, 1H), 7.64 (t, *J* = 7.7 Hz, 1H), 7.36 (d, *J* = 7.9 Hz, 1H), 7.26 (t, *J* = 8.1 Hz, 1H), 7.04 (d, *J* = 8.0 Hz, 1H), 6.94 (t, *J* = 7.7 Hz, 1H).

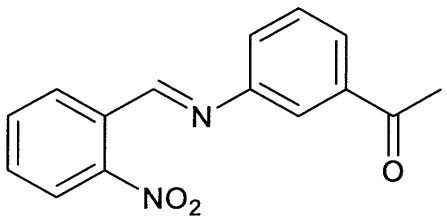

1-(3-((2-nitrobenzylidene)amino)phenyl)ethan-1-one (**2.24s**): ^{1}H NMR (400 MHz, Chloroform-*d*) δ 8.98 (s, 1H), 8.30 (d, *J* = 7.8 Hz, 1H), 8.11 (d, *J* = 8.2 Hz, 1H), 7.89 (d, *J* = 7.6 Hz, 1H), 7.84 (d, *J* = 2.3 Hz, 1H), 7.77 (t, *J* = 7.6 Hz, 1H), 7.66 (t, *J* = 7.8 Hz, 1H), 7.58 – 7.44 (m, 2H), 2.66 (s, 3H).

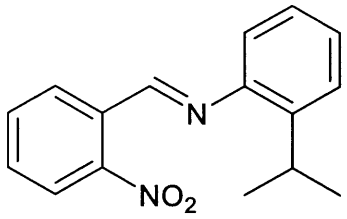

N-(2-isopropylphenyl)-1-(2-nitrophenyl)methanimine (**2.25s**): ^{1}H NMR (400 MHz, Chloroform-*d*) δ 8.84 (s, 1H), 8.31 (dd, *J* = 7.8, 1.6 Hz, 1H), 8.06 (dd, *J* = 8.2, 1.3 Hz, 1H), 7.75 (tdd, *J* = 7.8, 1.3, 0.7 Hz, 1H), 7.61 (ddd, *J* = 8.2, 7.4, 1.5 Hz, 1H), 7.37 – 7.31 (m, 1H), 7.29 – 7.20 (m, 2H), 7.04 – 6.97 (m, 1H), 3.54 (p, *J* = 6.9 Hz, 1H), 1.26 (d, *J* = 6.9 Hz, 6H).

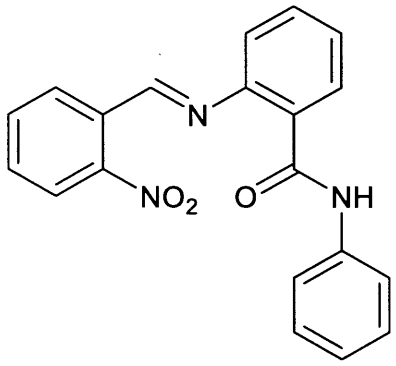

2-((2-nitrobenzylidene)amino)-N-phenylbenzamide (**2.27s**): ^{1}H NMR (400 MHz, $CDCl_3$) δ 11.04 (s, 1H), 9.06 (s, 1H), 8.41 (dd, *J* = 7.8, 1.6 Hz, 1H), 8.20 (ddd, *J* = 8.1, 3.3, 1.4 Hz, 2H), 7.83 (t, *J* = 7.3 Hz, 1H), 7.74 (t, *J* = 7.7 Hz, 1H), 7.65 (d, *J* = 7.4 Hz, 2H), 7.59 (t, *J* = 7.4 Hz, 1H), 7.49 (t, *J* = 7.7 Hz, 1H), 7.33 (t, *J* = 8.4 Hz, 2H), 7.25 (d, 1H), 7.10 (t, *J* = 7.4 Hz, 1H).

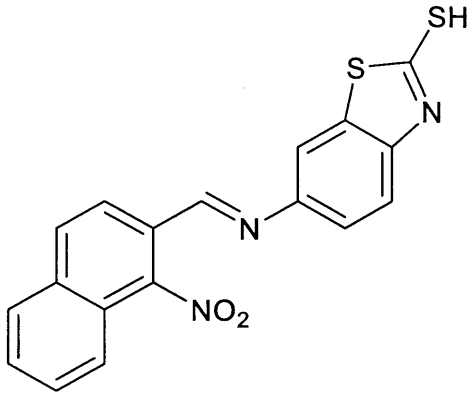

6-(((1-nitronaphthalen-2-yl)methylene)amino)benzo[d]thiazole-2-thiol[9] (**2.28s**): ^{1}H NMR (400 MHz, DMSO-d_6) δ 13.86 (s, 1H), 8.78 (s, 1H), 8.35 (d, J = 8.7 Hz, 1H), 8.27 – 8.17 (m, 2H), 7.85 – 7.77 (m, 4H), 7.44 (dd, J = 8.6, 2.1 Hz, 1H), 7.37 (d, J = 8.6 Hz, 1H).

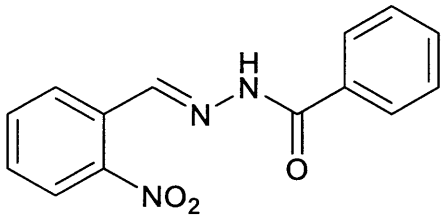

N'-(2-nitrobenzylidene)benzohydrazide (**2.29s**): ^{1}H NMR (360 MHz, DMSO-d_6) δ 8.82 (s, 1H), 8.15 (d, J = 8.0 Hz, 1H), 8.06 (d, J = 8.2 Hz, 1H), 7.90 (d, J = 7.6 Hz, 2H), 7.81 (t, J = 7.8 Hz, 1H), 7.64 (dt, J = 20.7, 7.5 Hz, 2H), 7.53 (t, J = 7.5 Hz, 2H), 5.65 (s, 2H).

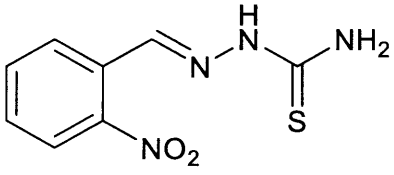

2-(2-nitrobenzylidene)hydrazine-1-carbothioamide (**2.31s**): ^{1}H NMR (360 MHz, DMSO-d_6) δ 11.74 (s, 1H), 8.52 – 8.33 (m, 3H), 8.13 (s, 1H), 8.02 (dd, J = 8.2, 1.3 Hz, 1H), 7.73 (t, J = 7.6 Hz, 1H), 7.68 – 7.55 (m, 1H).

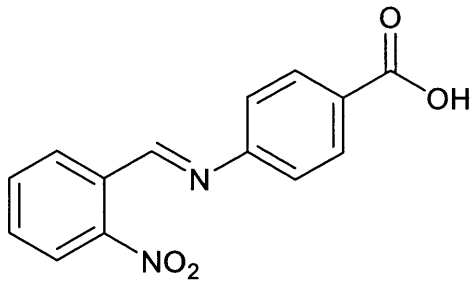

4-((2-nitrobenzylidene)amino)benzoic acid (**2.32s**): ^{1}H NMR (400 MHz, DMSO-d_6) δ 12.96 (s, 1H), 8.89 (s, 1H), 8.16 (dd, J = 18.2, 7.9 Hz, 2H), 8.02 (d, J = 8.1 Hz, 2H), 7.85 (dt, J = 36.0, 7.7 Hz, 2H), 7.34 (d, J = 8.0 Hz, 2H).

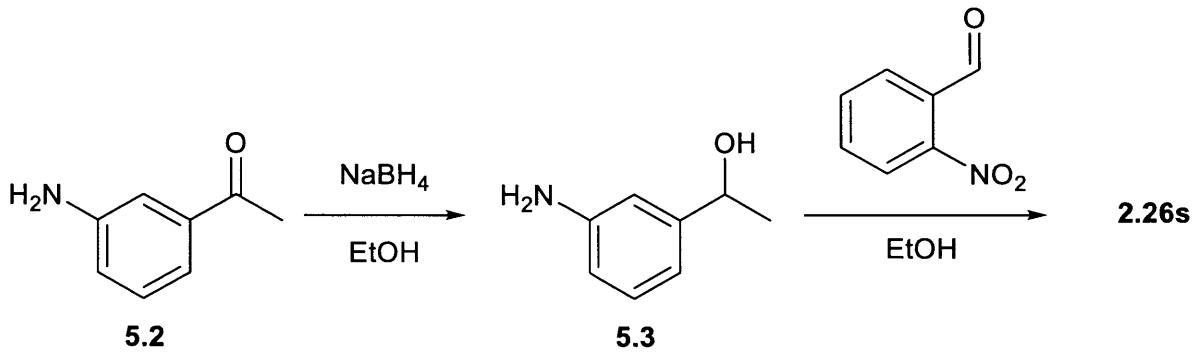

Figure 5.2. Synthetic route to imine **2.26s.**

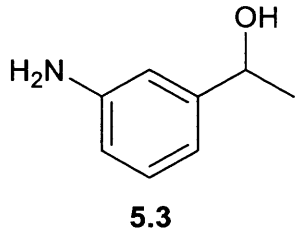

1-(3-aminophenyl)ethan-1-ol (**5.3**): 1-(3-aminophenyl)ethan-1-one **5.2** (2.00 g, 14.8 mmol) was dissolved in ethanol (25 mL, 0.6 M) in a round-bottom flask equipped with magnetic stirring. The flask was cooled to 0 °C, and sodium borohydride (1.44 g, 37.9 mmol) was added in several

portions. The flask was allowed to warm while under a positive nitrogen pressure. The reaction was heated at 30 °C for 4 h. The reaction mixture was poured into ice water and neutralized with 2N HCl to pH 6. The mixture was washed with aqueous sodium bicarbonate, and extracted with several portions of dichloromethane (120 mL), which was then washed with brine and dried over anhydrous sodium sulfate. Filtration and evaporation yielded an off-white solid. ^{1}H NMR (400 MHz, Chloroform-*d*) δ 7.13 (t, *J* = 7.7 Hz, 1H), 6.79 – 6.69 (m, 2H), 6.60 (ddd, *J* = 7.9, 2.4, 1.0 Hz, 1H), 4.81 (q, *J* = 6.5 Hz, 1H), 3.68 (s, 2H), 1.79 (s, 1H), 1.47 (d, *J* = 6.4 Hz, 3H).

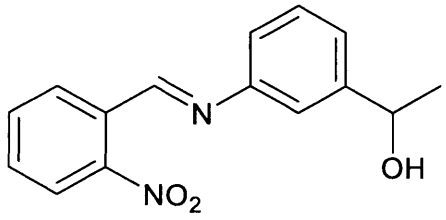

1-(3-((2-nitrobenzylidene)amino)phenyl)ethan-1-ol (**2.26s**): Prepared according to the general procedure. ^{1}H NMR (300 MHz, Chloroform-*d*) δ 8.87 (d, *J* = 0.6 Hz, 1H), 8.27 – 8.18 (m, 1H), 8.05 – 7.98 (m, 1H), 7.68 (tdd, *J* = 7.9, 1.3, 0.6 Hz, 1H), 7.56 (ddd, *J* = 8.1, 7.4, 1.5 Hz, 1H), 7.38 – 7.29 (m, 1H), 7.24 (dtd, *J* = 7.0, 1.4, 0.7 Hz, 2H), 7.15 – 7.08 (m, 1H), 4.89 (q, *J* = 6.5 Hz, 1H), 1.85 (s, 1H), 1.47 (d, *J* = 6.5 Hz, 3H).

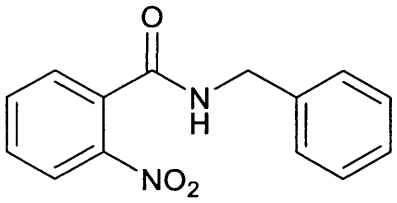

N-benzyl-2-nitrobenzamide (**2.30s**): To a solution of *o*-nitrobenzoyl chloride (2.6 mL, 20 mmol) in ethanol (40 mL, 0.5 M) was added benzylamine (4.2 mL, 40 mmol) dropwise via syringe at 0 °C. The reaction mixture was allowed to warm overnight with stirring. The reaction mixture was

diluted with 1 M HCl and ethyl acetate. After partitioning, the aqueous layer was extracted with ethyl acetate. The combined organics were washed with aqueous saturated sodium bicarbonate and brine, dried with anhydrous magnesium sulfate, filtered, and concentrated in vacuo to a brown solid. Recrystallization from hot ethanol (7 mL) gave a white powder. ^{1}H NMR (400 MHz, Chloroform-*d*) δ 8.02 (dd, *J* = 8.1, 1.2 Hz, 1H), 7.63 (td, *J* = 7.5, 1.3 Hz, 1H), 7.57 – 7.51 (m, 1H), 7.48 (dd, *J* = 7.5, 1.5 Hz, 1H), 7.39 – 7.26 (m, 5H), 6.27 (s, 1H), 4.59 (d, *J* = 5.7 Hz, 2H).

B. General Procedure for Catalytic Reductive Cyclization Reactions

General procedure: To an oven-dried 4 mL screw cap vial equipped with a magnetic stir bar was added imine substrate (0.5 mmol, 1.0 equiv.) and catalyst **2.8**•[O] (13 mg, 0.075 mmol, 15 mol%). The vial was then sealed with a Teflon-wrapped septum cap, and the atmosphere was replaced with nitrogen. Solvent (0.5 mL, 1.0 M), then phenylsilane (0.12 mL, 1 mmol, 2.0 equiv.) were added sequentially. The vial was heated to 100 °C with monitoring by TLC until completion (3-16 h, 24 h max). The product was isolated via column chromatography (silica gel, 0-50% ethyl acetate in hexanes, most commonly 10%). After cooling, solid occasionally precipitated from toluene; mild heating was necessary in some cases to be able to load the sample for chromatography.

*TBAF workup for **2.26***: Following cyclization, the reaction mixture was stirred with 1.5 equiv. of TBAF for 1 h at room temperature. The mixture was then diluted with water and extracted with ethyl acetate, dried, filtered, and concentrated to a residue. The product was isolated via column chromatography (silica gel, 25% ethyl acetate in hexanes).

C. Characterization Data for Reductive Cyclization Products

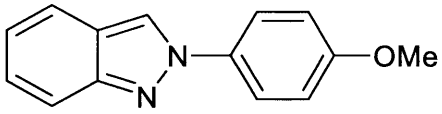

2-(4-methoxyphenyl)-2H-indazole (**2.20**): 6 h, 83%. ^{1}H NMR (300 MHz, $CDCl_3$) δ 8.29 (s, 1H), 7.86 – 7.74 (m, 3H), 7.69 (d, *J* = 8.5 Hz, 1H), 7.32 (t, *J* = 7.7 Hz, 1H), 7.11 (t, *J* = 7.6 Hz, 1H), 7.01 (d, *J* = 9.1 Hz, 2H), 3.84 (s, 3H). ^{13}C NMR (75 MHz, $CDCl_3$) δ 159.31, 149.62, 134.12, 126.62, 122.76, 122.43, 122.28, 120.36, 117.81, 114.67, 55.63. HRMS (DART) calculated for $C_{14}H_{12}N_2O$ $[M+H]^+$ 225.1022, found 225.1019.

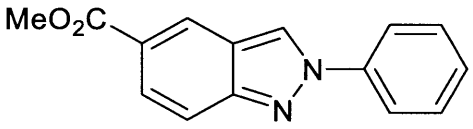

Methyl 2-phenyl-2H-indazole-5-carboxylate (**2.21**): 5 h, 73%. ^{1}H NMR (300 MHz, $CDCl_3$) δ 8.59 (s, 1H), 8.43 (s, 1H), 7.91 (d, *J* = 8.4 Hz, 2H), 7.74 (d, *J* = 1.1 Hz, 2H), 7.54 (t, *J* = 7.6 Hz, 2H), 7.43 (t, *J* = 7.6, 6.8 Hz, 1H), 3.96 (s, 3H). ^{13}C NMR (101 MHz, $CDCl_3$) δ 167.53, 149.12, 140.43, 129.82, 128.76, 128.59, 124.80, 122.21, 121.99, 121.28, 120.81, 120.58, 52.38. HRMS (DART) calculated for $C_{15}H_{12}N_2O_2$ $[M+H]^+$ 253.0972, found 253.0962.

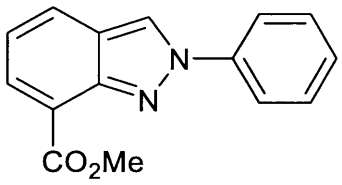

Methyl 2-phenyl-2H-indazole-7-carboxylate (**2.22**): 12 h, 12%. ^{1}H NMR (360 MHz, Chloroform-*d*) δ 8.55 (s, 1H), 8.15 (dd, *J* = 7.0, 1.0 Hz, 1H), 7.98 (ddd, *J* = 8.4, 5.9, 1.3 Hz, 3H), 7.54 (t, *J* = 7.9 Hz, 2H), 7.43 (t, *J* = 7.4 Hz, 1H), 7.20 (dd, *J* = 8.3, 7.1 Hz, 1H), 4.06 (s, 3H).

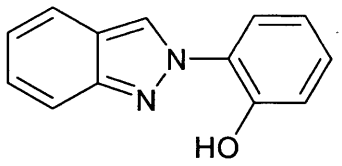

2-(2H-indazol-2-yl)phenol (**2.23**): 3 h, 63%. ^{1}H NMR (300 MHz, $CDCl_3$) δ 12.13 (s, 1H), 8.48 (s, 1H), 7.74 (d, J = 10.5 Hz, 2H), 7.59 (d, J = 8.1 Hz, 1H), 7.46 – 7.34 (m, 1H), 7.33 – 7.24 (m, 1H), 7.22 – 7.16 (m, 2H), 6.98 (t, J = 7.7 Hz, 1H). ^{13}C NMR (101 MHz, $CDCl_3$) δ 150.61, 147.74, 129.21, 127.82, 124.96, 123.08, 121.45, 120.41, 120.34, 119.76, 119.56, 119.34, 116.95. HRMS (DART) calculated for $C_{13}H_{10}N_2O$ $[M+H]^+$ 211.0866, found 211.0860.

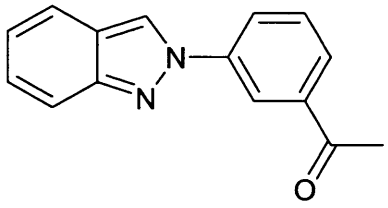

1-(3-(2H-indazol-2-yl)phenyl)ethan-1-one (**2.24**): 4 h, 49%. ^{1}H NMR (360 MHz, Chloroform-*d*) δ 8.48 (dd, J = 4.4, 1.7 Hz, 2H), 8.15 (ddd, J = 8.1, 2.3, 1.1 Hz, 1H), 7.96 (dt, J = 7.8, 1.2 Hz, 1H), 7.79 (d, J = 8.6 Hz, 1H), 7.75 – 7.68 (m, 1H), 7.63 (t, J = 7.9 Hz, 1H), 7.34 (ddd, J = 8.7, 6.6, 1.1 Hz, 1H), 7.17 – 7.08 (m, 1H), 2.69 (s, 3H). HRMS (DART) calculated for $C_{15}H_{12}N_2O$ $[M+H]^+$ 237.1022, found 237.1012.

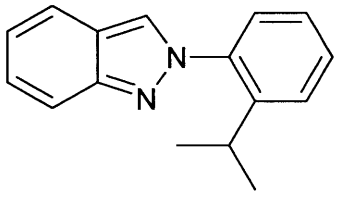

2-(2-isopropylphenyl)-2H-indazole (**2.25**): 5 h, 75%. ^{1}H NMR (400 MHz, Chloroform-*d*) δ 8.09 (d, J = 1.0 Hz, 1H), 7.83 (dq, J = 8.6, 1.1 Hz, 1H), 7.76 (dt, J = 8.4, 1.1 Hz, 1H), 7.54 – 7.46 (m,

2H), 7.41 – 7.28 (m, 3H), 7.16 (ddd, J = 8.5, 6.6, 0.9 Hz, 1H), 2.83 (p, J = 6.9 Hz, 1H), 1.19 (d, J = 6.9 Hz, 6H). HRMS (DART) calculated for $C_{16}H_{16}N_2$ $[M+H]^+$ 237.1386, found 237.1374.

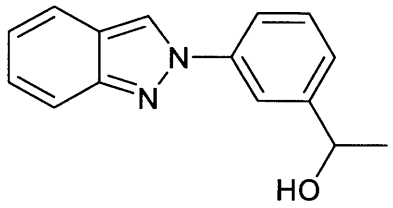

1-(3-(2H-indazol-2-yl)phenyl)ethan-1-ol (**2.26**): 6 h, 62%. ^{1}H NMR (400 MHz, Chloroform-*d*) δ 8.43 (d, J = 1.0 Hz, 1H), 7.98 – 7.92 (m, 1H), 7.79 (ddq, J = 8.0, 3.1, 1.0 Hz, 2H), 7.71 (dt, J = 8.4, 1.1 Hz, 1H), 7.49 (t, J = 7.8 Hz, 1H), 7.44 – 7.37 (m, 1H), 7.33 (ddd, J = 8.8, 6.6, 1.1 Hz, 1H), 7.12 (ddd, J = 8.5, 6.6, 0.9 Hz, 1H), 5.02 (q, J = 5.9 Hz, 1H), 2.07 (d, J = 2.4 Hz, 1H), 1.57 (d, J = 6.5 Hz, 3H). ^{13}C NMR (101 MHz, Chloroform-*d*) δ 149.92, 147.98, 140.81, 129.84, 127.05, 124.99, 122.90, 122.64, 120.67, 120.54, 119.99, 118.25, 118.06, 70.14, 25.54. HRMS (DART) calculated for $C_{15}H_{14}N_2O$ $[M+H]^+$ 239.1179, found 239.1156.

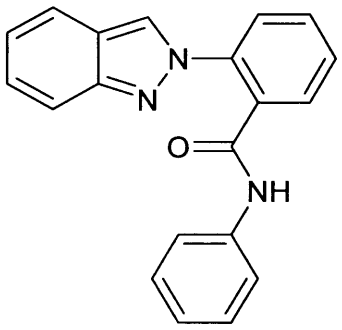

2-(2H-indazol-2-yl)-N-phenylbenzamide (**2.27**): 16 h, 50%. ^{1}H NMR (400 MHz, DMSO-d_6) δ 10.43 (s, 1H), 8.70 (s, 1H), 7.82 (d, J = 7.6 Hz, 1H), 7.79 – 7.69 (m, 3H), 7.64 (t, J = 7.4 Hz, 1H), 7.59 (d, J = 8.7 Hz, 1H), 7.54 (d, J = 7.6 Hz, 2H), 7.30 – 7.22 (m, 3H), 7.10 – 7.01 (m, 2H). ^{13}C NMR (101 MHz, DMSO-d_6) δ 165.27, 148.85, 138.96, 137.80, 133.13, 130.66, 128.93, 128.60,

128.58, 126.40, 125.52, 124.49, 123.63, 122.04, 121.79, 120.96, 119.87, 117.36. HRMS (DART) calculated for $C_{20}H_{15}N_3O$ $[M+H]^+$ 314.1288, found 314.1277.

V. Mechanistic Experiments

A. In situ NMR experiments

i. Speciation of Phosphorus in Indazolation

To an oven-dried purged septum-sealed NMR tube was added **3.2** (113 mg, 0.5 mmol, 1 equiv) and **3.1**•[O] (13 mg, 0.075 mmol, 15 mol%) in toluene-d_8 (0.5 mL). The tube was inserted into the NMR probe thermostatted at 100°C and a t = 0 spectrum was obtained. The tube was ejected from the probe, phenylsilane (0.12 mL, 1.0 mmol, 2 equiv) was added via syringe, and the NMR tube was reinjected into the probe. The decrease of the aldimine C-H signal for **3.2** (δ 8.76 ppm) and appearance of a heteroaromatic C-H for **3.3** (δ 7.86 ppm) were monitored by ^{1}H NMR spectroscopy at 100°C with data acquired every 15 min. In these experiments, substrate **3.2** is completely consumed in 90 min. ^{31}P NMR spectra, both proton-coupled and -decoupled, were also obtained contemporaneously. Phosphetane **3.1**•[O] (δ 53.2 ppm) is consumed within 30 min and replaced by two signals (δ 32.4 and 18.9 ppm, 3:1 *anti*:*syn*) which were shown by independent synthesis to be the epimers of tricoordinate phosphetane **3.1**.

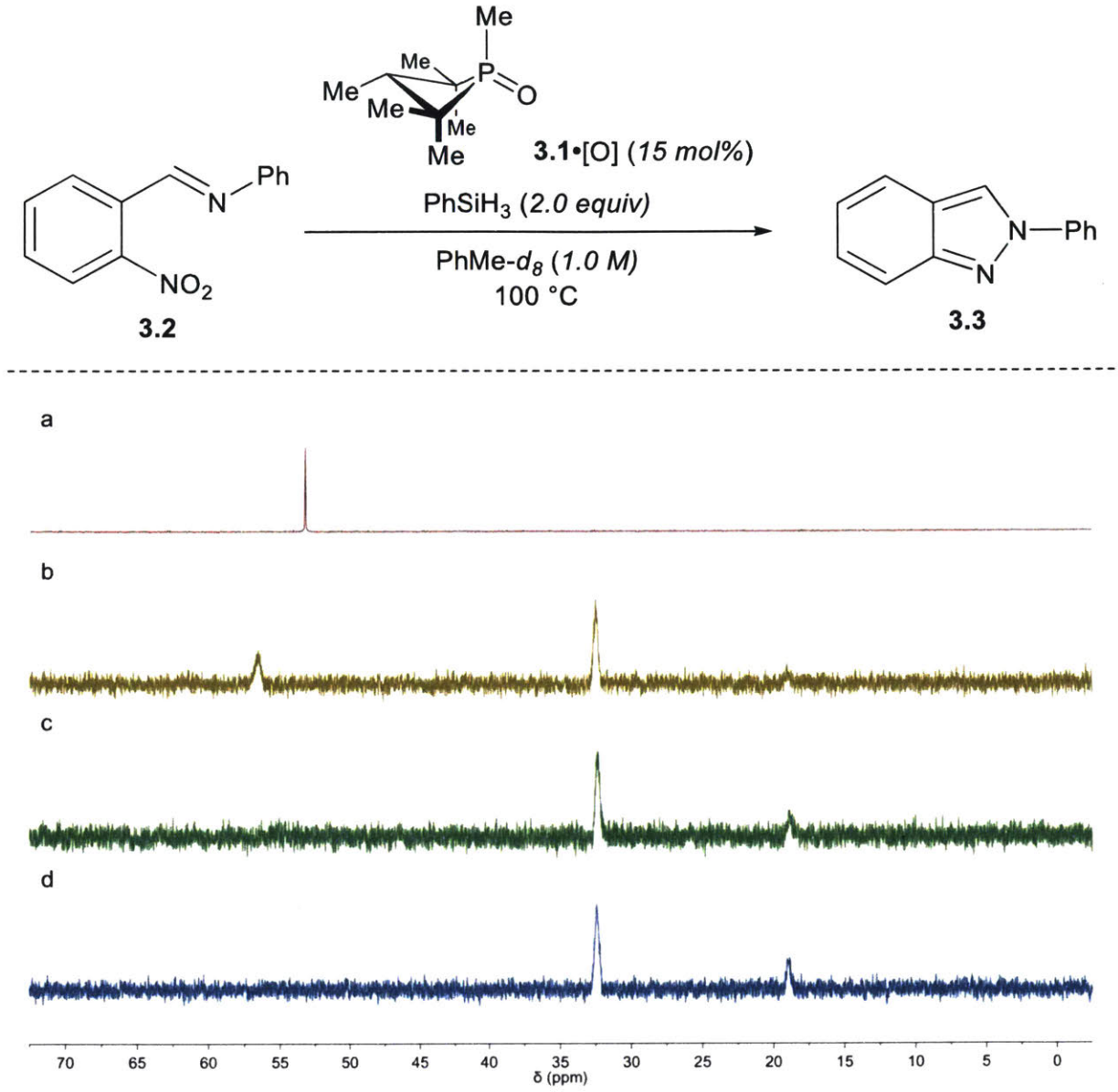

Figure 3.1 (from text)

ii. Speciation of Phosphorus in Carbazolation

To an oven-dried purged septum-sealed NMR tube was added biphenyl **3.4** (99 mg, 0.5 mmol, 1 equiv) and **3.1**•[O] (17 mg, 0.1 mmol, 20 mol%) in toluene-d_8 (0.5 mL). The tube was inserted into the NMR probe thermostatted at 100°C and a t = 0 spectrum was obtained. The tube was ejected from the probe, phenylsilane (0.12 mL, 1.0 mmol, 2 equiv) was added via syringe, and the NMR tube was reinjected into the probe. The appearance of a heteroaromatic C-H for **3.5** (δ 7.49 ppm) was monitored by ^{1}H NMR spectroscopy at 100°C with data acquired every 15 min. ^{31}P NMR spectra, both proton-coupled and -decoupled, were also obtained contemporaneously. Phosphetane **3.1**•[O] (δ 53.5 ppm) is consumed within 5 min and replaced by two signals (δ 32.4 and 18.9 ppm, 5:1 *anti*:*syn*) which were shown by independent synthesis to be the epimers of tricoordinate phosphetane **3.1**.

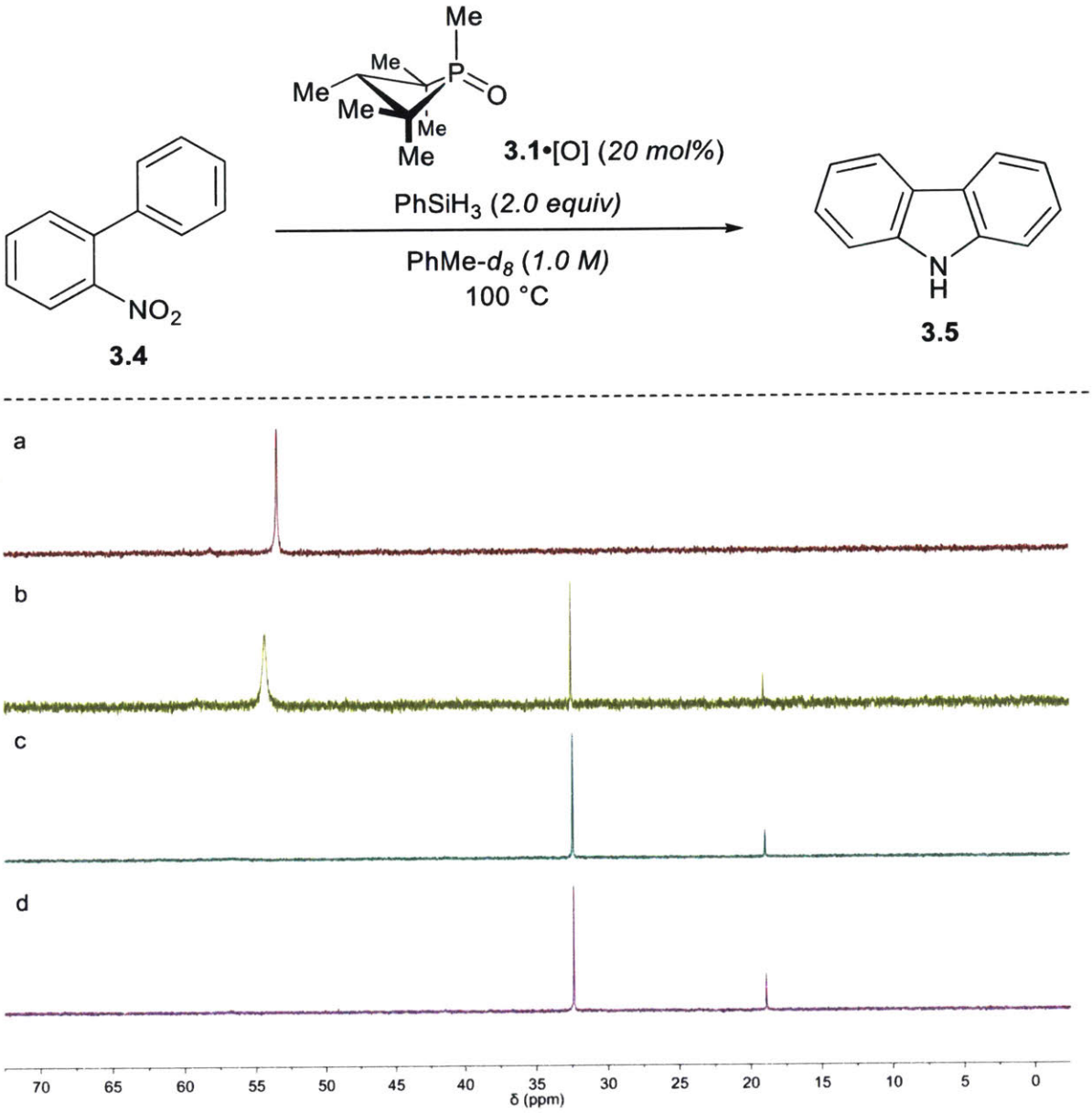

Figure 3.2 (from text)

iii. Low Temperature VT-NMR of Nitrosoarene (3.6)

To an oven-dried purged septum-sealed NMR tube was added **3.1** (8.4 mg, 0.053 mmol, 1 equiv.) in toluene-d_8 (0.4 mL, 0.13 M). The tube was frozen in liquid nitrogen, and a cold (−78 °C) solution of 2-nitrosobiphenyl (**3.6**, 12.3 mg, 0.067 mmol) in toluene- d_8 (0.6 mL, 0.11 M, 1.3 equiv) was layered on top via syringe injection. The resulting heterogeneous mixture was inserted into a -60 °C thermostatted NMR probe, where it underwent thawing and slow diffusional mixing over the course of ca. 80 min. ^{31}P NMR spectra, both proton-coupled and –decoupled, were recorded subsequently at 10 minute intervals. Phosphetane **3.1** (δ 24.2 *major*, 11.3 *minor* ppm) is converted to two new resonances (δ -24.4 *major*, -21.8 *minor* ppm) over the course of 2 h. At subsequent time points, these resonances diminish, concomitant with growth of signals corresponding to **3.1**•[O] (δ 54.1 *major*, 61.8 *minor* ppm). Upon termination of the experiment after 9 h, an aliquot of the mixture was analyzed by GCMS, with the presence of phosphetane *P*-oxide **3.1**•[O] and carbazole **3.5** as the only observable products.

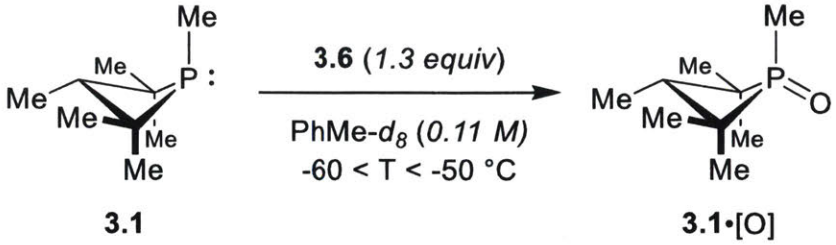

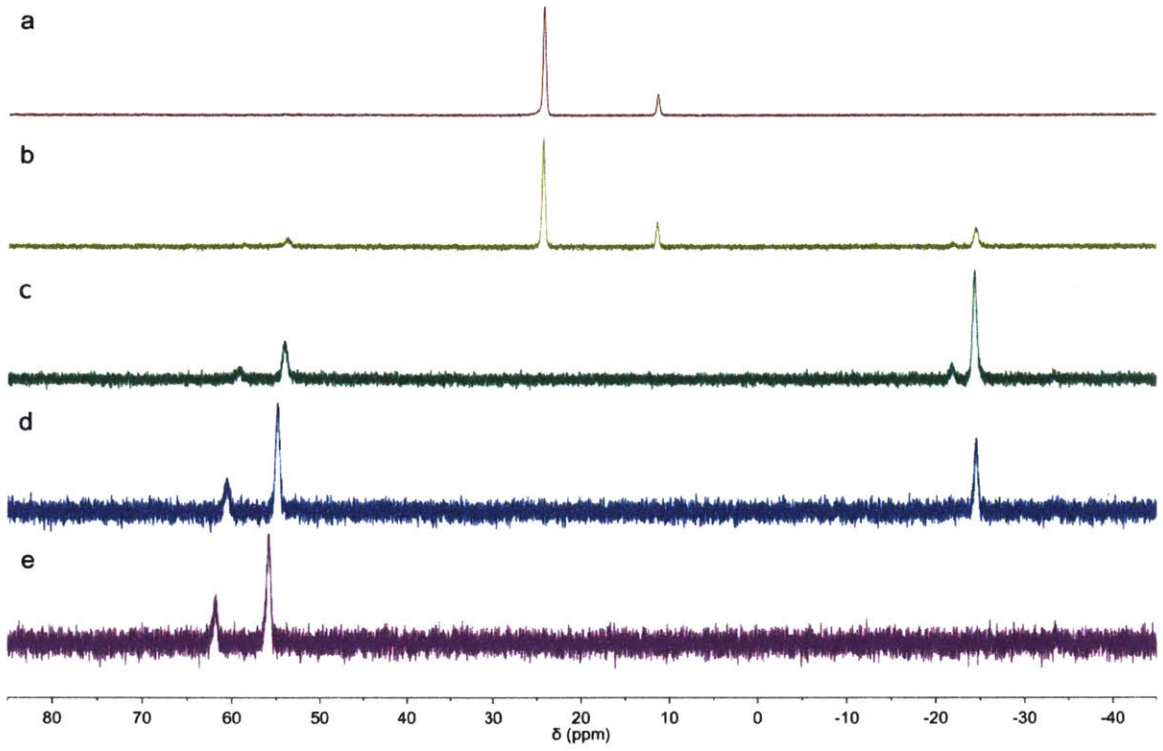

Figure 3.4 (from text)

iv. Low Temperature VT-NMR of ^{15}N-Nitrosoarene (3.6-^{15}N)

To an oven-dried purged septum-sealed NMR tube was added **3.1** (9.0 mg, 0.057 mmol, 1 equiv) in toluene-d_8 (0.4 mL, 0.14 M). The tube was frozen in liquid nitrogen, and a cold (−78 °C) solution of 2(^{15}N)-nitrosobiphenyl[10] (14.7 mg, 0.080 mmol) in toluene-d_8 (0.6 mL, 0.13M, 1.4 equiv) was layered on top via syringe injection. The resulting heterogeneous mixture was inserted

into a -60 °C thermostatted NMR probe, where it underwent thawing and slow diffusional mixing over the course of ca. 20 min. $^{31}P\{^{1}H\}$ and ^{15}N NMR spectra were obtained periodically. By 60 min, phosphetane **3.1** (δ 24.4 *major*, 11.5 *minor* ppm) is converted to two new doublets (δ -24.5 [J = 40.8 Hz] *major*, -21.9 [J = 39.5 Hz] *minor* ppm). Concomitantly, labeled nitrosobiphenyl (δ 922.3 ppm) is converted to two doublets (δ 238.9 [J = 40.6 Hz] *major*, 240.5 [J = 39.6 Hz] *minor* ppm). At subsequent time points, each of these resonances diminish, along with growth of signals corresponding to **3.1**•[O] (δ 54.1 *major*, 61.8 *minor* ppm) and ^{15}N-carbazole (δ 926.6 ppm). Upon termination of the experiment, an aliquot of the mixture was analyzed by GCMS, with the presence of phosphetane *P*-oxide **3.1**•[O] and ^{15}N-carbazole as the only observable products.

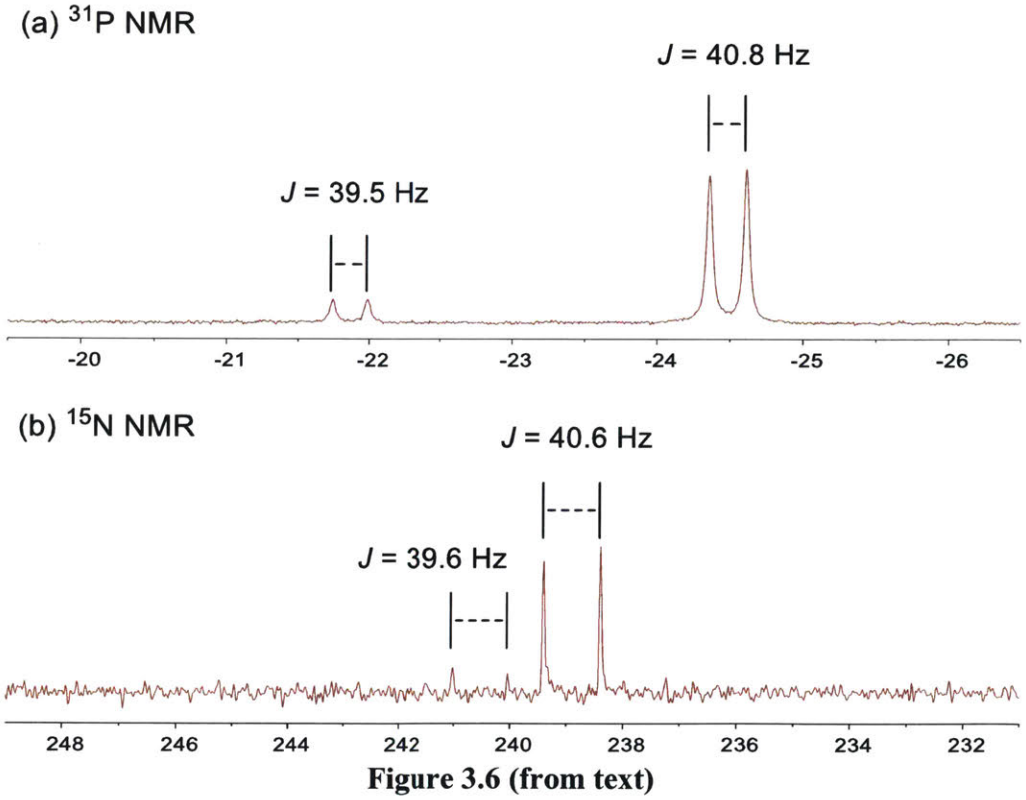

Figure 3.6 (from text)

B. Pseudo-first Order Kinetics with Excess Phosphine Reagent

In a nitrogen-filled glovebox, a stock solution of imine **3.2** (22.63 mM) and 1,3,5-trimethoxybenzene (31.96 mM) was prepared in toluene-d_8. To a volumetric flask was added 0.10 mL (0.002 mmol, 1 equiv.) of the prepared imine/internal standard stock solution and 0.37 mL of a 1.0 M solution of phosphetane **3.1** (0.32 mmol, 160 equiv.) or 0.36 mL of a 1.0 M solution of phosphine **2.2** (0.32 mmol, 160 equiv) and the resulting mixture was diluted to 1 mL with toluene-d_8. The diluted solution (0.5 mL) was then transferred to a septum-sealed NMR tube, and the loss of **3.2** was monitored with ^{1}H NMR at 80 °C (2 scans collected each minute). The concentrations of **3.2** were obtained from the ratio of the area of the imine methine (set to 1.00) relative to that of the internal standard. Duplicate runs were performed for each phosphine, which were used to determine the average and standard deviation of error.

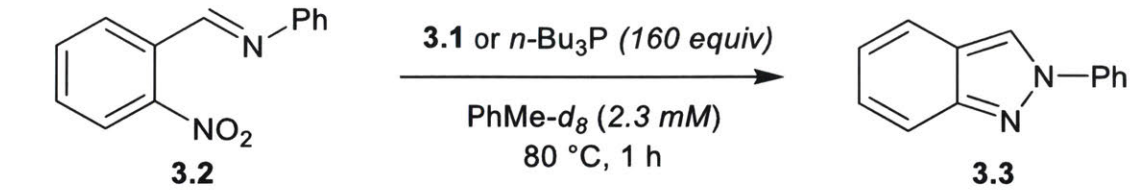

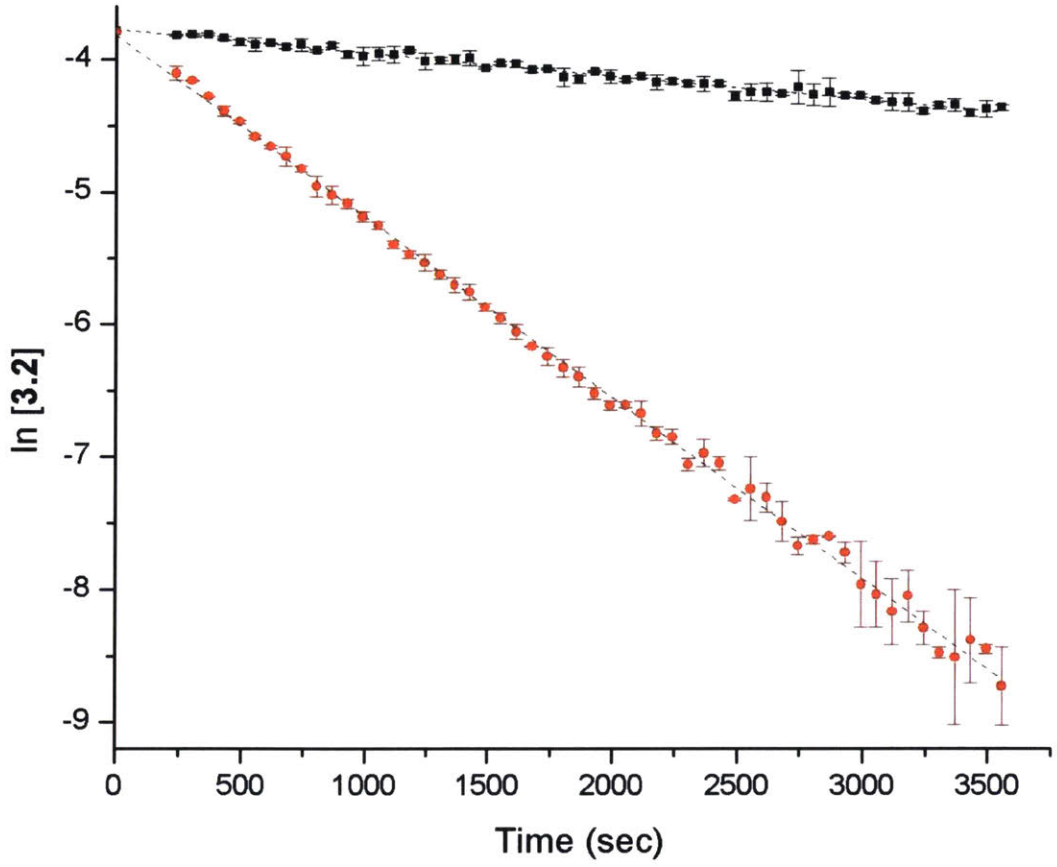

Figure 3.3 (from text)

VI. Control Experiment

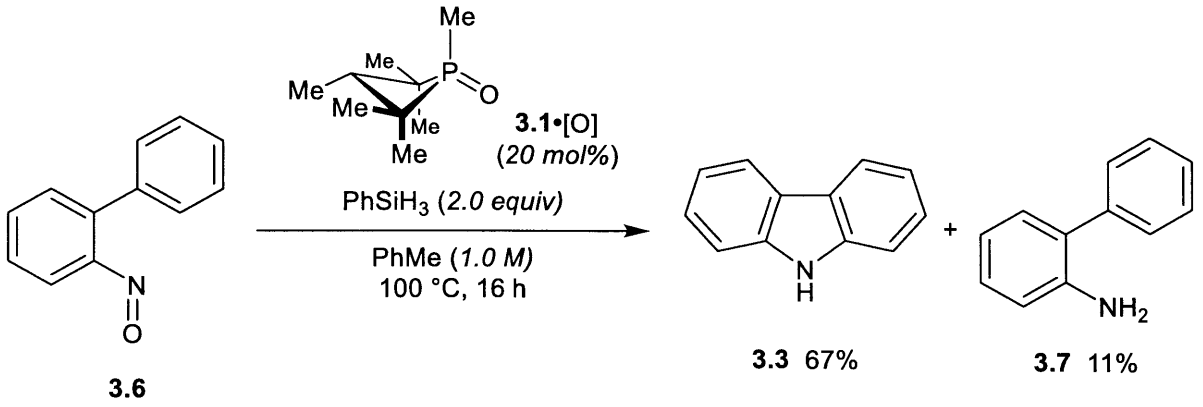

Figure 3.4 (from text)

2-nitrosobiphenyl **3.6** (92 mg, 0.5 mmol), **3.1**•[O] (13 mg, 0.075 mmol), and dodecane (84 mg, 0.49 mmol) were added to an oven-dried 4 mL screw cap vial equipped with a septum and a stir bar. After exchange of atmosphere for nitrogen, toluene (0.5 mL, 1.0 M) was added via syringe, followed by the silane (0.12 mL, 1.0 mmol). The sample was heated at 100 °C for 16 h, then cooled to room temperature and diluted with ethyl acetate (2 mL). After stirring, 40 μL of the diluted reaction mixture was added to 1.5 mL of ethyl acetate inside of a GC vial and the sample was analyzed (1.2 μL injection) using an Agilent 7890A gas chromatograph fitted with a J&W DB-1 column (10 m, 0.1 I.D.). Retention times: 2.8 min (dodecane), 3.9 min (2-aminobiphenyl **3.7**), 4.6 min (carbazole **3.3**). Calibration curves were made using authentic analytes prior to the start of this study.

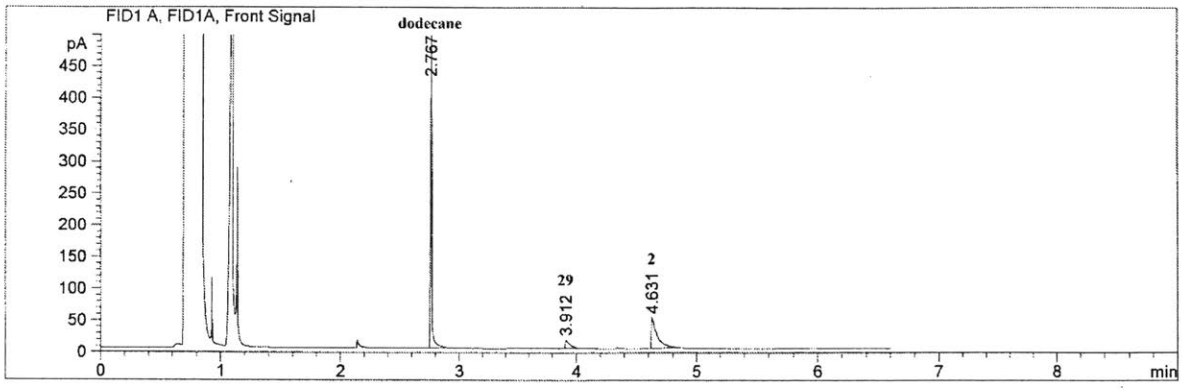

Peak #	RetTime [min]	Type	Width [min]	Area [pA*s]	Height [pA]	Area %
1	2.767	BB	0.0126	375.06497	463.41080	66.31631
2	3.912	BB	0.0354	32.75768	12.18528	5.79198
3	4.631	BB	0.0452	157.74709	47.39991	27.89171

VII. Initial Optimization of Catalytic Nitro Reduction Conditions

A. General Procedure A (NMR, no standard)

To a 4 mL oven-dried vial equipped with magnetic stirring was added nitro (1.0 equiv.) and phosphine oxide precatalyst (15 mol%). The vial was then sealed with a Teflon-wrapped septum cap, and the atmosphere was replaced with nitrogen. Solvent (1.0 M), then silane (2.0 equiv.) were added sequentially. The vial was heated to 100 °C for 21-22 h. Following cooling, an aliquot was removed and diluted with $CDCl_3$. The mixture was then analyzed by ^1H NMR, with yields determined by relative ^1H integration (integration of amine / integration of amine and nitro).

B. General Procedure B (NMR, internal standard)

To a 4 mL oven-dried vial equipped with magnetic stirring was added nitro (1.0 equiv.), phosphine oxide precatalyst (25 mol%) and 1,3,5-trimethoxybenzene internal standard (1.0 equiv.). The vial was then sealed with a Teflon-wrapped septum cap, and the atmosphere was replaced with nitrogen. Solvent (1.0 M), then silane (4.0 equiv.) were added sequentially. The vial was heated to

100 °C for 21 h. Following cooling, an aliquot was removed and diluted with $CDCl_3$. The mixture was then analyzed by ^1H NMR, with yields determined with respect to the internal standard.

C. General Procedure C (GC/MS, internal standard)

To a 4 mL oven-dried vial equipped with magnetic stirring was added nitro (1.0 equiv.), phosphine oxide precatalyst (25 mol%) and dodecane internal standard (1.0 equiv.). The vial was then sealed with a Teflon-wrapped septum cap, and the atmosphere was replaced with nitrogen. Solvent (1.0 M), then silane (4.0 equiv.) were added sequentially. The vial was heated to 100 °C for 17-21 h, then cooled to room temperature and diluted with ethyl acetate (2.0 mL). After stirring, 20 μL of the diluted reaction mixture was added to 1.5 mL of ethyl acetate inside of a GC vial, and the sample was analyzed (0.7 μL injection) using a Shimadzu GC-2010 gas chromatograph fitted with a SHRXI-5MS column (30 m, 0.25 I.D.). Calibration curves were made using authentic analytes prior to the start of this study.

D. Optimization with *p*-Nitrotoluene

Table 4.1 (from text). Solvent screen for reduction of *p*-nitrotoluene.[a]

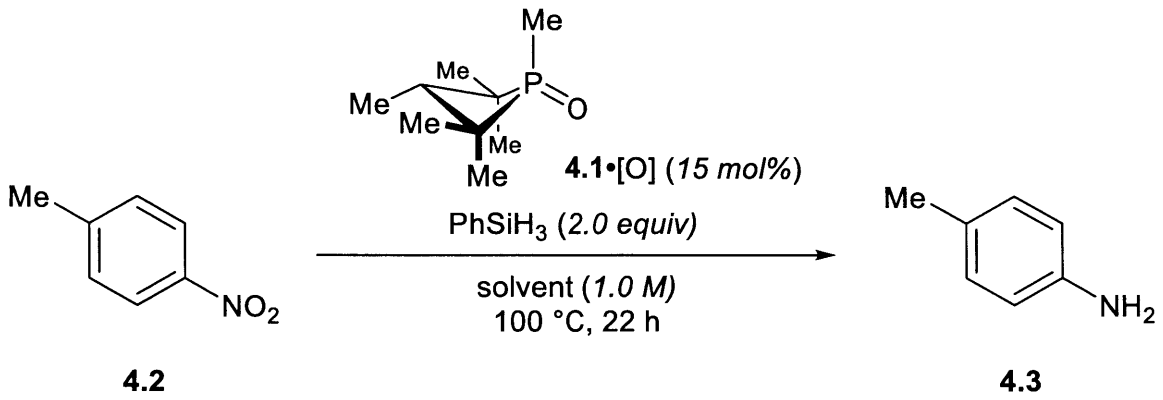

4.2 **4.3**

Entry	Solvent	Conversion (%)
1[b]	TFE	0[c]
2	*n*-BuOH	3
3	AcOH	0[c]
4	PhMe	4
5	Ethylene glycol	0
6	Glycerol	0

[a] Conversion determined by relative ^{1}H NMR integration (integration of amine / integration of amine and nitro). [b] Reaction performed at 70 °C. [c] Reduction of phosphetane *P*-oxide **4.1**•[O] not observed in absence of substrate.

Reactions were performed according to general procedure A. Chemical shifts: nitro **4.2** δ 2.46 ppm; aniline **4.3** δ 2.23 ppm.

^1H NMRs for data tabulated in Table 4.1.

Table 4.1, Entry 1

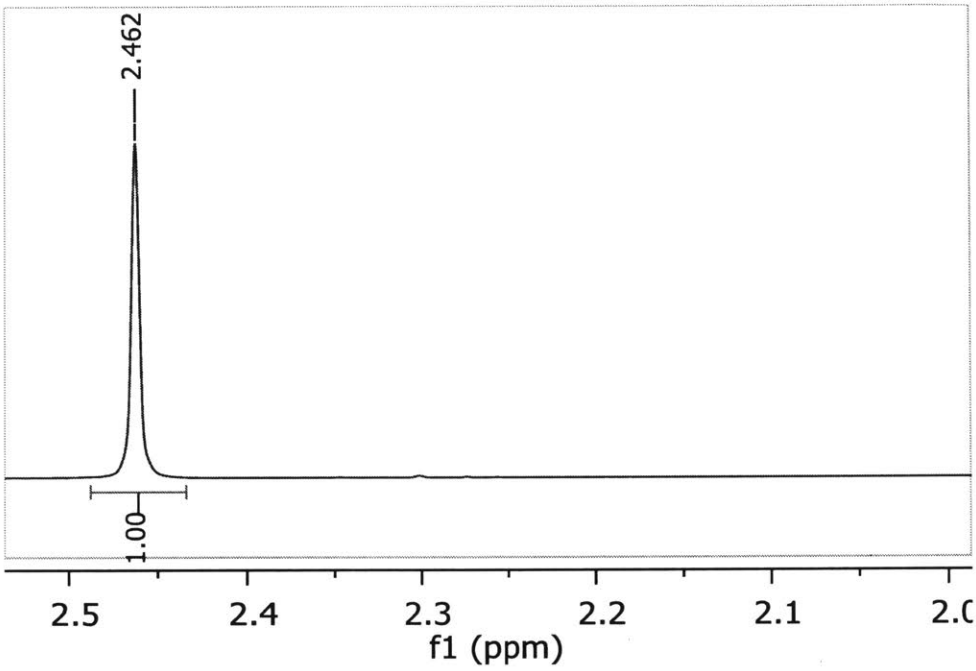

Table 4.1, Entry 2

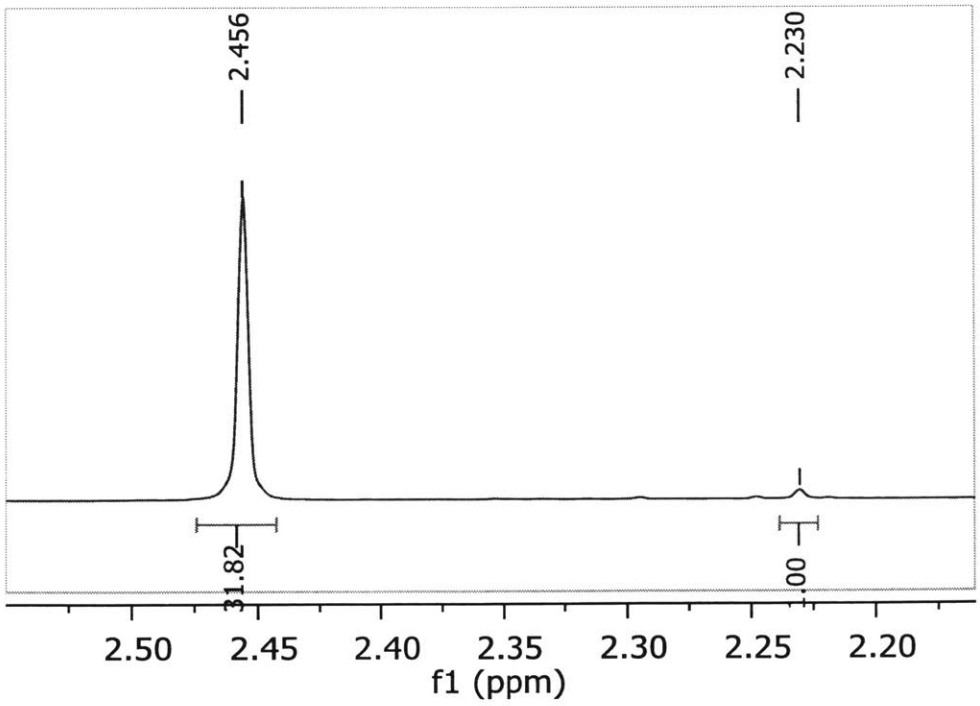

Table 4.1, Entry 3

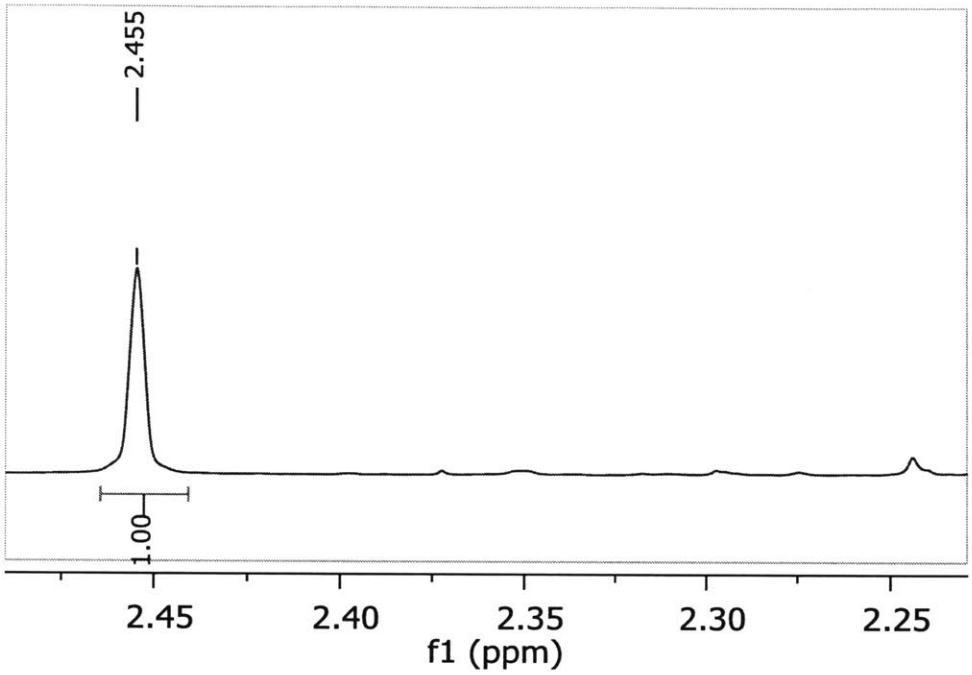

Table 4.1, Entry 4

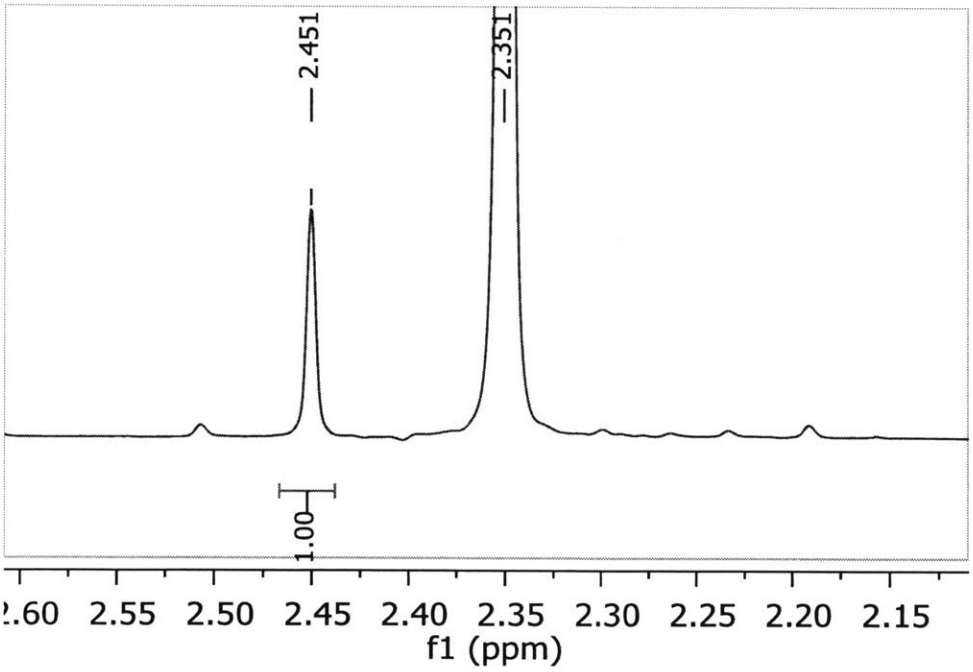

Table 4.1, Entry 5

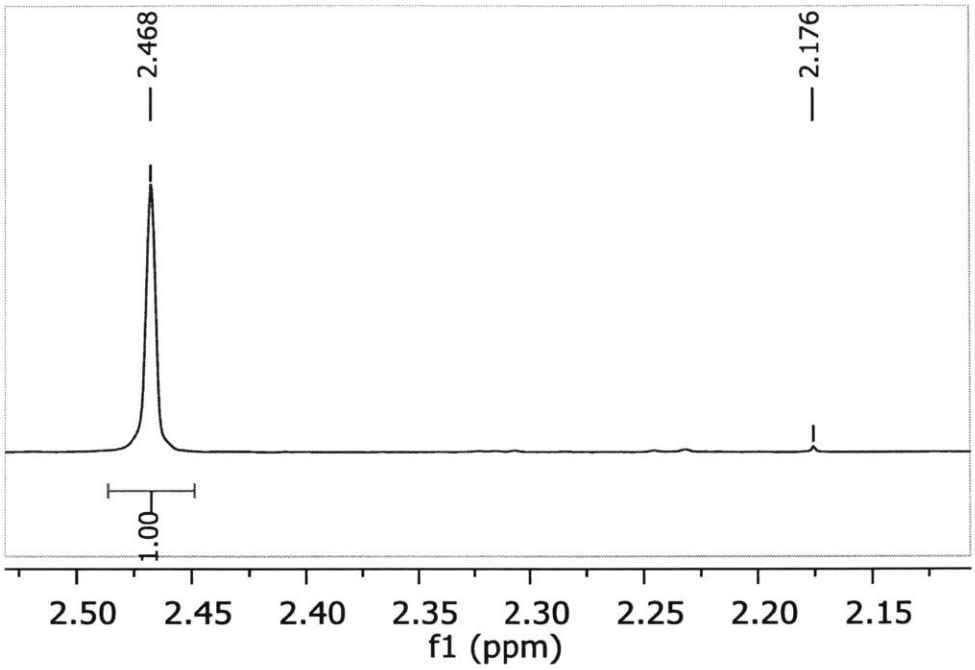

Table 4.1, Entry 6

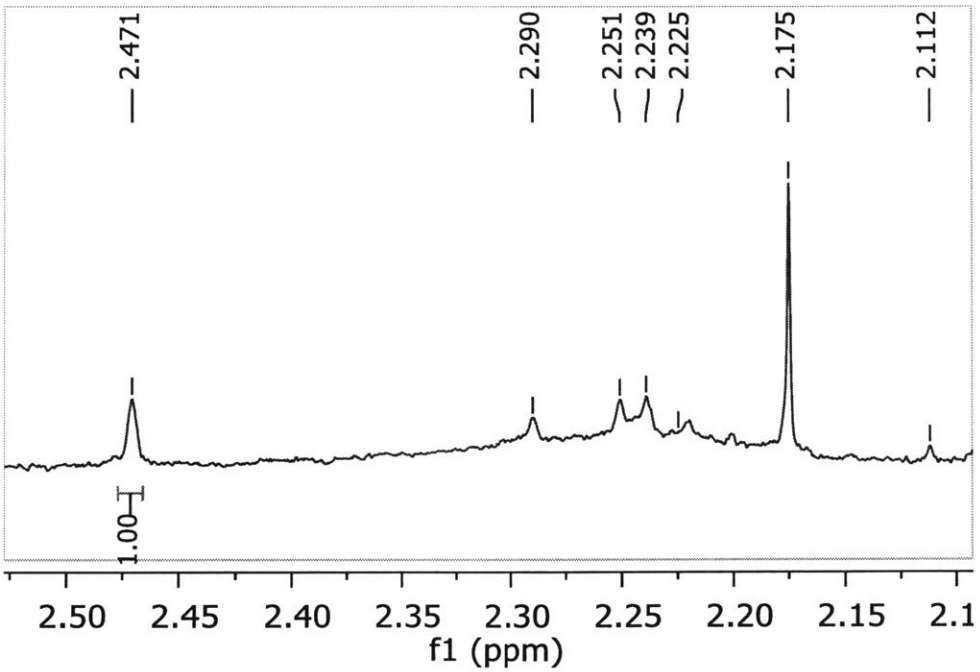

E. Optimization with *p*-Chloronitrobenzene

Table 4.2 (from text). Experiments involving electronically deficient *p*-chloronitrobenzene..[a]

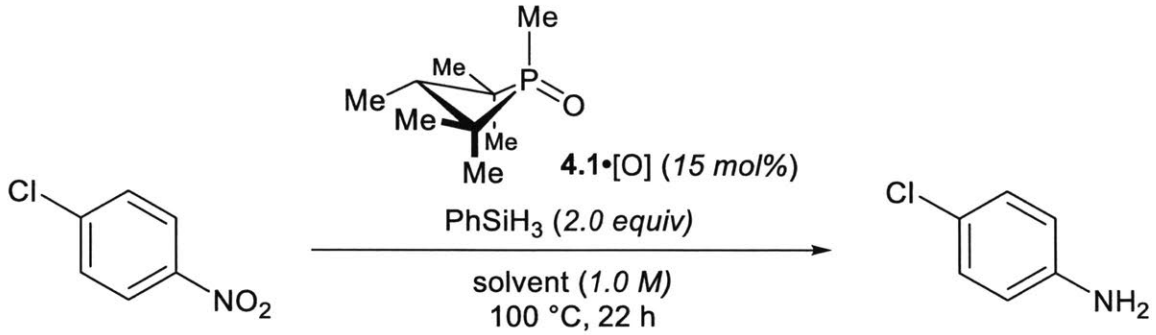

4.4 **4.5**

Entry	Solvent	Conversion (%)
1	TFE	1
2	*n*-BuOH	Trace[b]

[a] Conversion determined by relative ^{1}H NMR integration (integration of amine / integration of amine and nitro). [b] Trace aniline observed, but other signals prevent integration.

Reactions were performed according to general procedure A. Chemical shifts: nitro **4.4** δ 8.19, 7.53 ppm; aniline **4.5** δ 7.06, 6.53 ppm.

^{1}H NMRs for data tabulated in Table 4.2.

Table 4.2, Entry 1

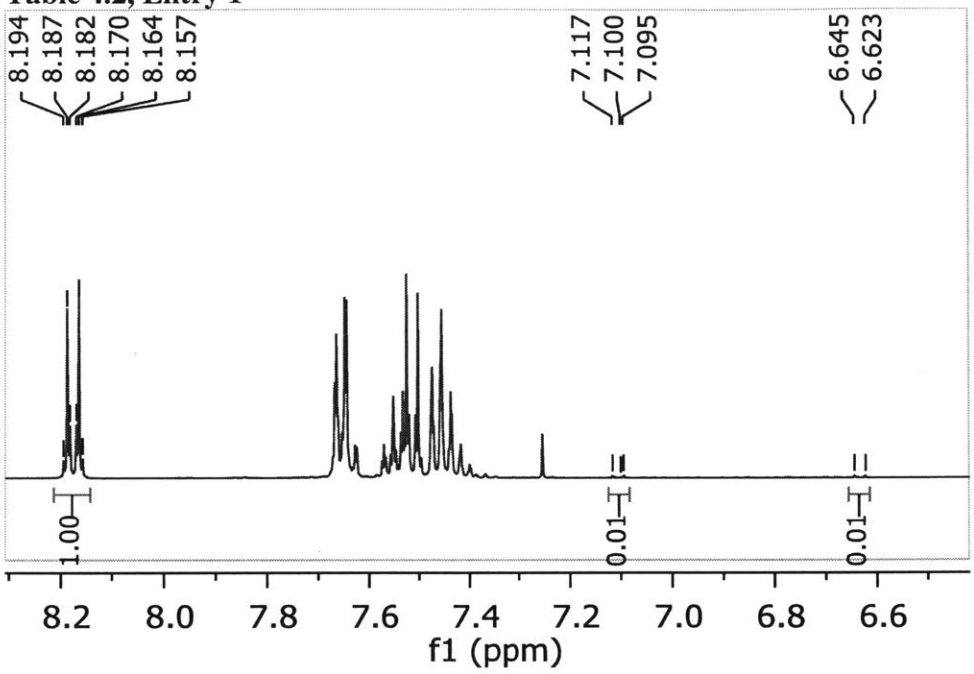

Table 4.2, Entry 2

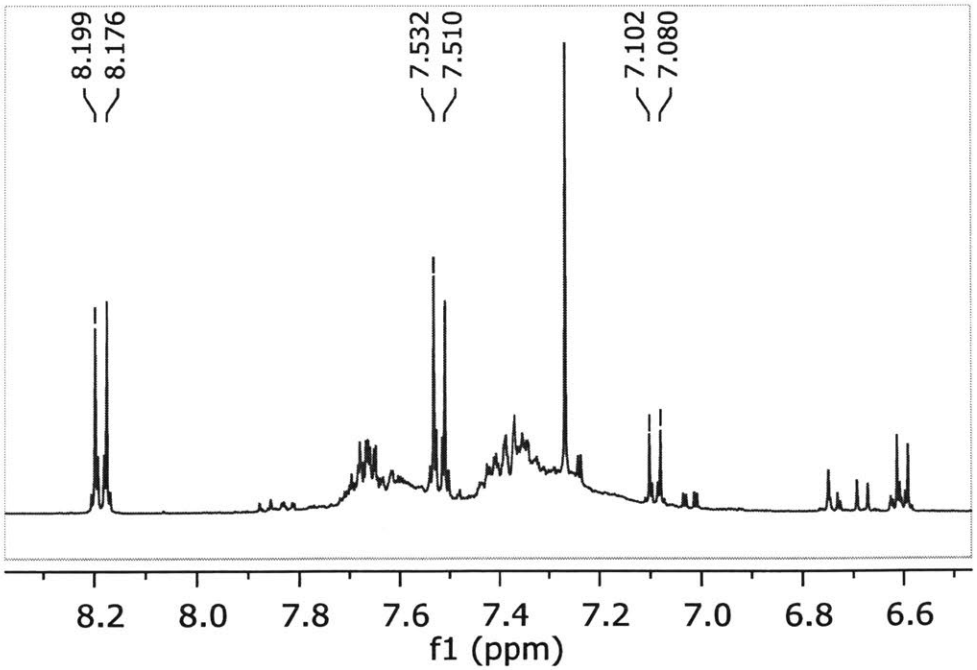

F. Optimization with *p*-Dinitrobenzene

Table 4.3 (from text). Optimization experiments involving *p*-dinitrobenzene without internal standard.[a]

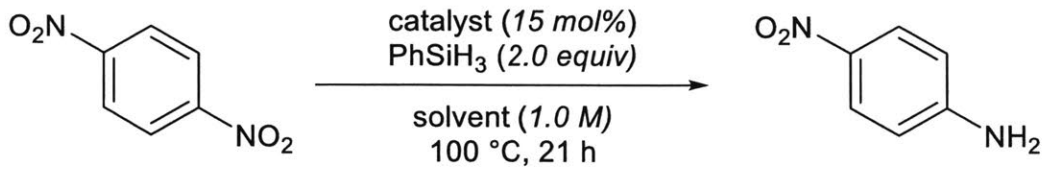

4.6 **4.7**

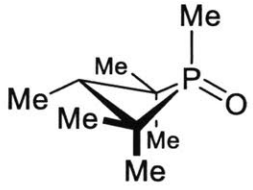

4.1•[O]

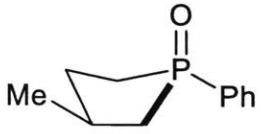

4.8•[O]

Entry	Catalyst	Solvent	Conversion (%)
1	**4.1**•[O]	TFE	2
2	**4.1**•[O]	n-BuOH	10
3	**4.8**•[O]	TFE	42
4	**4.8**•[O]	n-BuOH	19

[a] Conversion determined by relative ^{1}H NMR integration (integration of amine / integration of amine and nitro).

Reactions were performed according to general procedure A. Chemical shifts: nitro **4.6** δ 8.43 ppm; aniline **4.7** δ 8.07, 6.62 ppm.

^1H NMRs for data tabulated in Table 4.3.

Table 4.3, Entry 1

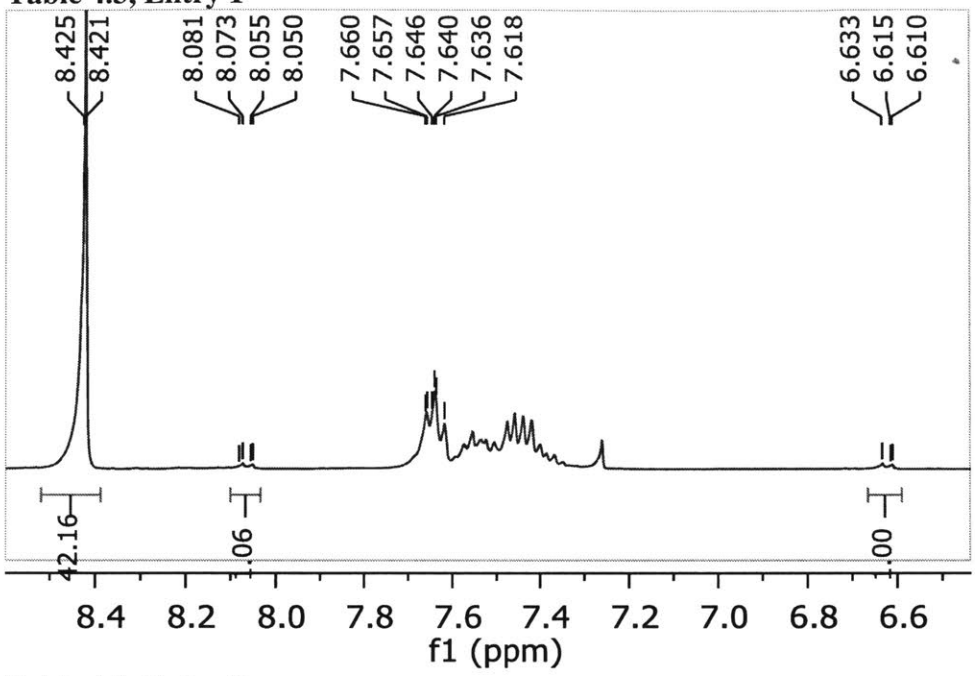

Table 4.3, Entry 2

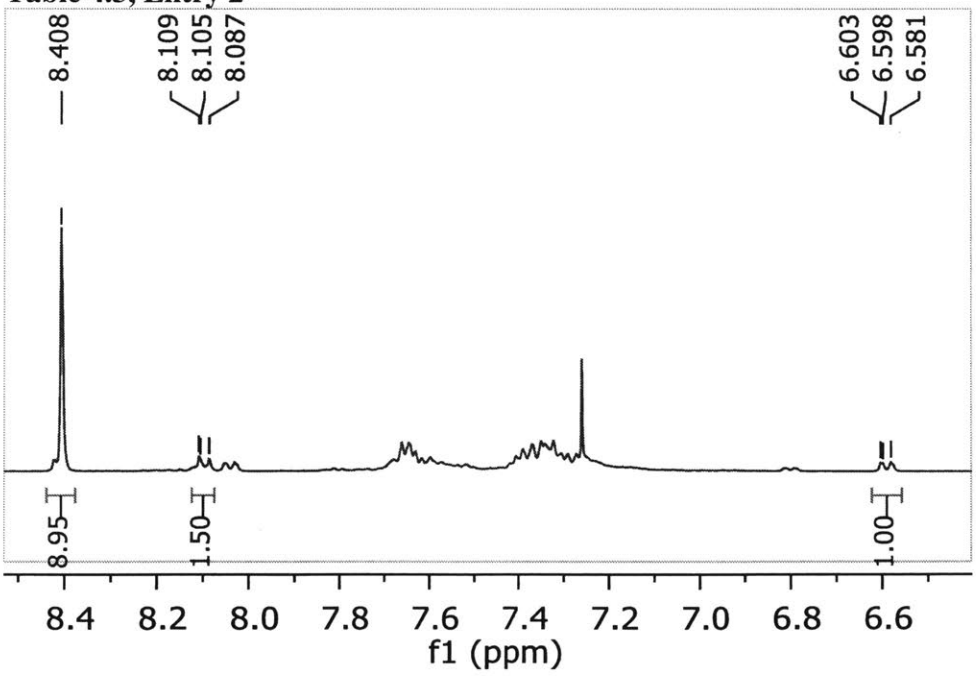

Table 4.3, Entry 3

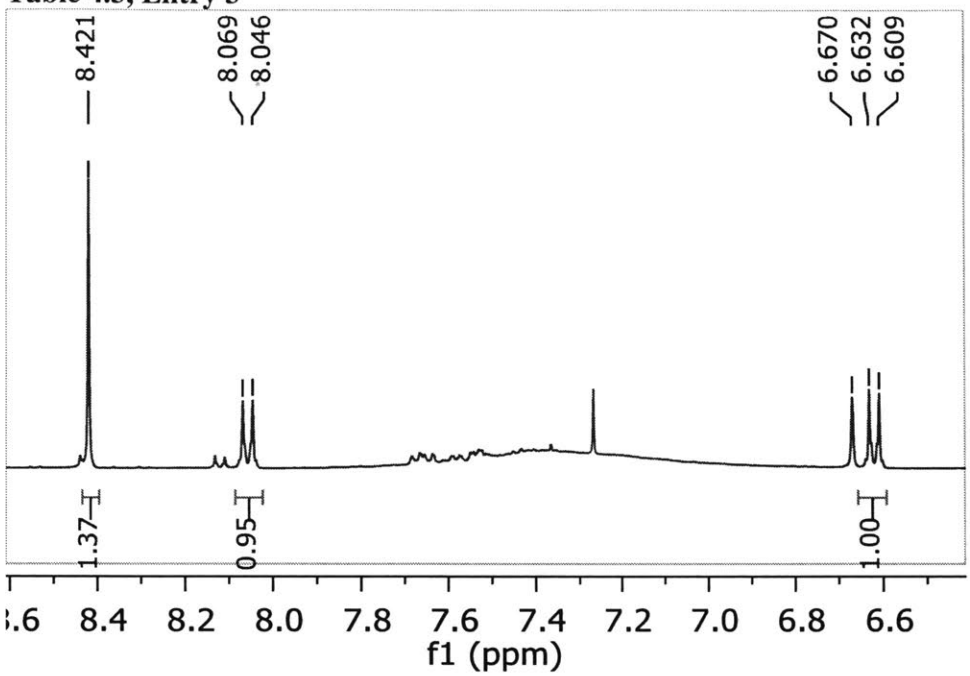

Table 4.3, Entry 4

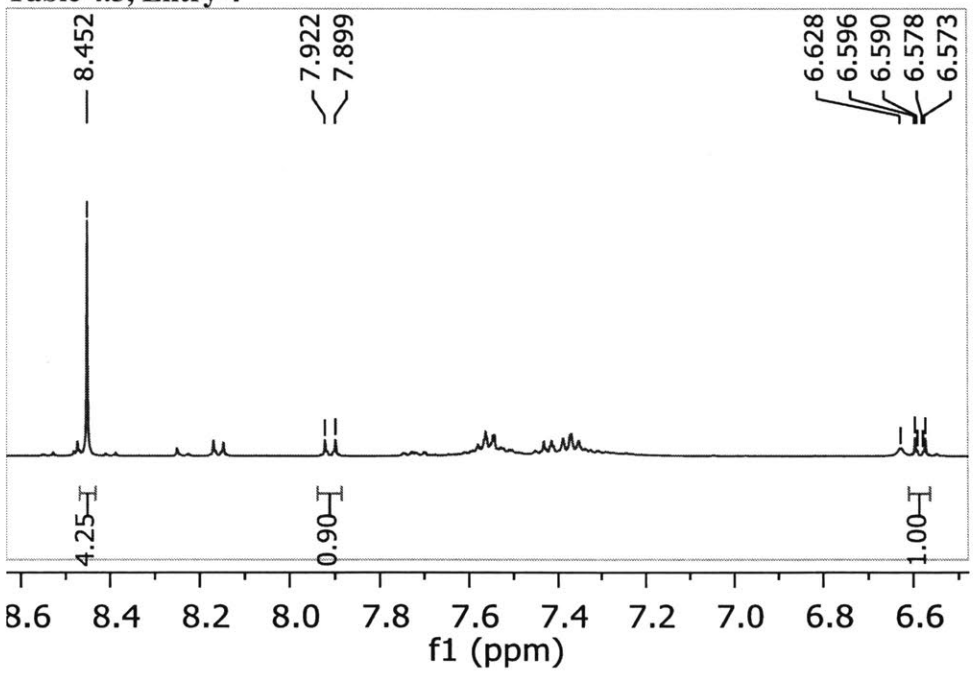

Table 4.4 (from text). Optimization experiments involving *p*-dinitrobenzene with internal standard.[a]

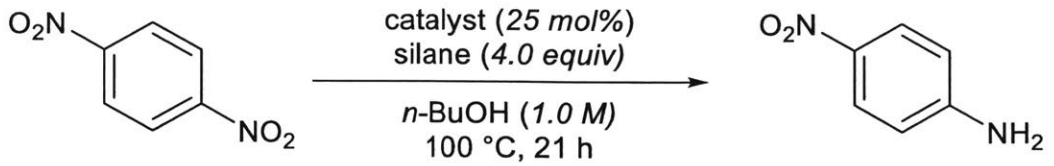

4.6 **4.7**

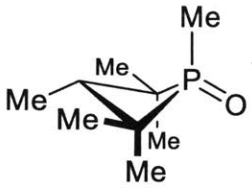

4.1•[O]

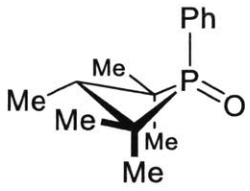

4.9•[O]

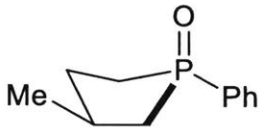

4.8•[O]

Entry	Catalyst	Silane	Conversion (%)	Yield (%)
1	**4.1**•[O]	$PhSiH_3$	97	36
2	**4.1**•[O]	$(MeO)_2MeSiH$	56	7
3	**4.1**•[O]	$(EtO)_2MeSiH$	64	9
4	**4.9**•[O]	$PhSiH_3$	59	28
5[b]	**4.8**•[O]	$PhSiH_3$	78	51

[a] Conversion and yield determined by ^1H NMR with respect to 1,3,5-trimethoxybenzene internal standard. [b] TFE used as solvent.

Reactions were performed according to general procedure B. Chemical shifts: nitro **4.6** δ 8.23 ppm; aniline **4.7** δ 7.91, 6.40 ppm; 1,3,5-trimethoxybenzene δ 5.99 ppm.

^{1}H NMRs for data tabulated in Table 4.4.

Table 4.4, Entry 1

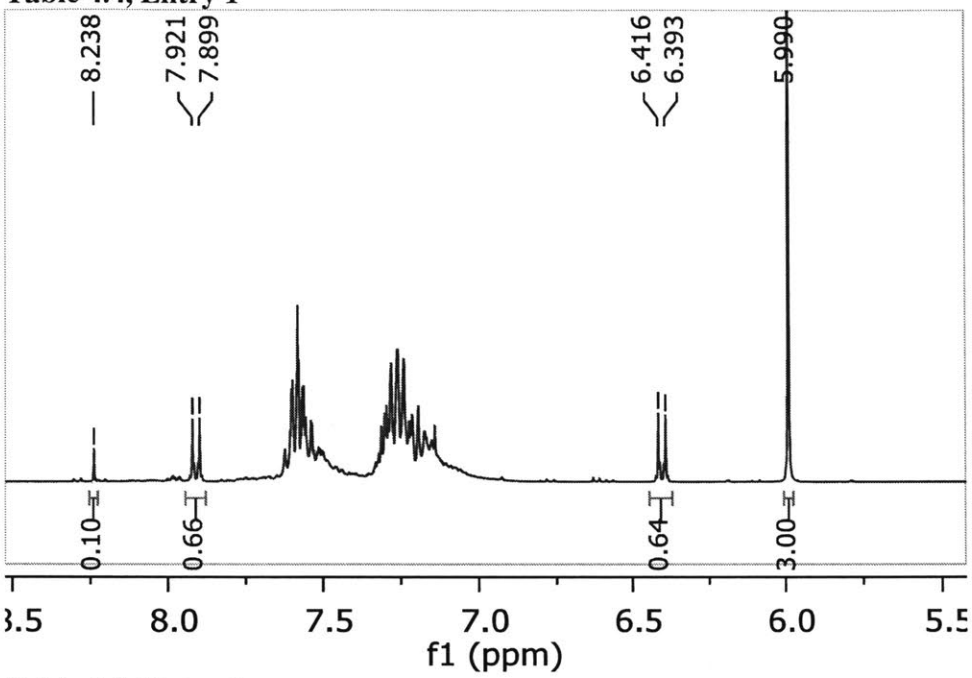

Table 4.4, Entry 2

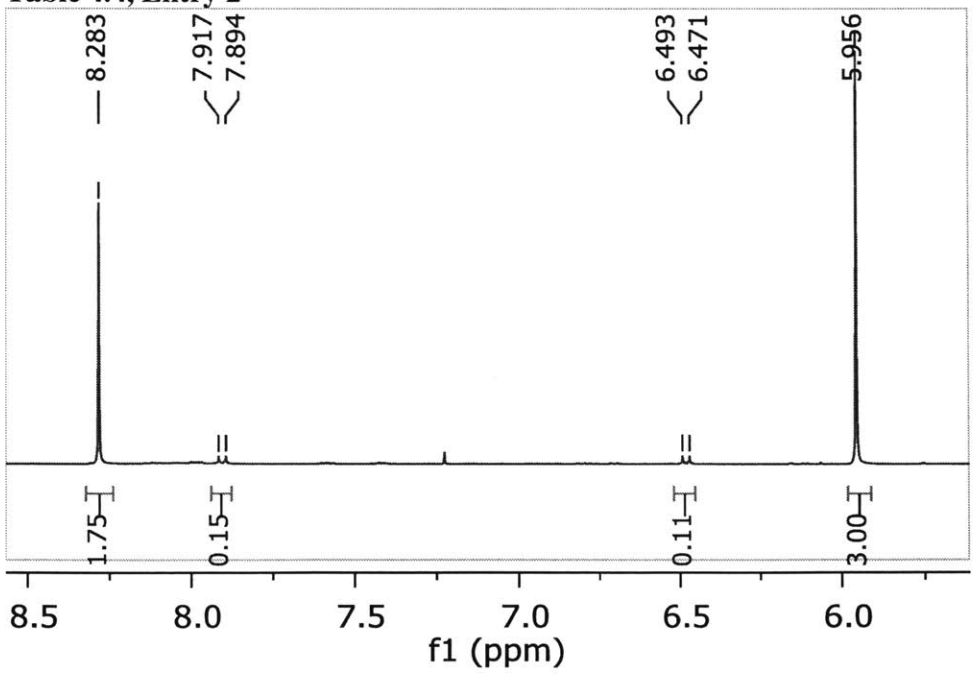

Table 4.4, Entry 3

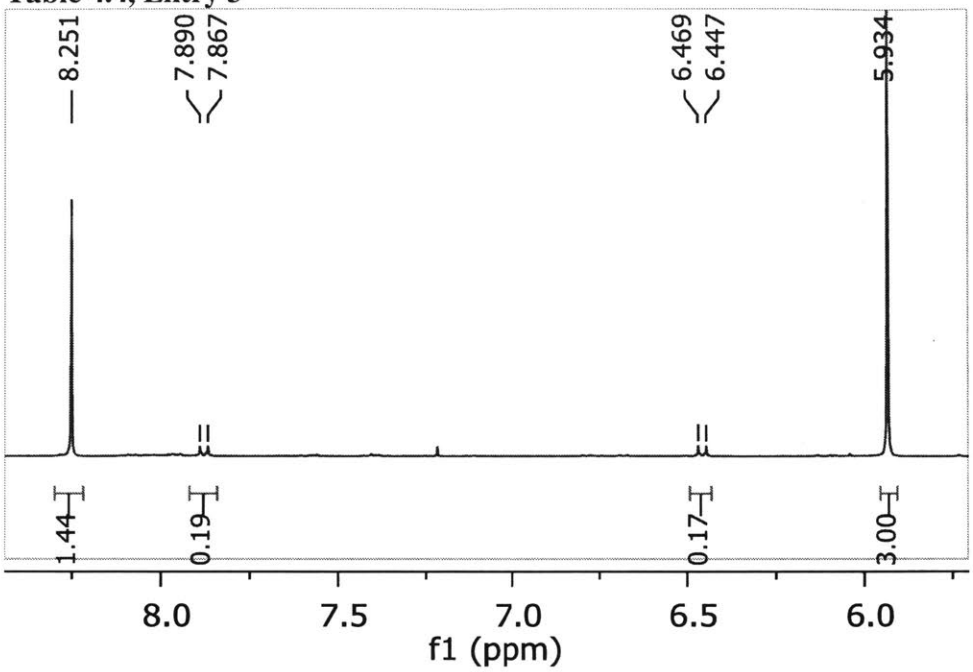

Table 4.4, Entry 4

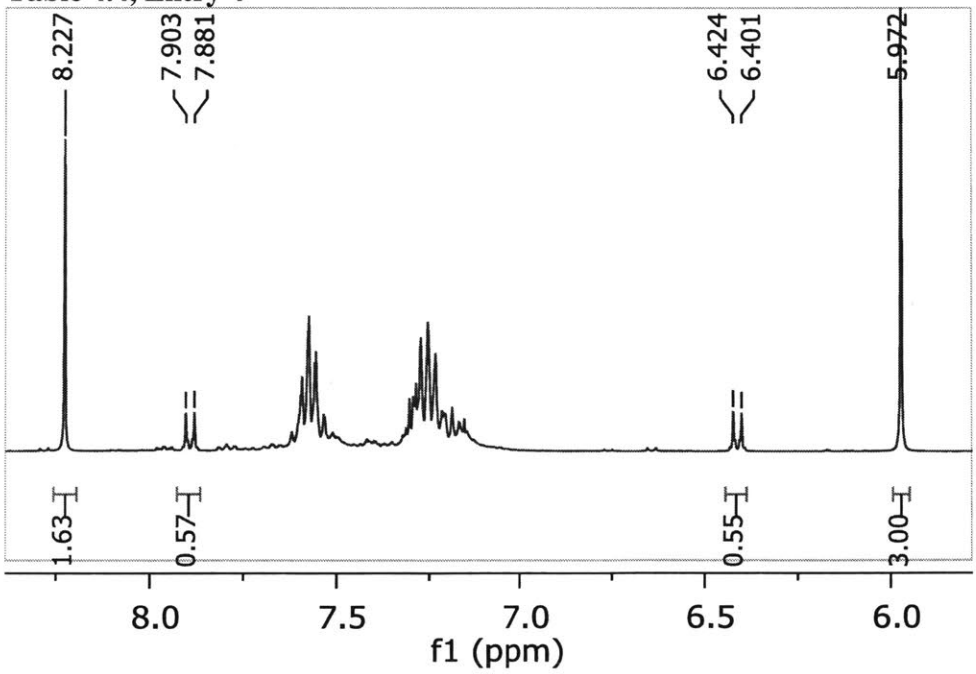

G. Optimization with *p*-Nitrobenzonitrile

Table 4.5. Optimization experiments involving *p*-nitrobenzonitrile.

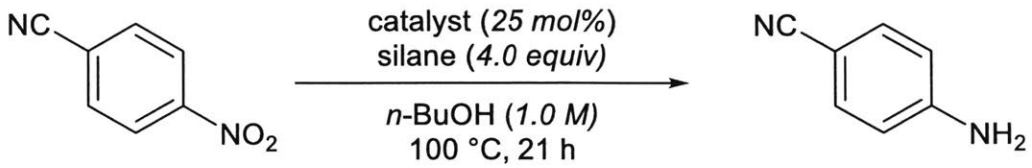

4.10 **4.11**

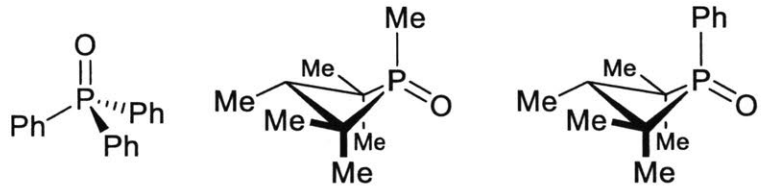

4.12•[O] **4.1•[O]** **4.9•[O]**

Entry	Catalyst	NMR Conversion (%) [a]	NMR Yield (%) [a]	GCMS Conversion (%) [b]	GCMS Yield (%) [b]	Unknown Yield (%) [b,c]
1	**4.12**•[O]	13	Trace	79[c]	Trace[c]	79
2	**4.1**•[O]	97	19	87	10	83
3	**4.9**•[O]	63	31	70	34	64

[a] Conversion and yield determined with respect to 1,3,5-trimethoxybenzene internal standard. [b] Conversion and yield determined with respect to dodecane internal standard. [c] Yield determined by relative GC integration (area of interest / sum of unknown, nitro, aniline areas).

Reactions were performed according to general procedure B and C. Chemical shifts: nitro **4.10** δ 8.35, 7.89 ppm; aniline **4.11** δ 7.37, 6.62 ppm; 1,3,5-trimethoxybenzene δ 6.07 ppm. Retention times: 5.83 min (dodecane), 7.03 min (nitro **4.10**), 7.67 min (aniline **4.11**).

[1]H NMRs and chromatographs for data tabulated in Table 4.5.

Table 4.5, Entry 1

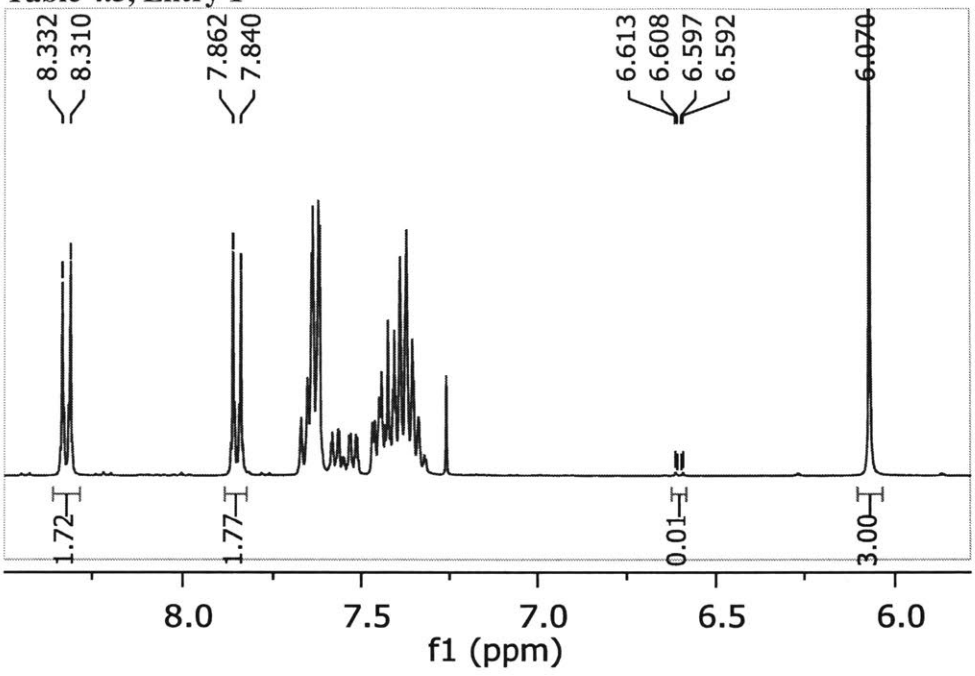

C:\GCMSsolution\Tyler\Nitro to Aniline\tsh_192-17.qgd

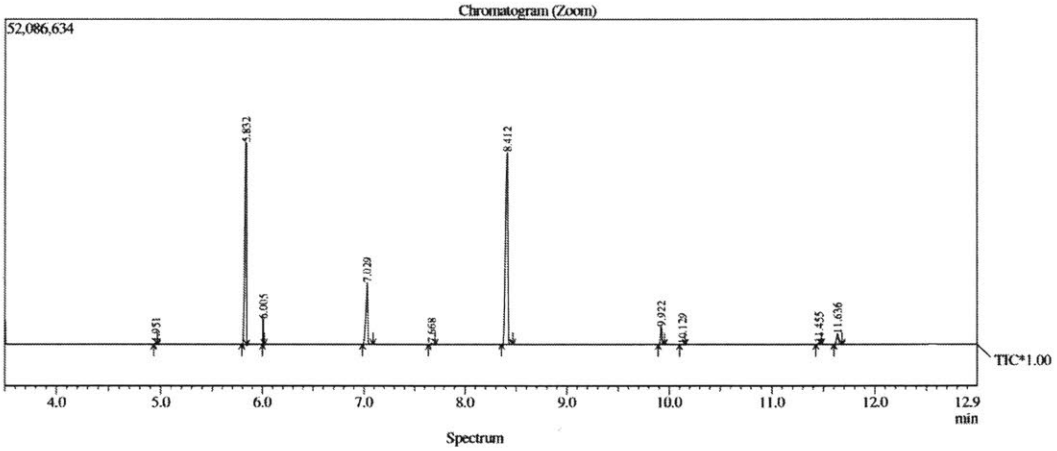

Peak Report TIC

Peak#	R.Time	I.Time	F.Time	Area	Area%	Height	Height%	A/H	Mark	Name
1	4.951	4.935	4.970	216864	0.20	243004	0.30	0.89	MI	
2	5.832	5.795	5.840	35605078	33.51	32423224	39.37	1.10	MI	
3	6.005	6.000	6.015	1228942	1.16	3995470	4.85	0.31	MI	
4	7.029	6.985	7.090	13290718	12.51	9896399	12.02	1.34	MI	
5	7.668	7.635	7.705	167976	0.16	168802	0.20	1.00	MI	
6	8.412	8.355	8.465	50222908	47.27	30808235	37.40	1.63	MI	
7	9.922	9.890	9.955	2788283	2.62	2841879	3.45	0.98	MI	
8	10.129	10.100	10.155	39320	0.04	44118	0.05	0.89	MI	
9	11.455	11.425	11.480	274426	0.26	247517	0.30	1.11	MI	
10	11.636	11.600	11.680	2421888	2.28	1696721	2.06	1.43	MI	
				106256403	100.00	82365369	100.00			

Table 4.5, Entry 2

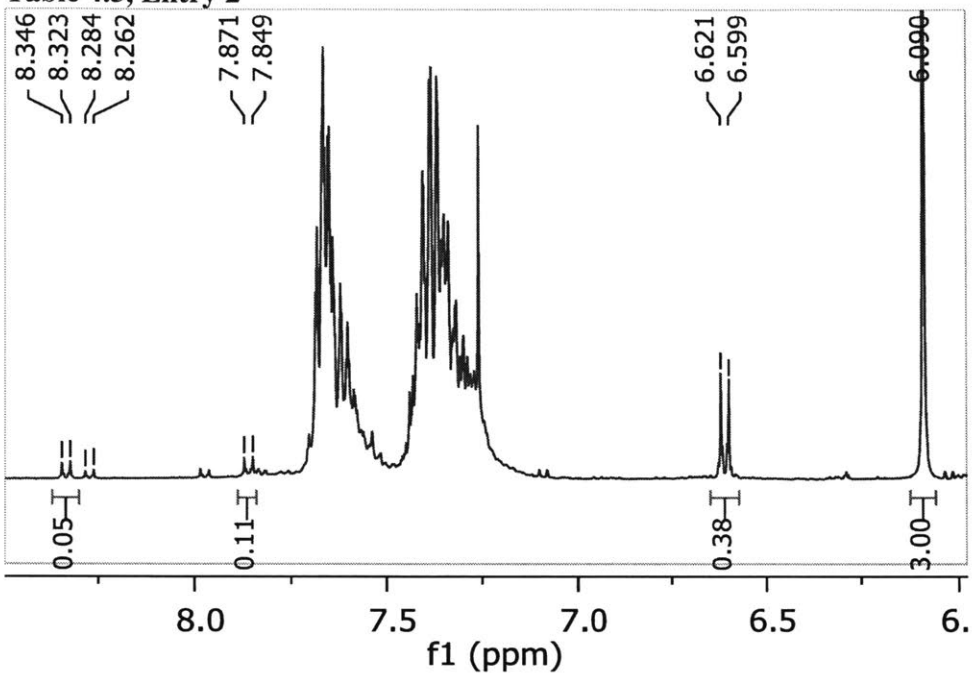

C:\GCMSsolution\Tyler\Nitro to Aniline\tsh_193-17.qgd

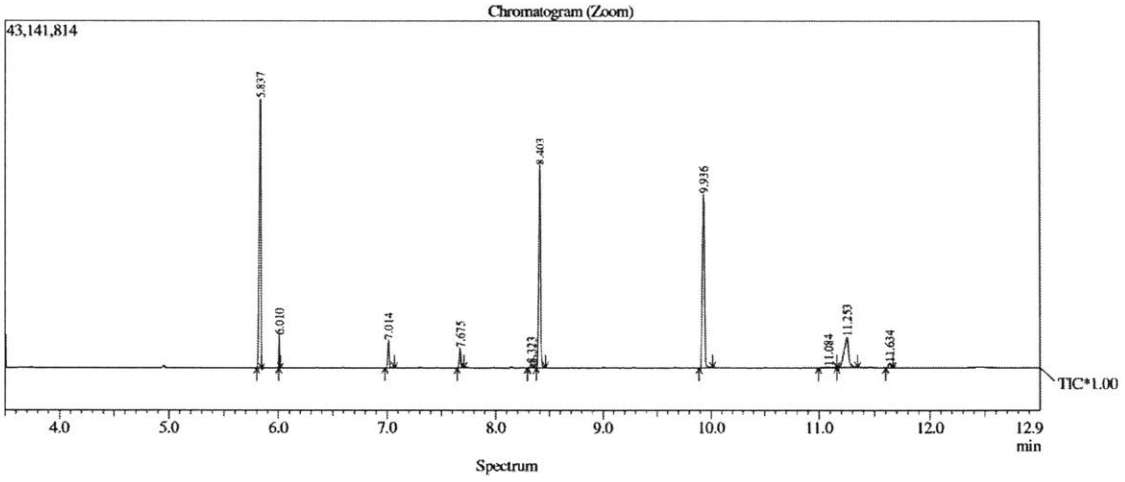

Peak Report TIC

Peak#	R.Time	I.Time	F.Time	Area	Area%	Height	Height%	A/H	Mark	Name
1	5.837	5.800	5.845	40815558	33.11	33504035	35.10	1.22	MI	
2	6.010	6.005	6.020	1237450	1.00	4042871	4.24	0.31	MI	
3	7.014	6.980	7.070	3089115	2.51	3457821	3.62	0.89	MI	
4	7.675	7.645	7.710	2272965	1.84	2430615	2.55	0.94	MI	
5	8.323	8.290	8.345	541645	0.44	522277	0.55	1.04	MI	
6	8.403	8.365	8.460	32847851	26.65	25272077	26.48	1.30	MI	
7	9.936	9.890	10.015	30261486	24.55	21702012	22.74	1.39	MI	
8	11.084	10.995	11.160	466780	0.38	105860	0.11	4.41	MI	
9	11.253	11.160	11.350	10825928	8.78	3796754	3.98	2.85	MI	
10	11.634	11.600	11.665	910488	0.74	618426	0.65	1.47	MI	
				123269266	100.00	95452748	100.00			

Table 4.5, Entry 3

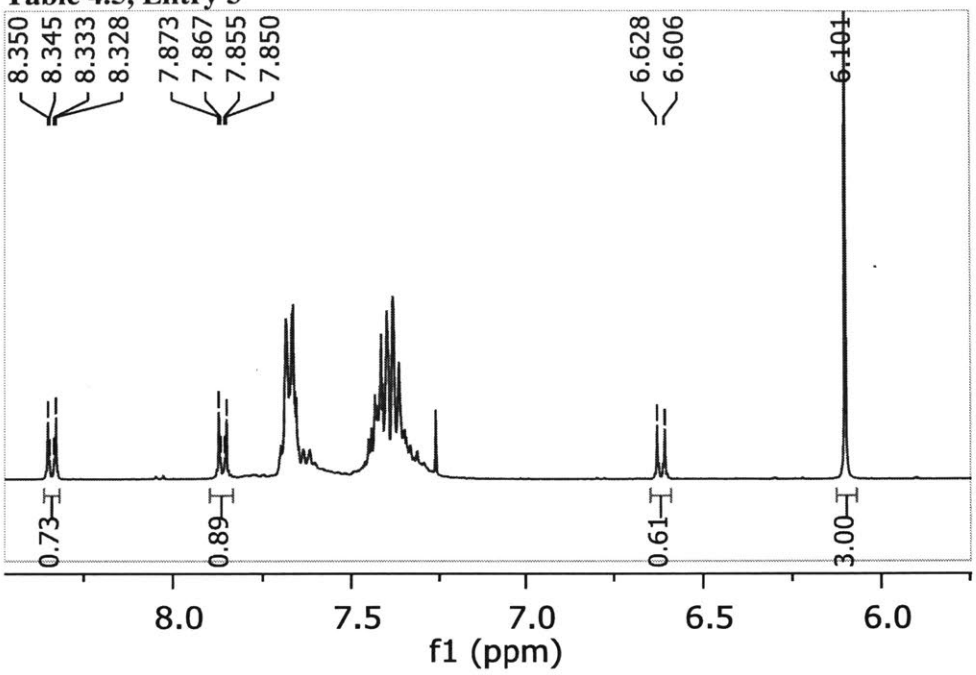

C:\GCMSsolution\Tyler\Nitro to Aniline\tsh_194-17.qgd

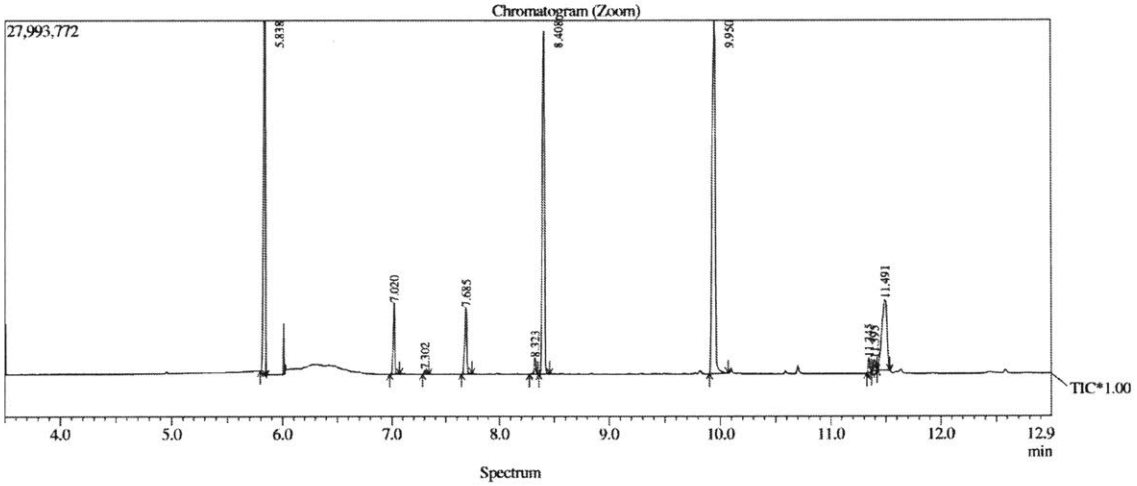

Peak Report TIC

Peak#	R.Time	I.Time	F.Time	Area	Area%	Height	Height%	A/H	Mark	Name
1	5.838	5.795	5.845	39127895	23.39	34014704	31.12	1.15	MI	
2	7.020	6.980	7.070	5587421	3.34	5651094	5.17	0.99	MI	
3	7.302	7.280	7.340	322217	0.19	335672	0.31	0.96	MI	
4	7.685	7.645	7.740	6073429	3.63	5281761	4.83	1.15	MI	
5	8.323	8.275	8.350	1319573	0.79	1303970	1.19	1.01	MI	
6	8.408	8.360	8.455	37668374	22.52	27118494	24.81	1.39	MI	
7	9.950	9.900	10.070	56185724	33.59	27913858	25.53	2.01	MI	
8	11.345	11.325	11.370	1260359	0.75	1171419	1.07	1.08	MI	
9	11.395	11.370	11.420	1369543	0.82	915142	0.84	1.50	MI	
10	11.491	11.420	11.535	18350767	10.97	5612517	5.13	3.27	MI	
				167265302	100.00	109318631	100.00			

Table 4.6 (from text). Control experiments to determine source and identity of unknown product. [a]

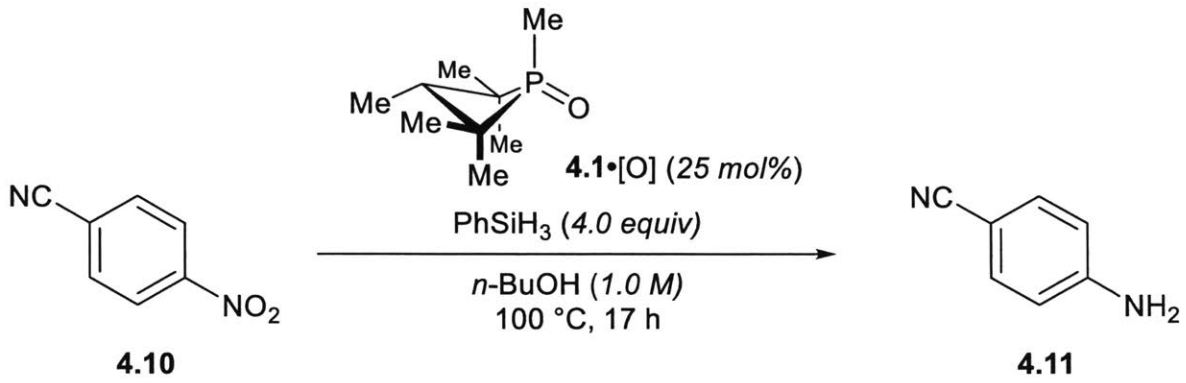

4.10 **4.11**

Entry	Variation	Conversion (%)	Yield of **4.11** (%)	Yield of unknown **4.13** (%)[b]
1	No internal standard	87[b]	6[b]	81
2	**4.11** as substrate	n/a	43[b]	57
3	Use of Ph_2SiH_2 as reductant	99	24	0
4	Use of PhMe as solvent	99	86	0
5	Use of PhMe as solvent, 2h	96	74	0

[a] Conversion and yields determined by GC with respect to dodecane internal standard.
[b] Determined by relative GC integration (area of interest / sum of unknown, nitro, aniline areas).

Reactions were performed according to general procedure C. Retention times: 5.83 min (dodecane), 7.03 min (nitro **4.10**), 7.67 min (aniline **4.11**), 8.40 min (unknown **4.13**).

Chromatographs for data tabulated in Table 4.6.

Table 4.6, Entry 1

C:\GCMSsolution\Tyler\Nitro to Aniline\tsh_198-17.qgd

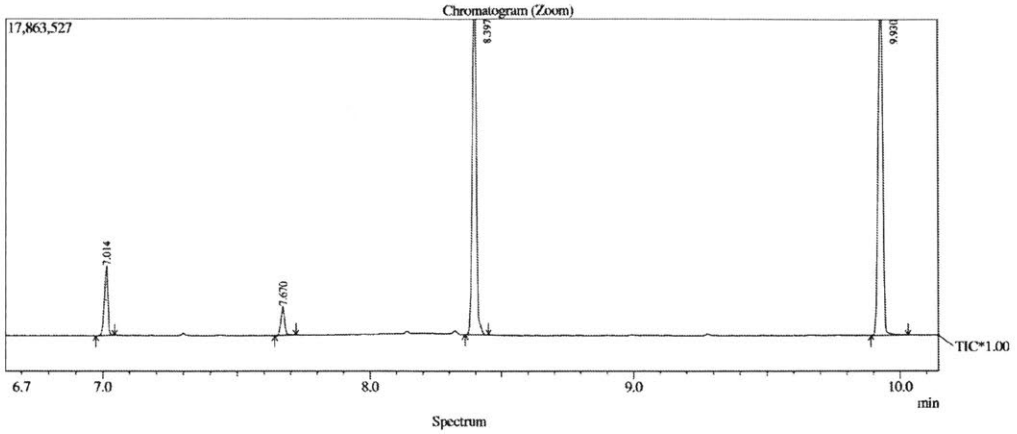

Peak Report TIC

Peak#	R.Time	I.Time	F.Time	Area	Area%	Height	Height%	A/H	Mark	Name
1	7.014	6.975	7.045	3616119	7.14	3916614	8.81	0.92	MI	
2	7.670	7.640	7.720	1504641	2.97	1633106	3.67	0.92	MI	
3	8.397	8.360	8.450	22114138	43.67	19730666	44.38	1.12	MI	
4	9.930	9.890	10.030	23405164	46.22	19181064	43.14	1.22	MI	
				50640062	100.00	44461450	100.00			

Table 4.6, Entry 2

C:\GCMSsolution\Tyler\Nitro to Aniline\tsh_199-17.qgd

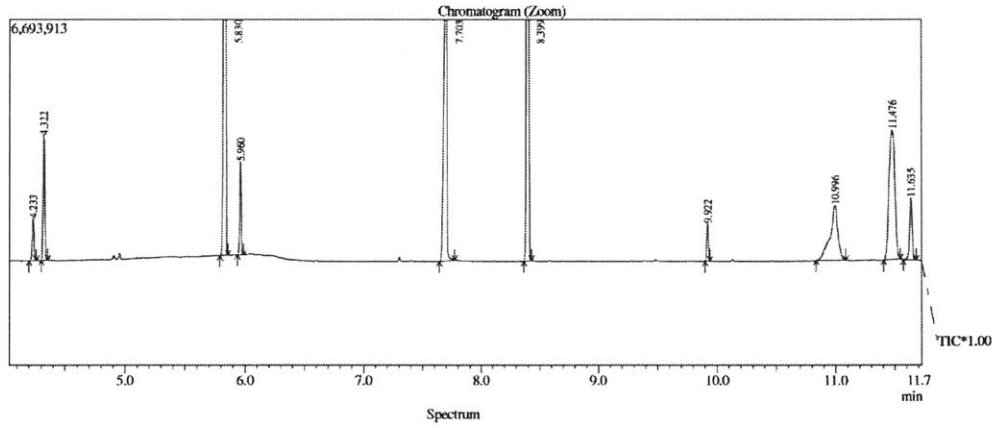

Peak Report TIC

Peak#	R.Time	I.Time	F.Time	Area	Area%	Height	Height%	A/H	Mark	Name
1	4.233	4.200	4.260	1177838	1.16	1161076	1.54	1.01	MI	
2	4.322	4.300	4.355	3452130	3.40	3451855	4.59	1.00	MI	
3	5.830	5.790	5.855	30757395	30.26	27972805	37.16	1.10	MI	
4	5.960	5.935	5.985	2135454	2.10	2552936	3.39	0.84	MI	
5	7.703	7.640	7.770	16960255	16.69	10028421	13.32	1.69	MI	
6	8.399	8.365	8.430	24215504	23.82	22261956	29.58	1.09	MI	
7	9.922	9.900	9.940	971799	0.96	1036434	1.38	0.94	MI	
8	10.996	10.835	11.085	7000521	6.89	1518262	2.02	4.61	MI	
9	11.476	11.405	11.545	12348683	12.15	3575078	4.75	3.45	MI	
10	11.635	11.570	11.680	2626376	2.58	1709450	2.27	1.54	MI	
				101645955	100.00	75268273	100.00			

Table 4.6, Entry 3

C:\GCMSsolution\Tyler\Nitro to Aniline\tsh_200-17.qgd

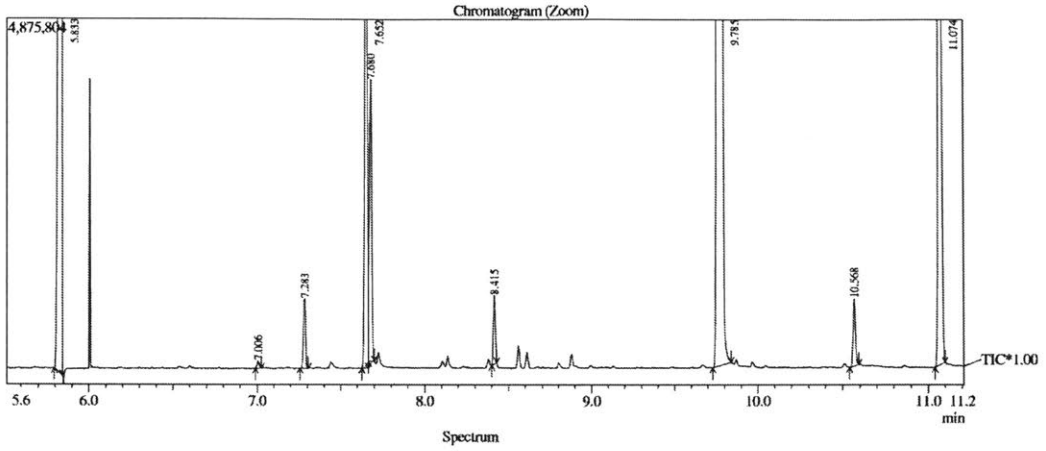

Peak Report TIC

Peak#	R.Time	I.Time	F.Time	Area	Area%	Height	Height%	A/H	Mark	Name
1	5.833	5.795	5.845	36957507	29.23	31530729	33.43	1.17	MI	
2	7.006	6.990	7.025	92731	0.07	102292	0.11	0.91	MI	
3	7.283	7.255	7.305	931098	0.74	973725	1.03	0.96	MI	
4	7.652	7.625	7.665	9632652	7.62	9616046	10.20	1.00	MI	
5	7.680	7.665	7.700	3741466	2.96	3917073	4.15	0.96	MI	
6	8.415	8.400	8.430	762536	0.60	954977	1.01	0.80	MI	
7	9.785	9.730	9.840	55952098	44.25	31014370	32.88	1.80	MI	
8	10.568	10.540	10.595	906918	0.72	940018	1.00	0.96	MI	
9	11.074	11.040	11.100	17467484	13.81	15271156	16.19	1.14	MI	
				126444490	100.00	94320386	100.00			

Table 4.6, Entry 4

C:\GCMSsolution\Tyler\Nitro to Aniline\tsh_201-17.qgd

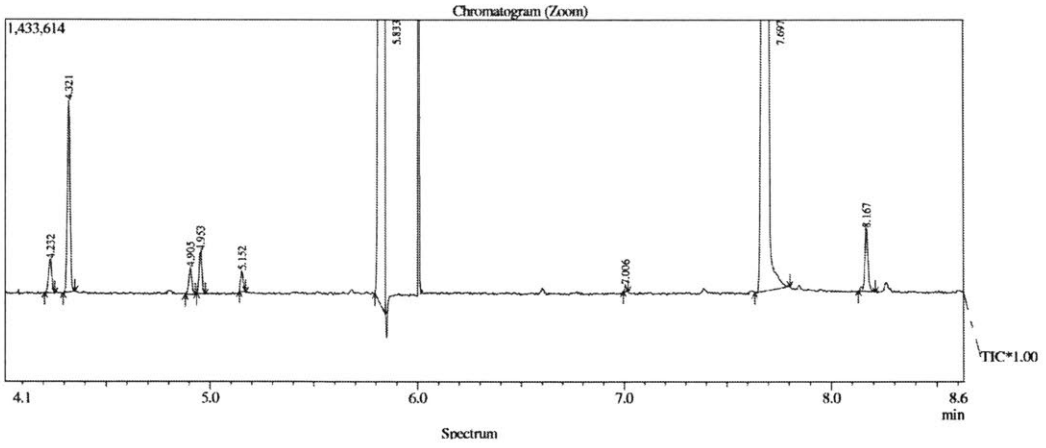

Peak Report TIC

Peak#	R.Time	I.Time	F.Time	Area	Area%	Height	Height%	A/H	Mark	Name
1	4.232	4.205	4.255	197233	0.38	172767	0.42	1.14	MI	
2	4.321	4.295	4.350	963660	1.84	985410	2.37	0.98	MI	
3	4.905	4.880	4.930	150988	0.29	139490	0.34	1.08	MI	
4	4.953	4.935	4.975	200569	0.38	219338	0.53	0.91	MI	
5	5.152	5.140	5.170	95308	0.18	104639	0.25	0.91	MI	
6	5.833	5.795	5.845	36821250	70.41	31204137	74.97	1.18	MI	
7	7.006	6.995	7.020	19234	0.04	33554	0.08	0.57	MI	
8	7.697	7.635	7.805	13501189	25.82	8436446	20.27	1.60	MI	
9	8.167	8.130	8.210	347115	0.66	324402	0.78	1.07	MI	
				52296546	100.00	41620183	100.00			

Table 4.6, Entry 5

C:\GCMSsolution\Tyler\Nitro to Aniline\tsh_201-2.qgd

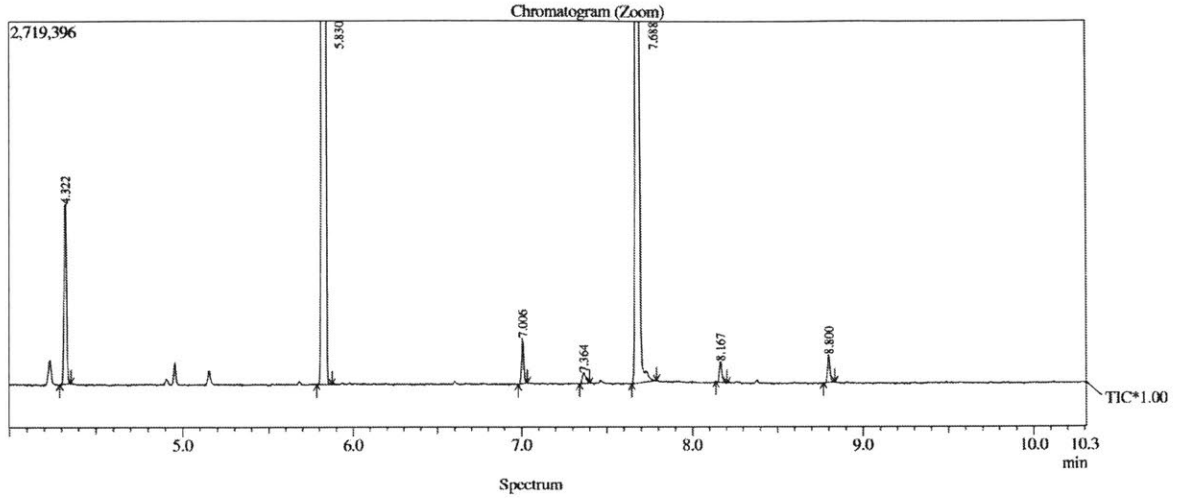

Peak Report TIC

Peak#	R.Time	I.Time	F.Time	Area	Area%	Height	Height%	A/H	Mark	Name
1	4.322	4.290	4.355	1340538	3.46	1328948	3.74	1.01	MI	
2	5.830	5.785	5.875	27837936	71.92	26666722	75.14	1.04	MI	
3	7.006	6.980	7.035	297692	0.77	336817	0.95	0.88	MI	
4	7.364	7.340	7.400	113087	0.29	78395	0.22	1.44	MI	
5	7.688	7.645	7.790	8777606	22.68	6720123	18.94	1.31	MI	
6	8.167	8.140	8.205	150806	0.39	153215	0.43	0.98	MI	
7	8.800	8.770	8.835	186513	0.48	203186	0.57	0.92	MI	
				38704178	100.00	35487406	100.00			

Table 4.7 (from text). Optimization in toluene. [a]

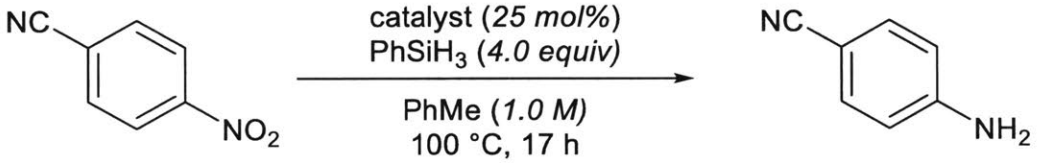

4.10 **4.11**

Entry	Catalyst	Conversion (%)	Yield (%)
1	**4.12**•[O]	1[b]	1[b]
2	**4.9**•[O]	68	19
3	**4.8**•[O]	100	11

[a] Conversion and yields determined by GC with respect to dodecane internal standard.
[b] Determined by relative GC integration (area of interest / sum of unknown, nitro, aniline areas).

Reactions were performed according to general procedure C. Retention times: 5.83 min (dodecane), 7.03 min (nitro **4.10**), 7.67 min (aniline **4.11**), 8.40 min (unknown **4.13**).

Chromatographs for data tabulated in Table 4.7.

Table 4.7, Entry 1

C:\GCMSsolution\Tyler\Nitro to Aniline\tsh_202.qgd

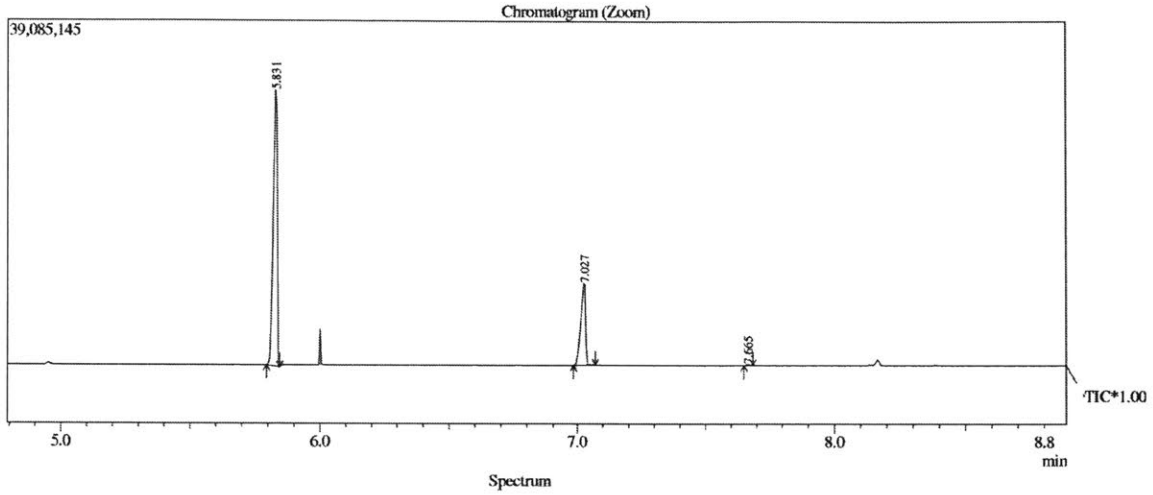

Peak Report TIC

Peak#	R.Time	I.Time	F.Time	Area	Area%	Height	Height%	A/H	Mark	Name
1	5.831	5.795	5.845	34896531	73.18	31298012	76.71	1.11	MI	
2	7.027	6.985	7.070	12656392	26.54	9351948	22.92	1.35	MI	
3	7.665	7.650	7.685	133250	0.28	151634	0.37	0.88	MI	
				47686173	100.00	40801594	100.00			

Table 4.7, Entry 2

C:\GCMSsolution\Tyler\Nitro to Aniline\tsh_203.qgd

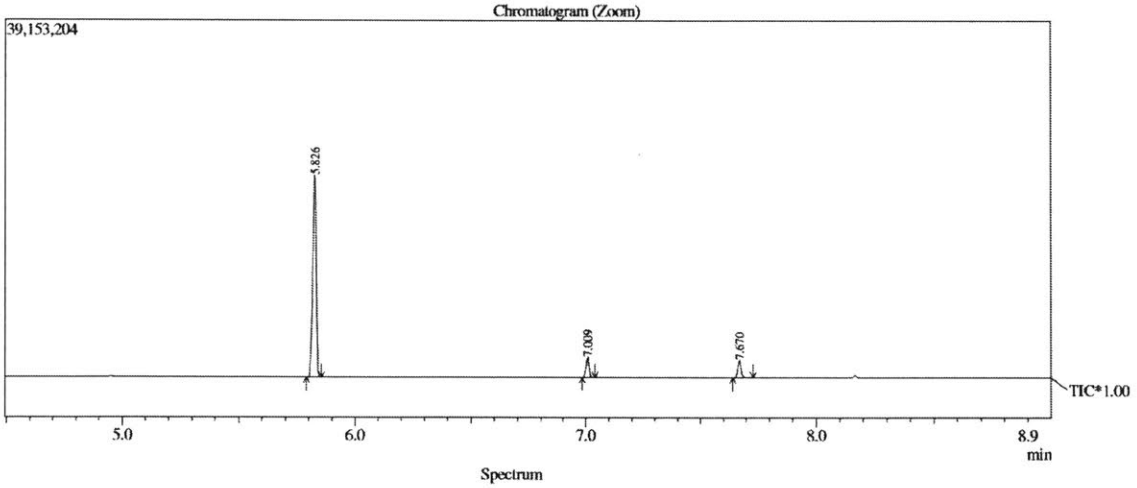

Peak Report TIC

Peak#	R.Time	I.Time	F.Time	Area	Area%	Height	Height%	A/H	Mark	Name
1	5.826	5.790	5.855	23132265	86.05	22086916	84.18	1.05	MI	
2	7.009	6.985	7.040	1908337	7.10	2214879	8.44	0.86	MI	
3	7.670	7.640	7.730	1840858	6.85	1936050	7.38	0.95	MI	
				26881460	100.00	26237845	100.00			

Table 4.7, Entry 3

C:\GCMSsolution\Tyler\Nitro to Aniline\tsh_205.qgd

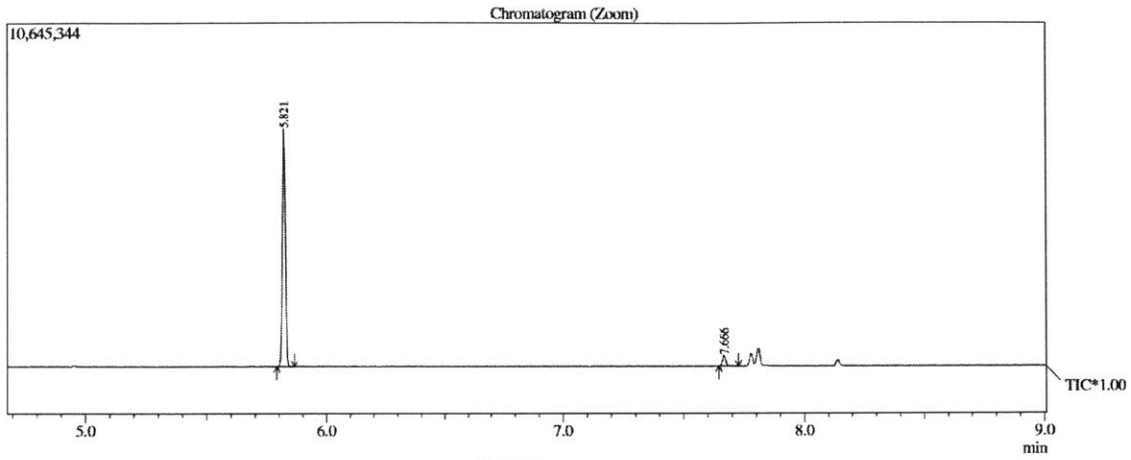

Spectrum

Peak Report TIC

Peak#	R.Time	I.Time	F.Time	Area	Area%	Height	Height%	A/H	Mark	Name
1	5.821	5.790	5.865	6618419	95.41	7352823	95.70	0.90	MI	
2	7.666	7.645	7.725	318440	4.59	330322	4.30	0.96	MI	
				6936859	100.00	7683145	100.00			

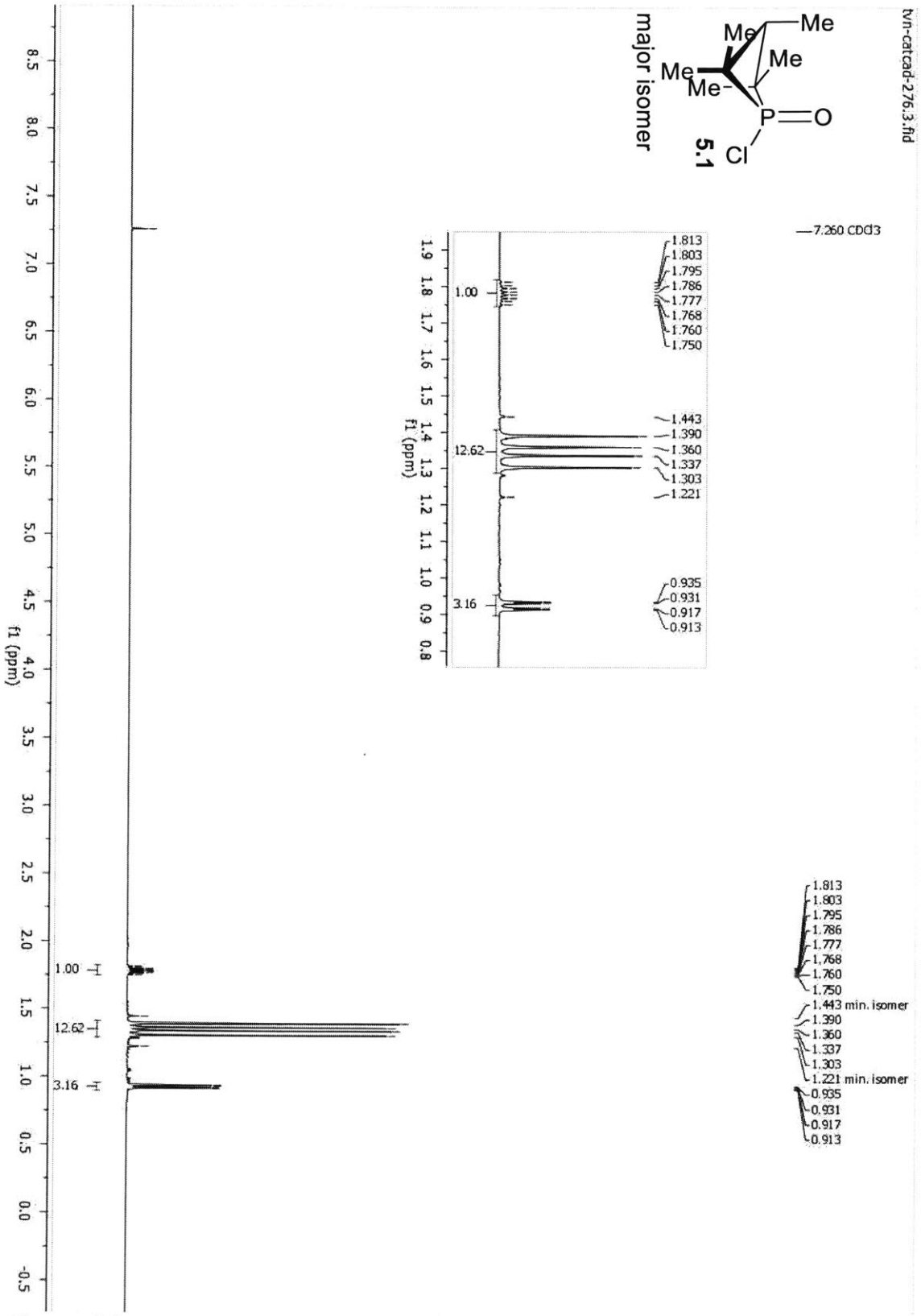

VIII. Spectral Data

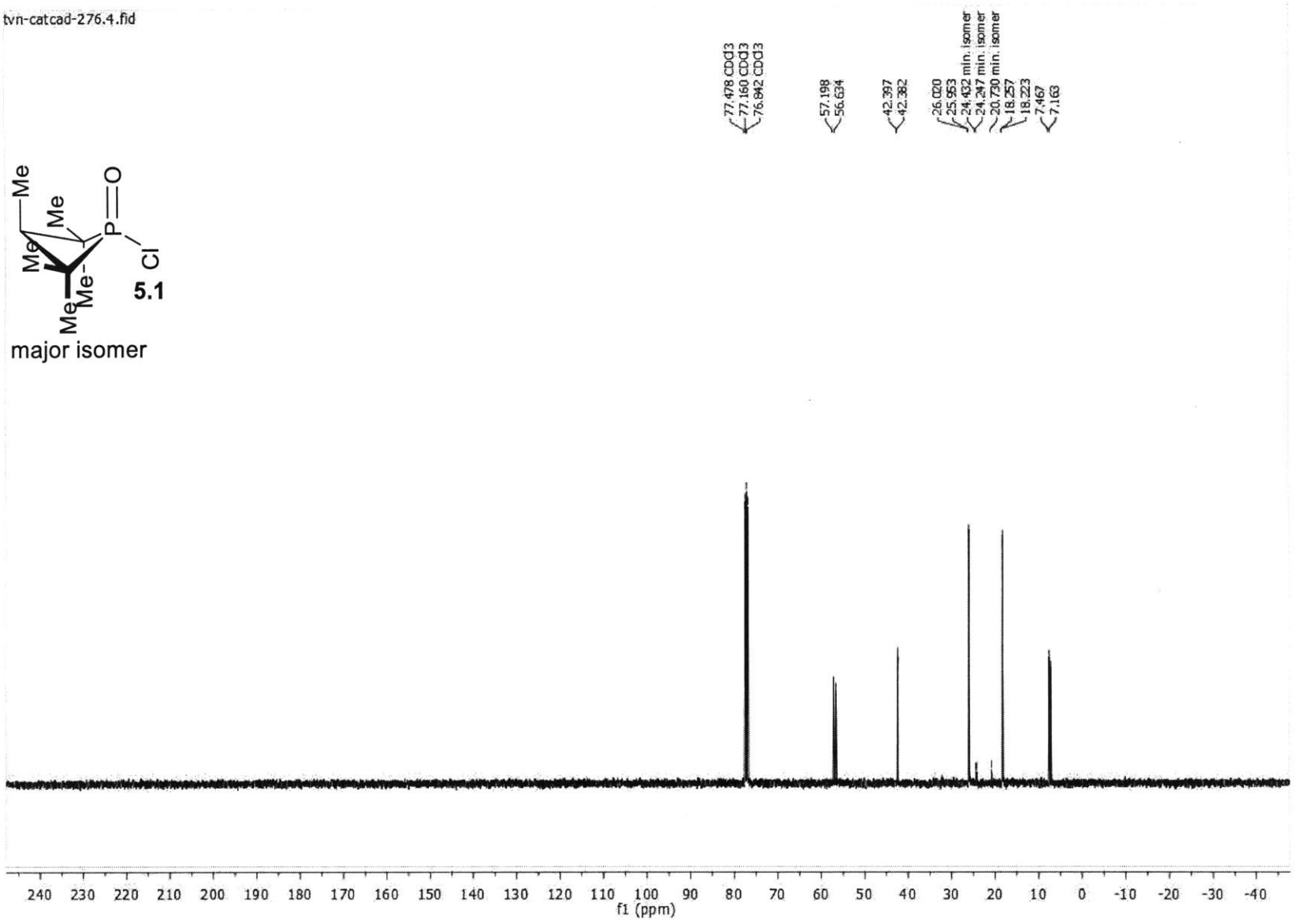
tvn-catcad-276.4.fid
77.478 CDCl3
77.160 CDCl3
76.842 CDCl3
57.198
56.634
42.397
42.382
26.020
25.953
24.432 min. isomer
24.247 min. isomer
20.730 min. isomer
18.257
18.223
7.467
7.163
Me
Me
Me
Me
P
O
Cl
5.1
major isomer
240 230 220 210 200 190 180 170 160 150 140 130 120 110 100 90 80 70 60 50 40 30 20 10 0 -10 -20 -30 -40
f1 (ppm)

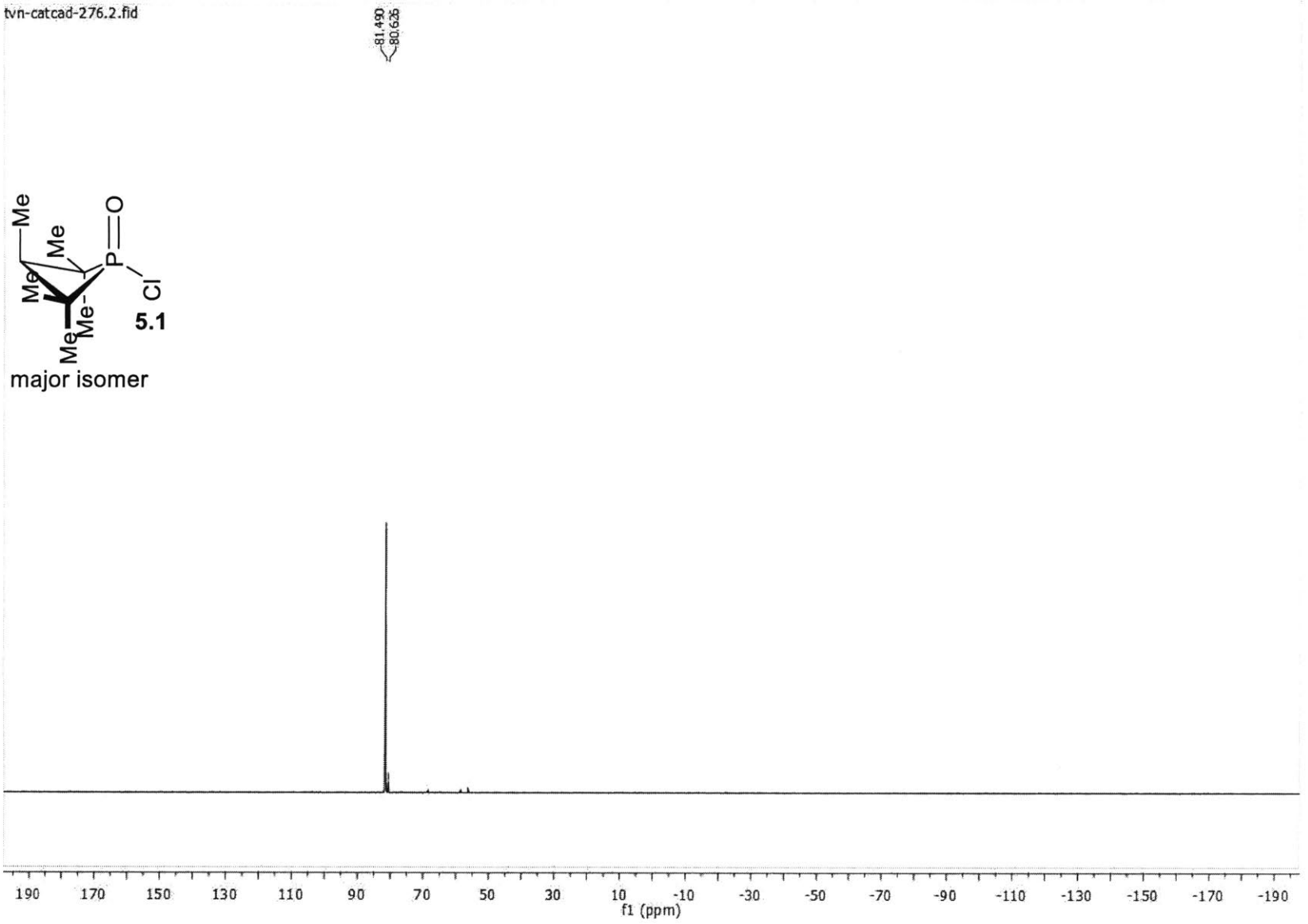
tvn-catcad-276.2.fid
81.490
80.626
Me
Me
Me
Me
P
O
Cl
5.1
major isomer
190
170
150
130
110
90
70
50
30
10
-10
-30
-50
-70
-90
-110
-130
-150
-170
-190
f1 (ppm)

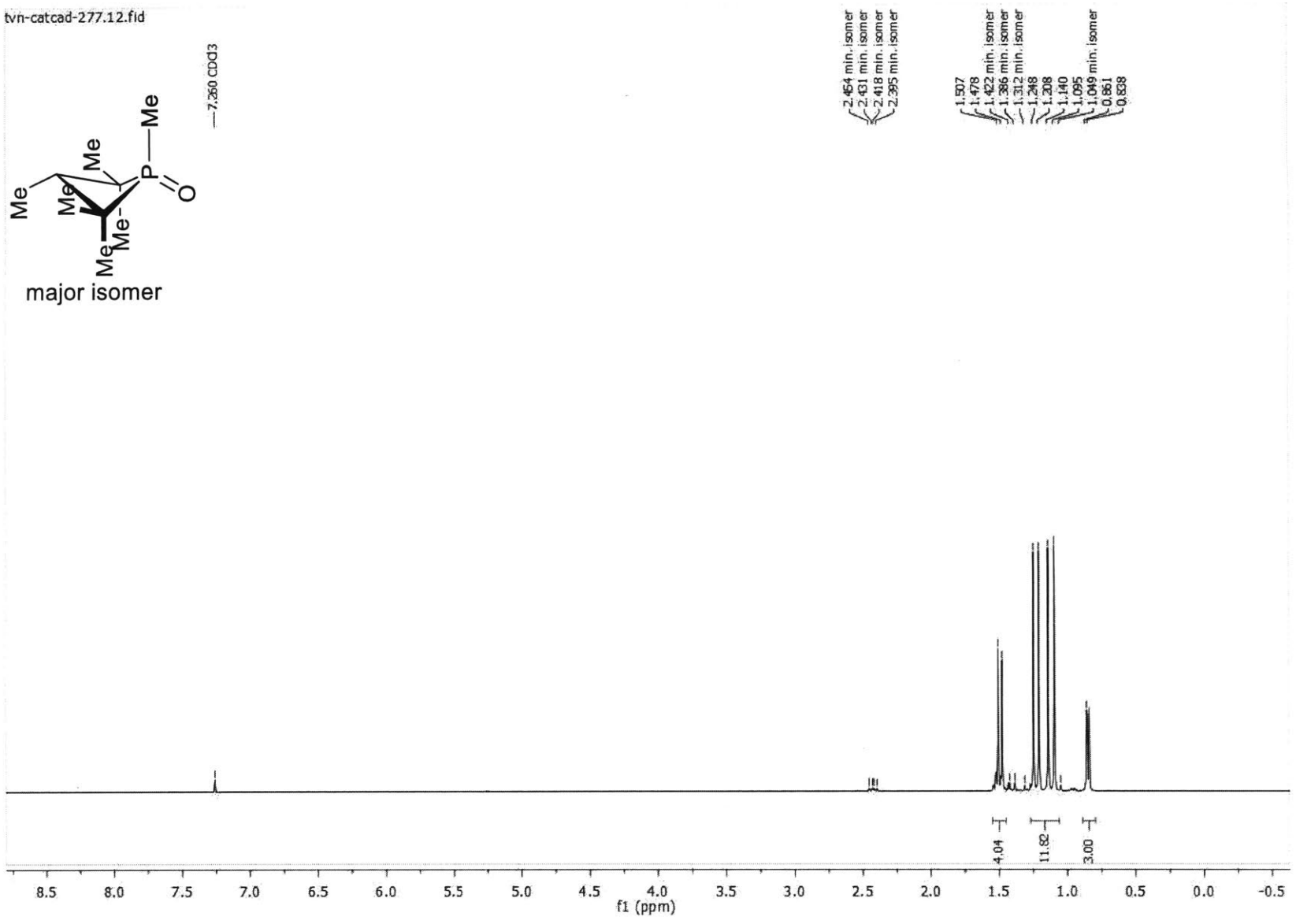
tvn-catcad-277.12.fid
7.260 CDCl3
Me
Me
Me
Me
Me
P
O
major isomer
2.454 min. isomer
2.431 min. isomer
2.418 min. isomer
2.395 min. isomer
1.507
1.478
1.422 min. isomer
1.386 min. isomer
1.312 min. isomer
1.248
1.208
1.140
1.095
1.049 min. isomer
0.861
0.838
4.04
11.82
3.00
8.5
8.0
7.5
7.0
6.5
6.0
5.5
5.0
4.5
4.0
3.5
3.0
2.5
2.0
1.5
1.0
0.5
0.0
-0.5
f1 (ppm)

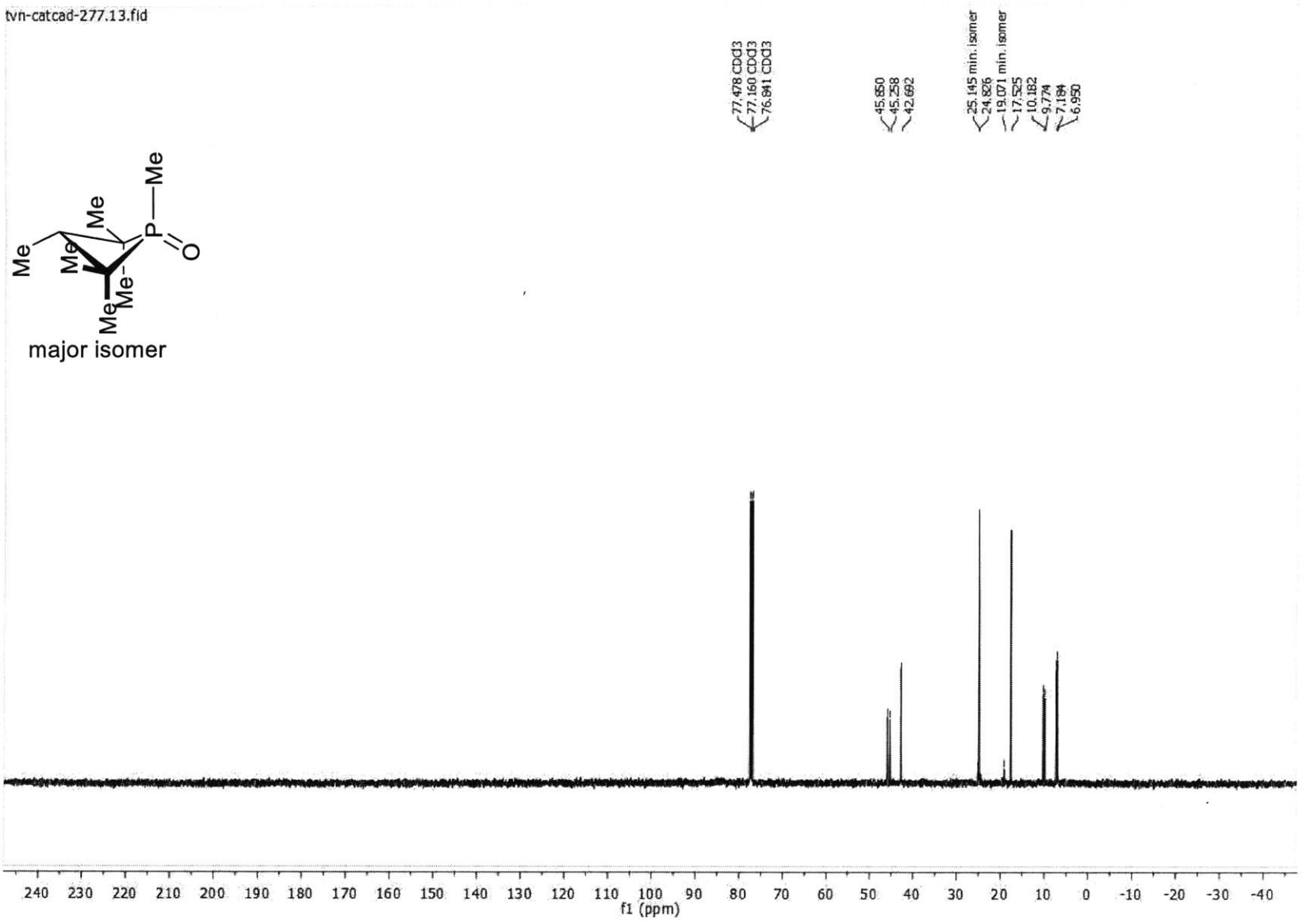
tvn-catcad-277.13.fid
77.478 CDCl3
77.160 CDCl3
76.841 CDCl3
45.850
45.258
42.692
25.145 min. isomer
24.826
19.071 min. isomer
17.525
10.182
9.774
7.184
6.950
Me
Me
Me
Me
Me
P
O
major isomer
240 230 220 210 200 190 180 170 160 150 140 130 120 110 100 90 80 70 60 50 40 30 20 10 0 -10 -20 -30 -40
f1 (ppm)

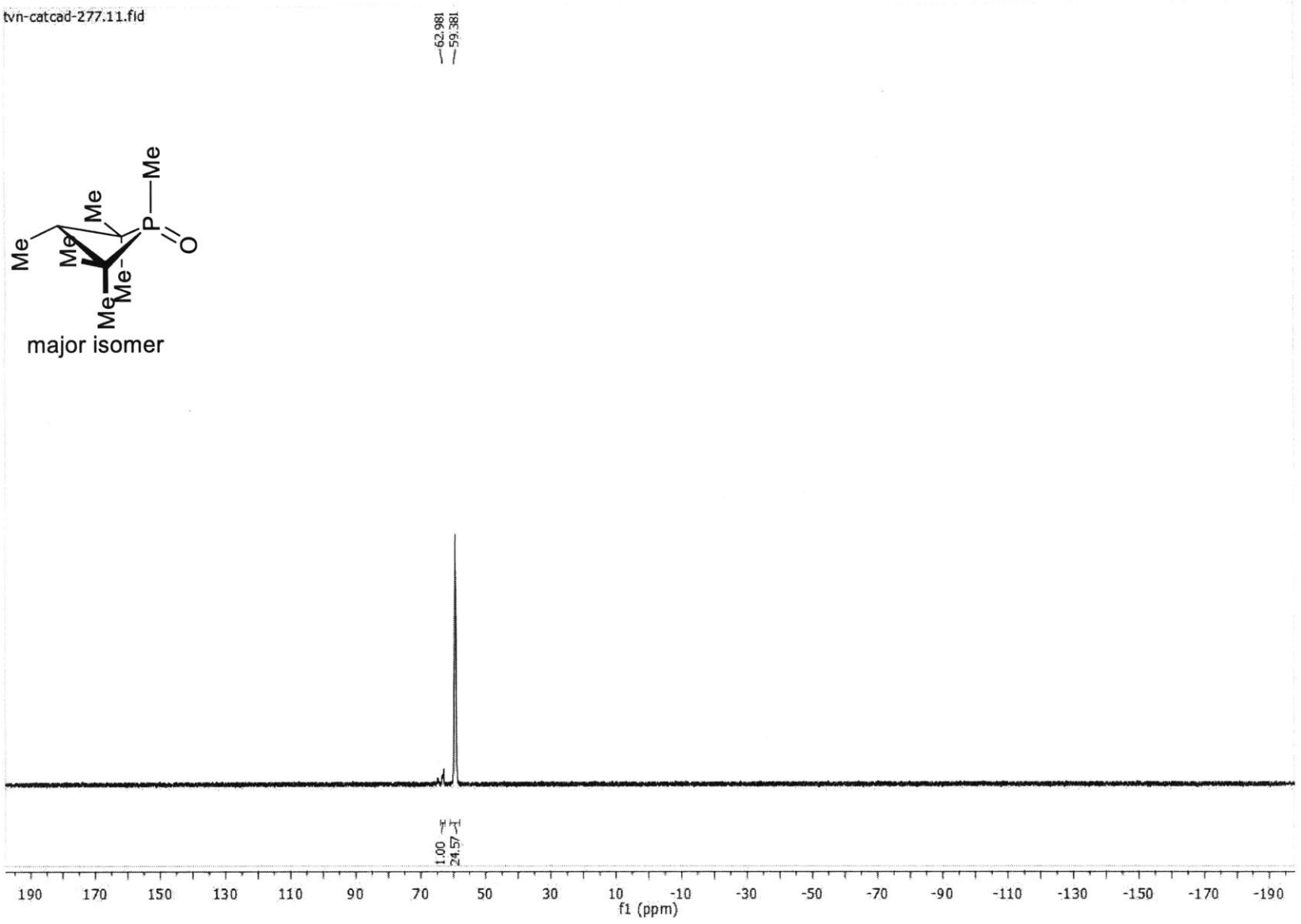
tvn-catcad-277.11.fid
62.981
59.381
Me
Me
Me
Me
Me
Me
P
O
major isomer
1.00
24.57
190
170
150
130
110
90
70
50
30
10
-10
-30
-50
-70
-90
-110
-130
-150
-170
-190
f1 (ppm)

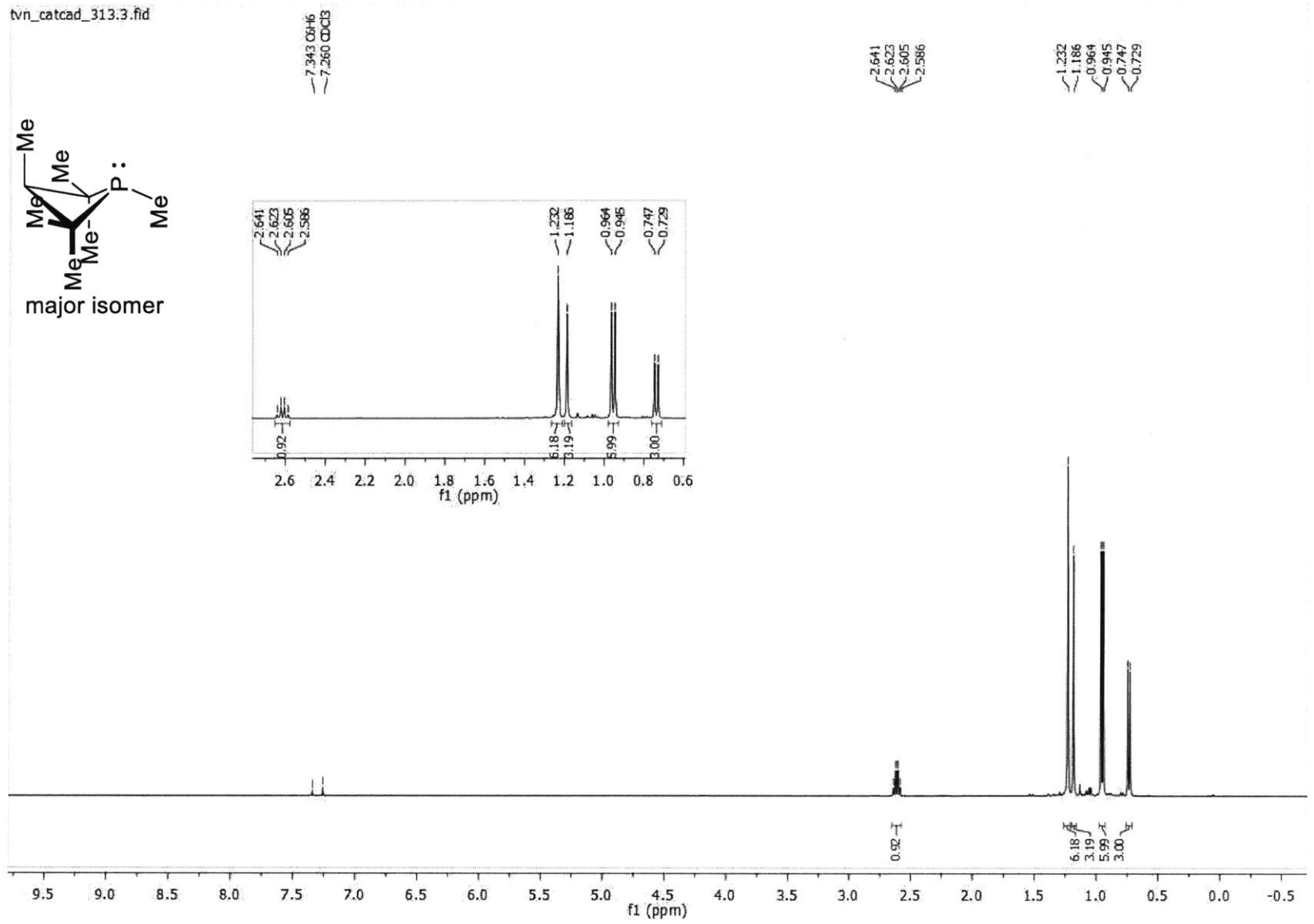
tvn_catcad_313.3.fid
7.343 C6H6
7.260 CDCl3
2.641
2.623
2.605
2.586
1.232
1.186
0.964
0.945
0.747
0.729
Me
Me
Me
P
Me
Me
Me
major isomer
0.92
6.18
3.19
5.99
3.00
f1 (ppm)

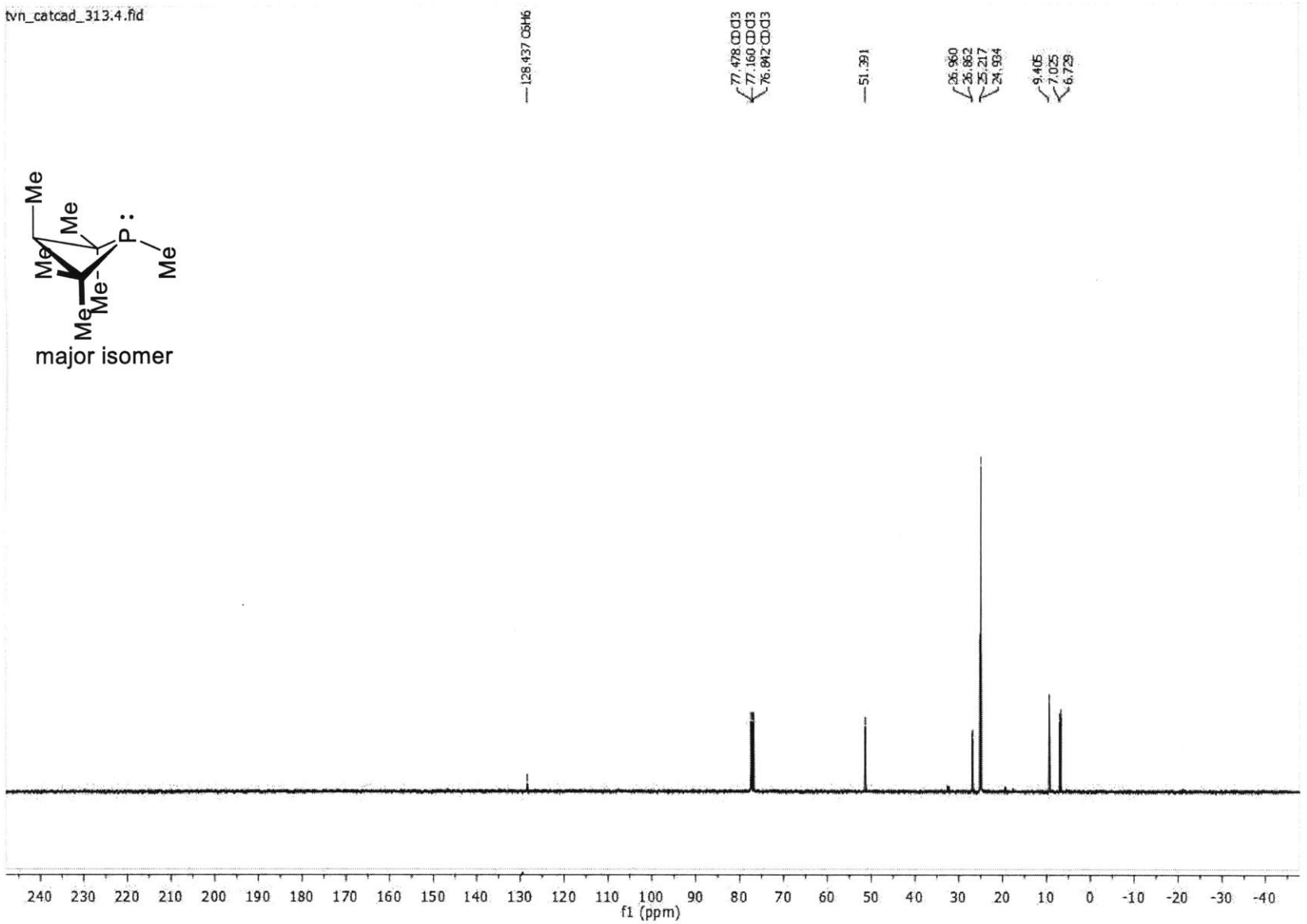
tvn_catcad_313.4.fid
128.437 C6H6
77.478 CDCl3
77.160 CDCl3
76.842 CDCl3
51.391
26.960
26.862
25.217
24.934
9.405
7.025
6.729
Me
Me
Me
P
Me
Me
Me
Me
major isomer
240 230 220 210 200 190 180 170 160 150 140 130 120 110 100 90 80 70 60 50 40 30 20 10 0 -10 -20 -30 -40
f1 (ppm)

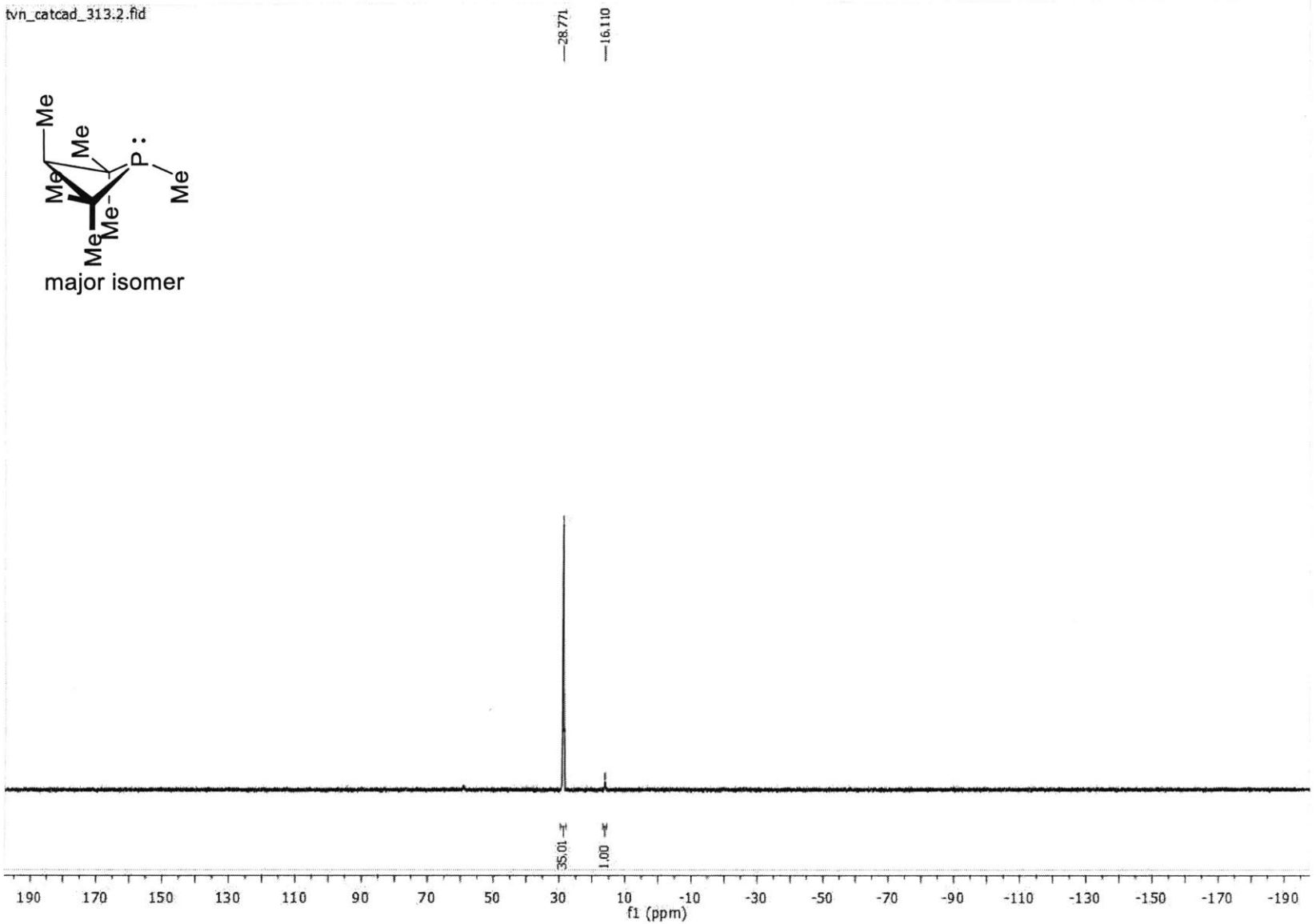
tvn_catcad_313.2.fid
28.771
16.110
Me
Me
Me
P
Me
Me
Me
major isomer
35.01
1.00
190
170
150
130
110
90
70
50
30
10
-10
-30
-50
-70
-90
-110
-130
-150
-170
-190
f1 (ppm)

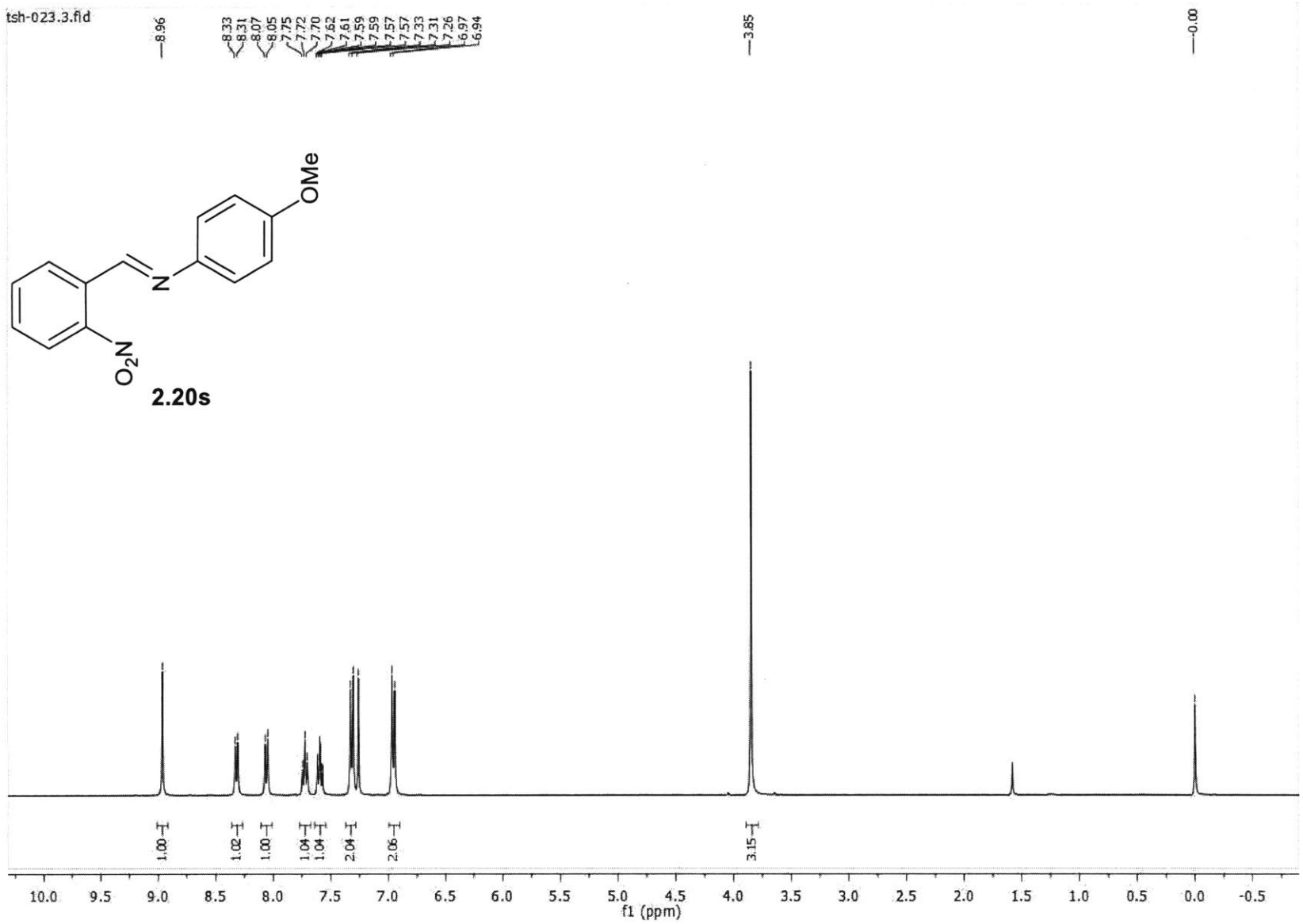
tsh-023.3.fid
8.96
8.33
8.31
8.07
8.05
7.75
7.72
7.70
7.62
7.61
7.59
7.59
7.57
7.57
7.33
7.31
7.26
6.97
6.94
3.85
0.00
OMe
N
O2N
2.20s
1.00
1.02
1.00
1.04
1.04
2.04
2.06
3.15
10.0
9.5
9.0
8.5
8.0
7.5
7.0
6.5
6.0
5.5
5.0
4.5
4.0
3.5
3.0
2.5
2.0
1.5
1.0
0.5
0.0
-0.5
f1 (ppm)

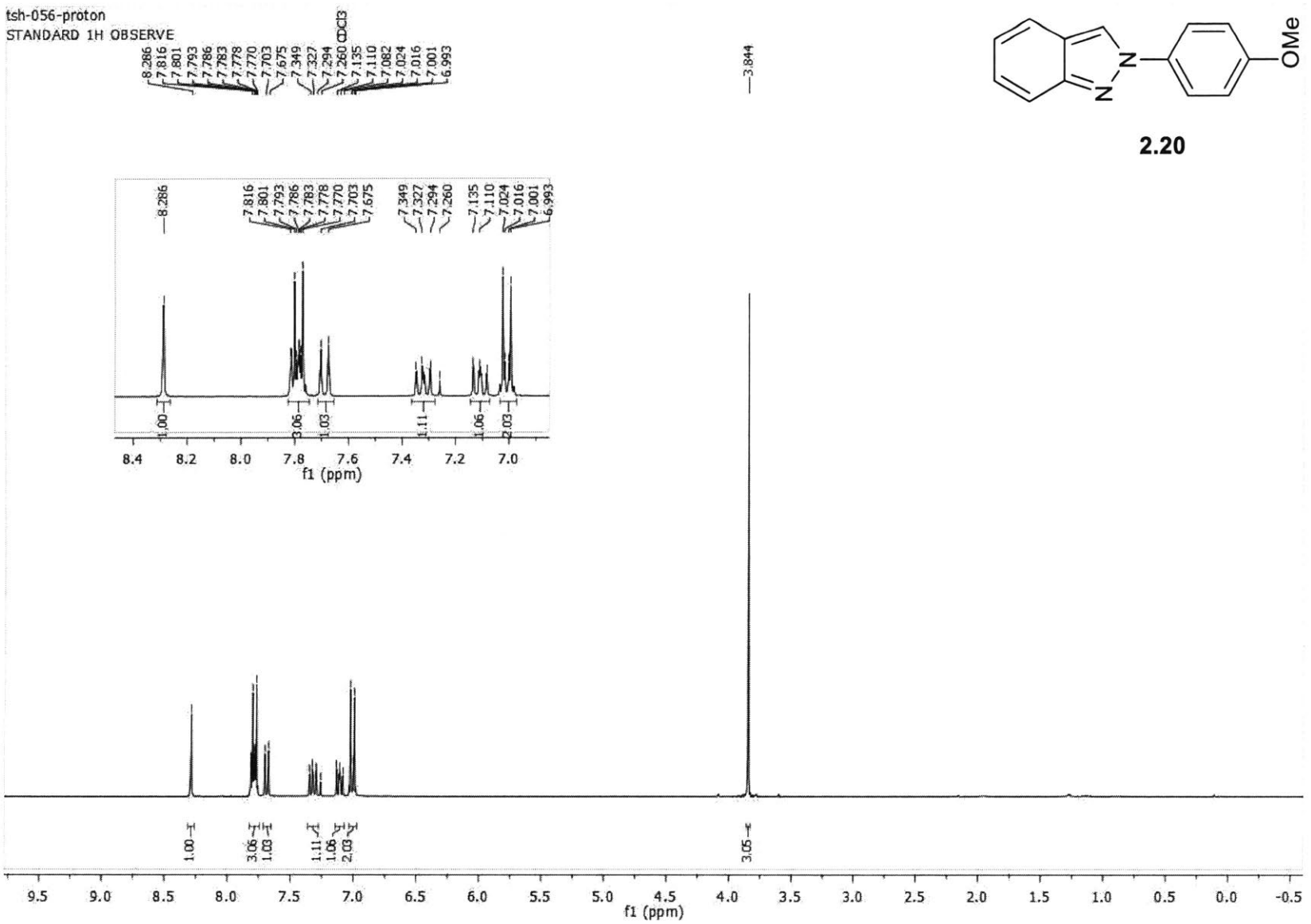
tsh-056-proton
STANDARD 1H OBSERVE
8.286
7.816
7.801
7.793
7.786
7.783
7.778
7.770
7.703
7.675
7.349
7.327
7.294
7.260
CDCl3
7.135
7.110
7.082
7.024
7.016
7.001
6.993
3.844
OMe
N
N
2.20
1.00
3.06
1.03
1.11
1.06
2.03
3.05
f1 (ppm)

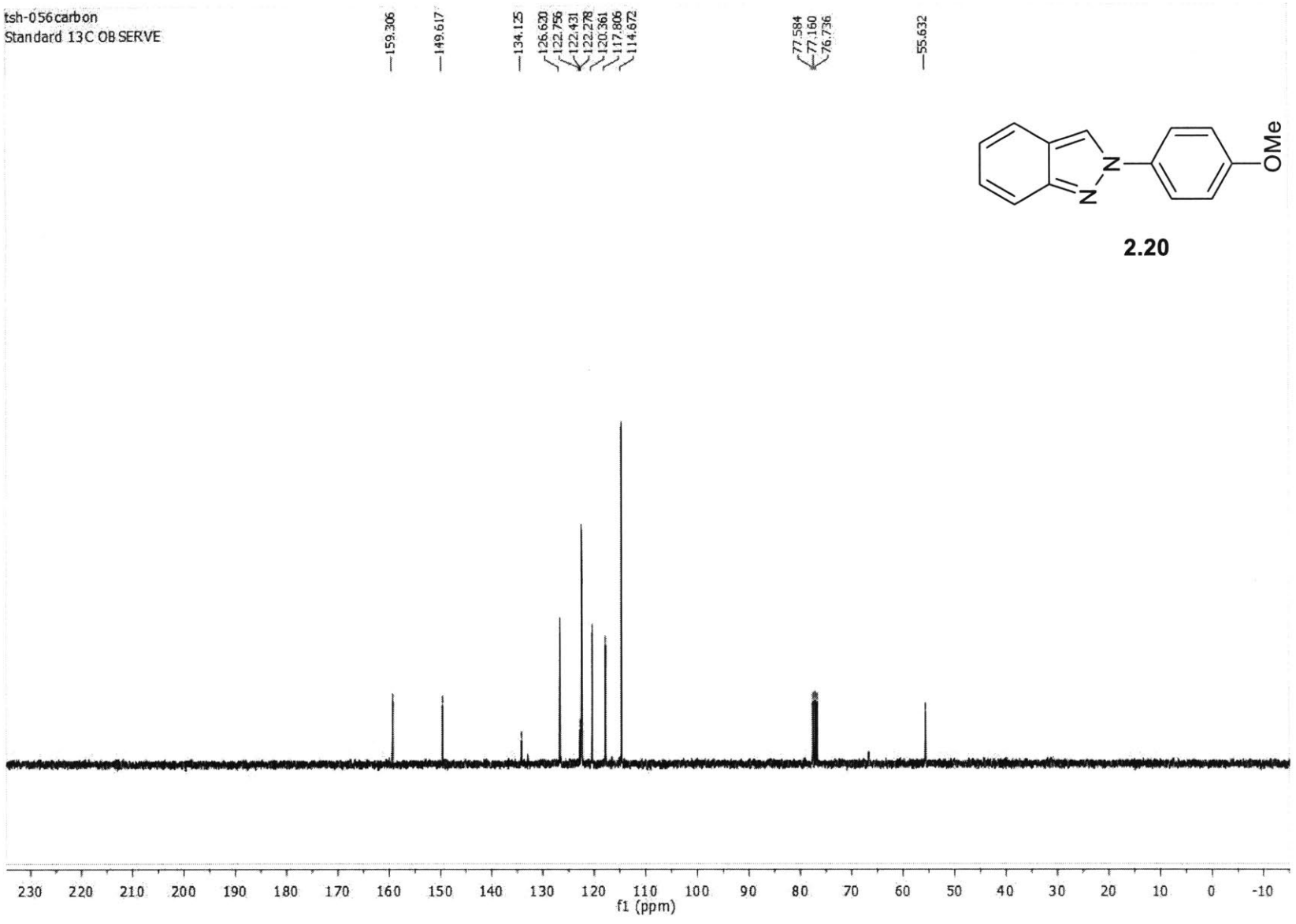
tsh-056carbon
Standard 13C OBSERVE
159.306
149.617
134.125
126.620
122.756
122.431
122.278
120.361
117.806
114.672
77.584
77.160
76.736
55.632
OMe
N
N
230 220 210 200 190 180 170 160 150 140 130 120 110 100 90 80 70 60 50 40 30 20 10 0 -10
f1 (ppm)

2.20

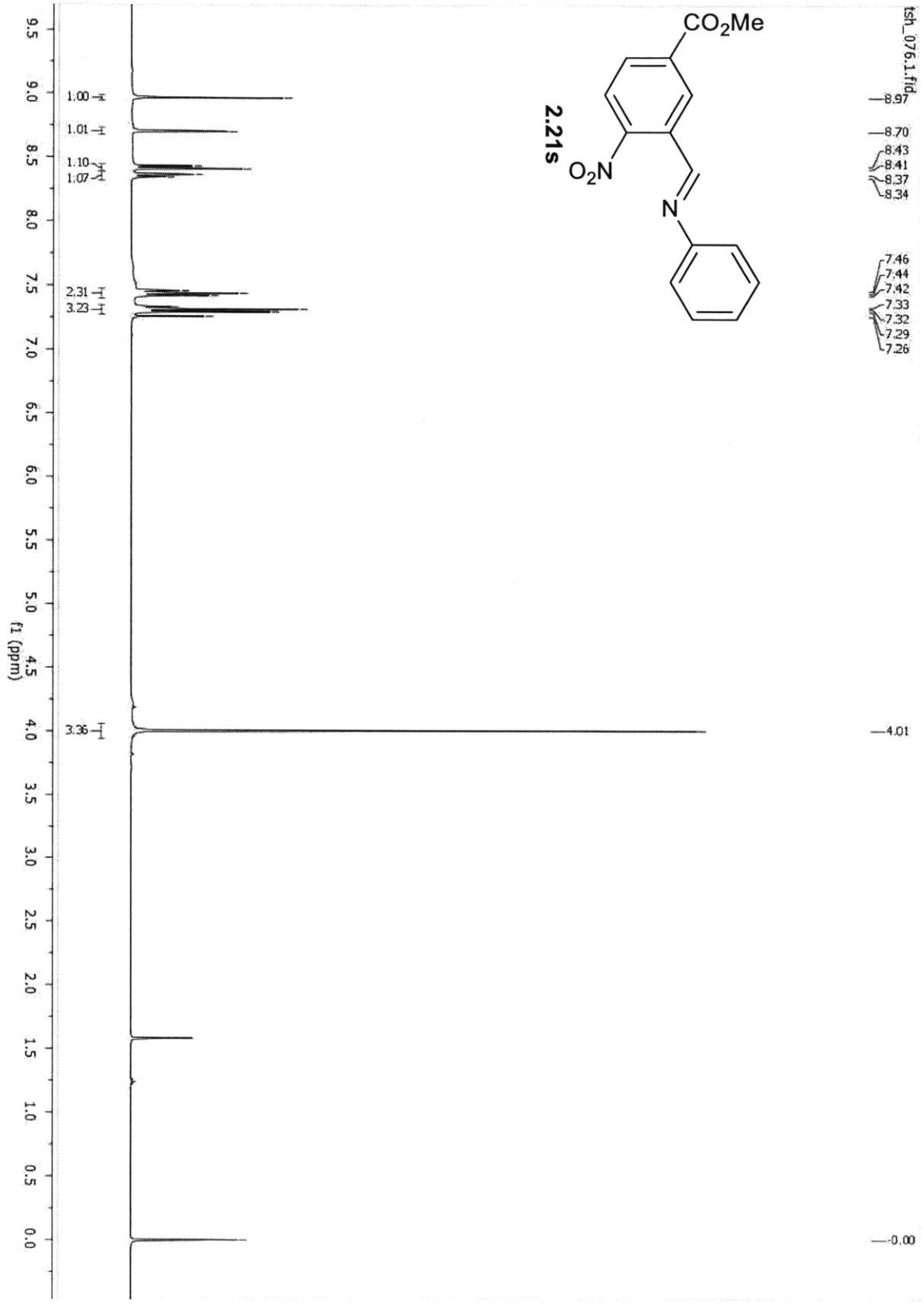
tsh_076.1.fid
CO2Me
O2N
N
2.21s
1.00
1.01
1.10
1.07
2.31
3.23
3.36
8.97
8.70
8.43
8.41
8.37
8.34
7.46
7.44
7.42
7.33
7.32
7.29
7.26
4.01
0.00
f1 (ppm)

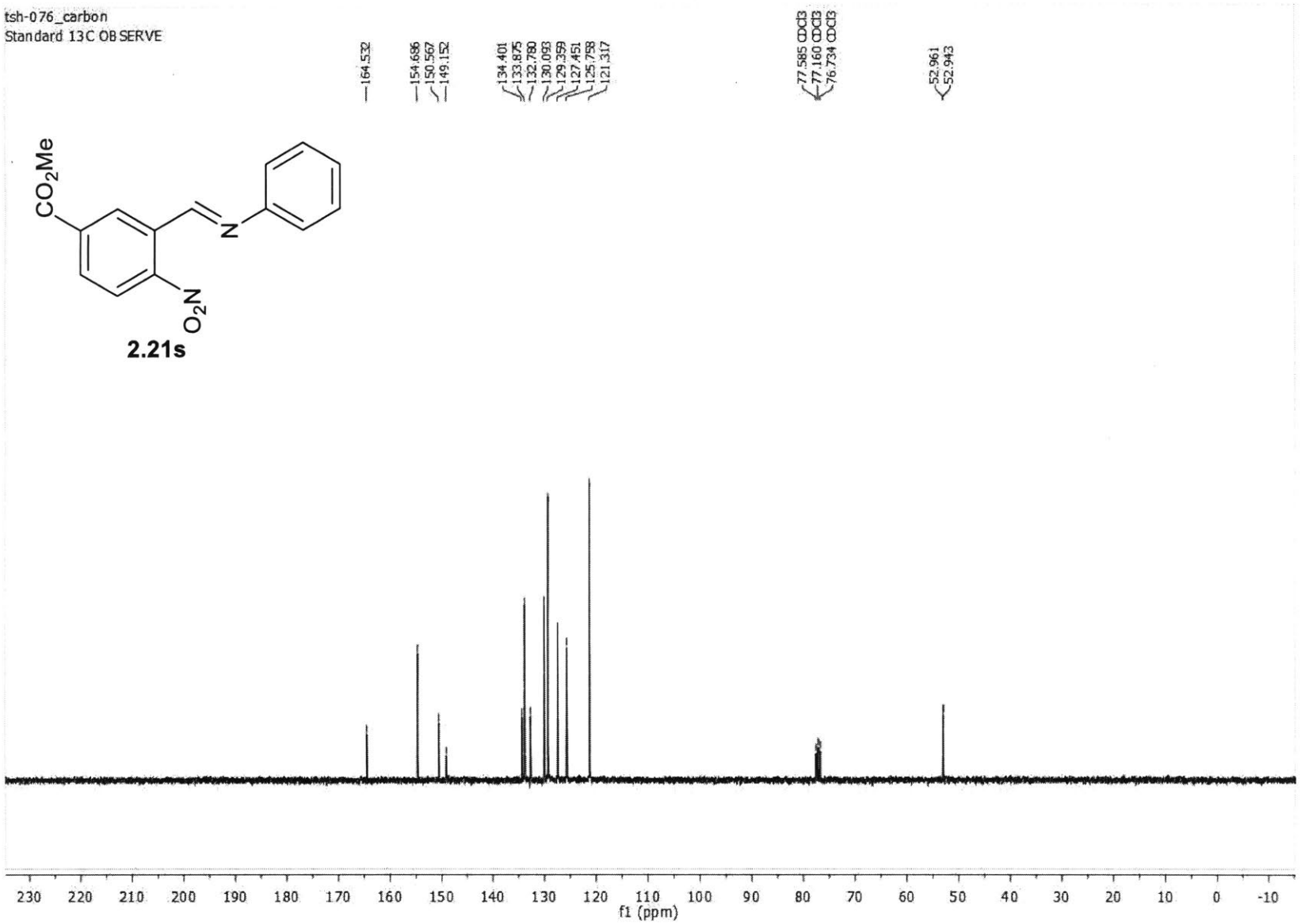
tsh-076_carbon
Standard 13C OBSERVE
164.532
154.686
150.567
149.152
134.401
133.875
132.780
130.093
129.359
127.451
125.758
121.317
77.585 CDCl3
77.160 CDCl3
76.734 CDCl3
52.961
52.943
CO2Me
N
O2N
2.21s
230 220 210 200 190 180 170 160 150 140 130 120 110 100 90 80 70 60 50 40 30 20 10 0 -10
f1 (ppm)

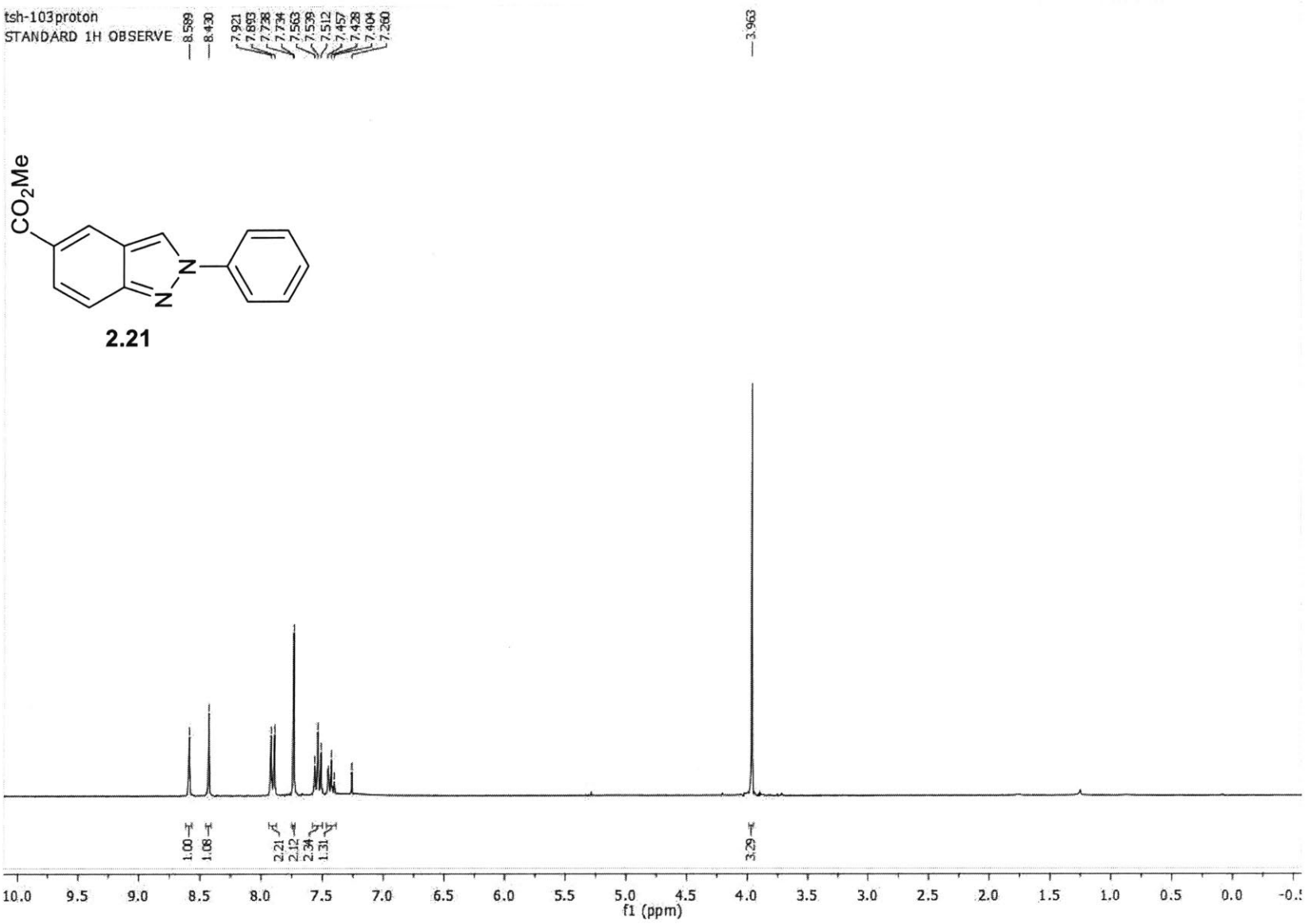
tsh-103proton
STANDARD 1H OBSERVE
8.589
8.430
7.921
7.893
7.728
7.734
7.563
7.539
7.512
7.457
7.428
7.404
7.260
3.963
CO2Me
N
N
2.21
1.00
1.08
2.21
2.12
2.34
1.31
3.29
10.0
9.5
9.0
8.5
8.0
7.5
7.0
6.5
6.0
5.5
5.0
4.5
4.0
3.5
3.0
2.5
2.0
1.5
1.0
0.5
0.0
f1 (ppm)

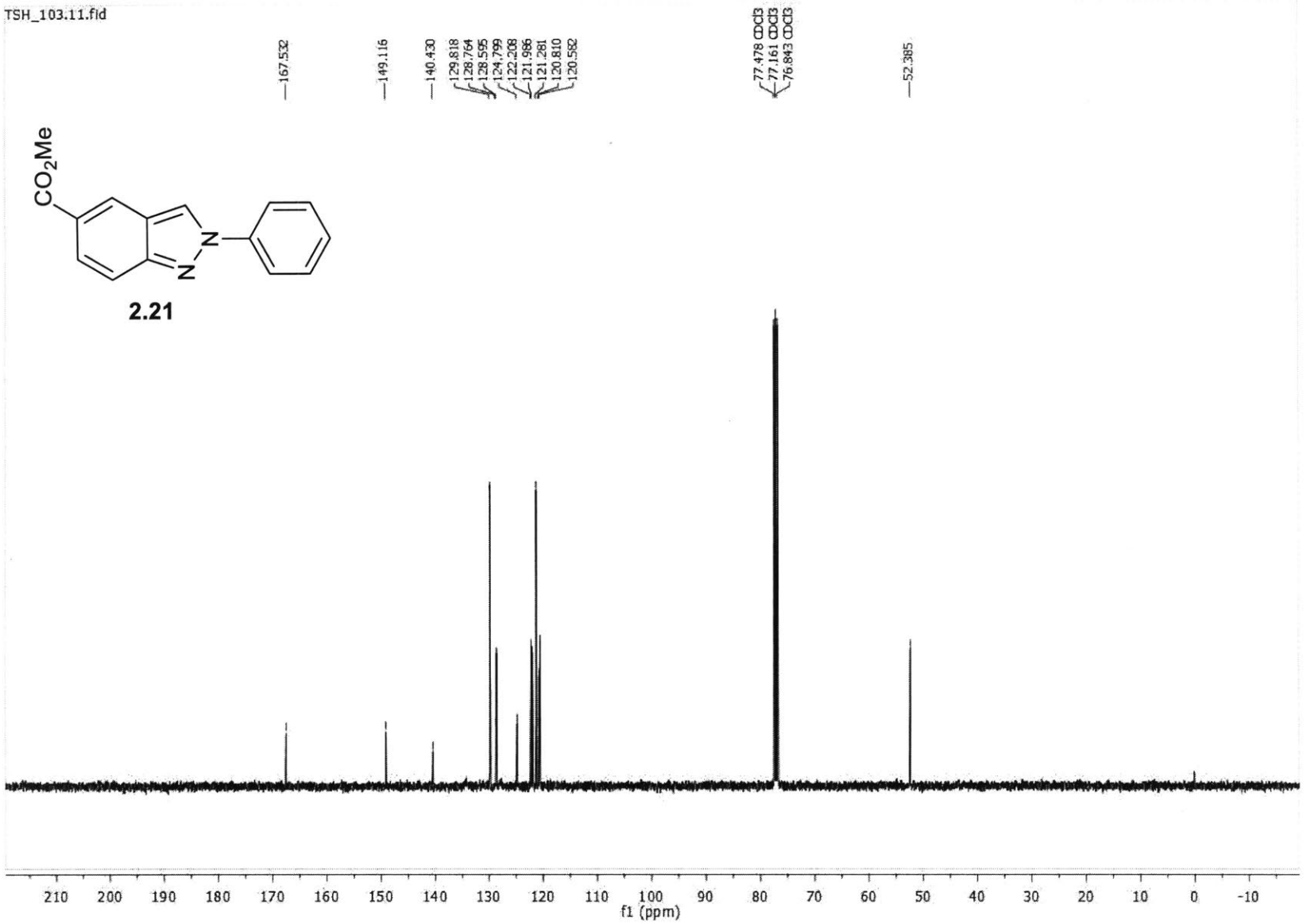
TSH_103.11.fid
167.532
149.116
140.430
129.818
128.764
128.595
124.799
122.208
121.986
121.281
120.810
120.582
77.478 CDCl3
77.161 CDCl3
76.843 CDCl3
52.385
CO2Me
N
N
2.21
210 200 190 180 170 160 150 140 130 120 110 100 90 80 70 60 50 40 30 20 10 0 -10
f1 (ppm)

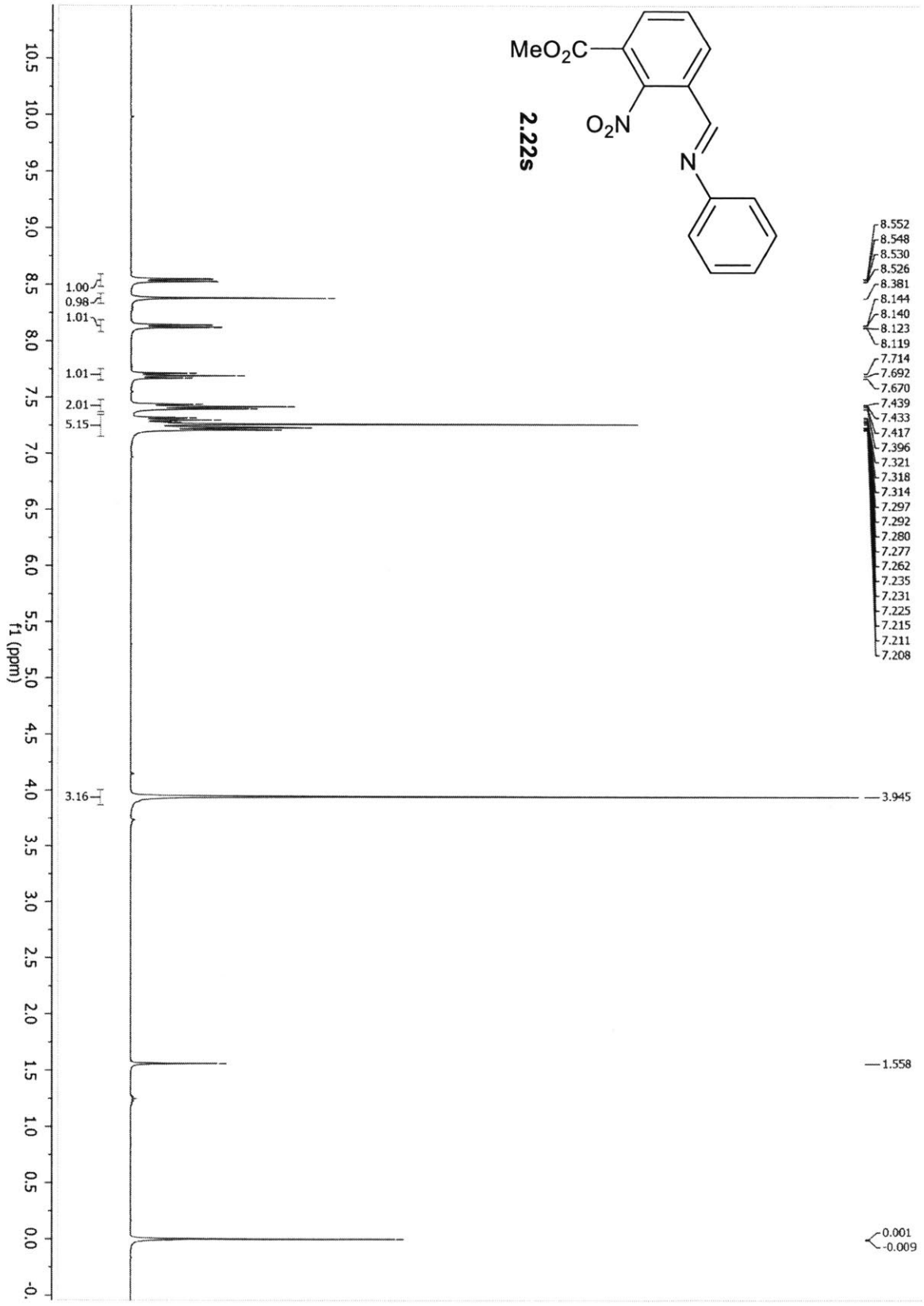
MeO2C
O2N
N
2.22s
f1 (ppm)
1.00
0.98
1.01
1.01
2.01
5.15
3.16
8.552
8.548
8.530
8.526
8.381
8.144
8.140
8.123
8.119
7.714
7.692
7.670
7.439
7.433
7.417
7.396
7.321
7.318
7.314
7.297
7.292
7.280
7.277
7.262
7.235
7.231
7.225
7.215
7.211
7.208
3.945
1.558
0.001
-0.009

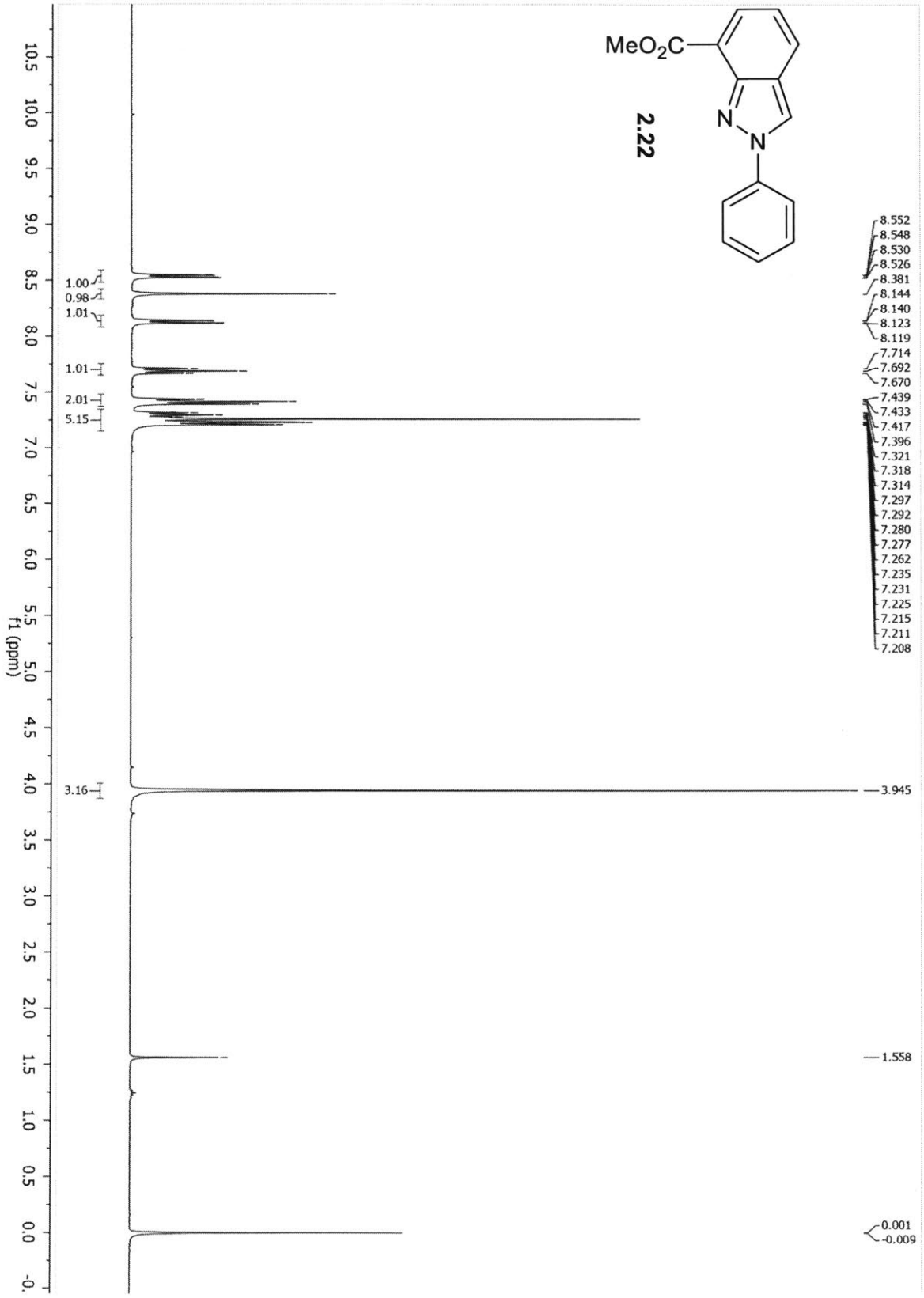
MeO2C
N
N
2.22
1.00
0.98
1.01
1.01
2.01
5.15
3.16
8.552
8.548
8.530
8.526
8.381
8.144
8.140
8.123
8.119
7.714
7.692
7.670
7.439
7.433
7.417
7.396
7.321
7.318
7.314
7.297
7.292
7.280
7.277
7.262
7.235
7.231
7.225
7.215
7.211
7.208
3.945
1.558
0.001
-0.009
f1 (ppm)

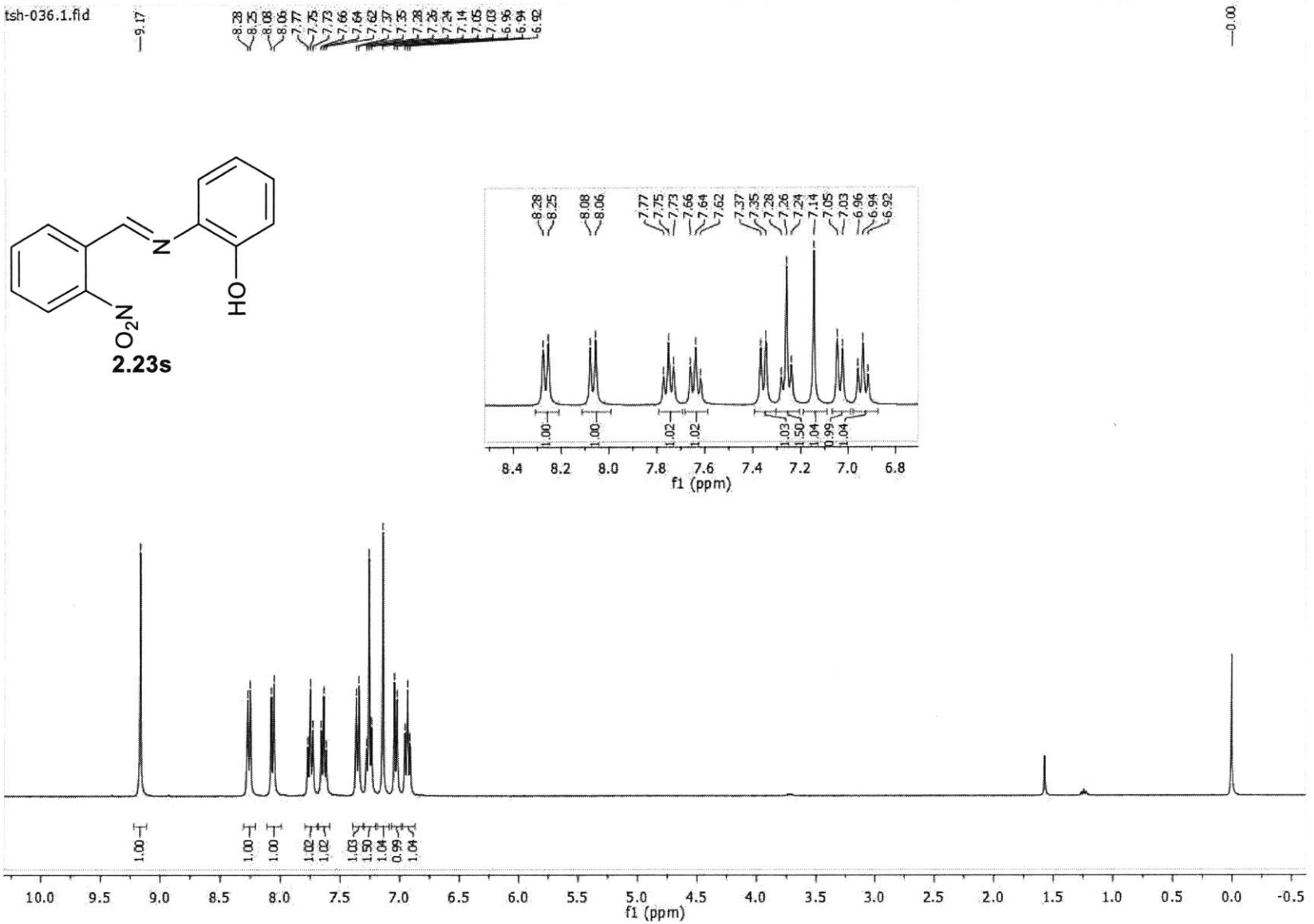
tsh-036.1.fid
9.17
8.28
8.25
8.08
8.06
7.77
7.75
7.73
7.66
7.64
7.62
7.37
7.35
7.28
7.26
7.24
7.14
7.05
7.03
6.96
6.94
6.92
0.00
N
HO
O2N
2.23s
f1 (ppm)

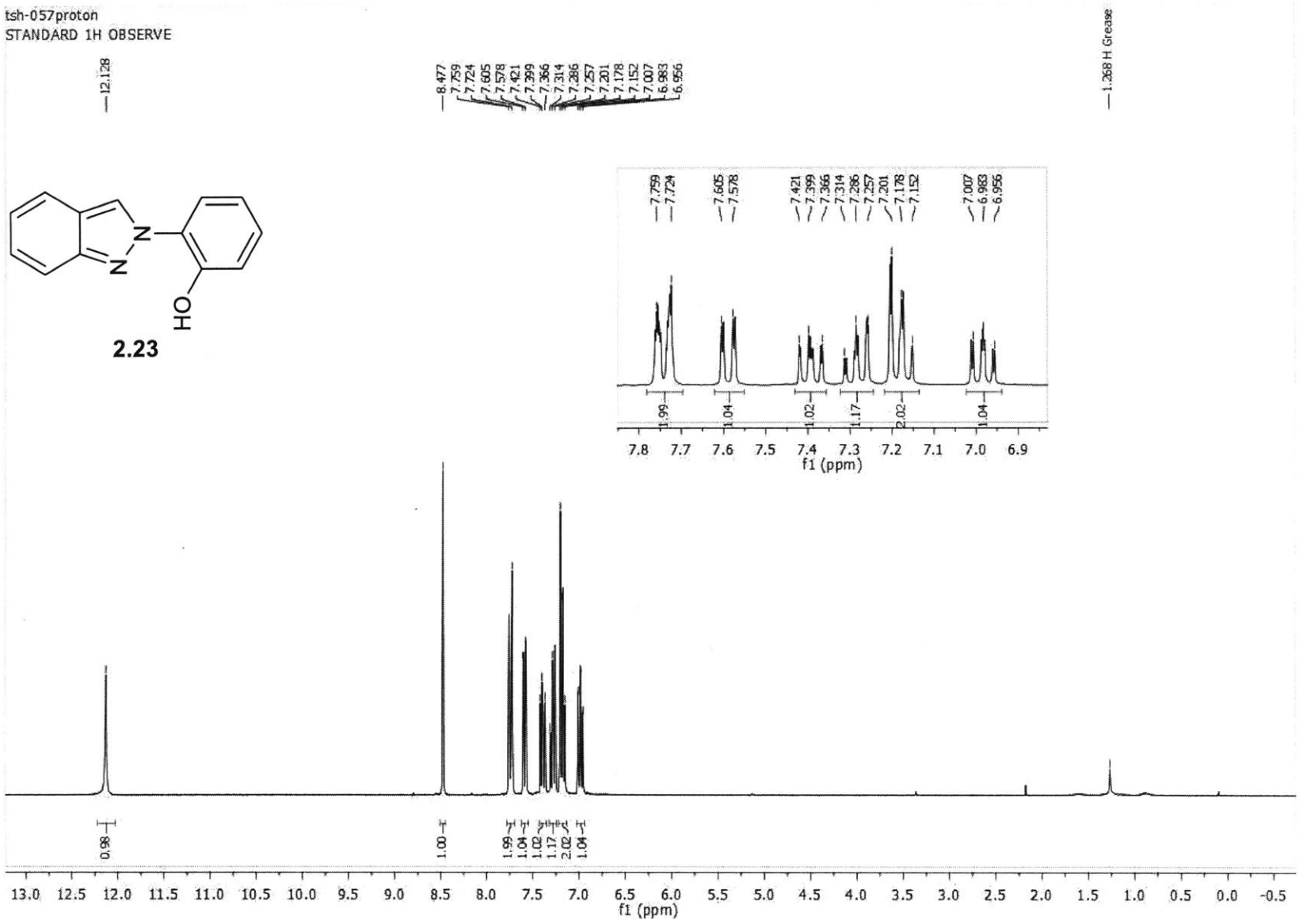
tsh-057proton
STANDARD 1H OBSERVE
12.128
8.477
7.759
7.724
7.605
7.578
7.421
7.399
7.366
7.314
7.286
7.257
7.201
7.178
7.152
7.007
6.983
6.956
1.268 H Grease
N
N
HO
2.23
0.98
1.00
1.99
1.04
1.02
1.17
2.02
1.04
f1 (ppm)

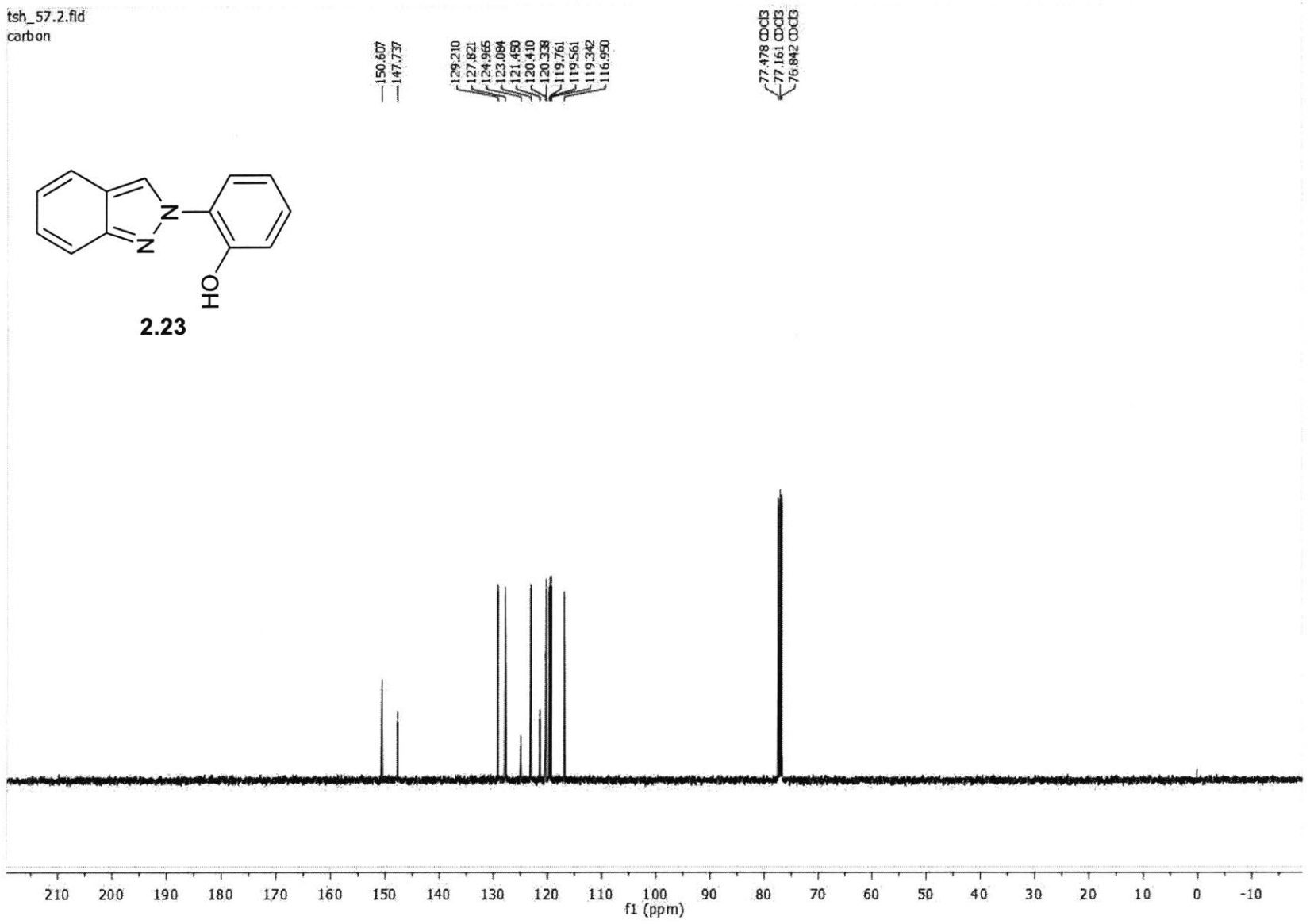
tsh_57.2.fid
carbon
150.607
147.737
129.210
127.821
124.965
123.084
121.450
120.410
120.338
119.761
119.561
119.342
116.950
77.478 CDCl3
77.161 CDCl3
76.842 CDCl3
N
N
HO
2.23
210
200
190
180
170
160
150
140
130
120
110
100
90
80
70
60
50
40
30
20
10
0
-10
f1 (ppm)

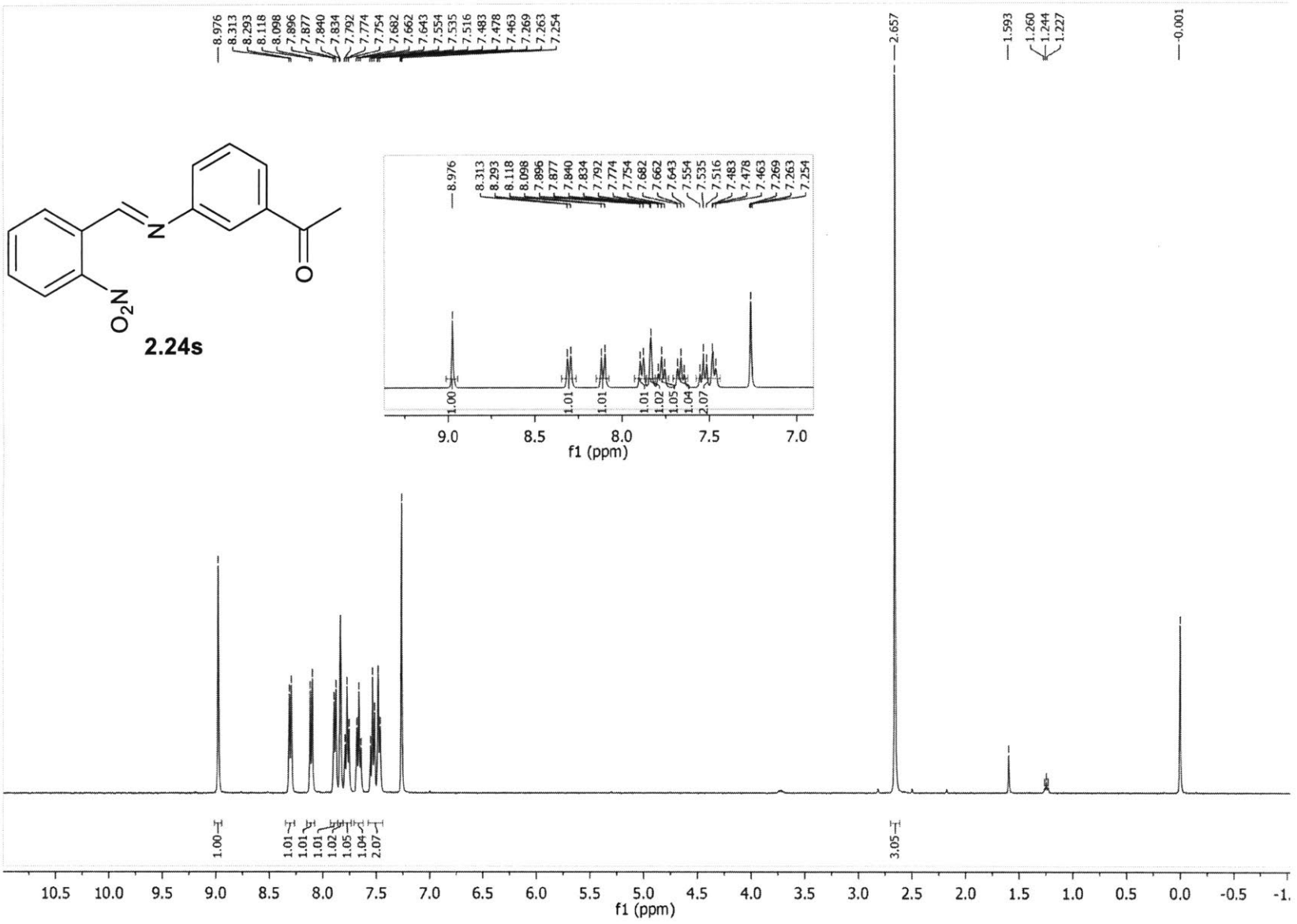
8.976
8.313
8.293
8.118
8.098
7.896
7.877
7.840
7.834
7.792
7.774
7.754
7.682
7.662
7.643
7.554
7.535
7.516
7.483
7.478
7.463
7.269
7.263
7.254
2.657
1.593
1.260
1.244
1.227
0.001
O
N
O2N
2.24s
f1 (ppm)

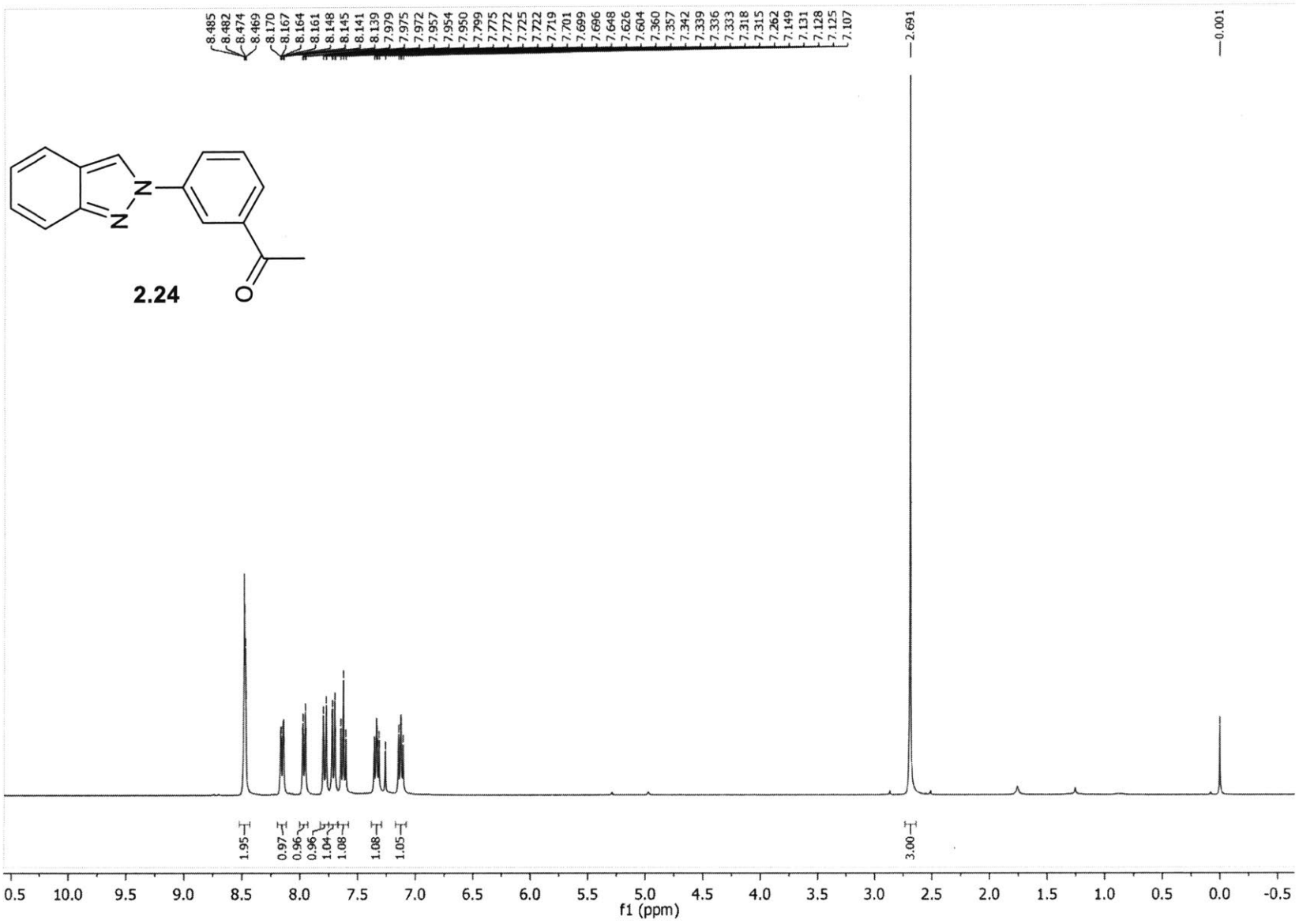
8.485
8.482
8.474
8.469
8.170
8.167
8.164
8.161
8.148
8.145
8.141
8.139
7.979
7.975
7.972
7.957
7.954
7.950
7.799
7.775
7.772
7.725
7.722
7.719
7.701
7.699
7.696
7.648
7.626
7.604
7.360
7.357
7.342
7.339
7.336
7.333
7.318
7.315
7.262
7.149
7.131
7.128
7.125
7.107
2.691
0.001
2.24
O
1.95
0.97
0.96
0.96
1.04
1.08
1.08
1.05
3.00
f1 (ppm)

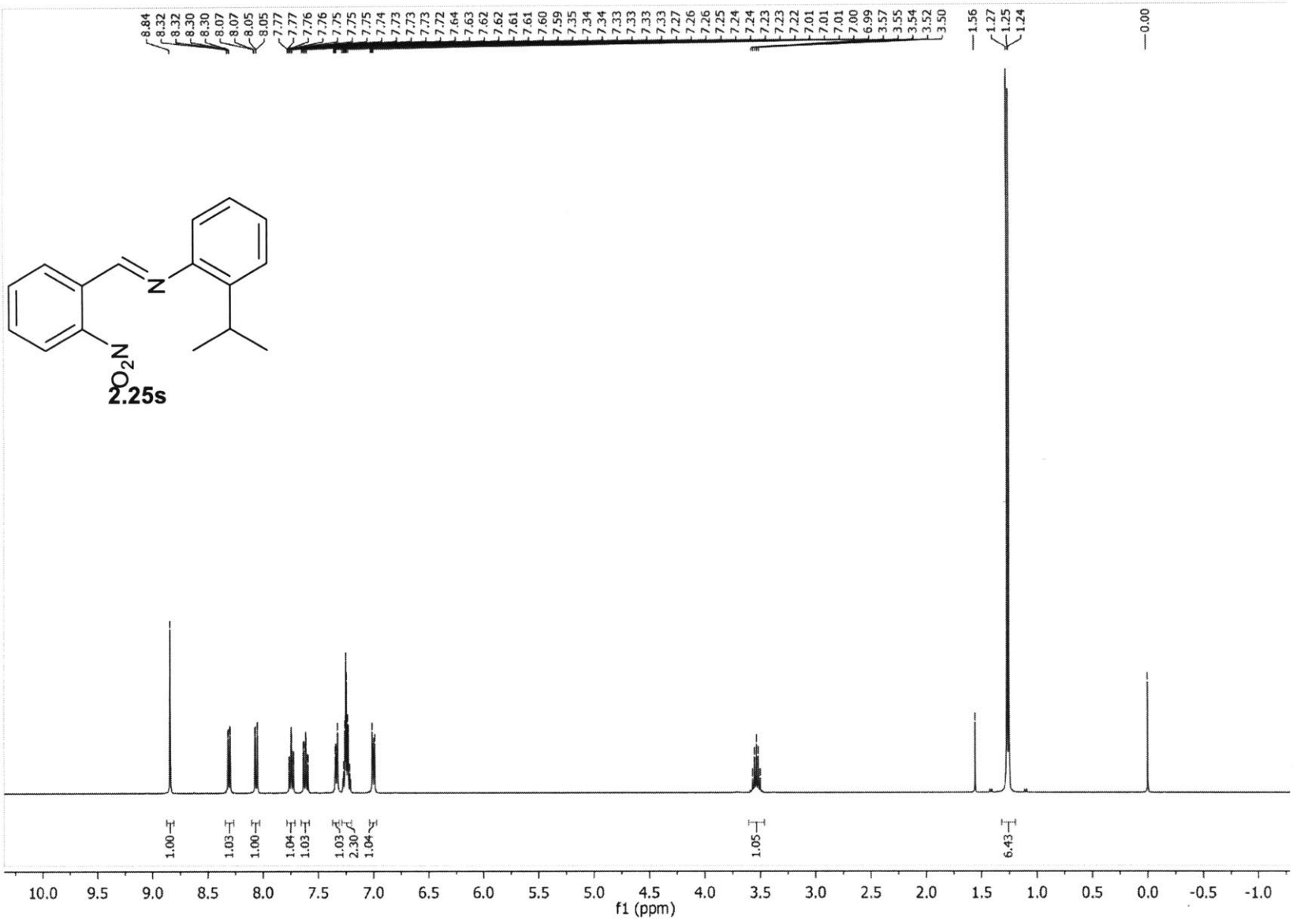
8.84
8.32
8.32
8.30
8.30
8.07
8.07
8.05
8.05
7.77
7.77
7.76
7.76
7.75
7.75
7.75
7.74
7.73
7.73
7.73
7.72
7.64
7.63
7.62
7.62
7.61
7.61
7.60
7.59
7.35
7.34
7.34
7.33
7.33
7.33
7.33
7.27
7.26
7.26
7.25
7.24
7.24
7.23
7.23
7.22
7.01
7.01
7.01
7.00
6.99
3.57
3.55
3.54
3.52
3.50
1.56
1.27
1.25
1.24
0.00
N
O2N
2.25s
1.00
1.03
1.00
1.04
1.03
1.03
2.30
1.04
1.05
6.43
10.0
9.5
9.0
8.5
8.0
7.5
7.0
6.5
6.0
5.5
5.0
4.5
4.0
3.5
3.0
2.5
2.0
1.5
1.0
0.5
0.0
-0.5
-1.0
f1 (ppm)

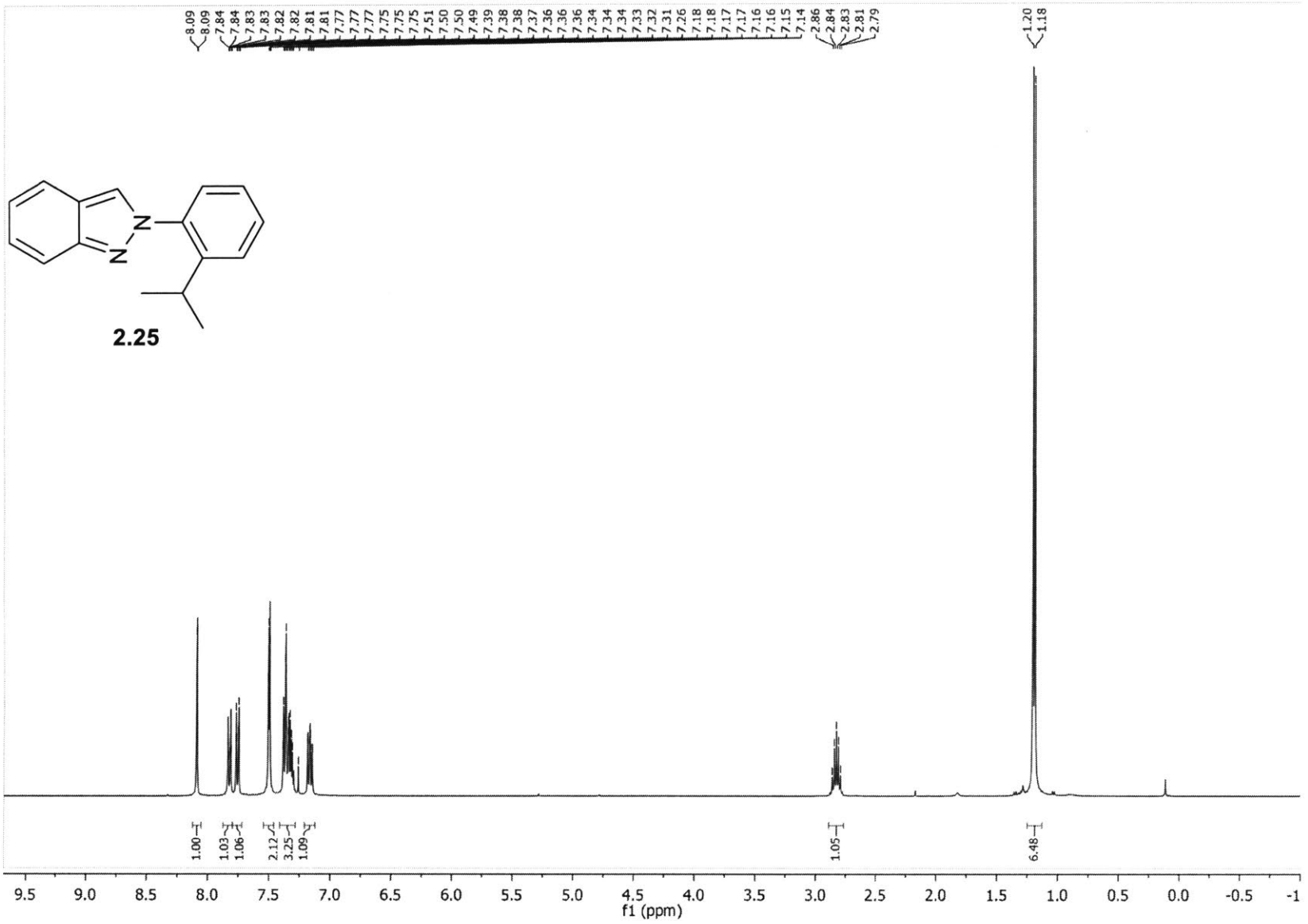
8.09
8.09
7.84
7.84
7.83
7.83
7.82
7.82
7.81
7.81
7.77
7.77
7.77
7.75
7.75
7.75
7.51
7.50
7.50
7.49
7.39
7.38
7.38
7.37
7.36
7.36
7.34
7.34
7.33
7.32
7.31
7.26
7.18
7.18
7.17
7.17
7.16
7.16
7.15
7.14
2.86
2.84
2.83
2.81
2.79
1.20
1.18
N
N
2.25
1.00
1.03
1.06
2.12
3.25
1.09
1.05
6.48
9.5
9.0
8.5
8.0
7.5
7.0
6.5
6.0
5.5
5.0
4.5
4.0
3.5
3.0
2.5
2.0
1.5
1.0
0.5
0.0
-0.5
-1
f1 (ppm)

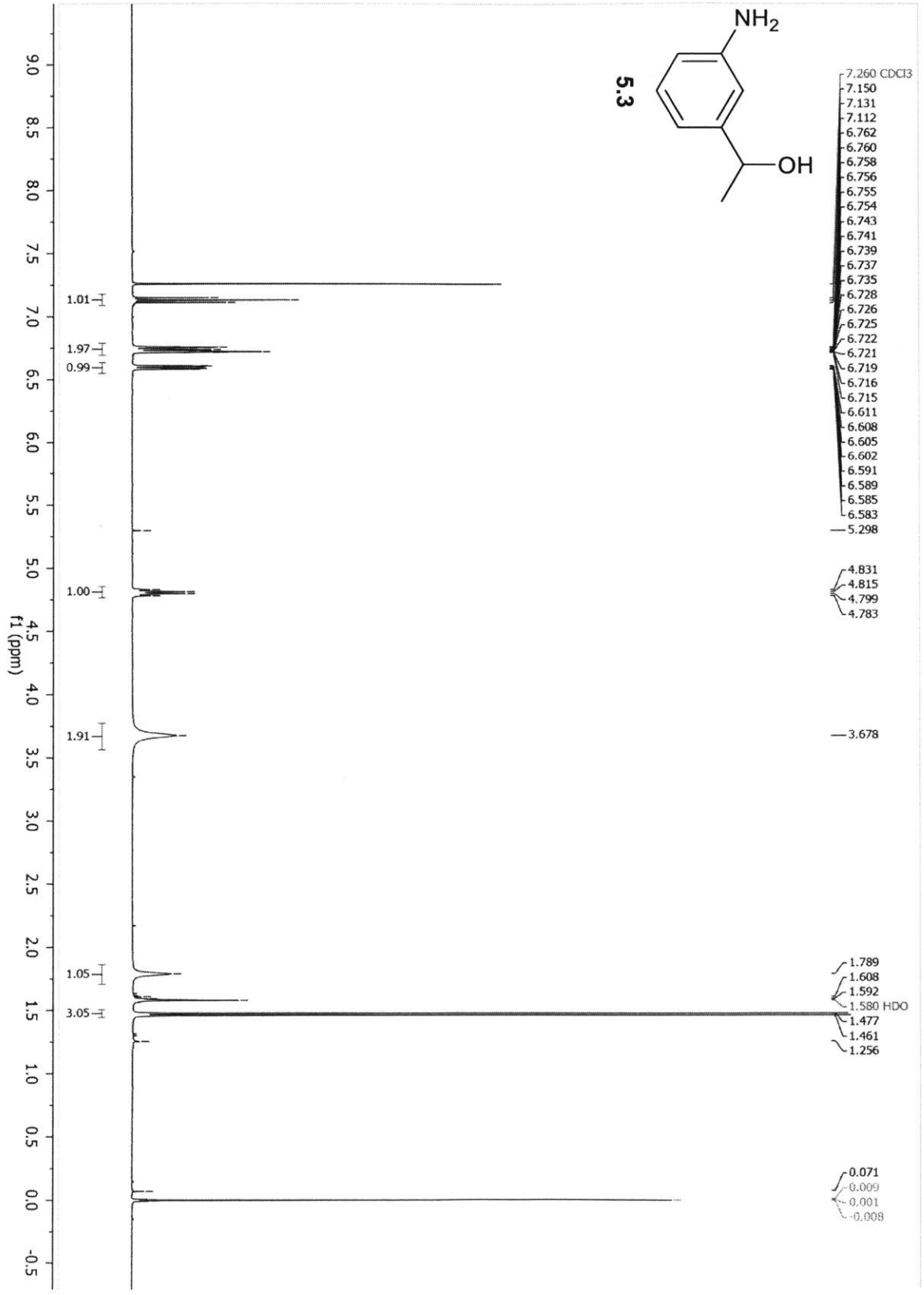
5.3
NH2
OH
7.260 CDCl3
7.150
7.131
7.112
6.762
6.760
6.758
6.756
6.755
6.754
6.743
6.741
6.739
6.737
6.735
6.728
6.726
6.725
6.722
6.721
6.719
6.716
6.715
6.611
6.608
6.605
6.602
6.591
6.589
6.585
6.583
5.298
4.831
4.815
4.799
4.783
3.678
1.789
1.608
1.592
1.580 HDO
1.477
1.461
1.256
0.071
0.009
0.001
-0.008
1.01
1.97
0.99
1.00
1.91
1.05
3.05
f1 (ppm)

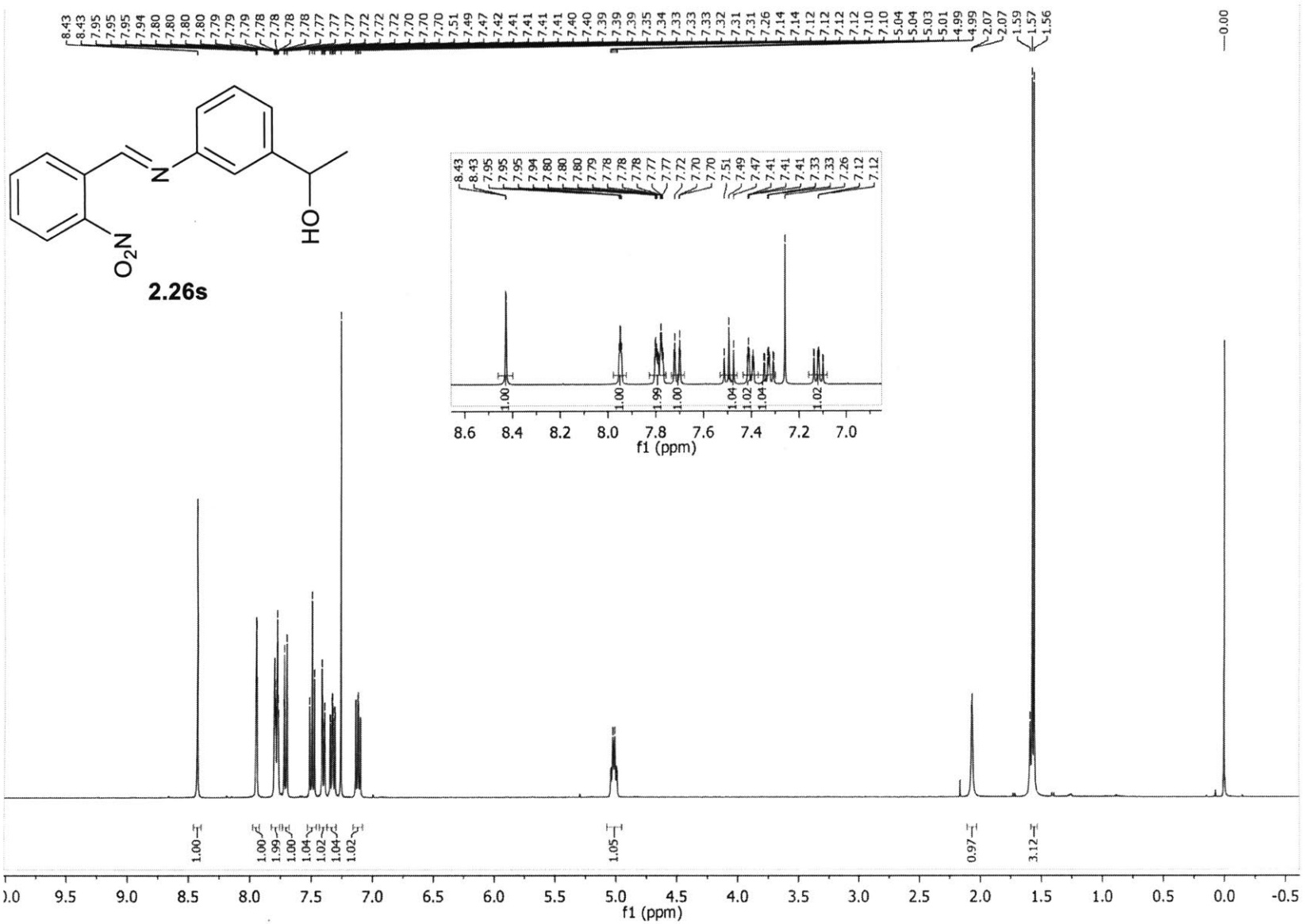
2.26s
f1 (ppm)

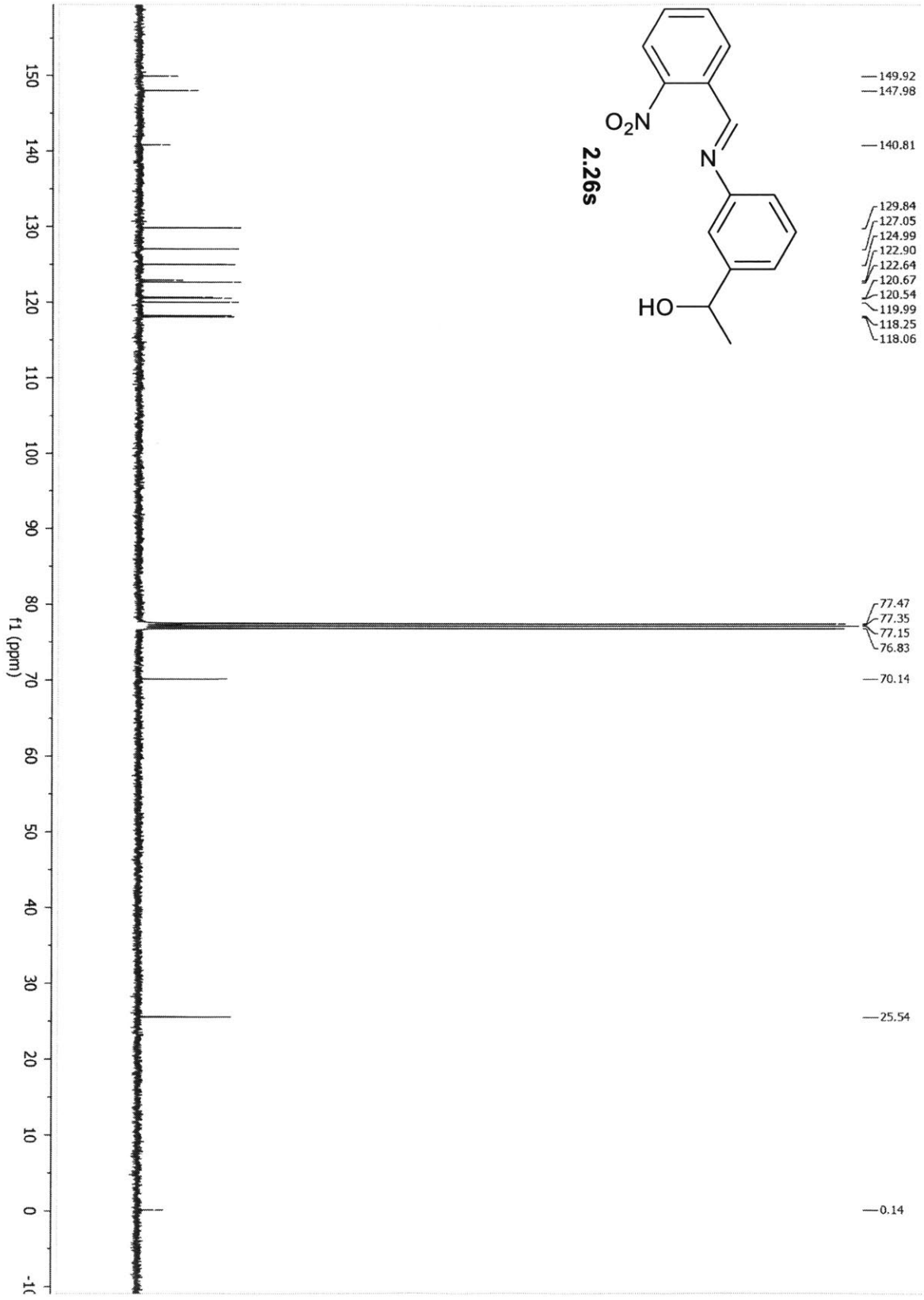
2.26s
O_2N
N
HO
149.92
147.98
140.81
129.84
127.05
124.99
122.90
122.64
120.67
120.54
119.99
118.25
118.06
77.47
77.35
77.15
76.83
70.14
25.54
0.14
f1 (ppm)

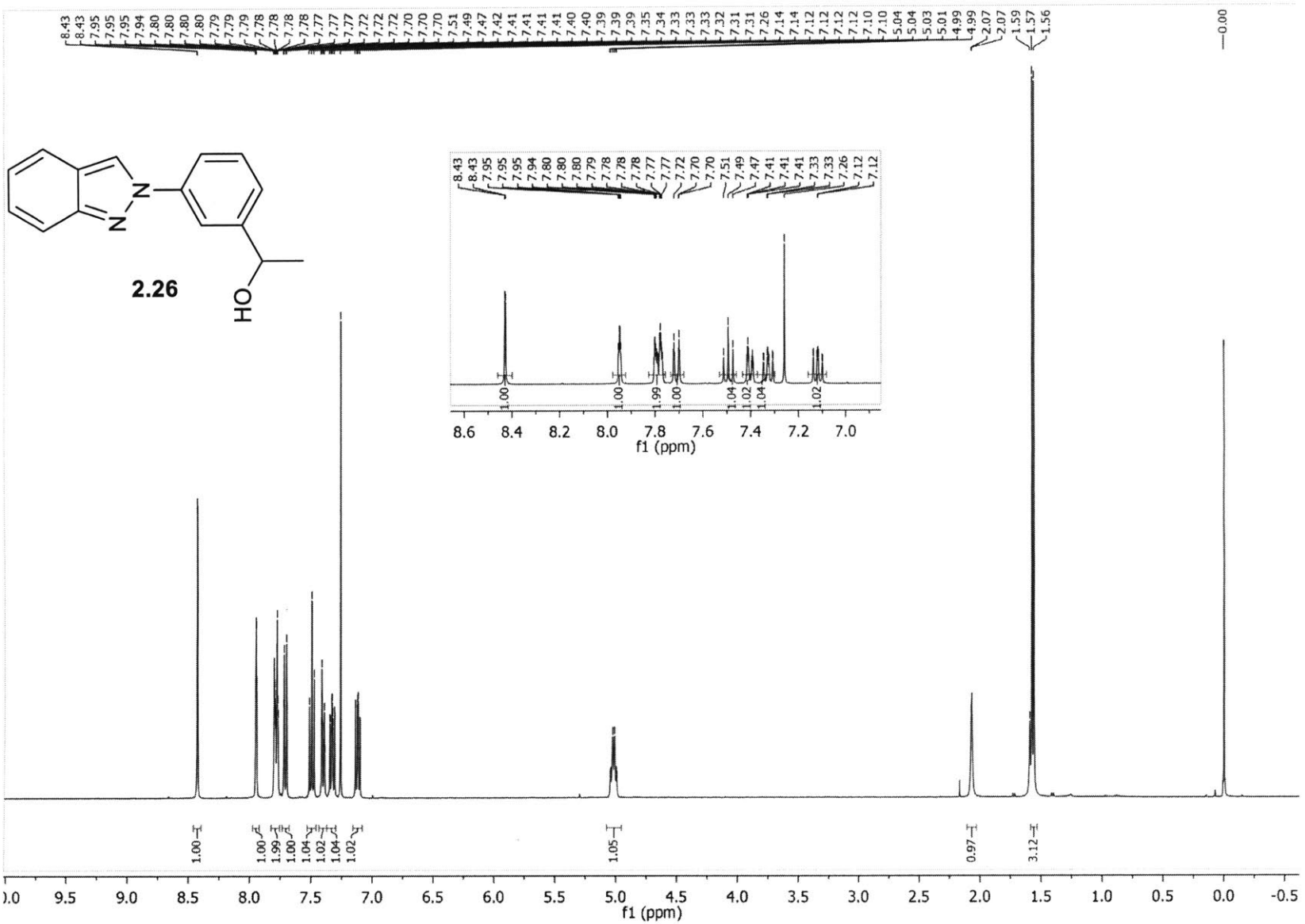
2.26
HO
N
N
f1 (ppm)

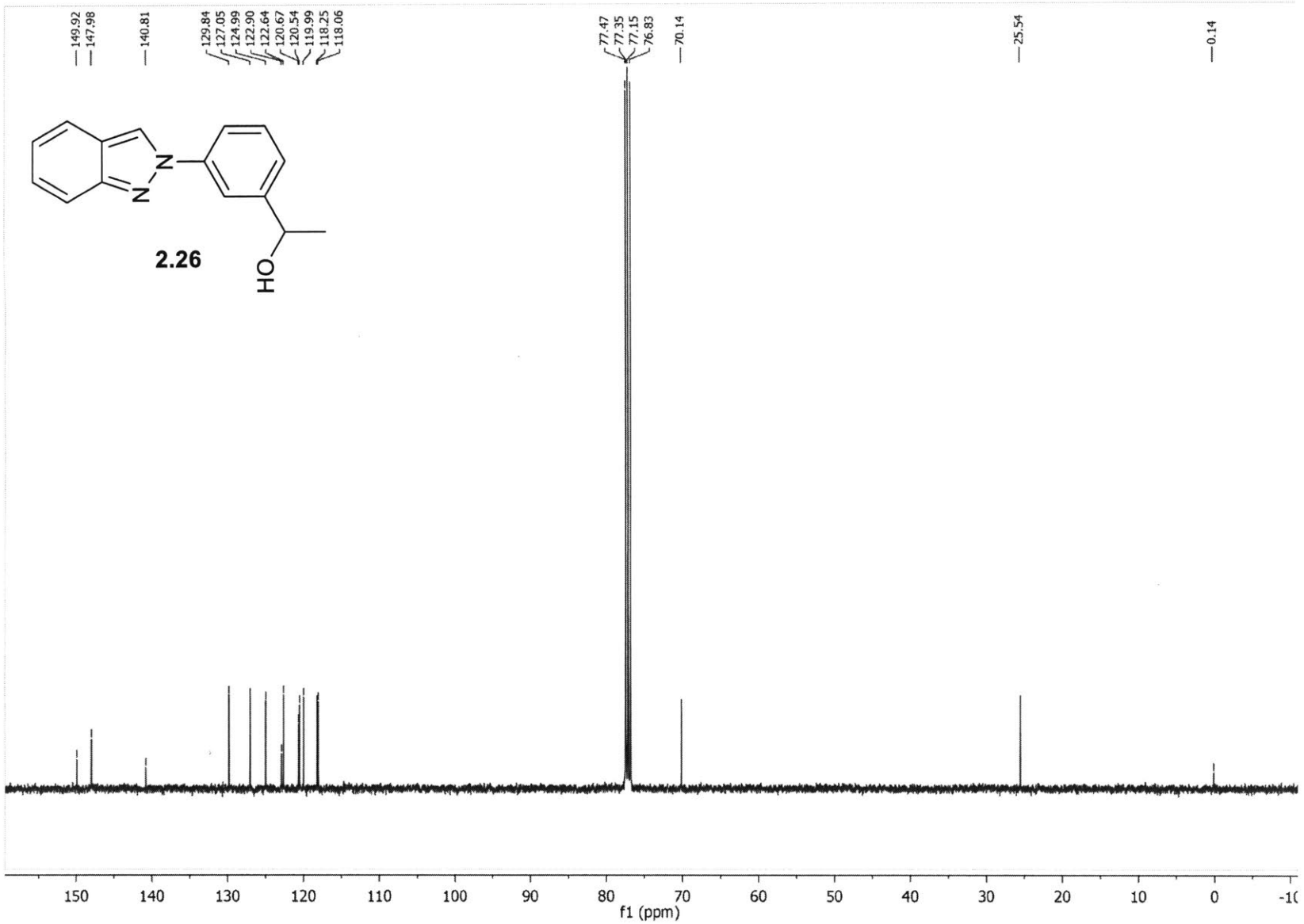
149.92
147.98
140.81
129.84
127.05
124.99
122.90
122.64
120.67
120.54
119.99
118.25
118.06
77.47
77.35
77.15
76.83
70.14
25.54
0.14
N
N
HO
2.26
150
140
130
120
110
100
90
80
70
60
50
40
30
20
10
0
f1 (ppm)

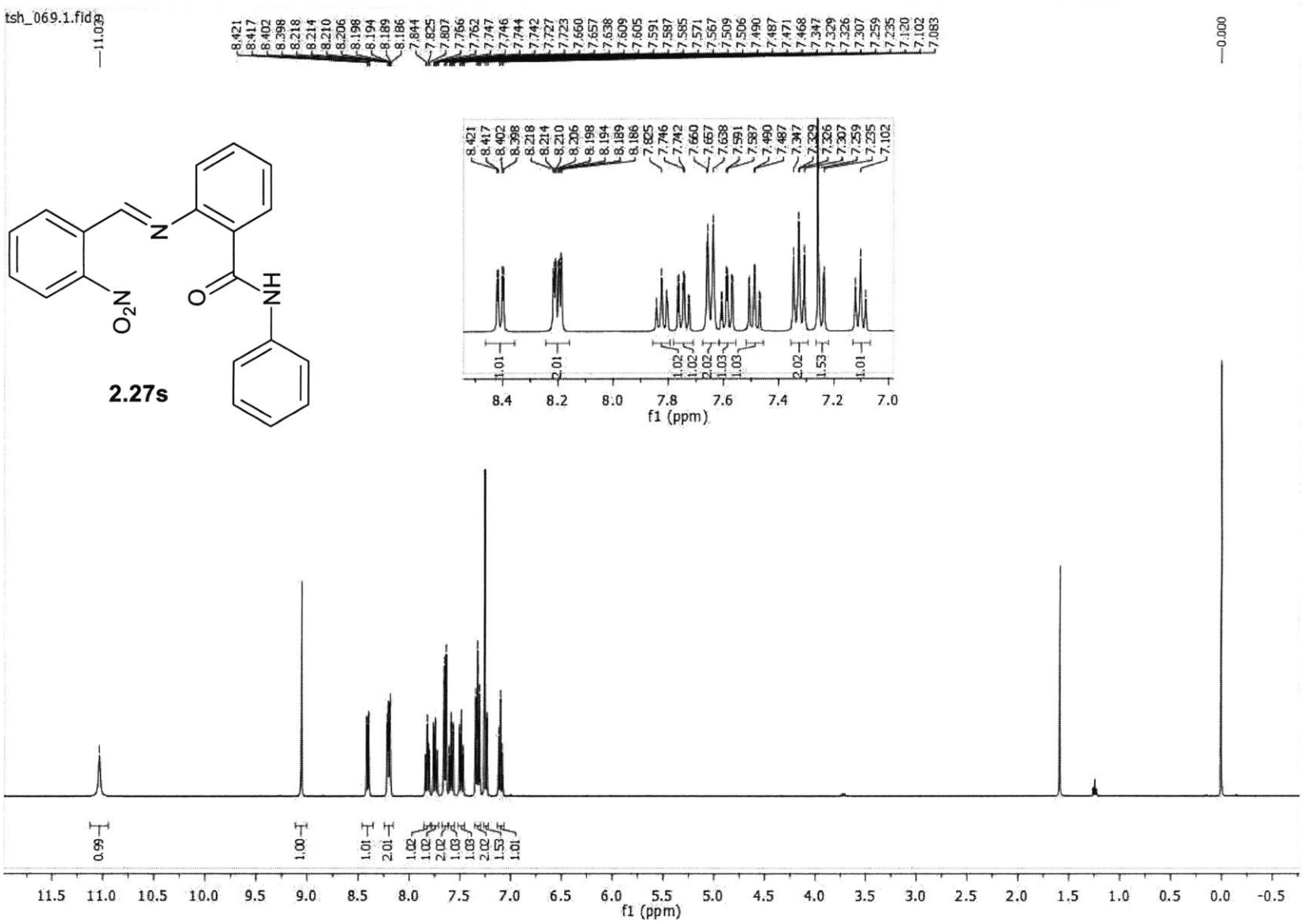
tsh_069.1.fid
11.039
8.421
8.417
8.402
8.398
8.218
8.214
8.210
8.206
8.198
8.194
8.189
8.186
7.844
7.825
7.807
7.766
7.762
7.747
7.746
7.744
7.742
7.727
7.723
7.660
7.657
7.638
7.609
7.605
7.591
7.587
7.585
7.571
7.567
7.509
7.506
7.490
7.487
7.471
7.468
7.347
7.329
7.326
7.307
7.259
7.235
7.120
7.102
7.083
0.000
N
O2N
O
NH
2.27s
1.01
2.01
1.02
1.02
2.02
1.03
1.03
2.02
1.53
1.01
8.4
8.2
8.0
7.8
7.6
7.4
7.2
7.0
f1 (ppm)
0.99
1.00
1.01
2.01
1.02
1.02
2.02
1.03
1.03
2.02
1.53
1.01
11.5
11.0
10.5
10.0
9.5
9.0
8.5
8.0
7.5
7.0
6.5
6.0
5.5
5.0
4.5
4.0
3.5
3.0
2.5
2.0
1.5
1.0
0.5
0.0
-0.5
f1 (ppm)

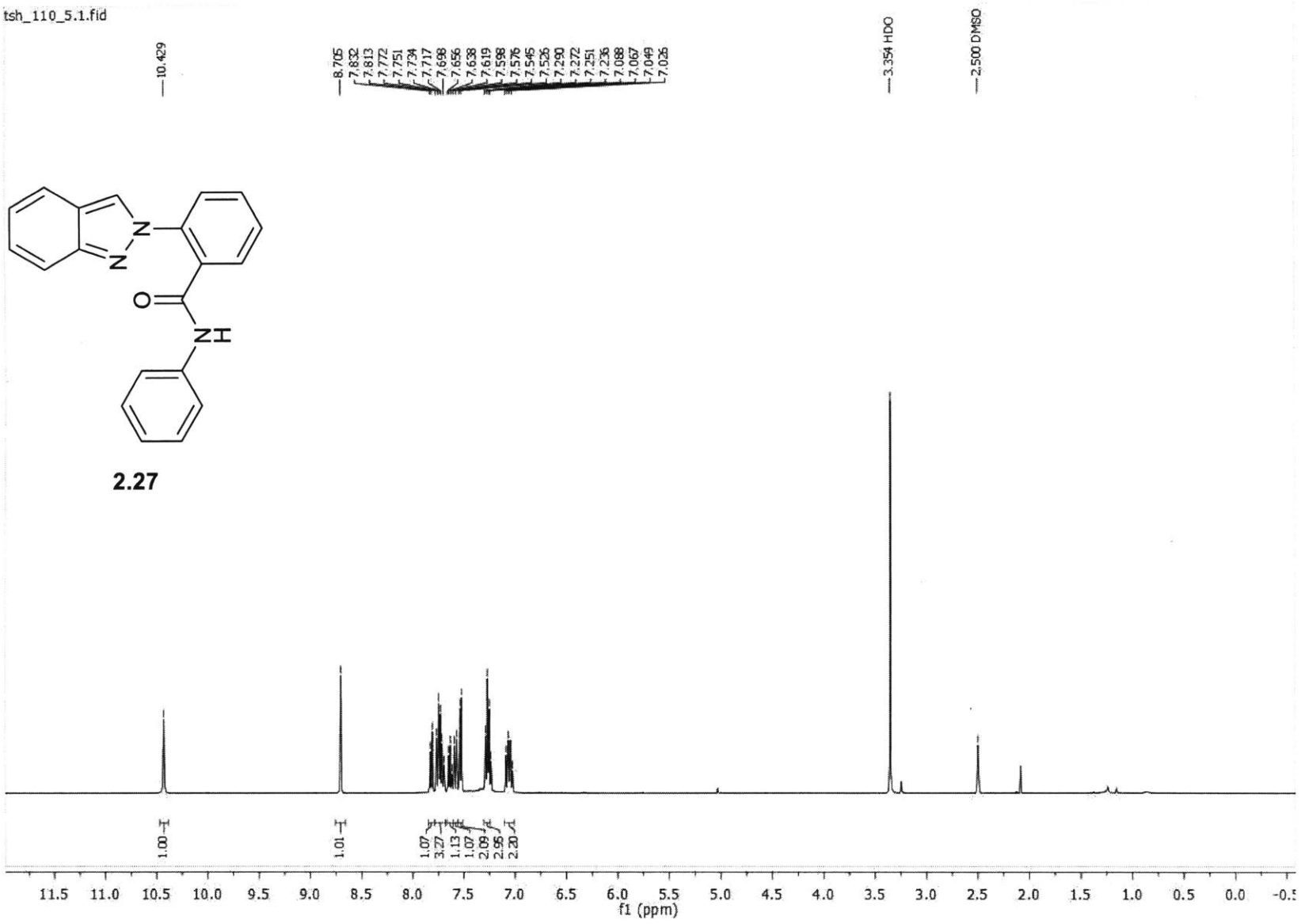
tsh_110_5.1.fid
10.429
8.705
7.832
7.813
7.772
7.751
7.734
7.717
7.698
7.656
7.638
7.619
7.598
7.576
7.545
7.526
7.290
7.272
7.251
7.236
7.088
7.067
7.049
7.026
3.354 HDO
2.500 DMSO
1.00
1.01
1.07
3.27
1.13
1.07
2.09
2.95
2.20
11.5 11.0 10.5 10.0 9.5 9.0 8.5 8.0 7.5 7.0 6.5 6.0 5.5 5.0 4.5 4.0 3.5 3.0 2.5 2.0 1.5 1.0 0.5 0.0
f1 (ppm)

2.27

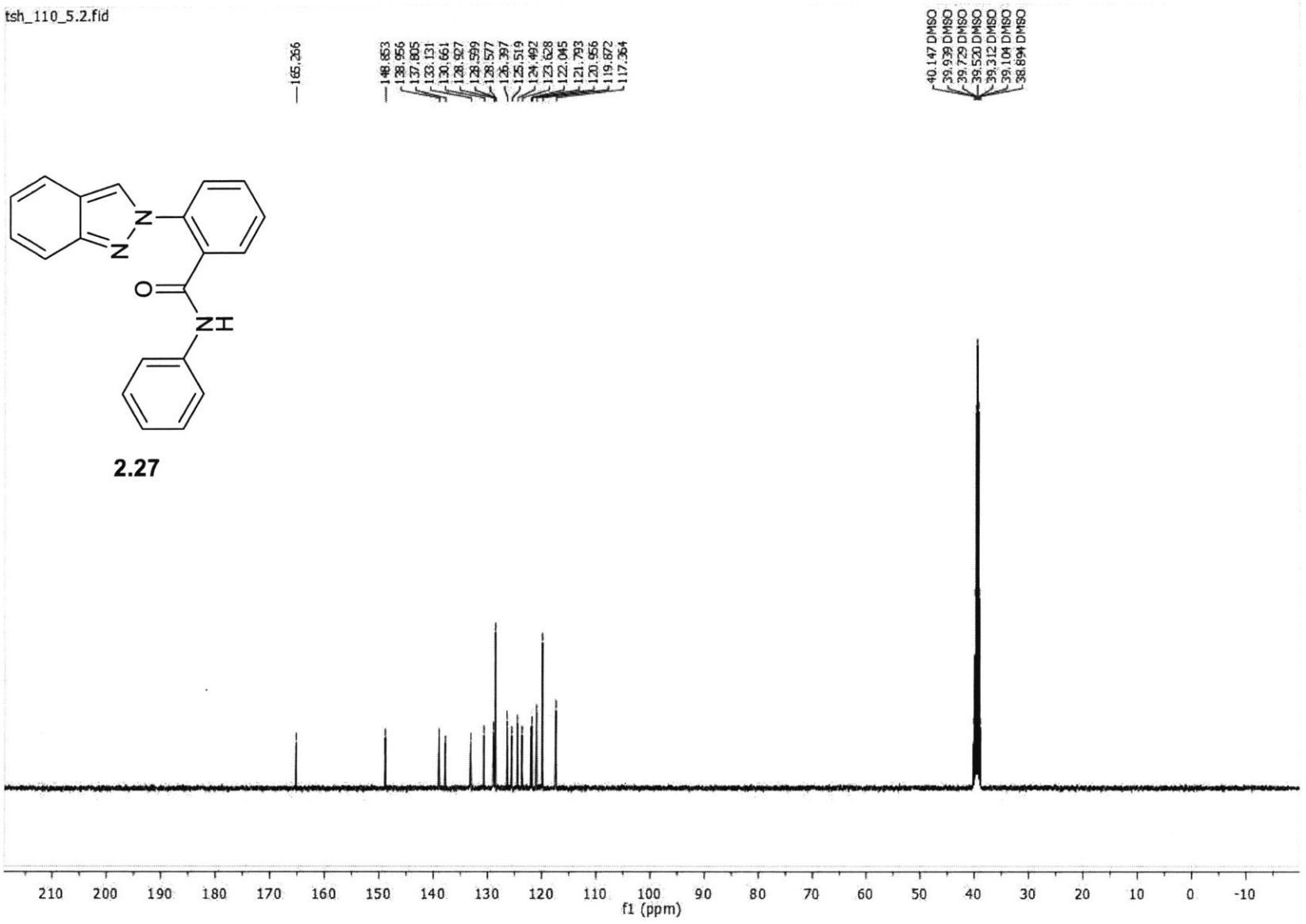
tsh_110_5.2.fid
165.266
148.853
138.956
137.805
133.131
130.661
128.927
128.599
128.577
126.397
125.519
124.492
123.628
122.045
121.793
120.956
119.872
117.364
40.147 DMSO
39.939 DMSO
39.729 DMSO
39.520 DMSO
39.312 DMSO
39.104 DMSO
38.894 DMSO
N
N
O
NH
2.27
210 200 190 180 170 160 150 140 130 120 110 100 90 80 70 60 50 40 30 20 10 0 -10
f1 (ppm)

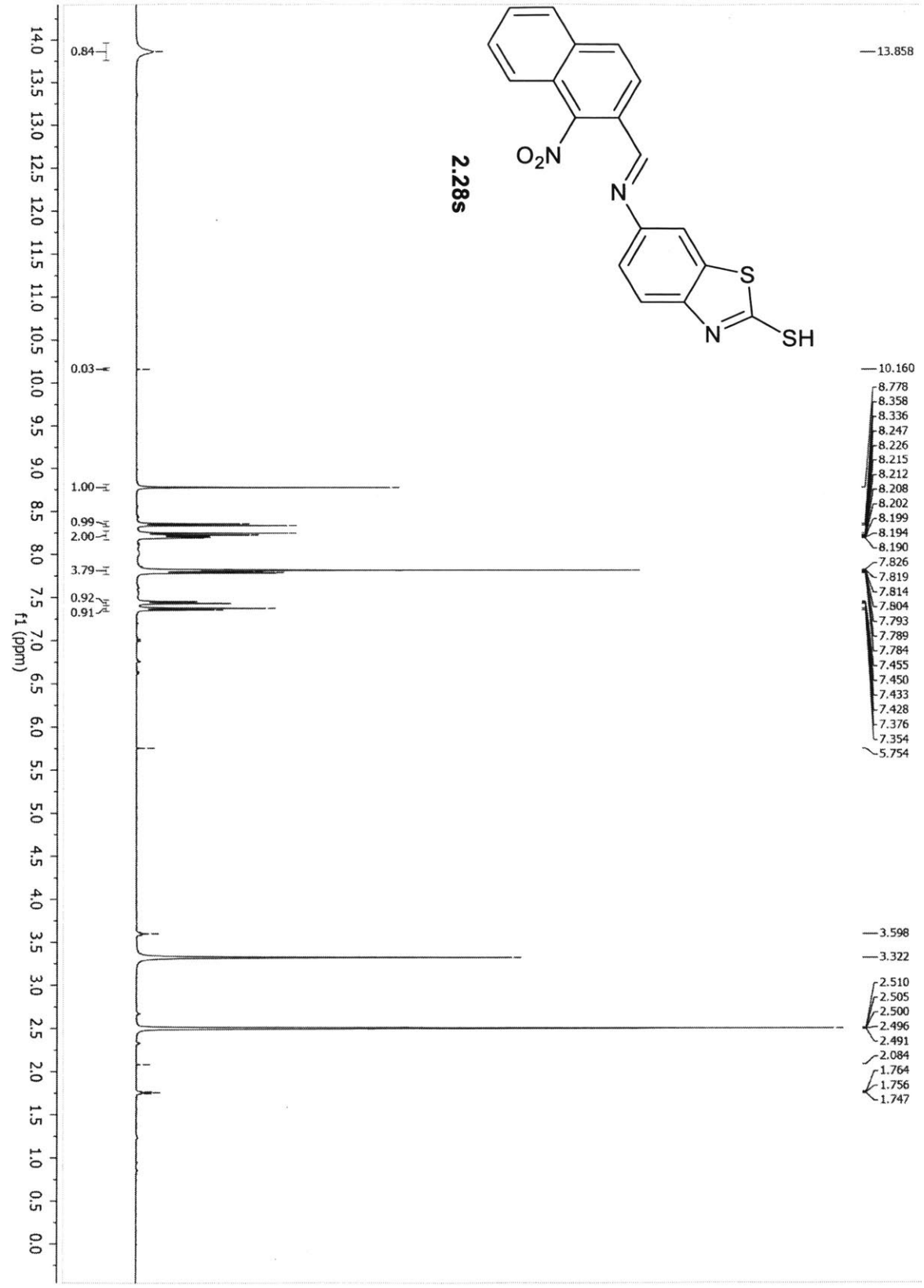
2.28s
O2N
N
S
N
SH
f1 (ppm)
0.84
0.03
1.00
0.99
2.00
3.79
0.92
0.91
13.858
10.160
8.778
8.358
8.336
8.247
8.226
8.215
8.212
8.208
8.202
8.199
8.194
8.190
7.826
7.819
7.814
7.804
7.793
7.789
7.784
7.455
7.450
7.433
7.428
7.376
7.354
5.754
3.598
3.322
2.510
2.505
2.500
2.496
2.491
2.084
1.764
1.756
1.747

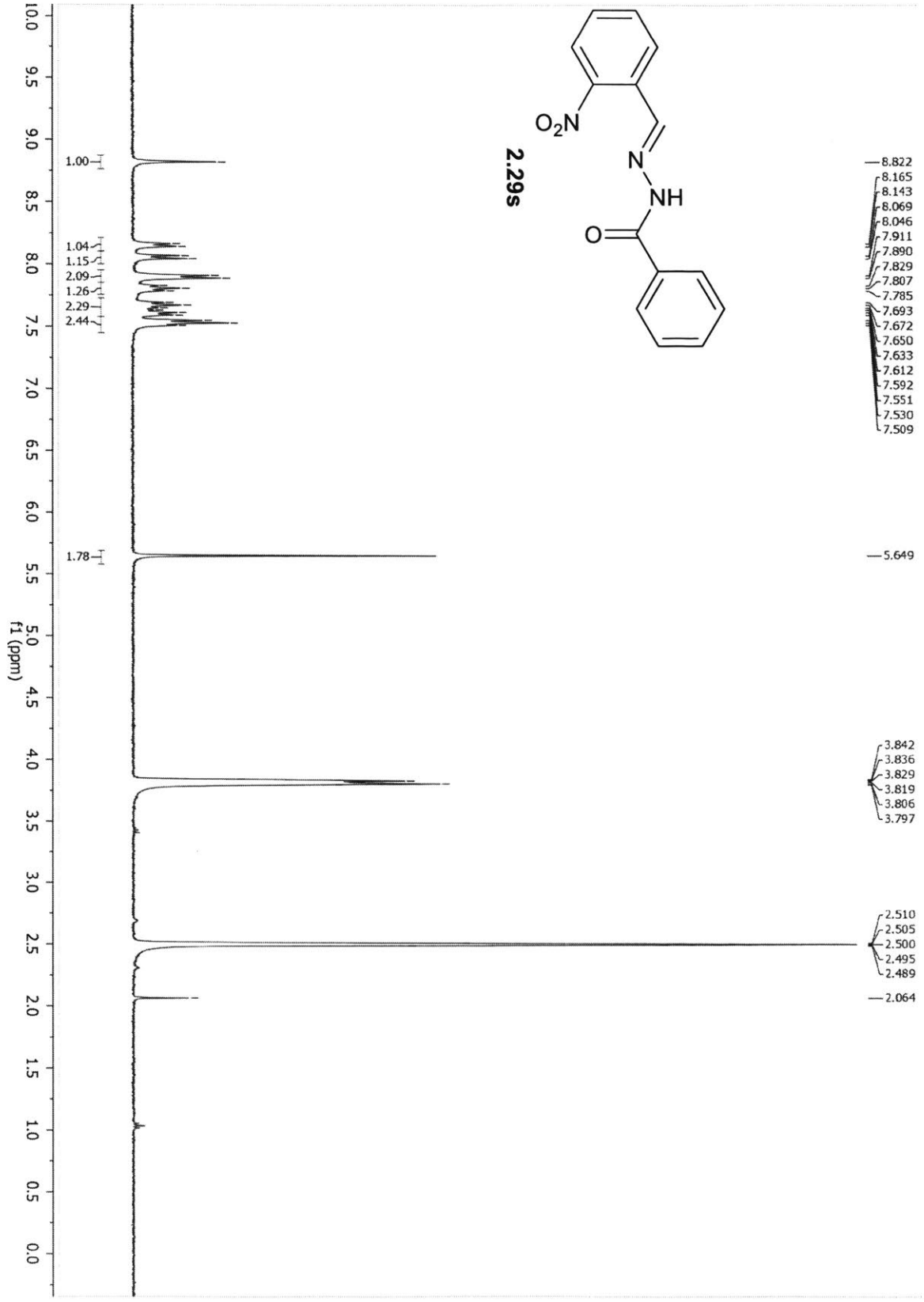
2.29s
O2N
N
NH
O
f1 (ppm)
10.0
9.5
9.0
8.5
8.0
7.5
7.0
6.5
6.0
5.5
5.0
4.5
4.0
3.5
3.0
2.5
2.0
1.5
1.0
0.5
0.0
1.00
1.04
1.15
2.09
1.26
2.29
2.44
1.78
8.822
8.165
8.143
8.069
8.046
7.911
7.890
7.829
7.807
7.785
7.693
7.672
7.650
7.633
7.612
7.592
7.551
7.530
7.509
5.649
3.842
3.836
3.829
3.819
3.806
3.797
2.510
2.505
2.500
2.495
2.489
2.064

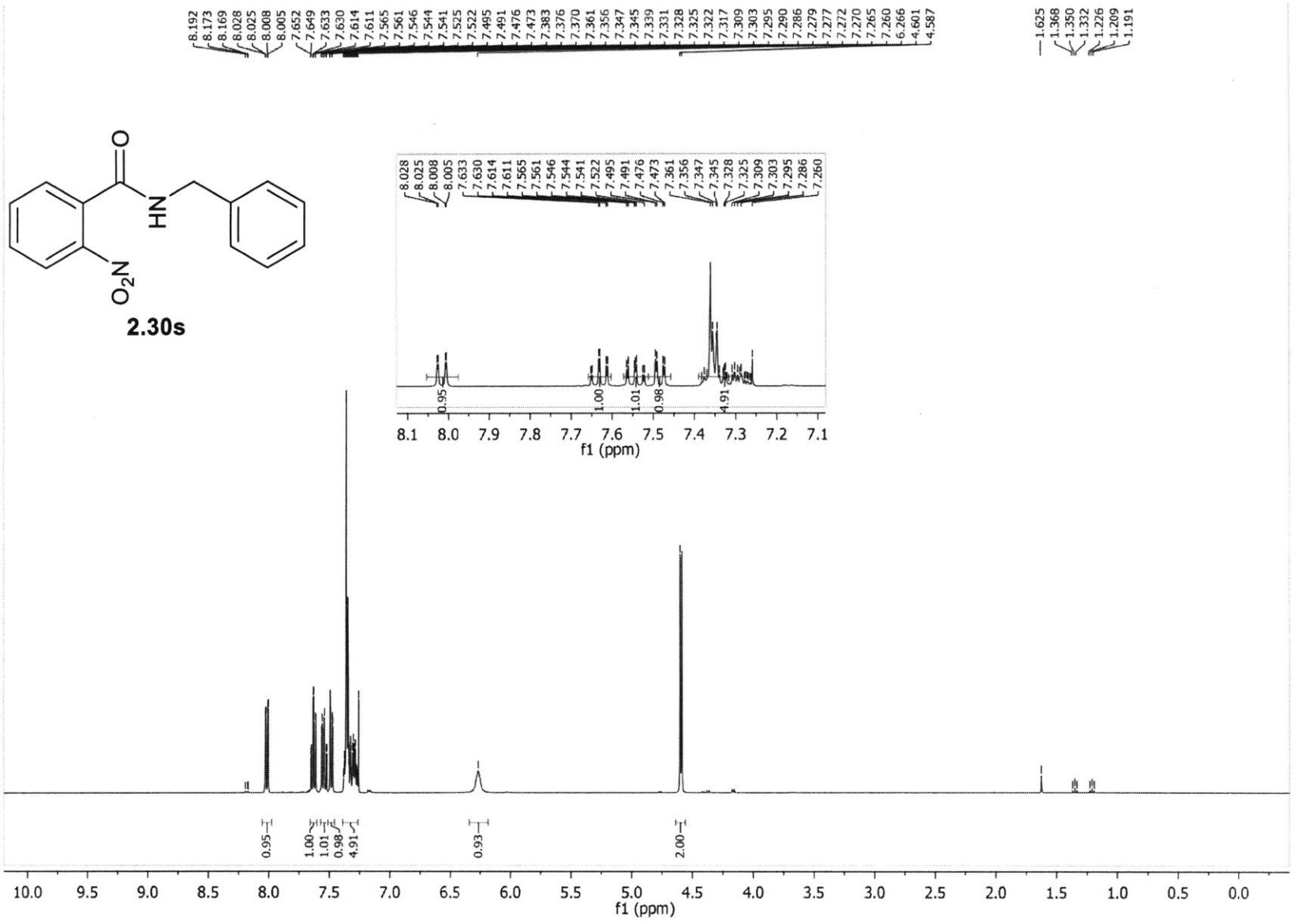
8.192
8.173
8.169
8.028
8.025
8.008
8.005
7.652
7.649
7.633
7.630
7.614
7.611
7.565
7.561
7.546
7.544
7.541
7.525
7.522
7.495
7.491
7.476
7.473
7.383
7.376
7.370
7.361
7.356
7.347
7.345
7.339
7.331
7.328
7.325
7.322
7.317
7.309
7.303
7.295
7.290
7.286
7.279
7.277
7.272
7.270
7.265
7.260
6.266
4.601
4.587
1.625
1.368
1.350
1.332
1.226
1.209
1.191
O
HN
O2N
2.30s
0.95
1.00
1.01
0.98
4.91
0.93
2.00
f1 (ppm)

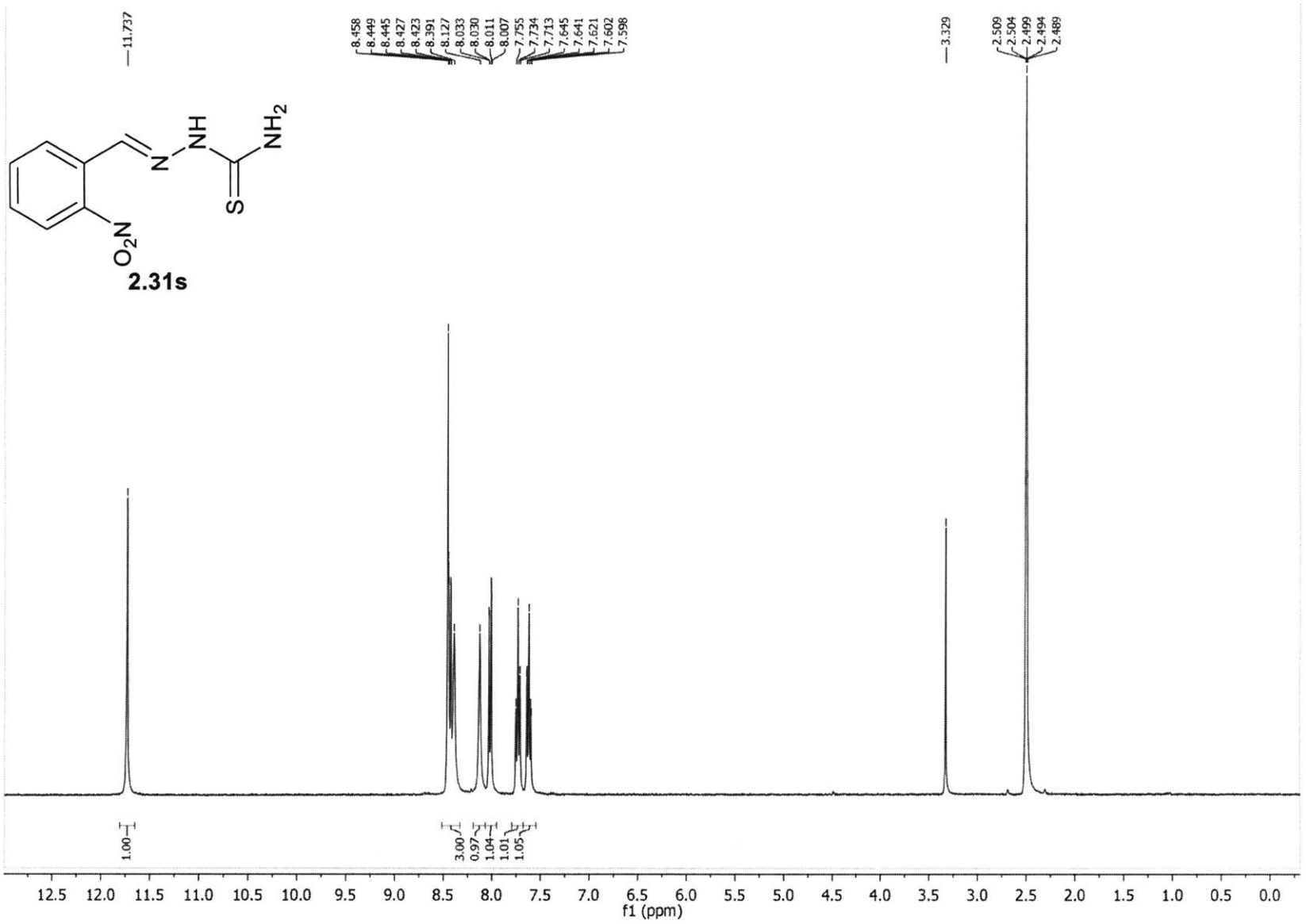
11.737
8.458
8.449
8.445
8.427
8.423
8.391
8.127
8.033
8.030
8.011
8.007
7.755
7.734
7.713
7.645
7.641
7.621
7.602
7.598
3.329
2.509
2.504
2.499
2.494
2.489
NH
NH2
S
O2N
2.31s
1.00
3.00
0.97
1.04
1.01
1.05
f1 (ppm)

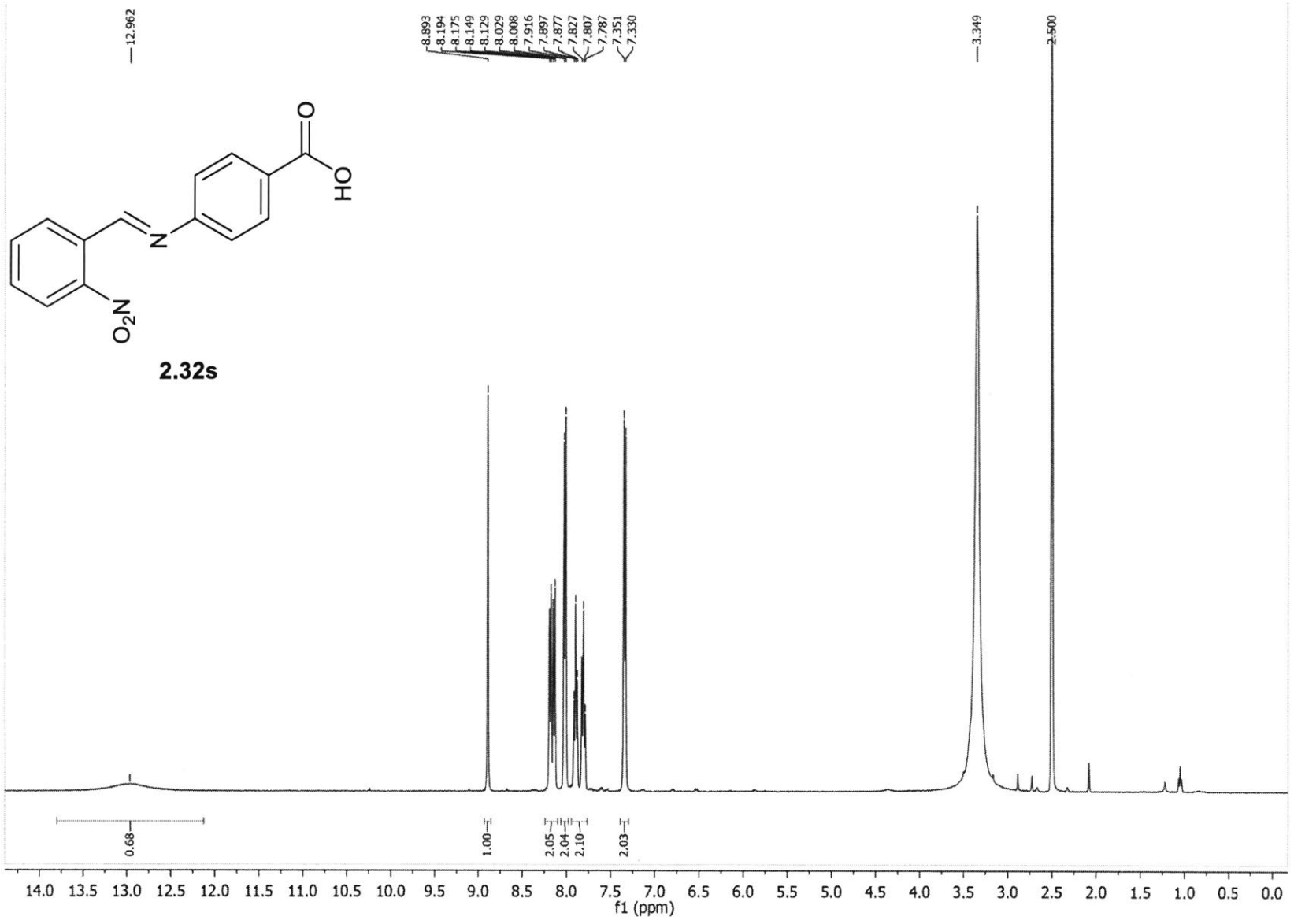
12.962
8.893
8.194
8.175
8.149
8.129
8.029
8.008
7.916
7.897
7.877
7.827
7.807
7.787
7.351
7.330
3.349
2.500
O
HO
N
O2N
2.32s
0.68
1.00
2.05
2.04
2.10
2.03
14.0 13.5 13.0 12.5 12.0 11.5 11.0 10.5 10.0 9.5 9.0 8.5 8.0 7.5 7.0 6.5 6.0 5.5 5.0 4.5 4.0 3.5 3.0 2.5 2.0 1.5 1.0 0.5 0.0
f1 (ppm)

IX. References

[1] Gray, G. A.; Cremer, S. E. "Carbon-13 Nuclear Magnetic Resonance of Organophosphorus Compounds. V. Effect of Changes in Phosphorus Oxidation State in Four-Membered Phosphorus Heterocycles." *J. Org. Chem.* **1972**, *37*, 3470–3475.

[2] O'Brien, C. J.; Nixon, Z. S.; Holohan, A. J.; Kunkel, S. R.; Tellez, J. L.; Doonan, B. J.; Coyle, E. E.; Lavigne, F.; Kang, L. J.; Przeworski, K. C. "Part I: The Development of the Catalytic Wittig Reaction." *Chem. Eur. J.* **2013**, *19*, 15281–15289.

[3] Ogawa, S.; Tajiri, Y.; Furukawa, N. "Simple Preparation of (2,2′-Biphenylylene)phenylphosphine Oxide and Role of Triphenylphosphine Oxide as a Mediator for Formation of Biaryl Derivatives." *Bull. Chem. Soc. Jpn.* **1991**, *64*, 3182–3184.

[4] Zhao, W.; Yan, P. K.; Radosevich, A. T. "A Phosphetane Catalyzes Deoxygenative Condensation of α-Keto Esters and Carboxylic Acids via P^{III}/P^{V}=O Redox Cycling." *J. Am. Chem. Soc.* **2015**, *137*, 616–619.

[5] Cremer, S. E.; Chorvat, R. J. "Syntheses of Substituted Phosphetanes and Related Derivatives." *J. Org. Chem.* **1967**, *32*, 4066–4070.

[6] Yao, E.; Szewczyk, J.; Quin, L. D. "Utilization of the ArH-PCl_3-$AlCl_3$ Reaction Product as the Source of Phosphorus in the Phosphetane Synthesis of McBride, *et al.*" *Synthesis* **1987**, 265–267.

[7] Cremer, S. E.; Chorvat, R. J. "Syntheses of Substituted Phosphetanes and Related Derivatives." *J. Org. Chem.* **1967**, *32*, 4066–4070.

[8] Oram, R. K.; Trippett, S. "Reactions of 1-Substituted 2,2,3,4,4-Pentamethylphosphetans with Hexafluoroacetone and the ^{19}F Nuclear Magnetic Resonance Spectra of the Resulting 1,3,2-Dioxaphospholans." *J. Chem. Soc., Perkin Trans. 1* **1973**, 1300–1310.

[9] Aldehyde synthesis adapted from: Wallace, D. J.; Baxter, C. A.; Brands, K. J. M.; Bremeyer, N.; Brewer, S. E.; Desmond, R.; Emerson, K. M.; Foley, J.; Fernandez, P.; Hu, W.; Keen, S. P.; Mullens, P.; Muzzio, D.; Sajonz, P.; Tan, L.; Wilson, R. D.; Zhou, G.; Zhou, G. "Development of a Fit-for-Purpose Large-Scale Synthesis of an Oral PARP Inhibitor." *Org. Process Res. Dev.* **2011**, *15*, 831–840.

[10] (a) Synthesis of [^{15}N]-2-aminobiphenyl: Peterson, M. A.; Nilsson, B. L. "An Efficient Synthesis of [^{15}N]-Carbazole from [^{15}N]-Aniline." *Synth. Commun.* **1999**, *29*, 3821–3827. (b) Aniline to nitroso oxidation conditions: Priewisch, B.; Rück-Braun, K. "Efficient Preparation of Nitrosoarenes for the Synthesis of Azobenzenes." *J. Org. Chem.* **2005**, *70*, 2350–2352. Reaction modifications (40 °C, 24 h, $CHCl_3$ instead of CH_2Cl_2).